School of Chemical and Petroleum Engineering

Department of Chemical Engineering

Heterogeneous Catalytic Oxidation of Organic Compound for Wastewater Treatment

Syaifullah Muhammad

This thesis is presented for the degree of

Doctor of Philosophy

of

Curtin University

May 2013

Declaration

To the best of my knowledge and belief this thesis contains no material previously published by any other person except where due acknowledgment has been made.

This thesis contains no material which has been accepted for the award of any other degree or diploma in any university.

Signature : ……

Date : ……

Acknowledgement

I would like to express my deepest gratitude to my supervisor and co-supervisor Prof. Shaobin Wang and Prof. Moses O. Tade for their guidance, encouragement and patience during my Ph.D Course at Chemical Engineering Department, Curtin University. Also I am thankful to Prof. Ming Ang as Chair Person of Thesis Committee who has organized regular meetings to support and help in resolving any issues raised in my research. Full support from all of them has made my Ph.D research and thesis be completed. Further, my sincere thank also goes to the technicians at Chemical Engineering Lab, Karen Haynes and all of her team members who have given very much assistance in experiments. I also wish to thank for my incredible research colleague, Edy Saputra, who gave very much contribution to the completion of this thesis.

I am thankful to DIKTI sponsor of National Education of Indonesia Government who has provided full scholarships for my Ph.D study. Thanks also go to Prof. Samsul Rizal, the rector of Syiah Kuala University, my home university, and Dr. Samadi as Scholarship Commission who gave so much help particularly in the delivery of the scholarship fund and other support. Further, a special thank is made to my wife Layli and my children, Buleun, Lubna and Ardan, for their continuous immense support. Finally, my kindest regards and thanks would go to all of my family: my mother, father, brother, sister and friends in Australia and Indonesia. Their interest and support have been of great comfort to me.

Summary

This research is focused on heterogeneous catalytic oxidation of phenol usually found in wastewater. Active metals of Ruthenium (Ru) and Cobalt (Co) have been impregnated on cheap support materials such as activated carbon (AC), fly ash (FA), red mud (RM), natural zeolite (NZ), ZSM5 and MCM48. Those synthesized catalysts, Ru/AC, Ru/ZSM5, Ru/Al_2O_3, Ru/TiO_2, Ru/MCM48, Co/FA, Co/RM, Co/NZ, Co/MCM48 have been tested in heterogeneous catalytic oxidation of phenol for waste water treatment in the presence of Oxone®. Particularly Ru/Al_2O_3 and Ru/TiO_2 catalysts have been tested in photocatalytic oxidation of phenol under UV-light. This research proves that the active metals impregnated on the support materials have well generated sulfate radicals from peroxymonosulphate (PMS) which serves as an oxidant agent to remove phenol pollutant from aqueous solutions. The catalyst activity in oxidation of phenol follows the order of Co/AC = Ru/AC > Co/MCM48 > Ru/ZSM5 = Co/RM-T > Co/FA-JL. It is found, AC that has large pores and surface area and MCM48 which has a very small particle size exhibit the best results as a support. In the photocatalytic tests, the activation of PMS is generated by the interaction PMS-Catalyst and PMS-UV. The photocatalysts of Ru/TiO_2 and Ru/Al_2O_3 can increase the phenol removal efficiency of 10-15% comparing PMS/UV only. Further, it was observed that catalyst loading, phenol concentration, oxidant concentration and temperature are the major factors influencing oxidation process of phenol. It is also noted, that degradation of phenol in heterogeneous catalytic oxidation is a combination of oxidation and adsorption process. However oxidation is much faster than adsorption.

Publication by the author

1. Muhammad, S., Shukla, P.R., Tade, M.O. and Wang, S. (2012). Heterogeneous activation of peroxymonosulphate by supported ruthenium catalysts for phenol degradation in water, *Journal of Hazardous Materials, 215-216, 183-190*

2. Muhammad, S., Saputra, E., Sun, H., Izidoro, J. d. C., Fungaro, D. A., Ang, H. M., Tade, M. O., Wang, S. Coal fly ash supported Co_3O_4 catalysts for phenol degradation using peroxymonosulfate. *RSC Advances 2012, 2, (13), 5645-5650.*

3. Muhammad, S., Saputra, E., Sun, H., Ang, H.M., Tade, M., Wang, S. Heterogeneous Catalytic Oxidation of Aqueous Phenol on Red Mud Supported Cobalt Catalysts. *Industrial & Engineering Chemistry Research, 51 (2012) 15351–15359.*

4. Saputra, E., Muhammad, S., Sun, H., Ang, H. M., Tadé, M. O., Wang, S. Red mud and fly ash supported Co catalysts for phenol oxidation. *Catalysis Today 2012, 190 (1), 68-72*.

5. Syaifullah Muhammad, Pradeep R. Shukla, Shaobin Wang, Moses O. Tadé, Heterogeneous catalytic oxidation of phenol for wastewater treatment using ruthenium catalyst, Proceeding of Chemeca Conference Sydney-Australia, 2011.

6. Syaifullah Muhammad, Edy Saputra, Hongqi Sun, Moses O. Tadé , Shaobin Wang, Phenol degradation in heterogeneous catalytic oxidation using Co-MCM48 and Co-Natural Zeolite Catalyst, Proceeding of Water Congress, Busan-Korea, 2012

7. Syaifullah Muhammad, Edy Saputra, Shaobin Wang, Moses O. Tadé. Phenol degradation on heterogeneous catalytic oxidation by using Cobalt-Natural Zeolite Catalyst, Proceeding of Annual International Conference Syiah Kuala University, Banda Aceh-Indonesia, 2011.

8. Edy Saputra, Panca Setia Utama, Syaifullah Muhammad, Ha-Ming Ang, Moses O Tadé, Shaobin Wang, Catalytic oxidation of toxic organic in aqueous solution for wastewater treatment : a review, Proceeding of TIChE International Conference, Songkhla-Thailand, 2011

Content

Chapter-1

Introduction

1.1 Some issues in water and wastewater

Water is a critical resource needed to sustain human life and other living creatures. Clean water is needed for drinking, hygiene and providing food. Water is also needed to produce energy and support for economic activities such as industry and transportation. Water in natural environment serves to ensure the provision of various ecosystem services to meet basic human needs and support economic and cultural activities.

According to the UNESCO report by the United Nations World Water Development Report 2012, the use of water by humans is driven by five main sectors of activity. *The first* is food and agriculture, which globally is the most consumed activity in water use. *The second* is energy; it is well known that water and energy have a reciprocal relationship. They are intricately connected, on one hand in many energy production processes water is always needed such as for the extraction of raw materials, cooling in thermal processes, cleaning materials, cultivation of crops for biofuels, and powering turbines. On the other hand, the energy is required to produce water for human resources through pumping, transportation, treatment, desalination and irrigation. *The third* is industry; this sector is pretty much in using clean water. It was reported that about 20% of underground world freshwater is used by this sector. This sector also affects the quality and quantity of water sources and environment. *The*

fourth is human settlement that includes drinking water and household use such as cooking, cleaning, hygiene and sanitation. And *the fifth* is ecosystems which are determined by the water needed to maintain or restore water benefits for the people (services) that supplied by the ecosystem including forests, wetlands and grassland components [1]

Water issues have been a major issue in many countries, from limited sources of fresh water for drinking to water pollution caused by industrial waste. According to the reports from the World Health Organization (WHO), about 13% of the world population is still consuming water from unprotected sources and it can be hazardous to health due to polluted compounds such as organic materials or toxic chemicals. About 2.5 billion people in the world lack access to adequate sanitation and nearly 1.2 billion have no sanitation facilities at all [2]. It also has led to endemic water-related disease threats to the world's population, especially in underdeveloped countries and developing countries like Diarrhea diseases, arsenic and fluoride poisoning, intestinal nematode infections, malnutrition, trachoma, schistosomiasis, malaria, onchocerciasis, dracunculiasis, Japanese encephalitis, lymphatic filariasis and dengue [3].

In many developing countries, a rapid growth of industrialization has not been watched by a tight control of the toxic effluents discharged into the environment. So the environmental pollution often occurs directly or not, contaminates surface water such as rivers, lakes and sea. As a result the dependence on fresh underground water increases. This was confirmed by a WHO report that the increase of consumption of underground freshwater in developing countries reaches 50% compared with developed countries by 18% [4]

In the global context, water contamination with pathogens and toxic substances, from municipal and industrial waste is recognized as the most serious risk in relation to human health. Toxic effects of hazardous chemicals are often not realized before the effect looks real and spreads out in community. Further, inorganic pollutants from industrial processes including toxic metals such as arsenic, lead, mercury and chromium become serious health problems when present in the water. These pollutants can cause toxic effects to human body including kidney, brain, and lung damage. They can also poison nerve tissue and blood. Further, arsenic poisoning of groundwater in drinking water can cause human organ failure and cancer. The contamination to humans mainly through contaminated food, such as through crop irrigation, fish and other seafood [5].

Water toxication is a major risk in industrial and agricultural production which is mainly due to the emission of wastes. Some cases become a crucial issue as the wastes from industry are discarded continuously into the environment. For example, intensive agriculture is highly dependent on the pest control thus has a high risk of contamination of pesticides to both surface water and groundwater. The similar issue happens in the mining industry that has a very large risk of the occurrence of toxic mining waste contamination in both the material and the mining process.

Industrial waste has also significantly contributed to the pollution of the environment through organic materials which are known as Persistent Organic Pollutants (POPs), which could be existed quite a long time in the environment, especially in the water without being able to be naturally degraded. These compounds can be bio-accumulated in human and animal tissues and cause death and disease, including endocrine disruption,

reproductive and immune systems, neurobehavioral disorders, and cancer. POPs include substances such as polychlorinated biphenyls (PCBs), pesticides such as DDT and pharmaceuticals and body care products. Further, some of the synthetic chemicals found in waste water are endocrine disruptors. Its effects on the endocrine hormonal system are disturbing because these chemicals can mimic natural hormones in both humans and wildlife [6].

Another organic contaminant generated by industrial waste such as chemical, petrochemical and pharmaceutical industries is phenol, because it widely used in the industry as a raw material. Phenol is a white crystalline solid with the molecular formula of C_6H_5OH. It has molecular weight of 94.113 g mol^{-1}, boiling point of 181.8 ^oC, freezing point of 40.9 ^oC and density of 1.071 g cm^{-3}. It is flammable and has a strong odor. When it loses the hydrogen of the –OH group it forms the negatively charged phenolate ion, and resonance stabilized, considering phenol as a relatively strong acidic compound. In the resonance stabilization, the negative charge on the oxygen atom is shared with the carbon atoms in the ring [7].

Phenol is moderately soluble in water, it can form hydrogen bonds with water and evaporates slower than water. Moreover, phenol is actually a phenyl derivative with a –OH group indicating that it is a hard degraded organic pollutant. Further, phenol is one of the important pollutants in waste water because of toxic effects on the environment including microorganisms even at very low concentrations such as above 70 ppm [8]. The chemical structure of phenol can be seen in Figure 1.1.

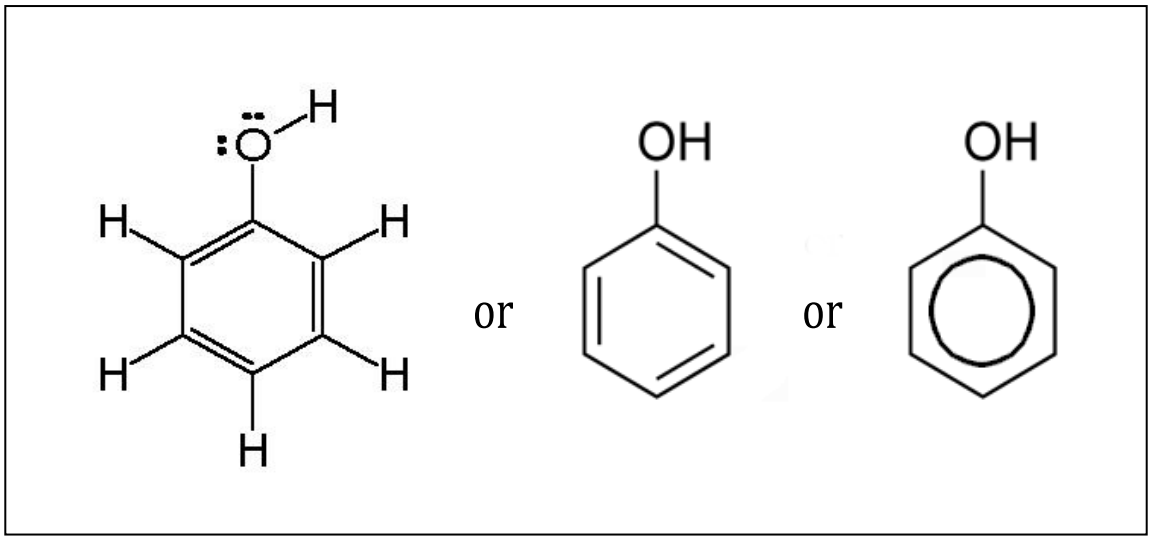

Figure 1.1 Phenol Structure.

As mentioned above, many industries use phenol in their processes. Table 1.1 shows the pollutants coming from phenol and its derivatives which are discharged into the environment [9]. As can be seen from Table 1.1, the huge phenol wastes produced by industry has led to the development of waste treatment technologies such as adsorption, incineration, wet air oxidation, catalytic wet air oxidation etc., to prevent the worse consequences experienced by the environment

Adsorption and Incineration are two methods which are widely used for degradation of organic pollutants, including phenol. However, these methods have significant drawbacks. By using activated carbon, for example, the adsorption processes can not remove completely the organic pollutants such as phenol from wastewater while the incineration technique generates emissions of byproducts into the environment and also requires the use of high energy to burn organic contaminant perfectly [10]. Furthermore, since phenol as a water pollutant that can not be easily degraded by both primary and secondary treatment processes, therefore

it will require the application of other technologies in the removal process. Tertiary treatment technology such as Advanced Oxidation Processes (AOPs) is to be implemented.

Table 1.1 Phenol-like pollutant release for the year of 2000 in United State

Compound	Emission (ton/year)	Overall Ranking
Phenol	22	35
2,4-Dinitriphenol	11	50
Catechol	8.3	59
Aniline	5.8	70
Hydroquinone	1.9	95
Quinone	0.64	115
Pentachlorophenol	0.55	120
Chlorophenol	0.046	203
2-Nitrophenol	0.026	213
4-Nitrophenol	0.007	239

Generally, AOPs include thermal oxidation, chemical oxidation, wet air oxidation, catalytic oxidation and some others. In principle, the treatment process is used to reduce the contaminants into harmless products such as CO_2 and H_2O through the oxidation process [11]. Among the various methods of these AOPs, heterogeneous catalytic oxidation typically has several advantages as it can be operated effectively at room temperature and normal pressure with high energy efficiency. Additionally, heterogeneous catalysts can be synthesized using cheap materials as catalyst supports such as activated carbon, zeolite, silica, red mud, fly ash, alumina etc., and can be regenerated for reuse in the process [12]. Thus,

the PhD thesis is focused on heterogeneous catalytic oxidation of organic compounds for wastewater treatment.

1.2 Aim and Scope of Research

The main objective of the research is to synthesize a variety of catalysts by impregnating several active metals such as Ruthenium (Ru) and Cobalt (Co) to the catalyst supports of inexpensive materials such as Activated Carbon (AC), Zeolite, Red mud, Fly ash, Alumina and Silica. The catalysts will be used in heterogeneous catalytic oxidation to degrade phenol as a model organic pollutant in wastewater treatment. The experiment is also conducted by involving photo catalytic oxidation in phenol removal. To meet the target of this research, several stages of research have been done with specific objectives as listed below.

1. To synthesis catalysts based on heavy metals of Ru and Co, on many supports such as activated carbon, redmud, flyash, zeolite (natural zeolite, ZSM5, MCM41 and MCM48), alumina, and titanium dioxide.
2. To identify the activity of the synthesised catalysts.
3. To investigate various processes with catalyst, oxidant and UV-light in heterogeneous catalytic oxidation of phenol for wastewater treatment and to identify their synergistic effect.
4. To identify the parameters of phenol degradation particularly the effects of catalyst amount, phenol concentration, oxidant concentration and temperature.
5. To determine the phenol degradation kinetics and activated energy of the synthesized catalysts in the heterogeneous catalytic oxidation processes.

1.3 Thesis Organization

This thesis is divided into eight chapters. ***Chapter 1*** presents an introduction which consists of the background of the research including several issues in water and wastewater. This chapter also presents Aim and Scope of Research with some specific objectives and organization of the thesis.

Chapter 2 deals with the literature review. This chapter presents the theoretical view of the research based on the studies of other researchers particularly about the various oxidation techniques for the treatment of phenol in waste water.

Chapter 3 investigates the heterogeneous activation of peroxymonosulphate by supported ruthenium catalysts for phenol degradation in water. This chapter will focus on catalytic oxidation of phenol by using Activated Carbon and ZSM-5 as catalyst supports. It also presents the kinetic and activation energy of phenol oxidation. The study has been presented at Chemeca Conference in Sydney, 18-21 September 2011 and also published in Journal of *Hazardous Materials 215– 216 (2012) 183– 190.*

Chapter 4 reports the study of Coal Fly Ash Supported Co_3O_4 catalysts for phenol degradation using peroxymonosulfate. Several fly ash (FA) samples derived from Australian (FA-WA) and Brazilian coals (FA-JL and FA-CH) were used as supports to prepare Co oxide (Co)-based catalysts. The experiment results have been published in *RSC Advances, 2012, 2, 5645–5650* and *Catalysis Today 190 (2012) 68–72.*

Chapter 5 reveals Heterogeneous Catalytic Oxidation of Aqueous Phenol on Red Mud Supported Cobalt Catalysts. The pre-treatment on red mud

support has been evaluated in regard to catalyst activation on phenol removal. The kinetic study of heterogeneous catalytic oxidation of phenol has also been presented in this chapter. This work has been published in *Industrial & Engineering Chemistry Research,* 51 *(2012)* 15351–15359*.*

Chapter 6 studies phenol degradation in heterogeneous catalytic oxidation using natural zeolite and MCM48 supported cobalt catalysts. The used catalysts consist of Australia Natural Zeolite (Clipnotilolite), Indonesia Natural zeolite (Clipnotilolite) and MCM48. Complete kinetic tests using these catalysts are also presented. The results of this experiment have been presented in a conference of *Water Congress in Busan Korea, 16-21 September 2012.*

Chapter 7 reports photo catalytic oxidation in phenol removal using Ru/TiO_2 and Ru/Al_2O_3 catalysts. This study will compare photo catalytic and photochemical reaction using different power of UV-light in the presence of the catalysts with peroxymonosulphate. Kinetic studies of the phenol oxidation are also presented in this chapter.

The last chapter, ***Chapter 8***, comprises of the conclusions and recommendations for future work. This chapter presents the summary of the research results and some suggestions for further research in this area. A lot of challenging issues are addressed for development of heterogeneous catalytic oxidation technology.

References

1. UN Water Report, the United Nations World Water Development Report 4*: Managing Water under Uncertainty and Risk*. Volume 1, 2012. p. 60.
2. Unicef, *Progress on Drinking water and Sanitation*, A.V.M. Chan, Editor. 2008. p. 58.

3. Erlanger, T. E., Keiser, J., Caldas De Castro, M., Bos, R., Singer, B. H., Tanner, M. and Utzinger, J. 2005. Effect of water resource development and management on lymphatic filariasis, and estimates of populations at risk. *American Journal of Tropical Medicine and Hygiene* Vol. 73, No. 3, pp. 523–33.
4. UN Water Report, The United Nations World water Development Report 2: *Water a shared responsibility.* 2006. p. 52.
5. Corcoran, E., Nellemann, C., Baker, E., Bos, R., Osborn, D. and Savelli, H. (eds). 2010. *Sick Water? The Central Role of Wastewater Management in Sustainable Development.* A Rapid Response Assessment. United Nations Environment Programme.
6. Colborn, T., vom Saal, F. S. and Soto, A. 1993. Developmental effects of endocrine-disrupting chemicals in wildlife and humans. *Environmental Health Perspectives,* Vol. 101, No. 5, pp. 378–84.
7. Phenol Properties & Specifications, retrieved 5 November 2012 from http://www51.honeywell.com/sm/chemicalintermediates/phenol-n3/phenol-properties-spec.html?c=21
8. Metcalf, E. and H.P. Eddy, *Wastewater engineering: treatment, disposal and reuse.* McGraw-Hill New York , 1991.
9. Athanasios Eftaxias, *Catalytic Wet Air Oxidation of Phenol in a Trickle Bed Reactor: Kinetics and Reactor Modelling*, 2002, Doctor Dissertation, the Rovira i Virgili University, Tarragona Spain.
10. Ahling, B. and A. Lindskog, *Emission of chlorinated organic substances from combustion.* Chlorinated dioxins and related compounds: impact on the environment. Pergamon, Oxford, 1980: p. 215-225.
11. S. Chiron, A. Fernandez-Alba, A. Rodriguez, E. Garcia-Calvo, Pesticide chemical oxidation: state-of-the-art, Water Res., 34 (2000) 366-377.
12. A. Camporro, M.J. Camporro, J. Coca, H. Sastre, Regeneration of an activated carbon bed exhausted by industrial phenolic waste-water, J. Hazard. Mater., 37 (1994) 207-214

Chapter-2

Literature Review

Abstract

Major issues in environmental protection lead all aspects of waste management into great attention. The pollutant that contaminates water is one of them, where the application of technology to degrade pollutants is experiencing rapid growth. This Chapter focuses on the evaluation of the developments in wastewater treatment methods particularly in completely destroying of organic pollutants by oxidation. Some oxidation techniques are highlighted and evaluated by looking at the advantages and disadvantages of each process. Further, heterogeneous catalytic oxidation for organic pollutants such as phenol in wastewater treatments is discussed in a greater depth as one of the efficient and economic wastewater treatment process. This chapter also reviews some cheap materials such as Activated Carbon, Fly ash, Natural Zeolite, ZSM-5, Red mud, Alumina and Silica which are widely used as catalyst supports in heterogeneous catalysis. Impregnation process of active metals on to a support material is also elaborated in this chapter.

2.1 Introduction

Based on the source, wastewater consists of domestic, industrial, public service and loss/leakage wastewater. Among them, the biggest contribution came from industrial and domestic wastewaters at 42.4% and 36.4%, respectively. Types of pollutants in the wastewater are suspended solids, biodegradable organic and priority pollutants such as carcinogeneous, pathogens, non-biodegradable organics and heavy metals [1]. Generally, the most reliable process to degrade the pollutants is through the conventional biological treatment. However, this process is relatively slow and for contaminants that are not biodegradable such as aqueous phenol solution, this method can not be applied [2]. On the other hand, phenol compound and its derivatives are the largest component existing in wastewater from industrial waste such as chemical, petrochemical and pharmaceutical plants which disposed of as effluent although it is prohibited due to environment contamination [3]. Because phenol is hazardous organic pollutant even at low concentrations such as 70 ppm or more, then wastewater treatment technology particularly organic compound treatment should be further developed [1].

Several methods of waste treatment which is widely used today for phenol removal are adsorption by using Activated Carbon (AC), thermal incineration and liquid phase chemical oxidation. The use of AC by adsorption method is very commonly used. Since AC has pores and large surface areas that can significantly remove phenol. However, AC can not exhibit complete removal of phenol through adsorption process [4]. Moreover, adsorption process using AC also needs extra planning and funding in regard to the regeneration and disposal of the adsorbent.

Other processes which are also widely used for removal of organic pollutants are incineration. With this process, organic contaminants can be destructed almost completely. However, the incineration of organic contaminants at temperatures between 1000 and 1700 ^{o}C will produce by products emissions into the environment in the form of dioxins and furans. Emissions of these chemicals have been proven to cause serious health problems to humans especially the workers around incineration plant unit [5, 6].

Further, another promising method is chemical oxidation. Complete removal of organic pollutants can be done well through this method while maintaining all of the components in the liquid phase. Liquid phase oxidation is influenced by several important factors such as type of oxidant, catalyst and selected operating conditions. In Wet Air Oxidation (WAO), the air can be used as an oxidant. Oxygen from the air can be dissolved in the system and assists the removal of organic pollutants through the process of oxidation at temperatures above 150 ^{0}C and a pressure of about 2 MPa [7-9]. The more effective process can also be obtained with a different oxidants such as hydrogen peroxide (H_2O_2)[10-12] or ozone (O_3) [13], but of course with a more additional cost.

However, for waste streams that have very small concentrations of pollutants, both inceneration and WAO becomes uneconomical to be implemented. Therefore, it required other waste treatment techniques such as Advanced Oxidation Process (AOP). Many techniques have been commonly used in AOP such as Fenton oxidation, UV-based technique and ozonation. Fenton oxidation is very effective, but at extremely low concentrations of pollutants, it also has limitations because the reaction rate is very slow and uneconomical utilization of the oxidants due to self-quenching. In order to be able to oxidize pollutants with very low

concentrations, it needs additional energy input which can come from UV-light or ozonation to achieve complete oxidation.

Furthermore, combining the use of oxidants with appropriate catalysts will reduce the use of high temperature and pressure in the oxidation process. Copper ion, for example, is a highly effective homogeneous catalyst to oxidize some organic pollutants by using the air as an oxidant [14]. Additionally, Fenton reaction that uses a combination of iron salts with hydrogen peroxide is also known as a very effective process to reduce various organic pollutants [15]. However, the use of homogeneous catalysts in the oxidation process causes other problems, because basically the catalyst metal ions are also a pollutant to water. So it will require additional processing to remove metal ions from water. Thus, a heterogeneous catalyst is quite promising to be adopted due to removal efficiency and no extra process to separate the catalyst from the system.

A lot of testings have been done to develop a heterogeneous catalytic system in degradation of organic pollutants. The used heterogeneous catalyst is generally coming from a noble metal and metal oxide with various combinations of oxidants. In laboratory-scale, many tests showed a pretty significant result in removing contaminants from wastewater. The main concern of this heterogeneous catalyst is the catalyst stability over sufficiently long time use. Several facts indicate that the catalyst has deactivation or loses active phase (active metal) from the catalyst structure. This could be caused by the leaching process [16], formation of carbonaceous deposits [17] and also catalyst sintering [18]. Another way to optimize the process of oxidation is through the application of external energy sources such as electrical or electrochemical [19, 20], radiation [21, 22] and ultrasound [23]. The process is quite successful at low flow rate and low effluent concentration at ambient conditions.

Furthermore, the effectiveness and efficiency of the pollutant removal should also be accompanied by economic processes. One that deserves attention is the use of a cheap and easy-to-obtain catalyst support. For that reason, the use of natural minerals and residual materials such as Activated Carbon (AC), Natural Zeolite (NZ), Fly Ash (FA), Red Mud (RM), Silica, Alumina etc. as a support impregnated with the active metal become very important to be developed.

2.2 Incineration

Incineration is the combustion process of pollutants by raising the system temperature up to 800 ^{o}C so that it is expected to form CO_2 and H_2O. Basic reactions that occur in this process are shown below [24].

$$R - H + O_2 \xrightarrow{\Delta} CO_2 + H_2O \quad 2.1$$

$$R - Cl + O_2 \xrightarrow{\Delta} CO_2 + H_2O + HCl \quad 2.2$$

$$R - N + O_2 \xrightarrow{\Delta} CO_2 + H_2O + NO_2 \quad 2.3$$

However, the combustion process is often not complete and produces exhaust gases other than CO_2 and H_2O such as HCl, SOx, NOx and Chlorine. These are toxic gases and must be removed from the waste effluent in range of permitted threshold before being discharged into the environment. Therefore, the incinerator must be complemented by air treatment equipment. In regard to this, various systems have been developed such as the rotary kiln incineration (for solid waste), liquid injection incineration, fluidized bed incineration, high temperature fluid-wall destruction, advanced electric reactor, infrared incineration, plasma pyrolysis, etc.

Although the technique is widely used and successful, the fact that the incineration process has serious health problems for the people around still remains. Because, the incineration units typically emit harmful substances such as fine particles, acid gases and aerosols, metal and organic compounds. Due to a lot of problems to the environment and health, some incinerators in the U.S. have been shutdown in recent years. Research shows that the impact on human health either carcinogenic or non-carcinogenic is mostly caused by fine particles such as cadmium, mercury, chromium and arsenic which are generated by this waste treatment unit [25].

Table 2.1 Organic compounds released from the Municipal Waste Incineration

Organic Products released during incineration at 680-1040 ^{o}C	***Concentration µg/m^3***
Formic Acids	500
Acetic Acid	2.5
Choloro Phenols	48
Formaldehyde	500
Acetaldehyde	500
PAH (Poly-aromatic Hydrocarbons)	5
Chlorinated Benzenes	20
Dioxins	0.038

Incineration of the organic contaminants such as chlorophenol has produced a number of toxic compounds into the air such as polychlorinated dibenzo-p-dioxins (PCDD). This compound is produced when process temperature is decreased to 500-600 ^{o}C from recommended temperature of 800-900 ^{0}C. The organic compounds that are released into the air from incineration process are shown in Table 2. 1.

2.3 Wet Air Oxidation (WAO)

It is well known that WAO is commonly used in the oxidation of organic contaminants. Currently there are more than 200 plants worldwide that use this process in wastewater treatment [27]. WAO involves waste water treatments at high temperature and pressure. During the process, organic compounds with high molecular weight split into a lower molecular weight such as formic acid, acetic acid, and aldehydes and subsequently further decomposed into CO_2 and H_2O. Oxidation mechanisms in parallel are shown in the following equation [28].

1) Direct oxidation to form carbon dioxide

$$R-H+O_2 \xrightarrow{k_1} CO_2 \qquad 2.4$$

2) Oxidation by intermediate compound

$$R-H+O_2 \xrightarrow{k_2} CH_3COOH \xrightarrow{k_3} CO_2 \qquad 2.5$$

The kinetic equation obtained from both direct oxidation and oxidation by formation of intermediate compound is given below [29]

$$\frac{[R-H+CH_3COOH]}{[R-H+CH_3COOH]_0} = \frac{k_2}{k_1+k_2-k_3} e^{-k_3 t} + \frac{k_1-k_3}{k_1+k_2-k_3} e^{-(k_1+k_2)t} \qquad 2.6$$

In principle, along the oxidation of organic compounds and the formation of the radical structure, there are 3 stages of the reaction: initiation, propagation and termination. These stages are shown in the following equations [30]. In each stage of the reaction, the oxidation of carboxylic acid controls the overall reaction rate due to its slowest reaction rate.

Initiation $$R-H+O_2 \rightarrow R^{\bullet} + HO_2^{\bullet} \qquad 2.7$$

Propagation $R^{\bullet} + O_2 \rightarrow RO_2^{\bullet}$ 2.8

$R - H + RO_2^{\bullet} \rightarrow ROOH + R^{\bullet}$ 2.9

Termination

$RO_2^{\bullet} + RO_2^{\bullet} \rightarrow ROOR + O_2$ 2.10

In this WAO process, organic substances contained in wastewater whether dissolved or precipitation will be oxidized by oxygen. The mentioned oxygen can be in the form of pure oxygen or air. Operating conditions are commonly at a relatively high temperature between 100 and 300 ^{o}C at pressures of 0.5-20 MPa. WAO can easily reach 90-95% conversion [31]. However, this is generally not sufficient to meet effluent requirements for waste disposal into the environment. Therefore, WAO usually must also be followed by biological treatment. Moreover, the existence of homogeneous catalysts in catalytic WAO process also has another issue that must be addressed and continued by additional treatment.

Chemical Oxygen Demand (COD) removal using WAO process can reach 75 to 90% depending on the oxidation of intermediate compounds that are formed during the process [28]. Alternative processes to improve COD removal can be done using Supercritical Wet Air Oxidation (SWAO), but with higher temperature and pressure at above 500 ^{o}C and pressures in the range of 20-50 MPa [32].

In some cases, the use of pure oxygen in the WAO can also improve the performance of the organic pollutant oxidation in wastewater. Several studies have shown that the use of pure oxygen produces higher removal efficiency and greater profitability than the use of air as an oxidant in the WAO [33].

In general, WAO is quite successfully to degrade a variety of organic pollutants in waste water. Table 2.2 presents various organic pollutants which were successfully removed using WAO processes [14, 28, 34, 35].

Table 2.2 Wet Air oxidation of various pollutants

Pollutants	Operating Temp ^{0}C	Operating Pressure MPa
Acetic Acid	270-300	2-20
Acetonitrile	275-320	1
Acetone	160-200	6.8-13.6
Butyric Acid	237-257	6.8-13.6
Black Liquor from Paper and Pulp unit	40-90	0.021 (P-O_2)
Diethanolamine	140-240	0.39-1.38 (P-O_2)
Formic Acid	300	1
Glucose	177-260	10.9
Morpholine	150-240	0.39-1.38 (P-O_2)
Nitriteacetic Acid	200-225	5-15.2
n-butanol	160-200	6.8-13.6
Oxalic Acid	227-288	2-20
Phenol	180-210	5.5-15.2
Propionic Acid	232-287	1.72-5.17 (P-O_2)
2-Chlorophenol	204-260	3.9-7.1
P-Cresol	150-200	3.9-7.1 (P-O_2)
Real Distillery Waste	150-210	0.1-2.5 (P-O_2)
Sec-butanol	160-200	6.8-13.6
Sewage sludge from paper industry	250-300	13
Tetrachloro ethylene	225	13.8

Some applications that have been implemented in the industry are also shown in Table 2.3 [11]. In general, the fundamental difference of WAO processes presented in the Table is related to the use of the reactor type and catalysts.

Tabel 2.3 Main Industrial Processes of Wet Air Oxidation

Process	Waste Type	Reactor Type	T (^oC)	P(MPa)	Catyst
Zimpro	Sewage sludge spent AC industrial	Bubble Column	280-325	20	none
Vertech	Sewage sludge	Deep Shaft	<280	<11	none
Wetox	ns	Stirred	200-250	4	none
Kenox	ns	Recirculation Reactor	<240	4.5	none
Oxyget	ns	Tubular Jet	<300	ns	none
Ciba-Geigy	Industrial	-	300	ns	Cu^{2+}
LOPROX[1]	Industrial	Bubble Column	<200	5-20	Fe^{2+}
NS-LC	ns	Monolith	220	4	Pt-Pd/TiO_2-ZrO_2
Osaka Gas	Coal Gasifier, Coke Oven, Cyanide, Sewage sladge	Slurry Bubble Column	250	7	ZrO_2 or TiO_2 with nobel or base metals
Kurita[2]	Ammonia	ns	ns	>100	Supported Pt

ns : not specified

[1] Organic Quinone substances was used to generate hydrogen peroxide

[2] Nitrite was used as an oxidant

As shown in Table 2.3 above, the use of heterogeneous catalysts in WAO process has also been done in the NS-LS, Osaka Gas and Kurita process. The interesting is that the third process uses temperature and pressure which are not much different from the WAO without heterogeneous catalysts. And they also use a noble metal catalyst which is relatively expensive. This reality is contrary to the fact that the laboratory-scale research has clearly proven that the use of noble metals as heterogeneous catalysts can run very well at room temperature and atmosphere pressure.

2.4 Catalytic Wet Air Oxidation

Several disadvantages which were found in the WAO especially inability to remove organic contaminants completely have become the main reason for the development of methods of Catalytic Wet Air Oxidation (CWAO). In fact, homogeneous catalysts are relatively more efficient than heterogeneous catalysts. However, the presence of homogeneous metal catalysts in the system resulted in another pollution problem in the water and requires further separation unit. Since most of the dissolved metal catalysts are toxic to the environment so that in many cases the separation of the catalyst technically or economically is not feasible to be implemented. In contrast, heterogeneous catalytic oxidation usually has some advantages such as operated at room temperature and normal pressure and high energy efficiency. Further, heterogeneous catalysts can also be synthesized using cheap material supports such as activated carbon, zeolite, fly ash, red mud, silica, alumina etc., and can be regenerated for reuse easily [36]. However, some limitations are shared by heterogeneous processes such as slow reaction due to limitation of mass transfer resistance, life time of the catalyst activity and catalyst damage.

In CWAO, the catalysts are usually made up of two main classifications: noble metal and metal oxide [37]. In the oxidation process, there are 5 stages between heterogeneous catalyst with involved reactants, the diffusion of the reactants on the catalyst surface, adsorption of reactants to the catalyst surface, the reaction on the catalyst surface, desorption of products from the catalyst surface and diffusion of products from the catalyst surface.

In most catalytic reactions, reaction kinetics depends on the molecular transport (diffusion and adsorption) of the reaction itself so that the development and modification of catalysts are required. Pollutant oxidation in the presence of a catalyst will follow redox mechanism as shown below [30]. The performance of the catalyst is related to the redox potential of the $Me^{n+}/Me^{(n-1)+}$ couple.

$$ROOH + Me^{(n-1)+} \rightarrow RO^{\bullet} + Me^{n+} + OH^{-} \quad 2.11$$

$$ROOH + Me^{n+} \rightarrow RO_2^{\bullet} + Me^{(n-1)+} + H^{+} \quad 2.12$$

Metal catalysts are generally a noble metal including Ru, Pt, Rh, Ir, and Pd [38]. The noble metal is usually loaded onto another metal oxide or supporting material to enhance the reactivity and stability of the catalyst. In certain cases the metal catalysts are also loaded onto a material that has the adsorption ability as activated carbon. Many studies have reported the effectiveness of the noble metal in the removal of organic pollutants such as phenol, carboxylic acids, ammonia, Kraft effluent etc., as summarized in Table 2.4.

The ability of noble metal oxidation of organic pollutants in the process varies depending on the type of oxidized pollutants. For example, with acetic acid, catalytic activity increases in the order Pd <Ir <Ru [39]. While in the oxidation of p-chlorophenol, removal capability of the catalyst increases in the order of Ru <Pd <Pt [40]. Other researchers have reported that the oxidation of polyethylene glycol at 200 ^{o}C the activity of nobel metals follows Ru = Rh = Pt> Ir> Pd [41].

Table 2.4 CWAO process using different noble metals.

Noble Metal	Support	Pollutant	T (°C)	P (MPa)	Ref.
Pt	γ-Al_2O_3	Phenol	>155	2	[42]
Pt, Ag	MnO_2/CeO_2	Phenol	>80	0.5	[43]
Pt-Ru	C	Phenol	>35		[44]
Ru	C, CeO_2/C	Phenol	>160	2	[45]
Pt	γ-Al_2O_3	Acetic Acid	>200		[46]
Ru, Ir, Pd, Ag	CeO_2, TiO_2, ZrO_2	Acetic Acid	200	2	[47]
Pt, Ru, Rh	TiO_2, CeO_2, C	Phenol/Acrylic Acid	170	2	[48]
Ru	CeO_2	Maleic Acid	>160	2	[49]
Ru	TiO_2	Succinic Acid	>150	5	[50]
Pt, Ru, Pd, Rh	CeO_2	Ammonia	>150	2	[51]
Pt-Ru	C	Trichoroethene	>90	>0.2	[52]
Pt	C	Carboxylic Acid	>20	>0.1	[53]
Ru	TiO_2, ZrO_2	Kraft Effluent	190	5.5	[54]
Pd	C	Ammonia	280	2	[55]
Ir	C	Butiric Acid	200	0.69	[56]
Ir	CeO_2, TiO_2, C	Ammonia	>150	1.5	[57]
Pt	C	p-chlorophenol	170	2.6	[58]

Noble metal supports also significantly determine catalyst activity. Many noble metal supports have been tested by various researchers, such as alumina, ceria, titania, zirconia, and others. Activated carbon which has high porosity is also used as a support material. In sewage Kraft treatment for instance, the surface area of the catalyst support proves as an important factor to increase the ability of the catalyst in the oxidation process. While in the process of phenol removal, dispersion of the active phase on the support material surface has become a significant impact in improving the performance of the catalyst. Furthermore, the deposition of noble metal on hydrophobic supports such as activated carbon is very effective to degrade volatile pollutants such as ammonia [55].

The other type of catalyst which is often used in CWAO either in pure form or mixed is metal oxide. For aqueous effluent, copper oxide is very widely used and become the study object of many researchers. For example, phenol has successfully oxidized using the Harshaw commercial catalyst, which consists of 10% copper oxide and alumina support [59, 60]. A commercial catalyst CuO/ZnO was also successful in oxidizing Formic Acid [61, 62]. Levec et al. combined Cu, Mn and La oxides with the support of Al_2O_3 and ZnO to oxidize acetic acid [63].

Table 2.5 Metal oxide based on CWAO

Oxide	Support	Pollutant	T (°C)	P (M.Pa)	Ref.
Cu/Cr oxides		phenol	>127	0.32	[74]
Cu/Cr/Ba/Al oxides		phenol	127	0.8	[75]
Co, Fe, Mn, Zn oxides	γ – Al2O3	phenol	140	0.9	[76]
CuO	γ – Al2O3	phenol	>120	>0.6	[77]
CuO	γ – Al2O3	phenol	140	0.9	[78]
Cu/Ni/Al oxides		phenol	140	0.9	[79]
CuO/ZnO/CoO	cement	phenol	>130	7	[80]
CuO/ZnO	γ – Al2O3	phenol	>105	>0.15	[81]
CuO	γ – Al2O3	phenol	>113	>0.44	[82]
CuO/CeO2		phenol	130	0.73	[83]
K –MnO2/CeO2		phenol	110	0.5	[84]
MnO2/CeO2		phenol	>80	>0.2	[85]
MnO2, Co2O3		phenol	>170	>1.3	[86]
CuO	C	phenol	>160	>2.6	[87]
MnO2, Co2O3		p-chlorophenol	>170	>1.3	[86]
CuO/ZnO	γ – Al2O3	p-chlorophenol	>105	>0.15	[88]
CuO/ZnO		formic acid	>200	4	[89]
Fe2O3		acetic acid	>252	>6.7	[90]
Cu/Mn/La	ZnO – Al2O3	acetic acid	>250		[90]
MnO/CeO		ammonia	263	1	[14]
MnO2/CeO2		alcohol distilery	>180	>0.5	[91]

The other commercial catalyst consisting of CuO, ZnO and γ-Al_2O_3 or CoO is very effective to degrade phenol and substituted phenols [64-67]. Furthermore, Hamoudi et al. reported that CeO/MnO catalysts can be effectively used in phenol removal [68, 69]. Similar to that, Chen et al. showed that the ratio of Mn/Ce mostly affects the efficiency in phenol oxidation [70]. In the phenol oxidation, activity of various metal oxides was also reported by Kochetkova et Al. with the following order: CuO> CoO> Cr_2O_3> NiO> MnO_2> Fe_2O_3> YO_2> Cd_2O_3> ZnO> TiO_2> Bi_2O_3 [71].

Next, some researchers showed that activated carbon has very good performance as a catalyst [72, 73]. Several tests based on metal oxide catalysts are shown in Table 2.5.

2.5 Chemical Oxidation

Chemical oxidation is a simple technique that uses a chemical oxidant to oxidize harmful chemicals in wastewater into harmless components. This technique is quite a lot used primarily for remediation of soil and groundwater, due to a simple application. A certain of chemical compounds are poured into waste water and serve as an oxidizing agent or better known as the oxidant. In general, the ability of the oxidation of chemical compounds against contaminants in the waste water is affected by oxidation reduction potential (redox) of each oxidant. Some frequently used oxidants with each potential redox standard are shown in the following table [92].

Table 2.6 Oxidation Potential of different Oxidants

Oxidants	**Redox Potential E^o (eV)**
Fluorine	3.03
Hydroxl radical	2.70
Sulphate Radical	2.60
Atomic Oxygen	2.42
Ozone	2.07
Persulphate	2.01
Hydrogen Peroxide	1.78
Permanganate	1.68
Chlorine Dioxide	1.57
Hypochlorous Acid	1.49
Chlorine	1.36

In general, the larger redox potential of the oxidant, the higher contaminant oxidation can be carried out. Some oxidants are very well known and have been widely applied in wastewater treatment include: Chlorine, Permanganate, Peroxide, Persulphate and Ozone. The use of chlorine as an oxidant in wastewater treatment is known as chlorination. Chlorine can destroy pathogenic organisms in water and is often used in drinking water treatment. However, the chorine has limited ability because it is only used by certain selective chemicals for mild oxidation process and can not be used in greater range of organic oxidation. The use of chlorine in high pollutant concentrations will stimulate the formation of intermediate compounds which are commonly harmful [93].

Another oxidant which is widely used in wastewater treatment, especially for organic compounds that cause color, taste and odor problems is potassium permanganate [94]. In the water, potassium permanganate will generate more than one type of active radicals which react with organic pollutants and turn them into harmless end products. Permanganate reactivity depends on the type of active radicals produced during

oxidation which was determined by the reaction conditions such as temperature and pH. Permanganate can form the following different reactive species in the waste solution.

$$MnO_4^- \xleftrightarrow{H^+} HMnO_4 \xleftrightarrow{H^+} H_2MnO_4^+ \xleftrightarrow{-H_2O} MnO_3^+ \qquad 2.13$$

Some researchers have reported the oxidation of benzene and alkyl benzene at pH greater than 2.5, oxidation is dominated by active species of MnO_4^- while at a pH less than 0.3, the active species of permanganate will be dominated by $HMnO_4$ [95, 96]. The disadvantage of this system is the formation of precipitation in form of magnesium oxide in end products which requires additional removal process [97].

Hydrogen peroxide is considered as an oxidant which has some advantages especially in its ability to produce hydroxyl radicals which is known as environmental friendly free radicals. Further, the oxidants can play as both oxidizing and reducing agents. In industry, hydrogen peroxide is widely used as an oxidant in the process of bleaching in textile industries as well as reducing permanganate to Mn^{2+}. Peroxide is also used to oxidize ferrous ion (Fe^{2+}) to ferric ion (Fe^{3+}) in the process involving the formation of active hydroxyl radicals, that has high ability to oxidize organic contaminants with high molecular weight in waste water. The oxidation reactions that can produce hydroxyl radical are known as advanced oxidation technique.

The next oxidant is potassium peroxydisulphate or better known as persulphate. This oxidant is commonly used in the processing of underground water and oxygen bleach in industry [98-100]. Persulphate has a high oxidation capacity with wider range of pH and able to generate highly active sulphate radicals ($SO4^{\cdot}$) at temperatures of 40-99 °C, as shown in the following equation [101].

$$S_2O_8^- \xrightarrow{\text{thermal}} 2SO_4^{\bullet} \quad 2.14$$

In the presence of divalent metal ions as active electron donor, such as Fe^{2+} ions, persulphate ion can be catalytically generated to sulphate radical at ambient temperature as seen in the equation below [102].

$$S_2O_8^- + Fe^{2+} \longrightarrow SO_4^{\bullet -} + Fe^{3+} + SO_4^{2-} \quad 2.15$$

Moreover, other popular oxidation process is ozonation which is involving ozone (O_3) compound. Reactivity of the process is higher than the process using peroxide and persulphate oxidants. In principle, the inclusion of ozone in the wastewater treatment process begins with the formation of ozone from oxygen (O_2) and bubbled into the waste water [103]. In the temperature range of 0-60 °C, ozone solubility is 10-15 times higher compared to oxygen [104]. Oxidation processes involving ozone can occur directly with ozone molecules or indirectly through the formation of hydroxyl radical. Usually direct ozonation process takes place at a pH less than 4, the combination of direct and indirect at a pH between 4 and 9 and indirect above pH of 9 [105]. The indirect process of hydroxyl radical formation in ozonation is shown in the following equation.

$$3O_3 + OH^- + H^+ \rightarrow 2OH^{\bullet} + 4O_2 \quad 2.16$$

2.6 Advance Oxidation Process

Advance Oxidation Process (AOP) in wastewater treatment or also known as Advanced Oxidation Technique (AOT) is an oxidation method of organic pollutants by generating active free radicals mostly hydroxyl radicals ($OH^{\bullet}$) in the liquid phase and convert them into end product of H_2O and CO_2 [106]. Hydroxyl radicals are the most powerful oxidants after florine.

The oxidation ability of hydroxyl radical on various organic contaminants is much faster than the ozone (O_3). Comparison between the hydroxyl radical with ozone in degrading different organic compounds is shown in Table 2.7 below [107].

Table 2.7 Comparison of rate constant for ozone and hydroxyl radical.

Organic Compound	**Rate constant (M^{-1} s^{-1})**	
	Ozone (O_3)	**Hydroxil radical ($OH^{\bullet}$)**
Benzene	2	7.8×10^9
Toluene	14	7.8×10^9
Chlorobenzene	0.75	4.0×10^9
Trichloroethylene	17	4.0×10^9
Tetrachloroethylene	<0.1	1.7×10^9
n-Butanol	0.6	4.6×10^9
t-Butanol	0.03	0.4×10^9

Compared with other oxidation techniques, AOP is relatively a new technology and thus it has a great potential to be explored in some aspects such as the type of oxidant, catalyst to activate the oxidant, the optimal reaction conditions and many others. More recently, there has been considerable research involving several oxidants, mostly a sulphate based oxidants for applications in AOP. Some combination of the wastewater treatment process of organic contaminants involves Fenton reagent, UV/H_2O_2, Modified Fenton reagent, UV/Ozone, Ozone/H_2O_2 technique also known as peroxone, TiO_2/UV and Co^{2+}/Oxone.

2.6.1 Fenton Reagent

Fenton reagent treatment involves the addition of hydrogen peroxide and iron ions into the wastewater treatment system. The reaction involves the generation of hydroxyl radicals as shown in equations below. The free radicals then become an agent in the oxidation process to degrade organic

compounds (Eq. 2.17 and 2.18) [108]. Many studies reported that the organic pollutant oxidation based Fenton reagent have successfully oxidize alcohol, ketones, phenols, chlorophenol, benzene, nitrobenzene, dichlorophenol and poly aromatic hydrocarbons which are also very difficult to be removed by other convensional treatments [109-114].

$$H_2O_2 + Fe^{2+} \longrightarrow OH^{\bullet} + OH^{-} + Fe^{3+} \quad 2.17$$

$$RH + OH^{\bullet} \longrightarrow R^{\bullet} + H_2O \quad 2.18$$

Generally, the reaction of free radical using Fenton reagent consists of 3 phases: Initiation in which the formation of active radicals, Propagation where additional formation of the active Radicals from the interaction and finally Termination which exhibits quenching of the active radical. Each stage takes place at varying reactions, as shown as an example in chlorophenol degradation in Table 2.8 below [115].

Table 2.8 Reaction involved in chlorophenol removal using Fenton Reaction

Reaction	**Rate constant (k $M^{-1}s^{-1}$)**
$Fe^{2+} + H_2O_2 \rightarrow Fe^{3+} + OH^{\bullet} + OH^{-}$	63
$Fe^{3+} + H_2O_2 \rightarrow Fe^{2+} + HO_2^{\bullet} + H^{+}$	0.01
$OH^{\bullet} + H_2O_2 \rightarrow HO_2^{\bullet} + H_2O$	2.7×10^7
$HO_2^{\bullet} \rightarrow O_2^{\bullet} + H^{+}$	1.58×10^5
$O_2^{-\bullet} + H^{+} \rightarrow HO_2^{\bullet}$	1×10^{10}
$OH^{\bullet} + Fe^{2+} \rightarrow Fe^{3+} + OH^{-}$	3.2×10^8
$HO_2^{\bullet} + Fe^{2+}(+H^{+}) \rightarrow Fe^{3+} + H_2O_2$	1.2×10^6
$HO_2^{\bullet} + Fe^{3+} \rightarrow Fe^{2+} + H^{+} + O_2$	3.1×10^5
$O_2^{-\bullet} + Fe^{2+}(+H^{+}) \rightarrow Fe^{3+} + H_2O_2$	1×10^7
$O_2^{-\bullet} + Fe^{3+} \rightarrow Fe^{2+} + O_2$	5×10^7
$OH^{\bullet} + OH^{\bullet} \rightarrow H_2O_2$	4.2×10^9
$HO_2^{\bullet} + HO_2^{\bullet} \rightarrow H_2O_2 + O_2$	8.3×10^5
$HO^{\bullet} + HO_2^{\bullet} \rightarrow H_2O + O_2$	1×10^{10}

$HO^{\bullet} + O_2^{-\bullet} \rightarrow HO^{-} + O_2$	1 x 10^{10}
$HO_2^{\bullet} + O_2^{-\bullet}(+H^{+}) \rightarrow H_2O_2 + O_2$	9.7 x 10^{7}
$OH^{\bullet} + p-chlorophenol \rightarrow (Cl)DHCD^{\bullet}$	~
$(Cl)DHCD^{\bullet} + Fe^{3+} \rightarrow Fe^{2+} + (Cl)benzendiols$	2 x 10^{10}
$OH^{\bullet} + (Cl)DHCD \rightarrow THB + Cl^{\bullet}$	~
$(Cl)benzenediols + Fe^{3+} \leftrightarrow Fe^{2+} + (Cl)semiquinones$	~
$THB + Fe^{3+} \rightarrow Fe^{2+} + (Cl)benzoquinones$	~
$THCD^{\bullet} + Fe^{3+} \rightarrow Fe^{2+} + THB$	7 x 10^{9}
$OH^{\bullet} + (Cl)benzoquinones \rightarrow MA^{\bullet}$	~
$OH^{\bullet} + THB \rightarrow (H)AA^{\bullet}$	~
$OH^{\bullet} + MA/(H)AA \rightarrow (H)AA^{\bullet}$	~
$MA^{\bullet}/(H)AA^{\bullet} + Fe^{3+} \rightarrow Fe^{2+} + MA/(H)AA$	1.2 x 10^{9}
$Fe^{3+} + \alpha(H)AA \rightarrow Fe^{3+} - organiccomplex$	~

$(Cl)DHCD^{\bullet}$ **- (chloro)dihydroxycyclohexadienyl radical**
THB – trihydroxybenzene
THCD – trihydroxycyclohexadienyl
MA – cic muconic acid
(H)AA – (hydroxylated) aliphatic acid

Although Fenton oxidation reaction is quite effective but some conditions often become constrain in this process. The first, the Fe^{2+}/H_2O_2 ratio, which influences the tendency of active hydroxyl radicals to react with the oxidant itself, thereby increasing the overall use of the oxidant amount. Therefore, the rate constant of hydroxyl radicals in the range of 10^{8}-10^{10} should be considered in designing the system reaction [105]. Research conducted by Beltran et al. on the Fenton oxidation suggested oxidation rate should be increased with increasing concentrations of H_2O_2 from 10^{-4} to 10^{-3} M and the amount of iron incorporated into the system in the 7.10^{-5} M [116]. The second, this system requires a low pH around 3 or lower. The tendency of pH increase in the system during the process will result in additional cost for pH control [117]. The third is the quenching of the hydroxyl radical caused by the large anion content of pollutants in waste water. This causes the removal efficiency decreased with reaction time.

Some studies reported that the removal of organic contaminants significantly decreases due to the presence of phosphate anions, chloride and nitrate in wastewater [118, 119]. And fourth is the precipitation of ferric ions due to uncontrolled pH of the solution so that the Fe^{3+} ions tend to merge into a complex oxide-hydroxide in the form of sediment that inhibits the regeneration of the ferrous ions.

2.6.2 UV/Oxidant System

To generate free radicals such as hydroxyl or sulphate radicals is not only by the addition of a chemical oxidant but also obtained by irradiating the solution using ultra violet light (UV-light). AOP is also often referred as photochemical Oxidation and is often used for the oxidation process in wastewater that has low Chemical Oxigen Demand (COD). The process generally also comprises initiation stage, propagation and termination. The reaction mechanism is shown below [120].

Initiation Reaction

$$H_2O_2 + h\nu \rightarrow 2OH^{\bullet} \qquad 2.19$$

Propagation Reaction

$$H_2O_2 + OH^{\bullet} \rightarrow HO_2^{\bullet} + H_2O \qquad 2.20$$

$$H_2O_2 + HO_2^{\bullet} \rightarrow OH^{\bullet} + H_2O + O_2 \qquad 2.21$$

$$HO_2^{-} + HO_2^{\bullet} \rightarrow OH^{\bullet} + OH^{-} + O_2 \qquad 2.22$$

Termination Reaction

$$OH^{\bullet} + HO_2^{\bullet} \rightarrow H_2O + O_2 \qquad 2.23$$

$$OH^{\bullet} + OH^{\bullet} \rightarrow H_2O_2 \qquad 2.24$$

This process also requires the use of H_2O_2 to obtain optimal generation of hydroxyl radicals. Some researchers suggest that at concentration of hydrogen peroxide of 0.01 M, some organo-halide compounds and atrazine were quite successfully oxidized [121-123]. Several other studies have tested this system with a variety of other organic compounds such as phenol, chlorophenol, dichlorophenol, nitro benzene, a major groundwater pollutant such as hydroxy phenyl acetic acid, and even actual industrial waste water [124-128]. The tests on UV/oxidant system in removal dichlorophenol with oxidants such as persulphate, peroxymonosulphate and hydroxide have been done by Anipsitakis et al [129]. According to this research, the removal efficiency followed the order of $UV/K_2S_2O_8 > UV/KHSO_5 > UV/H_2O_2$.

Besides, controlling the solution pH to optimize removal efficiency has to be noted. UV rays will be absorbed by humic acids containing in industrial waste. This absorption phenomenon will reduce the effectiveness of the UV to generate active radicals [130]. Humic acid is a major component of humic subtances which are found mainly in soil, peat, coal, many upland streams, dystrophic lakes, and ocean water. These compounds are produced from biodegradation of organic matters. It is not a single acid, but a complex mixture of many different acids containing carboxyl and phenolate groups. The humic acid structure is presented in the following Figure 2.1 [131].

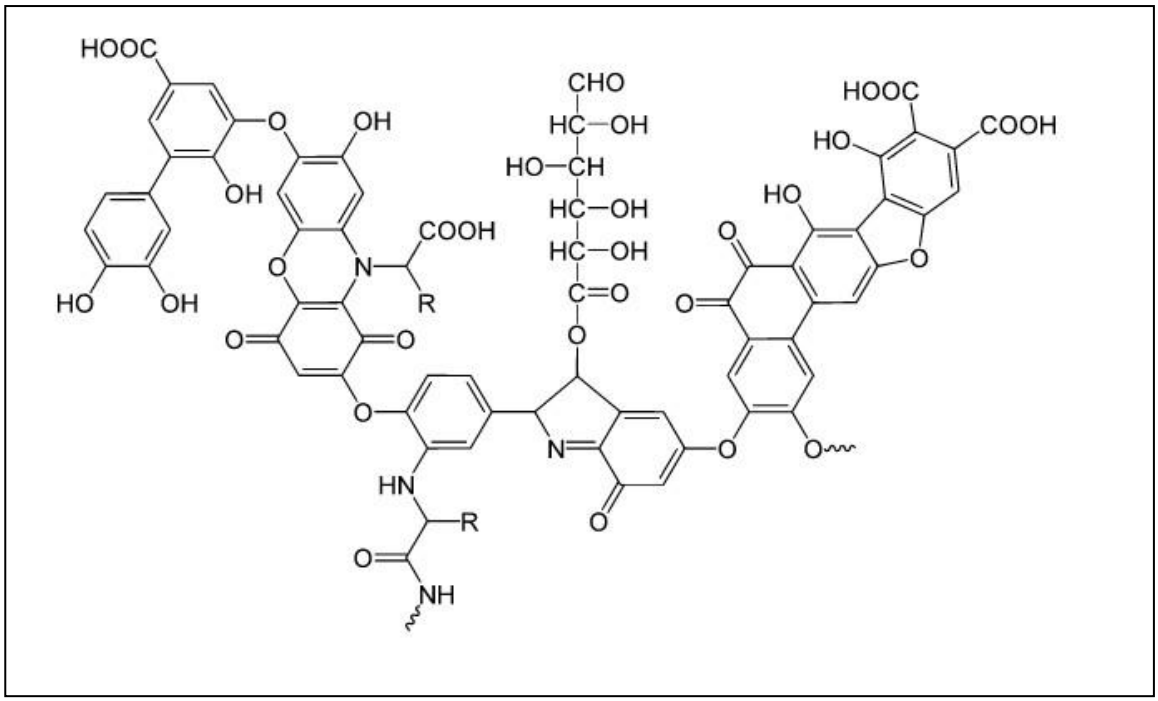

Figure 2.1 Humic Acid structure

Another oxidant which is well known and combined with UV in the application is ozone (O_3). UV/O_3 system has been widely used in waste water treatment especially the waste from the agro industry effluent. This system has the advantage of being able to take place at alkaline pH or in the pH which is relatively high [132]. In principle, wastewater solution saturated with ozone and then irradiation with UV-light radiation. In this process the wavelength of UV is important. By using a wavelength lower than 300 nm (under UV-C radiation), the formation of hydroxyl radicals can be seen in Eq. 2.25-2.27 below [133].

$$O_3 + H_2O \xrightarrow{h\nu} H_2O_2 + O_2 \qquad 2.25$$

$$H_2O_2 \xrightarrow{h\nu} 2OH^{\bullet} \qquad 2.26$$

As for the wavelength greater than 300 nm, the ozone molecule reacts with the peroxide to form hydroxyl radicals by the following reaction.

$$O_3 + H_2O_2 \xrightarrow{h\nu} OH^{\bullet} + HO_2^{\bullet} + O_2 \quad 2.27$$

2.6.3 Photo Fenton System

This system combines the Fenton reaction and UV/Oxidant system so that the benefit from both processes can be obtained. This combination will result in a more active radical than conventional Fenton Reaction and photochemical oxidation reaction their selves thereby increasing the reaction rate as well. Balcioglu et al. studied the degradation of textile dyes using photo Fenton reaction [134]. Under the influence of UV light, $Fe(OH)^{2+}$ ions obtained as a final product of Fenton reaction, absorbing radiation to change back into iron ions thereby increasing the rate of oxidation [135]. Several researchers reported their success in degradation of herbicides, nitro and di-nitro phenols, Anilines, toluene, Nitrotoluene, Atrizine, Effluent arising from dye industries, landfill leachate by Photo Fenton System. Interestingly, the sun (solar light) is quite effective as a light source replaces electrical power lamp [136-141]. By using this system dichlorophenol removal experiment with some combinations of active metal and oxidant removal efficiency was obtained in a sequence as follows: $UV/Fe^{3+}/H_2O_2 > UV/Fe^{2+}/H_2O_2 > UV/Co^{2+}/KHSO_5 > UV/Ag^{+}/K_2S_2O_8$ [129].

2.6.4 Photocatalytic System

Photocatalytic treatment is an excellent technique for the degradation of organic pollutant compounds with a high Total Organic Carbon (TOC) removal compared to other conventional techniques. This technique is based on the addition of catalyst into the liquid waste with illumination of UV radiation. This system can be conducted at neutral pH. In addition, this process also does not form by-product of complex sediment.

The reaction mechanism is based on the formation of active electron-hole pairs on the surface of the photocatalyst. When irradiated by UV on photocatalyst, the light photon promotes the electrons from the conduction band to the valance band. The amount of energy required to move the electron is equal to or more than the band gap energy of the photocatalyst. In the presence of contaminant molecules absorbed on the surface of the catalyst, the pollutant will also be oxidized by the electron transferred from the oxidative holes.

Many researchers have shown that a variety of halogenated compounds such as chlorophenols, nitrophenols, trichlorethylene, and toluene have been successfully removed by using both UV and combined photocatalyst/UV system [142-144]. Other researchers also reported the success of this system in reducing acids like salicyclic & t-cinnamic, dyes, and various biocalcitrant pesticides, and also actual industrial effluents and mixed pollutants [145, 146]. In the selection of catalysts for this system, some metal oxides such as TiO_2, ZnO, ZrO_2, SrO_2, CdS have been proven as effective catalysts [147]. In the oxidation of dyes, phenolic compounds and also for the treatment of groundwater pollutants, ZnO is reported to have a better removal efficiency of TiO_2, although both metal oxides have similar band gap of 3.2 eV [148-151].

It is well known that any additions to the system oxidants such as hydrogen peroxide treatment will increases the formation of active hydroxyl radical. Through a combination of oxidant with photocatalyst, the ability of the system to remove greater variety of organic wastes will also increase. Research conducted by Doong et al. who used a combination of H_2O_2/TiO_2/UV to degrade several pesticides reports that the surface of TiO_2 photocatalytic system can be activated optimally thereby the reaction rate is also increased [152]. Other researchers, Dhanalakshmi et al.

reported that peroxymonosulphate has higher capability than persulphate for dye degradation in the application of sulphate based oxidants such as persulphate and peroxymonosulphate and its relation to the use of TiO_2 as a catalyst [153].

AOP developments have led researchers to look for an alternative oxidant besides hydrogen peroxide which involved in conventional Fenton reaction. As an oxidant which has high standard of redox potential, the use of peroxymonosulphate based oxidant can become one of the alternative chemical that can be developed. Anipsitakis et al. reported reduction process of dichlorophenol and atrazine based on peroxymonosulphate oxidant in the presence of cobalt ions to generate active sulphate radicals. The mechanism of the reaction is shown in the following equation [154].

$$Co^{2+} + HSO_5^- \rightarrow Co^{3+} + SO_4^{-\bullet} + OH^- \quad 2.28$$

$$HSO_5^- + e^- \rightarrow SO_4^{-\bullet} + OH^- \quad 2.29$$

$$HSO_5^- + e^- \rightarrow SO_4^{2-} + OH^{\bullet} \quad 2.30$$

$$HSO_5^- \rightarrow SO_5^{-\bullet} + H^+ + e^- \quad 2.31$$

$$Co^{3+} + HSO_5^- \rightarrow Co^{2+} + SO_5^{-\bullet} + H^+ \quad 2.32$$

$$Co^{2+} + SO_4^{-\bullet} \rightarrow Co^{3+} + SO_4^{2-} \quad 2.33$$

$$RH + SO_4^{-\bullet} \rightarrow R^{\bullet} + HSO_4^- \quad 2.34$$

This technique is also used to oxidize a variety of other organic pollutants including dyes. The study proved that degradation of organic pollutants with various pH, the activity of Co/SO_4^- is higher than Fe/OH^-. It is also confirmed that the presence of UV in this system strengthenes the catalyst performance in reducing organic contaminant from wastewater.

2.7 Catalyst Support

Catalytic activity is determined by the chemical composition and some relevant physical properties. The catalyst support will also determine the effectiveness of a catalyst, as the characteristics of support material will affect catalyst properties. The catalyst support should be able to improve the mechanical properties of the catalyst. In many cases, a highly dispersed active phase can be stabilized by its deposition in the micropores of a support. Therefore, the catalyst support should be able to assist in the dispersion of the active phase to the surface of the support materials. The dispersion of active phase is defined as the ratio of the number of surface atoms of the active phase to the total number of atoms. This dispersion will determine the activity of a catalyst in the reaction process. For this purpose, proper preparation of catalysts is necessary. In general, the material as catalyst support must have certain characteristics such as inertness, mechanical properties (attrition resistance, hardness, compressive strength and flow resistance in packed bed), stability under reaction's conditions, porosity (average pore size, pore radius distribution) and surface area [155]. In many catalytic applications, carbon meets the above criteria as a catalyst support. Several other materials feasible in trials as support material are fly ash, redmud, zeolite, alumina, silica, etc.

2.7.1 Activated Carbon

Activated carbon is a crude form of graphite with a random or amorphous structure, which is very porous. It has a visible range of pore sizes from visible cracks, crevices and slits of molecular dimensions. Powdered activated carbon was first produced commercially in Europe in the early 19th century, using wood as a raw material. The use of activated carbon

for water treatment in the United States was first reported in 1930, for the removal of taste and odor of contaminated water. Activated carbon can be made out of coconut shell, wood char, lignin, petroleum coke, bone char, peat, sawdust, carbon black, rice bran, sugar, peach pit, fish waste, fertilizer, waste rubber tires, etc. [155]. Further, activated carbon has absorbing properties due to some factors such as highly surface area, micro-porous structure and high degree of surface reactivity.

Preparation of activated carbon can be done physically or chemically so that carbon particle is filled by hole and increased pore volume and surface area. In the activation process, the space between the elementary crystallites is cleared through removal of less organized loosely bound carbonaceous material resulting channel in the graphitic regions and also space (voids) between the elementary crystallites with fissures within and parallel to the graphite planes producing larger porous structure on carbon.

The physical activation process involves the carbonation stage at temperature of 500-600 °C to remove the volatile matters from carbon pore structure. Further, it is also made partial gasification using mild oxidizing gases such as CO_2, steam or fuel gas at 800-1000 °C. This process will Increase porosity and surface area of the raw carbon. On the other hand, the chemical activation involves inorganic chemical additives such as zinc chloride ($ZnCl_2$) or phosphate acid which was added to the precursor followed by a carbonization process at temperature range of 200-800 °C. Many other chemical compounds can be used for carbon activation such as ammonium salts, borates, calcium oxide, ferric and ferrous compounds, manganese dioxide, nickel salts, hydrochloric acid, nitric acid and sulfuric acid, etc. [156].

One gram of activated carbon can have a surface area between 500 m^2 to 2000 m^2. Due to its high porosity, activated carbon is then widely used as a catalyst support. Adsorption using activated carbon has proven to be one of the most effective and reliable physicochemical wastewater treatment methods. If carbon is used as a catalyst then the most decisive factor is the chemical composition of the active phase which dispersed on to the surface of the carbon [157].

Even today, AC without adding any active phase has also been used for the degradation of phenol. The most important conclusion made by some researchers, the oxidation of phenol on activated carbon occurs through the formation of a carbonaceous layer on the surface of activated carbon. In the oxidation processes, the AC surface functional groups oxidise the substrate and are consequently reoxidised by oxygen in a redox cycle and forming the initial formation of organic deposit coke from the initial oxidation on the AC surface. The measurements of the total micropore surface area indicated that the formed coke layer completely blocked the micropores of AC. It was also reported that during the process of Wet Air Oxidation Catalytic over Activated Carbon, it is not possible to balance the total carbon mass over the liquid and gas phase. Phenol removal is required relatively low activation energy of 40 kJ/mol compared the activation energy of 50 kJ/mol for phenol oxidation using, for instance, cuprous chloride [158].

In some cases, the carbon impurities can poison the catalyst. Most metals, such as iron, zinc and copper, contained in the mineral substance of the precursor material, are catalyst poisons. How ever, these obstacles can be overcome by special treatment or by using commercial pure carbon such as activated carbon as a catalyst precursor to generate support. Several techniques were performed on AC particles such as extrusion and

pelleting to increase uniformity in morphology and mechanical strength. This will provide a suitable carbon-based catalyst for fixed and fluidized beds.

2.7.2 Fly Ash

Fly ash is a residue of solid waste generated from coal, oil, and burning biomass. It is well known that the main components of fly ash are SiO_2 and Al_2O_3 which were produced after the combustion process at high temperature so that the two oxides have a very high thermal stability. In addition, other minor components of metal oxides containing in the fly ash are Fe_2O_3, TiO_2 CaO, MgO, K_2O, and Na_2O. The contents of metal oxides in the fly ash have made fly ash as a good catalyst or catalyst support. In the catalytic reaction, the alkali and alkaline earth metals will serve as promoters and transition metal components will be in the active phase. Further, it should be noted that fly ash also contains some elements such as Hg, which can be released during the use of fly ash and cause secondary pollution. Several investigations have found that Hg content in fly ash is relatively low, varying from 0.007 to 0.64 mg/kg depending on the source of coal and combustion conditions [159]. Also, some leaching tests on the fly ash showed the slightrelease of Hg into the air or water, and under certain conditions fly ash can also absorb Hg from the air [160]. Morphology and some of the main contents of the fly ash are shown in Figure 2.2 [161].

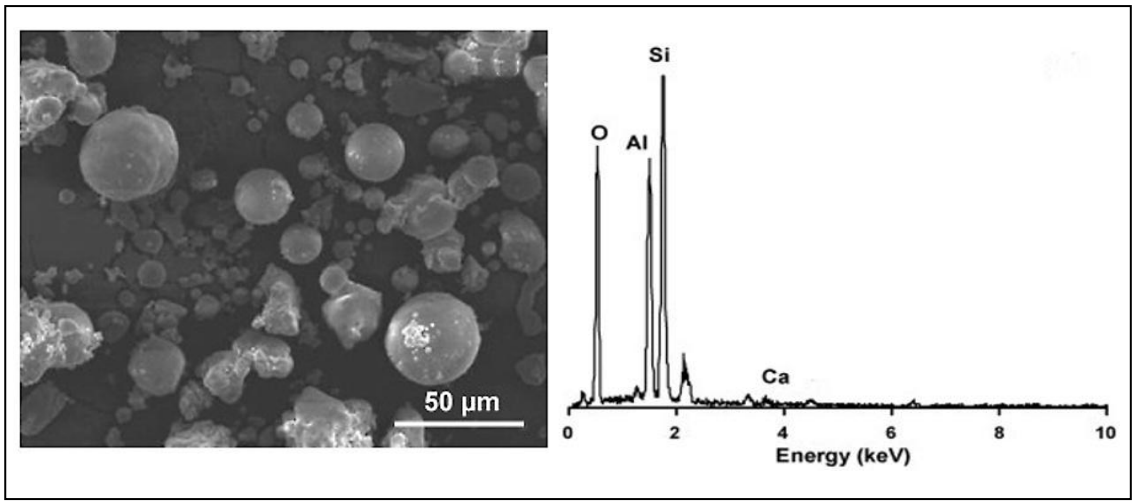

Figure 2.2 SEM Image and EDX analysis analysis of flyash particles

A large amount of fly ash is produced from power plants around the world every year. It is estimated that the world production of fly ash in 2003 was about 430 Mt and will continue to grow up in the future [159]. During this time, the large amount of fly ash has become an issue that could harm the environment. The fly ash disposal is usually dumped to the sea or into the trash, and fly ash derived from the industrial process and metal leaching, and contaminated organic compounds will pollute ground and surface water. Moreover, fly ash particles in the air are also a potential to disrupt human health. The huge production fly ash is also required maintenance and the use of spread land which will impact to economical cost for a long term. Because of the above reasons, reuse of fly ash to be a valuable product should be continued and developed.

The data show that the reuse of fly ash into value-added products has increased in the last two decades. For example, some applications have used fly ash as building and construction materials such as cement, geopolymer, ceramic materials, soil amendment, zeolite synthesis, a low-cost adsorbent for gases and water purifier, nuclear waste stabilization, and material recovery. However, the reuse of fly ash in the civil

engineering field is not able to keep the rate of fly ash regeneration. Worldwide fly ash recycling is estimated only about 25% of the generated fly ash each year, so that fly ash disposal into the sea or other landfills places still occurred. In Australia, less than 10% of fly ash was used in 2003. Compared with other countries, Australia has the lowest rate of utilization of fly ash so more work is needed to explore the recycling of fly ash [162].

Basically, fly ash is a heterogeneous material with various physical, chemical, and mineralogical properties depends on the mineralogical composition of burned coal and the combustion technology. Currently, the classification of fly ash is based on the content of CaO. Two classes of fly ash are defined by ASTM C618, the class F and class C. Class C fly ash refers to having more than 8% CaO and usually from lignite and subbituminous coal combustion. Class F fly ash derived from bitumen and anthracite coals and contain less than 8% CaO. Fly ash from subbituminous and lignite has high levels of CaO and MgO, but contains SiO_2 and Al_2O_3 lower than bituminous coal fly ash. Fly ash particles are generally spherical with a size of 0.5 to 100 μm. Particle size distribution is important for the properties of fly ash, because the smaller particles will have a larger surface area and affect the interaction of fly ash with a variety of solutions to mobilize every element on the surface of the particles. Many studies showed a bimodal particle size distribution of fly ash, with a major peak in the particle size between 0.1 and 1 am and the other with a particle size greater between 10 and 200 μm [163].

Table 2.9 Conversion of Fly Ash supported catalysts in reactions.

Reaction	Catalyst	Temperature (^{0}C)	Conversion (%)
Methane reforming	Ni/FA	700	29.1
	Ni/FA-HNO_3	700	2.3
	Ni/FA-NH_3	700	50.7
	Ni/FA-$Ca(OH)_2$	700	54.7
	Ni/FA-CaO	700	74.6
NO Reduction	Fe/FA	450	90
	Cu/FA	300	90
	Ni/FA	350	70
	V/FA	350	90
NO Reduction Aqueous dye oxidation hydrocracking	TiO_2/FA	Room Temp.	90
	FA-ZY	Room Temp.	100 (2 hours)
	Ni/FA-ZY	320	30
		320	60

FA : Fly Ash, ZY : Zeolite Y

Catalytic activity of the fly ash is highly dependent on the active components which are loaded onto the surface with some metal oxides such as Al_2O_3, SiO_2, TiO_2, and MgO and also their interaction with the catalyst support. Many studies have shown that fly ash supported catalysts showed high activity in the CO_2 reforming of methane, ammonia decomposition, catalytic reduction of NOx and SOx, methane oxidation, dye decomposition, and petroleum hydrocracking. Table 2.9 shows some of the reactions and the activities of fly-ash supported catalyst systems [163].

2.7.3 Natural Zeolite

Zeolites (consisted of corner-sharing AlO_4 and SiO_4 tetrahedral) are crystalline alminosilicate containing pores and cavities of molecular dimension. Many of them can be found as natural minerals but synthetic

zeolites are also widely used. Zeolites are also porous on a molecular scale, their structures revealing regular array of channels and cavities, creating a nanoscale labyrinth which can be filled with water or other guest molecules. The resulting molecular sieving ability has enabled the creation of new types of selective separation processes such as ion exchange, molecular sieving, catalysis and sorption. SEM image and XRD pattern of natural zeolite (clipnotilolite) can be seen below [164].

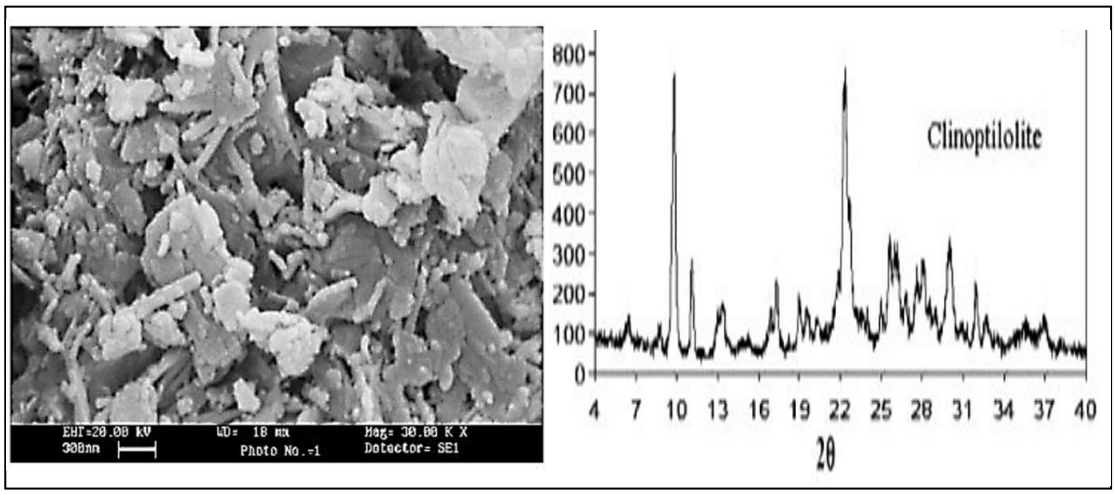

Figure 2.3 SEM Image and XRD Pattern of natural zeolite (clipnotilolite)

Further, zeolites are one of the most important heterogeneous acid catalysts used in industry. Their key properties are size and shape selectivity, together with the potential for strong acidity. Zeolites also have ion exchangeable sites and highly hydrothermal stability. Because of the properties of zeolite and its availability in abundance throughout the world, the use of natural zeolite in environmental pollution control is always interesting to be studied. The use of natural zeolite in water and water treatment for instance, is always promising a new technique in their utilization.

Table 2.11 Structural properties of some natural zeolites.

Zeolite	**Chemical formula**	**Struct. type**	**Symmetry, space group**
Clinoptilolite	$(K_2, Na_2, Ca)_3Al_6Si_{30}O_{72}\cdot 21H_2O$	HEU	Monoclinic, C2/m
Mordenite	$(Na_2, Ca)_4Al_8Si_{40}O_{96}\cdot 28H_2O$	MOR	Orthorhombic, Cmcm
Chabazite	$(Ca, Na_2, K_2)_2Al_4Si_8O_{24}\cdot 12H_2O$	CHA	Rhombohedral or triclinic P1
Phillipsite	$K_2(Ca, Na_2)_2Al_8Si_{10}O_{32}\cdot 12H_2O$	PHI	Monoclinic, $P2_1/m$
Scolecite	$Ca_4Al_8Si_{12}O_{40}\cdot 12H_2O$	NAT	Monoclinic,Cc
Stilbite	$Na_2Ca_4Al_{10}Si_{26}O_{72}\cdot 30H_2O$	STI	Monoclinic, C2/m
Analcime	$Na_{16}Al_{16}Si_{32}O_{96}\cdot 16H_2O$	ANA	Cubic Ia3d
Laumontite	$Ca_4Al_8S_{16}O_{48}\cdot 16H_2O$	LAU	Monoclinic, C2/m
Erionite	$(Na_2K_2MgCa_{1.5})_4Al_8Si_{28}O_{72}\cdot 28H_2O$	ERI	Hexagonal $P6_3/mmc$
Ferrierite	$(Na_2, K_2, Ca, Mg)_3Al_6Si_{30}O_{72}\cdot 20H_2O$	FER	Orthorhombic, Immm Monoclinic, $P2_1/n$

Many types of natural zeolites have been identified throughout the world such as clinoptilolite, mordenite, phillipsite, chabazite, stilbite, analcime, laumontite, offretite, paulingite, barrerite and mazzite. Among the natural zeolite, clinoptilolite is the most abundant and widely used for various applications. In the structure of the zeolite, there are 3 main components: the aluminosilicate framework, exchangeable cations, and zeolitic water. The general chemical formula of zeolites is $Mx/n[AlxSiyO2(x+y)]\bullet pH_2O$ where M is (Na, K, Li) and/or (Ca, Mg, Ba, Sr), n is cation charge; y/x = 1–6, p/x = 1–4. The structural properties of some natural zeolites are presented in Table 2.11 [165].

In the past, the use of natural zeolite was focused on removal of ammonium and heavy metal due to the nature of the ion exchange characteristics on zeolites. But lately a lot of natural zeolites have been

modified for the purpose of removal of anions and organic compounds in water and wastewater. Most applications of anions and organic compounds degradation in waste water using modified natural zeolite is involving adsorption process. Adsorption is considered as the most economical way due to low cost, simplicity of design, ease of operation and insensitivity to toxic substances. Further, due to the nature of its ion exchange, natural zeolite showed high performance in the absorption of cations in aqueous solution such as ammonium and heavy metals.

However, these materials are not good adsorbents for adsorption of anionic ions and organics so that it is required a certain modifications to the zeolite for the removal purpose of these components. Organic pollutant removal process by using natural zeolite has also been used extensively like dye adsorption, humic substance adsorption, and other organic compounds which are more toxic such as phenolic compounds, petroleum, surfactants, pesticides, and pharmaceuticals, from various industrial wastes. However, for toxic organic compounds, it should use surfactant modification of zeolite.

In addition, natural zeolite was also quite successfully used for humic substance degradation. Humic substances such as humic acid, fulvic acid or humin are mostly resulting from the natural process of decay. The presence of humic substance in surface water and groundwater will produce a toxic chemical during the disinfection process and it should be eliminated. Many techniques have been developed to remove humic substance including the use of natural zeolite adsorption. These researches reported that natural zeolites can also be good adsorbent for humic substance. The adsorption capacity would be depended on the structure and chemical composition of the natural zeolite. Table 2.12

shows the adsorption capacity of natural zeolite in some dye removal [165].

Table 2.12 Dye adsorption on natural zeolite.

Material	Dye	Adsorption (mg/g)
Clinoptilolite	Methylene blue	19.9
Clinoptilolite	Rhodamine B	12.4
Clinoptilolite	Malachite green	19.7
HTAB-clinoptilolite	Reactive black 5	60.6
HTAB-clinoptilolite	Reactive red 239	111.1
HTAB-clinoptilolite	Reactive yellow 176	88.5
CTAB-clinoptilolite	Reactive black 5	12.1–12.9
CTAB-clinoptilolite	Reactive red 239	11.0–15.9
Clinoptilolite	Basic red 46	8.6
HTAB-clinoptilolite	Reactive yellow 176	13.2
CTAB-clinoptilolite	Reactive yellow 176	5.5
Clinoptilolite	Toluidine blue O	33.0–58.7

Li and Bowman reported the adsorption of non-polar organic compound such as perchlorethylene (PCE) and the HDTMA using modified natural zeolite. They also tested the adsorption of ionized organic solutes, benzene, phenol and aniline on natural zeolite [166]. Research shows that the uptake of phenol on natural zeolite is strongly influenced by the pH of the solution. Further, various other researchers reported their research work on the use of natural zeolite to remove organic compounds such as toluene, o-xylene, and naphthalene benzene, toluene, phenol and of water through the adsorption process [167, 168]. Unfortunately this process can not completely degrade organic compounds from the water.

2.7.4 Zeolite ZSM-5

ZSM-5 is a zeolite that has a high silica content with the framework code of MFI that has a channel dimension of [100] 10 5.1x5.5 ↔ [010] 10 5.3 x 5.6 ***. The ratio of silica to alumina in the zeolite ZSM-5 is over 25. These zeolites have three dimensions of the channel which is indicated with three numbers of asterisks and also the bold numbers indicating the number of T-atoms. Further, in MFI channels it can also see the presence of double arrows which indicate the interconnecting channel system [169]. Fig. 2.4 shows the structures and morphology of ZSM-5.

ZSM-5 is often used as a catalyst in petroleum refining and petrochemicals for cracking, hydrocracking, isomerization, alkylation and reforming reaction. The morphologies and properties of ZSM-5 are related to crystalline structure, high internal surface area, uniform pore and good thermal stability resulting in the high selectivity and efficiency. Several variables such as silica and alumina sources, the alumina content, the template/silica ratio, the characteristics of cations in the synthesis mixture, crystallization temperature etc influence the crystallization process [170].

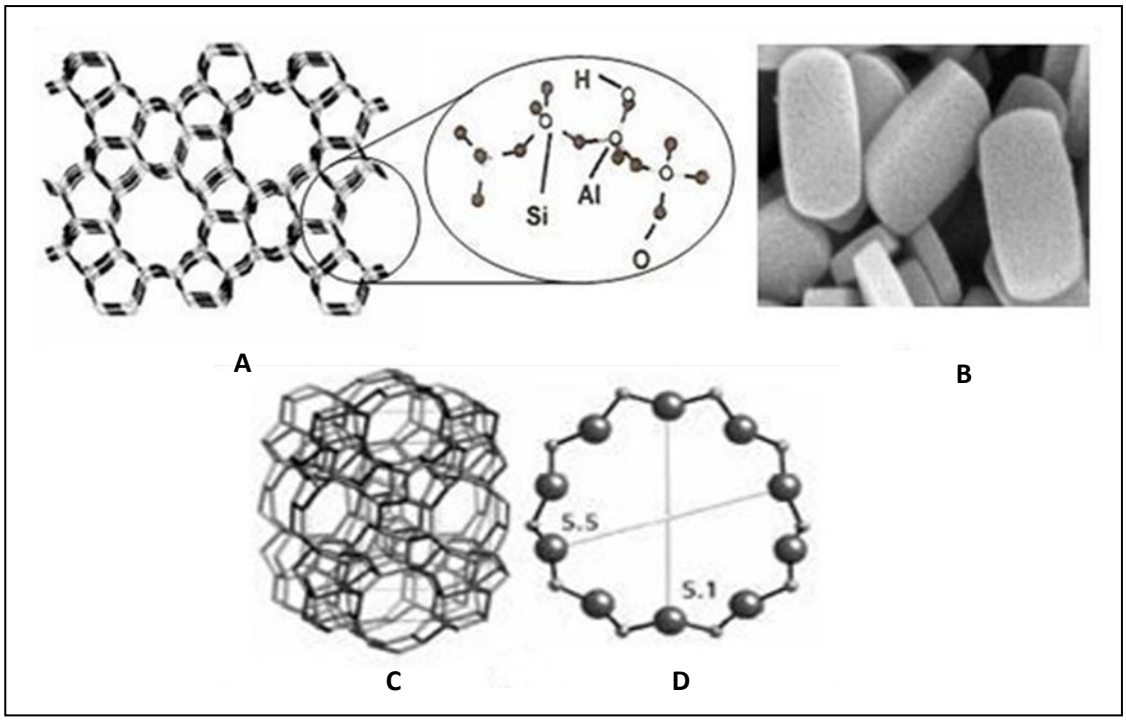

Figure 2.4 Zeolite ZSM-5 structures: (A) Part of ZSM-5 structure, (B) Crystal morphology of ZSM-5, (C) MFI Framework and (D) Channel Dimension

The crystallization mechanism of ZSM-5 was reported by Grieken et al. ZSM-5 crystals are formed in two stages. The first stage is solid-solid transformation of amorphous solid in homogeneous supersaturated solution. This amorphous solid is then becoming agglomeration and zeolitization until formation of the nanocrystalline ZSM-5. In the second stage, the initial solution which is less saturated in silicon and aluminium due to their consumption in the first stage, has nucleation process and transformed into zeolite. The second stage is running slowly compared with the first stage [171].

2.7.5 Red mud

Red mud is red sludge generated from waste in the bauxite processing which is the most common aluminum ore. The main components of red mud contain Fe_2O_3, Al_2O_3, SiO_2, TiO_2, Na_2O, CaO, MgO and a small number of constituents such as K, Cr, V, Ni, Cu, Mn, Zn, etc. Generally, iron oxide (Fe_2O_3) is the main constituent of red mud and gives the characteristic of brick red. In addition, the rich content of alumina has also allowed red mud to be reprocessed to produce alumina. Various mineralogical constituents were identified by X-ray analysis of the red mud between hematite (α-Fe_2O_3), gutit (FeOOH), iron hydroxide ($Fe(OH)_3$), magnetite (Fe_3O_4), rutile (TiO_2), anatase (TiO_2) , bayerite ($Al(OH)_3$), halloysite ($Al_2Si_2O_5(OH)_4$), boehmite (ALO (OH)), diaspore (ALO (OH)), gibsit ($Al(OH)_3$), kaolinite ($Al_2Si_2O_5(OH)_{4)}$, quartz (SiO_2), calcite ($CaCO_3$), perovskite ($CaTiO_3$), Sodalite ($Na_2OAl_2O_3$ $1.68SiO_2$ $1.73H_2O$), cancrinite ($3NaAlSiO_4$ • NaOH), whewellite (CaC_2O_4 • H_2O), katoite ($Ca_3Al_2SiO_2(OH)_{12}$), gypsum (CaSO4 • $2H_2O$), etc. [172].

Further, red mud has low surface area with fine particle size distribution. Red mud has specific BET surface area in the range of 20-30 m^2/g depending on the preparation method. Red mud surface area can be increased substantially by using multiple methods of treatment as shown in Table 2.13 [172].

Table 2.13 Surface area of red mud following treatments.

No	Surface area before treatment (m^2/g)	Surface area after treatment (m^2/g)	Surface area increase (%)	Treatment
1	64.0	155.0	1.42	ARM[a]
2	25.5	184.1	6.21	ARM[a]
3	29.4	60.7	1.06	ARM[a]
4	24.3	82.4	2.39	ARM[a]
5	24.3	85.4	2.51	SARM[c]
6	24.3	29.5	0.21	SRM[c]
7	28.3	131.1	3.63	ARM[a]
8	28.3	111.7	2.94	PARM[b]

a ARM-HCl activated red mud, b PARM-HCl + H_3PO_4 activated red mud,
c SRM-Sulphided red mud.

Further, Australia is one of the world's largest producers of red mud. Many applications of water and waste water treatment have used redmud as an adsorbent such as phenol removal from the aqueous phase and heavy metal removal, nitrate removal, phosphate removal, color dye removal and others. Red mud is generally highly alkaline with a pH between 10 and 12. This nature causes red mud highly caustic and is considered as hazardous to the environment and it should be neutralized. Iron oxide (Fe_2O_3) as the main component red mud, at high temperature of 400-850 ^oC will be gradually reduced to be Fe. The reaction stages are presented below [172].

$$3Fe_2O_3 + H_2 \rightarrow 2Fe_3O_4 + H_2O \quad 2.35$$

$$Fe_3O_4 + H_2 \rightarrow 3FeO + H_2O \quad 2.36$$

$$FeO + H_2 \rightarrow Fe + H_2O \quad 2.37$$

$$3Fe_2O_3 + 9H_2 \rightarrow 6Fe + 9H_2O \quad 2.38$$

SEM image and XRD pattern of red mud are shown in Figure 2.5 [173].

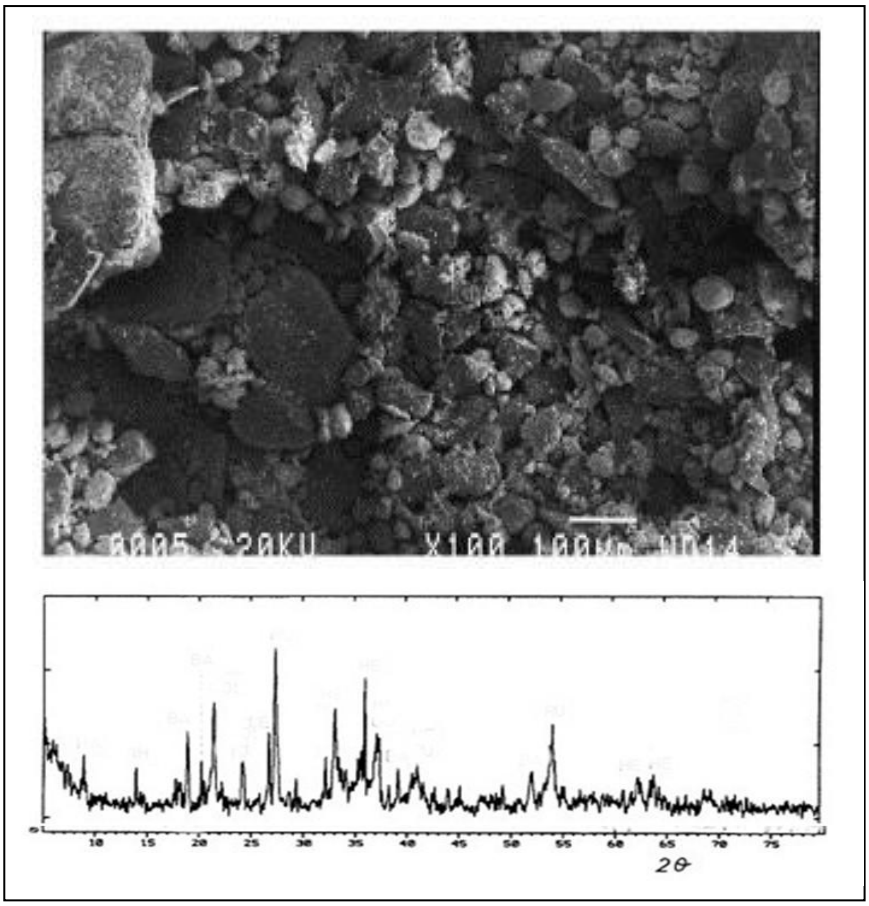

Figure 2.5 SEM image and XRD pattern of red mud.

2.7.6 Alumina

Alumina is also a material that is widely used as a catalyst support because of relatively inexpensive and has good thermal stability, high surface area and porosity and enough availability for many catalytic applications. The texture of alumina is influenced by many factors. The predominant phase is believed to have important effects to determine surface area and porosity. Generally, the porosity will increase when the surface area increases. Some types of alumina with lattice geometry of α, η, γ, θ, λ, δ etc. have long been known. Among the various types of alumina, α-alumina is reported to be the most stable type of alumina.

The following scheme (Fig. 2.6) shows the calcinations of boehmite and pseudo-boehmite for α-Al_2O_3 formation [174]. SEM image and XRD pattern of alumina are shown in Figure 2.7 [175].

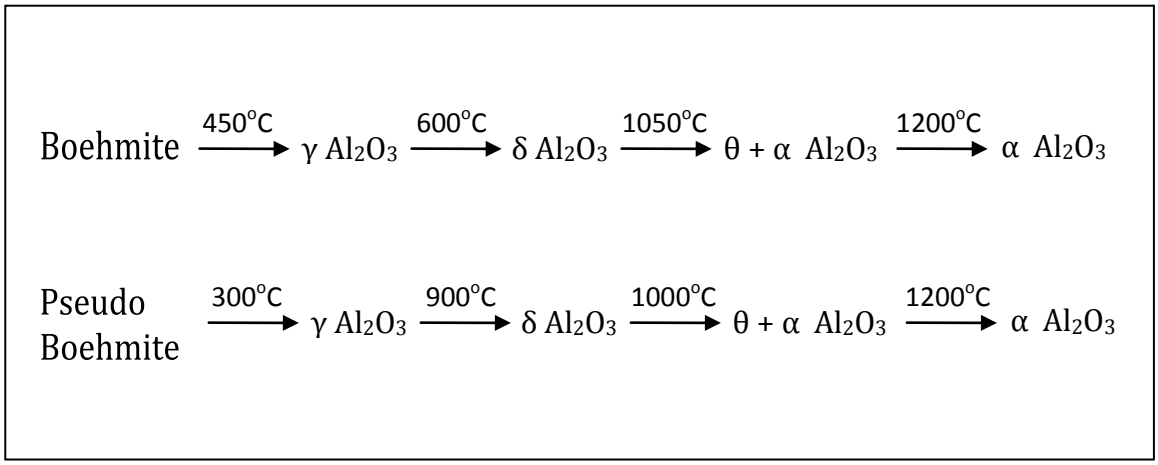

Figure 2.6 Calcination Process of boehmite and pseudo-boehmite

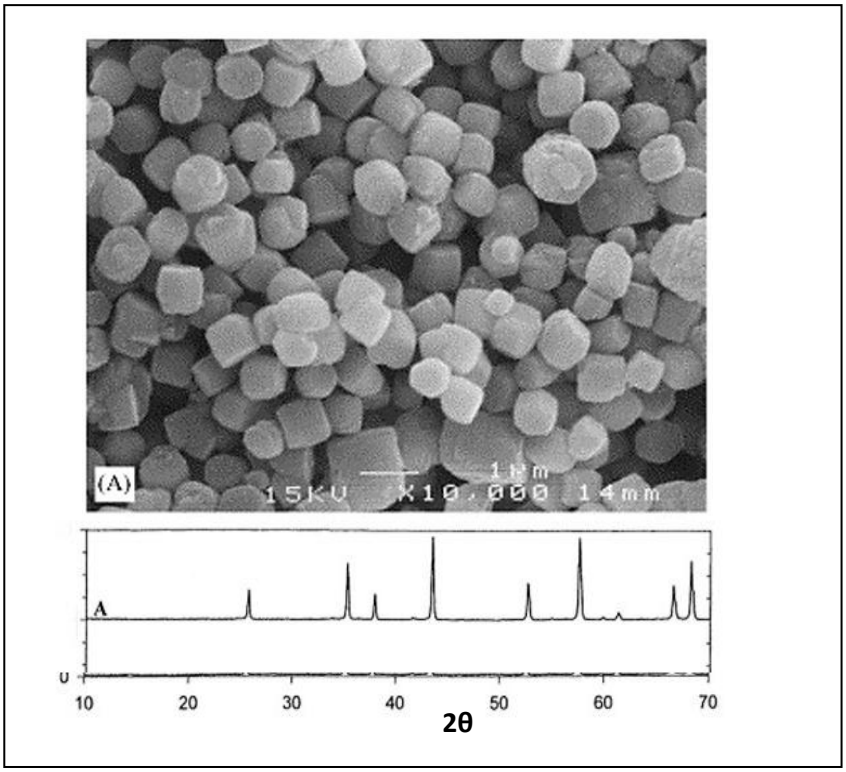

Figure 2.7 SEM image and XRD pattern of α-alumina.

2.7.7 Mesoporous Silicas

Mesoporous silicas such as MCM-41 and MCM-48 are sintetic materials developed by Mobil group and become popular as a research object particularly as a catalyst support. The high surface area owned by MCM-41 and MCM-48 allowing a large number of highly dispersed active sites within the material framework is the main reason for the widespread use of these materials. MCM-41 with a 2-D hexagonal structure and MCM-48 with a 3-D cubic structure can be disynthesised using n-alkyl ammonium salts as templates. Hydroxyl clusters contained their surface structure is an important characteristics which determines the performance of materials such as adsorption, surface modification, wetting and others. The particle porosity and pore wall thickness of MCM-48 is higher than MCM-41 [176].

MCM-48 material is more attractive with the three-dimensional structure and interconnected channels, providing advantages in more rapid diffusion and resistance to pore blocking of molecules coming compared with the two-dimensional pores of MCM-41. The characteristics such as long-range order, large surface area, and narrow pore size distribution make the MCM-48 widely used as adsorbent, catalyst and catalyst support, sensors, as well as an inorganic template for the synthesis of advanced nanostructure. Figure 2.8 presents the X-ray pattern and morphology images of MCM-48 and MCM-41 [177, 178].

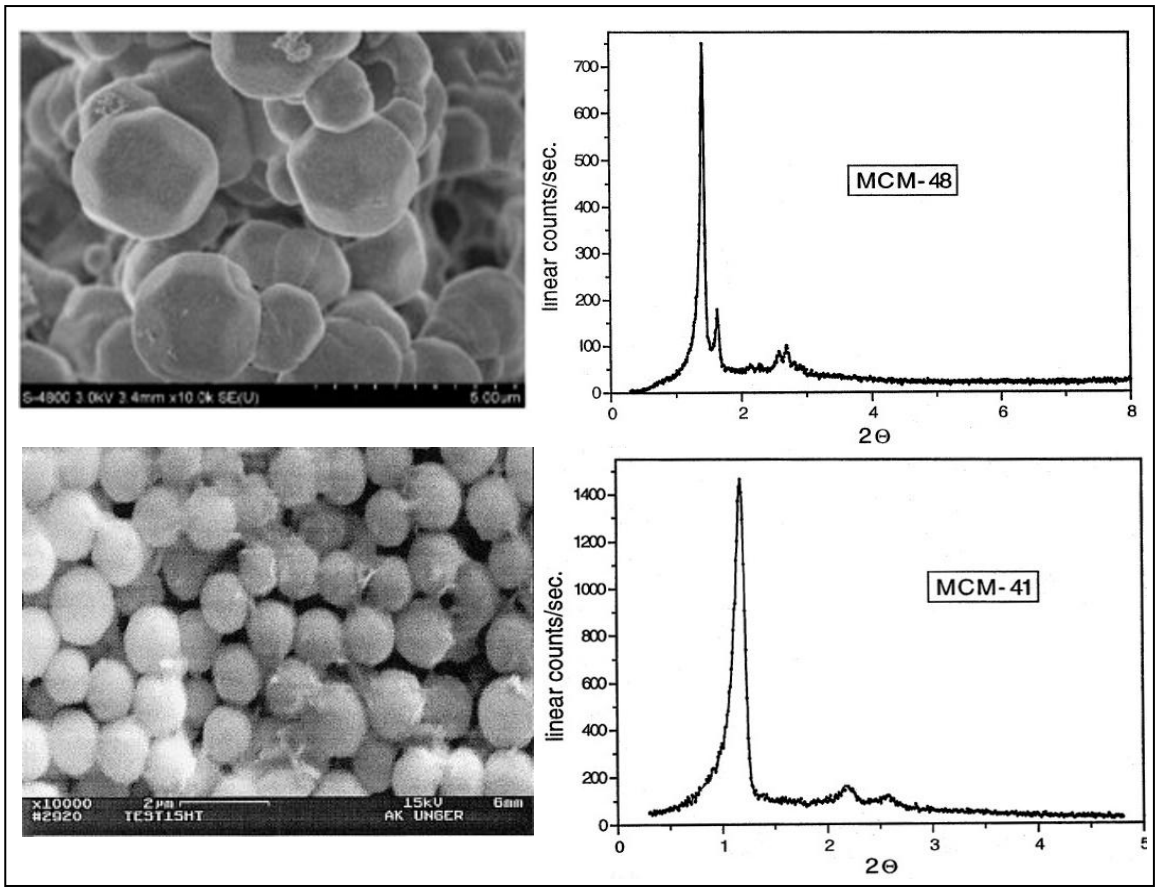

Figure 2.8 SEM Image and XRD Pattern: A) MCM48, B). MCM41

2.8 Impregnation

Impregnation is a very common and widely used method to synthesize a heterogeneous catalyst. In principle, impregnation is referred to dispersion of the active component to support surface so that it has a better reactivity in the chemical reaction process. The preparation of heterogeneous catalysts with a support material involves at least three steps: firstly, deposition of active components on the support surface through impregnation. This step can be done either by wet process or dry support impregnation [179]. For wet support impregnation, before impregnation process is done, support material is first wetted by liquid solvent where capillary forces do not come into play and the distribution

of metal in the support surface is based on diffusion and adsorption. Therefore this impregnation is also known as diffuse impregnation.

On the other hand, for dry support impregnation, support material is soaked in a solution with the desired metal precursor. In this case, the solvent and the metal precursors penetrate into the support material mainly because of capillary forces. In this type of impregnation, sometimes fluid is added just to fill the pores, so that it is often referred as pore volume impregnation. In many reports, it is known that the dry support impregnation has a shorter processing time compared to the wet support impregnation. Further, in the impregnation process, it was found that composition of the impregnation solution, impregnation time, drying rate and the initial metal are important while the effect of temperature is not significant on the final metal distribution [179].

Second step is drying which is required to vaporize solvent from material support. In the drying process, at least three stages of processes are required: preheating period, a constant-rate period and a falling-rate period. During drying, the liquid solvent is moving towards the outer surface through capillary flow while dissolved metals are transported by diffusion and convection of liquid [180]. Generally, it is believed that the quality dispersion of active metal on the material support surface is determined by the impregnation process. However, further research proved that the drying process also determines whether or not the active metal is well distributed within the support. The drying stages can significantly change the metal profile established during the impregnation process when adsorption between the active metal with material support is weak [181].

And third step is reduction and calcinations. Calcinations are one of the most important factors that can affect the texture, specific surface area and morphology of the catalyst and subsequently affect the catalytic performance of the catalyst. At this stage, impurities are removed through evaporation by burning at high temperatures. The pores of the support material which was filled by water can be removed, so that the new catalyst has a pore for relatively better ability to adsorb pollutants .

Although it typically only refers to the thermal treatment, the calcination is generally used to describe all process variables associated with the process in the furnace such as gas phase composition in the atmosphere in contact with the catalyst during the process of burning that led to the oxidizing, reducing, inert, and functionalizing and the thermal profile also affects catalyst such as ramp rate, hold temperature, and hold time. After the formation of the catalyst precursor, further heat treatment is required to convert the catalyst precursor to form the catalyst shape as desired. Calcination stage is also quite important in synthesizing heterogeneous catalyst because it affects the morphology, surface area, the crystallite size distribution and the catalytic properties. Arsalanfar et al. report the effect of calcination to the phase changes of the catalyst which are thermodynamically more stable. Scheme during the phase change process for some types of catalyst calcination is shown in Figure 2.9 [182].

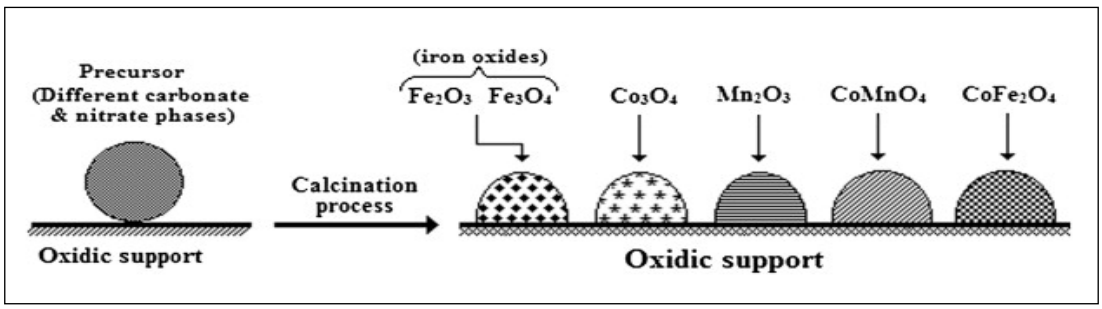

Figure 2.9 Phase changes during calcination process

2.9 Summary

As described above, phenol and its derivatives are the largest component in wastewater from industrial waste such as chemical, petrochemical and pharmaceutical plants. This compound has been disposed of as effluent although it is prohibited due to environmental contamination. Several methods have been developed to reduce the phenol pollutant from wastewater such as adsorption using activated carbon, thermal incineration and liquid phase chemical oxidation. The use of activated carbon is very commonly due to economical method. However, activated carbon can not exhibit complete removal of phenol through adsorption process. It also needs extra planning and funding in regard to the regeneration and disposal of the adsorbent. Other processes which are also widely used for removal of organic pollutants include incineration. Although this method can destroy the contaminant completely, it produces by-products emissions into the environment in the form of dioxins and furans causing serious health problems to humans. Chemical oxidation is another promising method including Wet Air Oxidation (WAO), Catalytic Wet Air Oxidation (CWAO), Heterogeneous Catalytic Oxidation and Advance Oxidation Process (AOP). Many techniques have been commonly used in AOP such as Fenton oxidation, UV-based technique and ozonation. These techniques are based on the formation of hydroxyl radical or sulfate radical as an oxidant agent to degrade phenol contaminant from aqueous solution. Further, combining the use of oxidants with appropriate catalysts will reduce the use of high temperature and pressure in the oxidation process. Therefore, heterogeneous catalyst is quite promising to be adopted due to removal efficiency and no extra process to separate the catalyst from the system. The used heterogeneous catalyst is generally coming from a noble metal and metal oxide with various combinations of

oxidants. One that deserves attention is the use of a cheap and easy-to-obtain catalyst support. For that reason, the use of natural minerals and residual materials such as Activated Carbon (AC), Natural Zeolite (NZ), Fly Ash (FA), Red Mud (RM), Silica, Alumina etc. as a support for impregnation of the active metal become very important to be developed.

References

1. Metcalf, E. and H.P. Eddy, *Wastewater Engineering: Treatment, Disposal and Reuse*, 3rd edition, revised by: G. Tchobanoglous, F.L. Burton, McGraw-Hill, New York, 1991, p.17

2. C.F. Foster, Biotechnology and Wastewater Treatment, Cambridge University Press, Cambridge,1985, p.303

3. Eftaxias A. *Catalytic Wet Air Oxidation of Phenol in a Trickle Bed Reactor: Kinetics and Reactor Modeling*, Ph.D Disertation at the Rovira i Virgili University, Tarragona Spain, 2002.

4. T. C. Voice, Activated carbon adsorption, Standard Handbook of Hazardous Waste Treatment and Disposal, H.M. Freeman (ed), McGraw-Hill, New York, 1988

5. J.J. Santoleri, Liquid-Injection Incinerators, Standard Handbook of Hazardous Waste Treatment and Disposal, H.M. Freeman (ed), McGraw-Hill, New York, 1988

6. S. C. Rowat, Medical Hypotheses 52 (1999) 389.

7. F.J. Zimmermann, Chem. Eng. 25 (1958) 117.

8. W. M. Copa, W. B. Gitchel, Wet Oxidation, Standard Handbook of Hazardous Waste Treatment and Disposal, H.M. Freeman (ed), McGraw-Hill, New York, 1988

9. V. S. Mishra, V. V. Mahajani, J. B. Joshi, Ind. Eng. Chem. Res. 34 (1995) 2.

10. R. Andreozzi, V. Caprio, A. Insola, R. Marotta, Catalysis Today 53 (1999) 51.

11. F. Luck, Catalysis Today 27 (1996) 195.

12. J. Barrault, M. Abdellaoui, C. Bouchoule, A. Majeste, J.M. Tatibouet, A. Louloudi, N. Papayannakos, N.H. Gangas, Applied Catalysis B: Environmental 27 (2000) L225.

13. B. Legube, N. Karpel Vel Leitner, Catalysis Today 53 (1999) 61.

14. Imamura, S., *Catalytic and noncatalytic wet oxidation.* Ind. Eng. Chem. Res, 1999. 38(5): p. 1743-1753.

15. R.J. Bigda, Chem. Eng. Prog. 91 (1995) 62

16. A. Fortuny, C. Bengoa, J. Font, A. Fabregat, J. Hazard. Mater. 64 (1999) 181.

17. S. Hamoudi, F. Larachi and A. Sayari, J. Catal. 177 (1998) 247.

18. Z.Y. Ding, M.A. Frisch, L. Li, E.F. Gloyna, Ind. Eng. Chem. Res. 35 (1996) 3257.

19. D. R. Grymonpre, W. C. Finney, B. R. Locke, Chem. Eng. Sci. 54 (1999) 3095.

20. L. Szpyrkowicz, C Juzzolino, S. N. Kaul, S Daniele, M D. De Faveri, Ind. Eng. Chem. Res. 39 (2000) 3241.

21. R. Andreozzi, V. Caprio, A. Insola, R. Marotta, Catalysis Today 53 (1999) 51.

22. C. Dominguez, J. Garcia, M. A. Pedraz, A. Torres, M. A. Galan, Catalysis Today

23. Y. G. Adewuyi, Ind. Eng. Chem. Res. 40 (2001) 4681

24. Laine, D.F. and I.F. Cheng, *The destruction of organic pollutants under mild reaction conditions: a review.* Microchemical Journal, 2007. 85(2): p. 183-193.

25. Rushton, L., *Health hazards and waste management.* Br Med Bull, 2003. 68(1): p. 183-197.

26. Ahling, B. and A. Lindskog, *Emission of chlorinated organic substances from combustion.* Chlorinated dioxins and related compounds: impact on the environment. Pergamon, Oxford, 1980: p. 215-225.

27. S. T. Kolaczkowski, P. Plucinski, F. J. Beltran, F. J. Rivas, D. B. McLurgh, Chem. Eng. J. 73(1999) 143.

28. Luck, F., *Wet air oxidation: past, present and future.* Catalysis today, 1999. 53(1): p. 81-91.

29. Lixiong, L., C. Peishi, and F.G. Earnest, *Generalized kinetic model for wet oxidation of organic compounds.* AIChE Journal, 1991. 37(11): p. 1687-1697.

30. Zhang, Q. and K.T. Chuang, *Alumina-Supported Noble Metal Catalysts for Destructive Oxidation of Organic Pollutants in Effluent from a Softwood Kraft Pulp Mill.* Industrial & Engineering Chemistry Research, 1998. 37(8): p. 3343-3349.

31. H. Debellefontaine, J. N. Foussard, Waste Management 20 (2000) 2

32. Kritzer, P. and E. Dinjus, *An assessment of supercritical water oxidation (SCWO) existing problems, possible solutions and new reactor concepts.* Chemical Engineering Journal, 2001. 83(3): p. 207-214.

33. Prasad, J., et al. *Comparative Study of Air-and Oxygen-Based Wet Oxidation Systems*. in *Proc of 7th Natl Conf., Hazard waste Hazard mater.;*. 1990: Hazard Mater Res Control Inst; Silver spring MD.

34. Mishra, V.S., V.V. Mahajani, and J.B. Joshi, *Wet air oxidation.* Industrial & Engineering Chemistry Research, 1995. 34(1): p. 2-48.

35. Bhargava, S.K., et al., *Wet Oxidation and Catalytic Wet Oxidation.* Industrial & Engineering Chemistry Research, 2006. 45(4): p. 1221-1258.

36. A. Camporro, M.J. Camporro, J. Coca, H. Sastre, Regeneration of an activated carbon bed exhausted by industrial phenolic waste-water, J. Hazard. Mater., 37 (1994) 207-214.

37. Y.I. Matatov-Meytal, M. Sheintuch, Ind. Eng. Chem. Res. 37 (1998) 309.

38. Pirkanniemi, K. and M. Sillanpää, *Heterogeneous water phase catalysis as an environmental application: a review.* Chemosphere, 2002. 48(10): p. 1047-1060.

39. J. Barbier Jr., F. Delanoe, F. Jabouille, D. Duprez, G. Blanchard, P. Isnard, J. Catal. 177 (1998) 378.

40. J. Qin, Q. Zhang, K. T. Chuang, Appl. Cat. B: Environ. 29 (2001) 115.

41. Imamura, S., I. Fukuda, and S. Ishida, *Wet oxidation catalyzed by ruthenium supported on cerium (IV) oxides.* Industrial & Engineering Chemistry Research, 1988. 27(4): p. 718-721.

42. S-K Kim, S-K Ihm, Ind. Eng. Chem. Res. 41 (2002) 1967.

43. S. Hamoudi, A. Sayari, K. Belkacemi, L. Bonneviot, F. Larachi, Catalysis Today 62 (2000) 379.

44. J. E. Atwater, J. R. Akse, J. A. McKinnis, J. O. Thompson, Chemosphere 34 (1997) 203.

45. L. Oliviero, J. Barbier Jr., D, Duprez, A. Guerrero-Ruiz, B. BAchiller-Baeza, I. Rodriguez-Ramos, Appl. Cat. B: Environ. 25 (2000) 267.

46. A. A. Klingoffer, R. L. Cerro, M. A. Abraham, Catalysis Today 40 (1998) 59.

47. J. Barbier Jr., F. Delanoe, F. Jabouille, D. Duprez, G. Blanchard, P. Isnard, J. Catal. 177 (1998) 378.

48. S. Duprez, F. Delano, J. Barbier, P. Isnard, G. Blanchard, Catal. Today 29 (1996) 317.

49. L. Oliviero, J. Barbier Jr., D. Duprez, H. Wahyu, J. W. Pnton, I. S. Metcalf, D. Mantzavinos, Apll. Cat. B: Environ. 35 (2001) 1.

50. J. C. Beziat, M. Besson, P Gallezot, S. Durecu, Ind. Eng. Chem. Res. 38 (1999) 1310.

51. J. Barbier Jr., L. Oliviero, B. Renard, D. Duprez, Catalysis Today 75 (2002) 29.

52. J. E. Atwater, J. R. Akse, J. A. McKinnis, J. O. Thompson, Appl. Cat. B: 11 (1996) L11.

53. P. Gallezot, N. Laurain, P. Isnard, Appl. Cat. B: Environ 9 (1996) L11.

54. A. Pintar, M. Besson, P. Gallezot, Appl. Cat. B: Environ. 30 (2001) 123.

55. H. Takayama, Q. Jiang-Yan, K. Inazu, K. Aika, Chemistry Letters (1999) 377.

56. H. T. Gomes, J. L. Figueiredo, J. L. Faria, Catalysis Today 75 (2002) 23.

57. R. Ukropec, B. F. M. Kuster, J. C. Schoten, R. A. van Santen, Appl. Cat. B: Environ. 23 (1999) 45.

58. J. Qin, Q. Zhang, K. T. Chuang, Appl. Cat. B: Environ. 29 (2001) 115.

59. A. Sadana, J.R. Katzer, J. Catal. 35 (1974) 140.

60. H. Ohta, S. Goto, H. Teshima, Ind. Eng. Chem. Fundam. 19 (1980) 180.

61. G. Baldi, S. Goto, C. K. Chow, J. M. Smith, Ind. Eng. Chem. Proc. Des. Dev. 13 (1974) 447.

62. S. Goto, J. M. Smith, AIChE J. 21 (1974) 714.

63. J. Levec, M. Herskowitz, J. M. Smith, AIChE J., 22 (1976) 919.

64. A. Pintar, J. Levec, Chem. Eng. Sci. 47 (1992) 2395.

65. A. Pintar, J. Levec, J. Catal. 135 (1992) 345.

66. A. Pintar, J. Levec, Ind. Eng. Chem. Res. 33 (1994) 3070.

67. A. Pintar, J. Levec, 49 (1994) 4391.

68. S. Hamoudi, F. Larachi, G. Cerrella, M. Cassanello, Ind. Eng. Chem. Res. 37 (1998) 3561.

69. S. Hamoudi, K. Belkacemi, F. Larachi, Chem. Eng. Sci. 54 (1999) 3569

70. H. Chen, A. Sayari, A. Adnot, F. Larachi Appl. Cat. B: Environ. 32 (2001) 195.

71. Kochetkova R P, B.A.F., Shiplevskaya L I, Shiplevskaya I P, Eppel S A, Smidt F K, *Liquid phase oxidation of Phenol.* Khim.Tekhnol.Topl.Masel, 1992. 4(31): p. Chem Abstract 1992, 117, 156952.

72. A. Fortuny, J. Font, A. Fabregat, Appl. Cat. B: Environ. (1998)

73. J. Qin, Q. Zhang, K. T. Chuang, Appl. Cat. B: Environ. 29 (2001) 115.
74. A. Santos, P. Yustos, A. Quintanilla, S. Rodriguez, F. Garcia-Ochoa, Appl. Cat. B: Environ. 39 (2002) 97.

75. A. Santos, E. Barroso, F. Garcia-Ochoa, Catalysis Today 48 (1999) 109.

76. A. Fortuny, C. Bengoa, J. Font, A. Fabregat, J. Hazard. Mater. 64 (1999) 181.

77. A. Fortuny, C. Bengoa, J. Font, F. Castells, A. Fabregat, Catal. Today 53 (1999) 107

78. C. Miro, A. Alejandre, A. Fortuny, C. Bengoa, J. Font, A. Fabregat, Water Research 33 (1999) 1005

79. A. Alejandre, F. Medina, X. Rodriguez, P. Salagre, Y. Cesteros, J. E. Sueiras, Appl. Cat. B: Environ 30 (2001) 195.

80. A. Pintar, G. Bercic, J. Levec, Chem. Eng. Sci. 52 (1997) 4143.

81. A. Pintar, J. Levec, J. Catal. 135 (1992) 345.

82. H. Ohta, S. Goto, H. Teshima, Ind. Eng. Chem. Fundam. 19 (1980) 180.

83. S. Hocevar, U. O. Krasovec, B. Orel, A. S. Arico, H. Kim, Appl. Cat. B: Environ.28 (2000) 113.

84. S. T. Hussain, A. Sayari, F. Larachi, Appl. Cat. B: Environ. 34 (2001) 1.

85. H. Chen, A. Sayari, A. Adnot, F. Larachi Appl. Cat. B: Environ. 32 (2001) 195.

86. C. J. Chang, C.-M. Ko, K. Shih, Chem. Eng. Com. 156 (1996) 201.

87. P. M. Alvarez, D. McLurgh, P. Plucinsky, Ind. Eng. Chem. Res. 41 (2002) 2147.

88. A. Pintar, J. Levec, Chem. Eng. Sci. 47 (1992) 2395

89. G. Baldi, S. Goto, C. K. Chow, J. M. Smith, Ind. Eng. Chem. Proc. Des. Dev. 13 (1974) 447.

90. J. Levec, M. Herskowitz, J. M. Smith, AIChE J., 22 (1976) 919.
91. K. Belkacemi, F. Larachi, A. Sayari, J. Catal. (2000) 224

92. Hunsberger, J.F., *Standard reduction potentials; in: R.C. Weast (Ed.), Handbook of Chemistry and Physics*. 58 ed. 1977, Ohio: CRC Press, Ohio.

93. Gallard, H. and U. von Gunten, *Chlorination of natural organic matter: kinetics of chlorination and of THM formation.* Water research, 2002. 36(1): p. 65-74.

94. Vella, P.A., et al., *Treatment of Low Level Phenols (g/L) with Potassium Permanganate.* Research journal of the water pollution control federation, 1990: p. 907-914.

95. Yan, Y.E. and F.W. Schwartz, *Oxidative degradation and kinetics of chlorinated ethylenes by potassium permanganate.* Journal of Contaminant Hydrology, 1999. 37(3-4): p. 343-365.

96. Waldemer, R.H. and P.G. Tratnyek, *Kinetics of contaminant degradation by permanganate.* Environ. Sci. Technol, 2006. 40(3): p. 1055-1061.

97. Seol, Y., H. Zhang, and F.W. Schwartz, *A review of in situ chemical oxidation and heterogeneity.* Environmental and Engineering Geoscience, 2003. 9(1): p. 37.

98. Huang, K.C., R.A. Couttenye, and G.E. Hoag, *Kinetics of heat-assisted persulfate oxidation of methyl tert-butyl ether (MTBE).* Chemosphere, 2002. 49(4): p. 413-420.

99. Watts, R.J. and A.L. Teel, *Treatment of contaminated soils and groundwater using ISCO.* Practice Periodical of Hazardous, Toxic, and Radioactive Waste Management, 2006. 10: p. 2.

100. Dahmani, M.A., K. Huang, and G.E. Hoag, *Sodium persulfate oxidation for the remediation of chlorinated solvents (USEPA superfund innovative technology evaluation program).* Water, Air, & Soil Pollution: Focus, 2006. 6(1): p. 127-141.

101. Johnson, R.L., P.G. Tratnyek, and R.O.B. Johnson, *Persulfate Persistence under Thermal Activation Conditions.* Environmental Science & Technology, 2008. 42(24): p. 9350-9356.

102. Block, P.A., R.A. Brown, and D. Robinson. *Novel activation technologies for sodium persulfate in situ chemical oxidation*. in *Proceedings of 4th International Conference on the Remediation of chlorinated and Recalcitrant Compounds*. 2004.

103. Langlais, B., D.A. Reckhow, and D.R. Brink, *Ozone in water treatment: Application and engineering: Cooperative research report*. 1991: CRC Press.

104. Battino, R., T.R. Rettich, and T. Tominaga, *The solubility of oxygen and ozone in liquids.* J. Phys. Chem. Ref. Data, 1983. 12(2): p. 164-177.

105. Munter, R., *Advanced oxidation processes—current status and prospects.* Proc. Estonian Acad. Sci. Chem, 2001. 50(2): p. 59-80.

106. Glaze, W.H., J.W. Kang, and D.H. Chapin, *The chemistry of water treatment processes involving ozone, hydrogen peroxide and ultraviolet radiation.* Ozone: Science & Engineering, 1987. 9(4): p. 335-352.

107. Parson, S. (ed), Advance Oxidation Processes for Water and Wastewater Treatment, IWA Publishing, London, 2004, p.4

108. De Laat, J., G. Truong Le, and B. Legube, *A comparative study of the effects of chloride, sulfate and nitrate ions on the rates of decomposition of H2O2 and organic compounds by Fe (II)/H2O2 and Fe (III)/H2O2.* Chemosphere, 2004. 55(5): p. 715-723.

109. Benitez, F.J., et al., *Oxidation of several chlorophenolic derivatives by UV irradiation and hydroxyl radicals.* Journal of Chemical Technology &# 38; Biotechnology, 2001. 76(3): p. 312-320.

110. Huang, C.P., C. Dong, and Z. Tang, *Advanced chemical oxidation: its present role and potential future in hazardous waste treatment.* Waste management, 1993. 13(5): p. 361-377.

111. Walling, C. and S. Kato, *Oxidation of alcohols by Fenton's reagent. Effect of copper ion.* Journal of the American Chemical Society, 1971. 93(17): p. 4275-4281.

112. Li, Z.M., P.J. Shea, and S.D. Comfort, *Nitrotoluene destruction by UV-catalyzed Fenton oxidation.* Chemosphere, 1998. 36(8): p. 1849-1865.

113. Kavitha, V. and K. Palanivelu, *Destruction of cresols by Fenton oxidation process.* Water Research, 2005. 39(13): p. 3062-3072.

114. Potter, F.J. and J.A. Roth, *Oxidation of chlorinated phenols using Fenton's reagent.* Hazardous Waste and Hazardous Materials, 1993. 10(2): p. 151-170.

115. Kang, N., D.S. Lee, and J. Yoon, *Kinetic modeling of Fenton oxidation of phenol and monochlorophenols.* Chemosphere, 2002. 47(9): p. 915-924.

116. Beltran, F.J., et al., *Fenton reagent advanced oxidation of polynuclear aromatic hydrocarbons in water.* Water, Air, & Soil Pollution, 1998. 105(3): p. 685-700.

117. Wadley, S. and T.D. Waite, *Fenton processes.* 2006.

118. Pignatello, J.J., *Dark and photoassisted iron (3+)-catalyzed degradation of chlorophenoxy herbicides by hydrogen peroxide.* Environmental Science & Technology, 1992. 26(5): p. 944-951.

119. Lu, M.C., J.N. Chen, and C.P. Chang, *Effect of inorganic ions on the oxidation of dichlorvos insecticide with Fenton's reagent.* Chemosphere, 1997. 35(10): p. 2285-2293.

120. Benitez, F.J., et al., *Rate constants for the reactions of ozone with chlorophenols in aqueous solutions.* Journal of hazardous materials, 2000. 79(3): p. 271-285.

121. Tanaka, K., T. Hisanaga, and K. Harada, *Efficient photocatalytic degradation of chloral hydrate in aqueous semiconductor suspension.* Journal of photochemistry and photobiology. A, Chemistry, 1989. 48(1): p. 155-159.

122. Tanaka, K., T. Hisanaga, and K. Harada, *Photocatalytic degradation of organohalide compounds in semiconductor suspension with added hydrogen peroxide.* New journal of chemistry(1987), 1989. 13(1): p. 5-7.

123. Beltran, F.J., G. Ovejero, and B. Acedo, *Oxidation of atrazine in water by ultraviolet radiation combined with hydrogen peroxide.* Water research(Oxford), 1993. 27(6): p. 1013-1021.

124. Hirvonen, A., T. Tuhkanen, and P. Kalliokoski, *Formation of chlorinated acetic acid during UV/H 2 O 2 -oxidation of ground water contaminated with chlorinated ethylenes.* Chemosphere(Oxford), 1996. 32(6): p. 1091-1102.

125. De, A.K., S. Bhattacharjee, and B.K. Dutta, *Kinetics of phenol photooxidation by hydrogen peroxide and ultraviolet radiation.* Ind. Eng. Chem. Res, 1997. 36(9): p. 3607-3612.

126. Andreozzi, R., et al., *The oxidation of metol (N-methyl-p-aminophenol) in aqueous solution by UV/H2O2 photolysis.* Water Research, 2000. 34(2): p. 463-472.

127. Benitez, F.J., et al., *The role of hydroxyl radicals for the decomposition of p-hydroxy phenylacetic acid in aqueous solutions.* Water Research, 2001. 35(5): p. 1338-1343.

128. Hou, W.J., S. Tsuneda, and A. Hirata, *TOC removal of raw industrial wastewater from LSI photo-resist processing with H 2 O 2 /UV in a batch reactor.* Journal of chemical engineering of Japan, 2001. 34(3): p. 444-447.

129. Anipsitakis, G.P. and D.D. Dionysiou, *Transition metal/UV-based advanced oxidation technologies for water decontamination.* Applied Catalysis B, Environmental, 2004. 54(3): p. 155-163.

130. Ku, Y., L.S. Wang, and Y.S. Shen, *Decomposition of EDTA in aqueous solution by UV/H sub (2) O sub (2) process.* Journal of Hazardous Materials, 1998. 60(1): p. 41-55.

131. Stevenson F.J., *Humus Chemistry: Genesis, Composition, Reaction*, John Wiley & Son, New York, 1994.

132. Benitez, F.J., et al., *Simultaneous photodegradation and ozonation plus UV radiation of phenolic acids-major pollutants in agro-industrial wastewaters.* Journal of Chemical Technology and Biotechnology, 1997. 70(3): p. 253-260.

133. Peyton, G.R., *Oxidative treatment methods for removal of organic compounds from drinking water supplies.* Significance and Treatment of Volatile Organic Compounds in Water Supplies, 1990: p. 313-362.

134. Balcioglu, I.A. and I. Arslan, *Treatment of textile industry wastewater by enhanced photocatalytic oxidation reaction.* Journal of Advanced Oxidation Technologies, 1999. 4(2): p. 189-195.

135. Lee, C. and J. Yoon, *Determination of quantum yields for the photolysis of Fe (III)-hydroxo complexes in aqueous solution using a novel kinetic method.* Chemosphere, 2004. 57(10): p. 1449-1458.

136. Li, Z.M., P.J. Shea, and S.D. Comfort, *Nitrotoluene destruction by UV-catalyzed Fenton oxidation.* Chemosphere, 1998. 36(8): p. 1849-1865.

137. Kim, S.M. and A. Vogelpohl, *Degradation of organic pollutants by the photo-Fenton-process.* Chemical Engineering & Technology, 1998. 21(2): p. 187-191.

138. Brand, N., G. Mailhot, and M. Bolte, *Degradation photoinduced by Fe (III): method of alkylphenol ethoxylates removal in water.* Environ. Sci. Technol, 1998. 32(18): p. 2715-2720.

139. Huston, P.L. and J.J. Pignatello, *Degradation of selected pesticide active ingredients and commercial formulations in water by the photo-assisted Fenton reaction.* Water Research, 1999. 33(5): p. 1238-1246.

140. Arslan, I., I. Akmehmet Balcioglu, and T. Tuhkanen, *Oxidative treatment of simulated dyehouse effluent by UV and near-UV light assisted Fenton's reagent.* Chemosphere, 1999. 39(15): p. 2767-2783.

141. Engwall, M.A., J.J. Pignatello, and D. Grasso, *Degradation and detoxification of the wood preservatives creosote and pentachlorophenol in water by the photo-Fenton reaction.* Water Research, 1999. 33(5): p. 1151-1158.

142. Wang, K.H., et al., *Photocatalytic degradation of 2-chloro and 2-nitrophenol by titanium dioxide suspensions in aqueous solution.* Applied Catalysis B, Environmental, 1999. 21(1): p. 1-8.

143. Luo, Y. and D.F. Ollis, *Heterogeneous Photocatalytic Oxidation of Trichloroethylene and Toluene Mixtures in Air: Kinetic Promotion and Inhibition, Time-Dependent Catalyst Activity.* Journal of Catalysis, 1996. 163(1): p. 1-11.

144. Crittenden, J.C., et al., *Photocatalytic oxidation of chlorinated hydrocarbons in water.* Water Research, 1997. 31(3): p. 429-438.

145. Farré, M.J., et al., *Degradation of some biorecalcitrant pesticides by homogeneous and heterogeneous photocatalytic ozonation.* Chemosphere, 2005. 58(8): p. 1127-1133.

146. Ranjit, K.T., et al., *Lanthanide Oxide Doped Titanium Dioxide Photocatalysts: Effective Photocatalysts for the Enhanced Degradation of Salicylic Acid and t-Cinnamic Acid.* Journal of Catalysis, 2001. 204(2): p. 305-313.

147. Serpone, N., et al., *Exploiting the interparticle electron transfer process in the photocatalysed oxidation of phenol, 2-chlorophenol and pentachlorophenol: chemical evidence for electron and hole transfer between coupled semiconductors.* Journal of Photochemistry & Photobiology, A: Chemistry, 1995. 85(3): p. 247-255.

148. Villasen8or, J., P. Reyes, and G. Pecchi, *Photodegradation of Pentachlorophenol on ZnO.* J. Chem. T echnol. Biotechnol, 1998. 72: p. 105È110.

149. Akyol, A., H.C. Yatmaz, and M. Bayramoglu, *Photocatalytic decolorization of Remazol Red RR in aqueous ZnO suspensions.* Applied Catalysis B, Environmental, 2004. 54(1): p. 19-24.

150. Khodja, A.A., et al., *Photocatalytic degradation of 2-phenylphenol on TiO2 and ZnO in aqueous suspensions.* Journal of Photochemistry & Photobiology, A: Chemistry, 2001. 141(2-3): p. 231-239.

151. Khalil, L.B., W.E. Mourad, and M.W. Rophael, *Photocatalytic reduction of environmental pollutant Cr (VI) over some semiconductors under UV/visible light illumination.* Applied Catalysis B, Environmental, 1998. 17(3): p. 267-273.

152. Doong, R. and W. Chang, *Photoassisted titanium dioxide mediated degradation of organophosphorus pesticides by hydrogen peroxide.* Journal of Photochemistry & Photobiology, A: Chemistry, 1997. 107(1-3): p. 239-244.

153. Dhanalakshmi, K.B., et al., *Photocatalytic degradation of phenol over TiO2 powder: The influence of peroxomonosulphate and peroxodisulphate on the reaction rate.* Solar Energy Materials and Solar Cells, 2007.

154. Anipsitakis, G.P., T.P. Tufano, and D.D. Dionysiou, *Chemical and microbial decontamination of pool water using activated potassium peroxymonosulfate.* Water Research, 2008. 42(12): p. 2899-2910.

155. Juntgen H, *Activated carbon as catalyst support*. Fuel, 1998. Vol. 65, p. 1436-1446

156. Pala A., Tokat, E. *Color removal from cotton textile industry wastewater in an activated sludge system with various additives.* Water Res. 36(2002) p. 2920–2925.

157. Stavropoulos G.G., Samaras P., Sakellaropoulos G.P. *Effect of activated carbons modification on porosity surface structure and phenol adsorption*, Journal of Hazardous Materials 151 (2008) p. 414–421

158. Kadirvelu, K., Karthika, C., Vennilamani, N., Pattabhi, S., 2005. *Activated carbon from industrial solid waste as an adsorbent for the removal of Rhodamine-B from aqueous solution: kinetic and equilibrium studies.* Chemosphere 60(2005) p. 1009–1017.

159. Mukherjee, A. B.; Zevenhoven, R.; Bhattacharya, P.; Sajwan, K. S.; Kikuchi, R. *Mercury flow via coal and coal utilization by-products: A global perspective*. *Resour. Conserv. Recyl.* 2008, *52* (4), 571–591.

160. Gustin, M. S.; Ladwig, K. *An assessment of the significance of mercury release from coal fly ash. J. Air Waste Manage. Assoc.* 2004, *54* (3), 320–330.

161. Shijitha T., Baiju K.V., Shukla, S., Patil, K. Warrier K.G.K. Novel electroless process for copper coating of flyash using titania/ultraviolet-radiation/metal catalyst-system, Applied Surface Science 255 (2009) p. 6696–6704

162. Wang S. *Application of Solid Ash Based Catalysts in Heterogeneous Catalysis*, Environ. Sci. Technol. 2008, 42, p. 7055–7063

163. Manz, O. E. Coal fly ash: A retrospective and future look. *Fuel* 1999, *78* (2), p. 133–136.

164. Olad A., Naseri B. *Preparation, characterization and anticorrosive properties of a novel polyaniline/clinoptilolite nanocomposite*, Progress in Organic Coatings 67 (2010) p. 233–238.

165. Wang S., Peng Y. *Natural zeolites as effective adsorbents in water and wastewater treatment*, Chemical Engineering Journal 156 (2010) p. 11–24

166. Li Z.H., Bowman R.S. *Sorption of perchloroethylene by surfactant-modified zeolite as controlled by surfactant loading*, Environmental Science & Technology 32 (1998) p. 2278–2282.

167. Huttenloch P., Roehl K.E., Czurda K. *Sorption of nonpolar aromatic contaminants by chlorosilane surface modified natural minerals,* Environmental Science & Technology 35 (2001) p. 4260–4264.

168. Ersoy B., Celik M.S. *Uptake of aniline and nitrobenzene from aqueous solution by organo-zeolite*, Environmental Technology 25 (2004) p. 341–348.

169. http://www.iza-stucture.org, retrieved: 10 August 2012.

170. Cundy C.S., Cox P.A. *The hydrothermal synthesis of zeolites: History and development from the Earliest to the present time,* Chem. Rev. 103 (2004), p. 663-701.

171. Grieken R.V., Sotelo J.L., Menendez J.M., Melero J.A. *Anomalous crystallization mechanism in the synthesis of nanocrystalline ZSM-5*, Microporous and Mesoporous material, 39 (2000), p. 135-147.

172. Sushil S., Batra V.S. Catalytic applications of red mud, an aluminium industry waste: A review, Applied Catalysis B: Environmental 81 (2008) p. 64–77

173. Alvarez J., Rosal R., Sastre H., DõÂez F.V. *Characterization and deactivation studies of an activated sulfide red mud used as hydrogenation catalyst,* Applied Catalysis A: General 167 (1998) p. 215-223

174. Trimm D.L., Stanislaus *A. The control of pore size in alumina catalyst supports: a review*, Applied Catalysis, 21 (1986) p. 215-238

175. Bell N.S., Adair J.H. Adsorbate elects on glycothermally produced α-alumina particle morphology, Journal of Crystal Growth 203 (1999) p. 213-226.

176. D. Kumar D., Schumacher K., du Fresne von Hohenesche C., Gru¨n M.. Unger K.K. *MCM-41, MCM-48 and related mesoporous adsorbents: their synthesis and characterization*, Colloids and Surfaces: Physicochemical and Engineering Aspects 187–188 (2001) p. 109–116.

177. Yun J.S., Seong M.Y., Ihm S.K. *The synthesis of MCM-41 with different macropore morphologies: Residual volume and skeletal-structure*, Journal of Physics and Chemistry of Solids 69 (2008) p. 1129–1132.

178. Qiang Z., Bao X., Ben W. MCM-48 modified magnetic mesoporous nanocomposite as an attractive adsorbent for the removal of sulfamethazine from water. Article in Press: Water Research xxx (2012) p. 1-8.

179. Liua X., Khinast J.G., Glassera B.J. *A parametric investigation of impregnation and drying of supported catalysts,* Chemical Engineering Science 63 (2008) p. 4517-4530

180. Lekhal, A., Glasser, B.J., Khinast, J.G. *Impact of drying on the catalyst profile in supported impregnation catalysts*. Chemical Engineering Science 56 (2001) p. 4473–4487.

181. Li, W.D., Li, Y.W., Qin, Z.F., Chen, S.Y. *Theoretical prediction and experimental validation of the egg-shell distribution of Ni for supported Ni=Al2O3 catalysts*. Chemical Engineering Science 49 (1994), p. 4889–4895.

182. Arsalanfar M., Mirzaei A.A., Bozorgzadeh H.R. Effect of calcination conditions on the structure and catalytic performance of MgO supported FeeCoeMn catalyst for CO hydrogenation, Journal of Natural Gas Science and Engineering 6 (2012) p. 1-13

Chapter-3

Heterogeneous activation of peroxymonosulphate by supported ruthenium catalysts for phenol degradation in water

Abstract

Activated carbon (AC) and Zeolite Socony Mobil-5 (ZSM5) supported ruthenium oxide catalysts were prepared and tested to degrade aqueous phenol in the presence of peroxymonosulphate. The physicochemical properties of ruthenium oxide based catalysts were characterised by several techniques such as XRD, SEM-EDS, and N_2 adsorption. It was found that RuO_2/AC was highly effective in heterogeneous activation of peroxymonosulphate to produce sulphate radicals, presenting higher reaction rate in phenol degradation compared with RuO_2/ZSM-5. Degradation efficiency of phenol could be achieved at 100% of phenol decomposition and 60% of total organic carbon (TOC) removal in 1 h at the conditions of 50 ppm phenol, 0.2 g catalyst, 1 g Oxone® in 500 mL solution at 25 ^oC using the two catalysts. It was also found that phenol degradation was strongly influenced by catalyst loading, phenol concentration, Oxone® concentration and temperature. Kinetic studies proved that a pseudo first order kinetics would fit to phenol decomposition and the activation energies for RuO_2/AC and RuO_2/ZSM5 were obtained to be 61.4 and 42.2 kJ/mol, respectively.

3.1 Introduction

Phenol is one of important pollutants in wastewater due to its toxic effect on the environment even at very low concentration. Phenol is widely used as a raw material in many industries such as chemical, petrochemical, and pharmaceutical industries [1]. Moreover, phenol is a water pollutant which can not be easily degraded with primary and secondary treatment processes so that a tertiary treatment of wastewater has to be adopted. These tertiary treatments include thermal oxidation, chemical oxidation, wet air oxidation, catalytic oxidation etc, which are generally known as advanced oxidation processes (AOPs). In principle, a tertiary treatment process is used to reduce the contaminants to harmless products such as CO_2 and H_2O [2]. Among the methods, heterogeneous catalytic oxidation usually has some advantages such as operation at room temperature and normal pressure with high energy efficiency. Furthermore, heterogeneous catalysts can be synthesised using cheap materials as supports such as activated carbon, zeolite, silica, alumina etc., and can be regenerated for reuse in treatment processes [3].

Generally, the most popular method to degrade organic compounds in wastewater is Fenton oxidation, which involves hydrogen peroxide and Fe ions (Fenton reagent) to generate hydroxyl radicals in solutions [4, 5]. Nowadays, this principle has been developed with some other oxidants such as peroxymonosulphate (PMS) and persulphate, which are found effective in chemically mineralising various organic pollutants [6]. Many researchers have proved that some heavy metals such as cobalt and iron can activate PMS to produce sulphate radicals for oxidation of organic pollutants to harmless end products. The following reactions show the formation of sulphate radicals in Co activation[7].

$$Co^{2+} + HSO_5^- \rightarrow Co^{3+} + SO_4^{-\bullet} + OH^- \quad 3.1$$

$$Co^{3+} + HSO_5^- \rightarrow Co^{2+} + SO_5^{-\bullet} + H^+ \quad 3.2$$

It was reported, in comparison with the conventional Fenton reagent, the rate of organic oxidation by sulphate radicals is faster. Moreover, the oxidation by sulphate radicals is less dependent on pH of solution, providing an alternative route to efficiently degrade organic contaminants [7, 8]. However, a major issue in using heavy metal ions as catalysts is the toxicity of the heavy metals in the treatment system. The metal ions can cause many health problems to humans such as asthma and pneumonia. Therefore, heterogeneous catalytic oxidation has to be conducted. For this purpose, the heavy metals should be loaded into solid supports such as activated carbon (AC), zeolite (ZSM5), silica, alumina etc., via different methods including impregnation and ion exchange. In the past few years, several investigations have been attempted for supported Co catalysts in activation of PMS for the degradation of organic compounds [9-17].

Ruthenium (Ru) is one of the popular noble metals and it can also be used as a catalyst in chemical degradation of organic compounds. Pirkanniemi and Sillanp [18] reported that ruthenium has traditionally been used as a heterogeneous catalyst for water treatment. Oliviero et al. [19] used activated carbon supported Ru as a catalyst in catalytic wet air oxidation of phenol and acrylic acid. They found that the catalyst was very reactive to oxidise phenol. Further, Cybulski and Trawczynski [20] studied a ruthenium catalyst loaded on carbon black in catalytic wet air oxidation to degrade phenol solution and also concluded that this catalyst was very reactive for phenol removal. Similar studies in mineralising organic contaminants by using ruthenium based catalysts in wet air oxidation have been reported [21-26]. All of them reported that this heavy metal had

very good performance. However, the use of ruthenium based catalysts with the presence of PMS to generate sulphate radicals for phenol oxidation is less developed.

In this research we investigate the use of ruthenium catalysts supported on AC and ZSM5 in heterogeneous catalytic oxidation process with the presence of peroxymonosulphate (using Oxone®) to generate sulphate radicals for chemical mineralising of phenol in aqueous solution. Several key parameters in the kinetic study such as phenol concentration, catalyst loading, Oxone® concentration and temperature were also investigated.

3.2 Experimental

3.2.1 Synthesis of ruthenium catalysts on AC and ZSM5 supports

Catalyst synthesis was carried out following a general impregnation method. For ruthenium (RuO_2)/activated-carbon (AC), a fixed amount of ruthenium chloride (Sigma-Aldrich) was added into 200 mL ultrapure water until the ruthenium compound was dissolved. Next, AC (Picactif) with particle size of 60-100 μm was added into the solution and kept stirring for 24 h. After that, the suspension was evaporated in a rotary evaporator at temperature of 50 ^oC under vacuum. The solid was then recovered and dried in an oven at 120 ^oC for 6 h. Calcination of the catalyst was conducted in a tube furnace at 550 ^oC for 6 h in nitrogen. For RuO_2/ZSM5, the same method was also implemented but with a different calcination process. The used ZSM5 was supplied by Zeolite and Allied Products, Mumbai India with particle size of 500-1000 nm. The RuO_2/ZSM5 was calcined in air. The loading of Ru on the two supports was maintained at 5 wt%.

3.2.2 Characterisation of catalysts

The synthesised catalysts were characterised by X-ray diffraction (XRD), scanning electron microscopy (SEM) with energy dispersive X-ray spectroscopy (EDS), and N_2 adsorption. The XRD (Siemen, D501 diffractometer) was used to identify the structural features and the mineralogy of the catalysts. The XRD pattern was obtained using filtered Cu Kα radiation with accelerating voltage of 40 kV and current of 30 mA. The samples were scanned at 2θ from 5-100^o. Scanning electron microscopy (SEM, Philips XL30) with secondary and backscatter electron detectors was used to obtain a visual image of the samples to show the texture and morphology of the catalysts with magnification more than 20,000. Energy-dispersive X-ray spectroscopy (EDS) was also used to detect Ru particles on supported catalysts. The catalysts were also characterised by nitrogen adsorption-desorption (Autosorb-1) to identify the BET surface area and pore volume. Prior to the analysis, the catalyst samples were degassed under vacuum at 200 ^{o}C for 12 h.

3.2.3 Kinetic study of phenol oxidation

Catalytic oxidation of phenol was conducted in 500 mL phenol solutions at concentrations of 25, 50, 75 and 100 ppm. A reactor attached to a stand was dipped into a water bath with a temperature controller. The solution was stirred constantly at 400 rpm to maintain homogeneous solution. Next, a fixed amount of peroxymonosulphate (Oxone®, DuPont's triple salt $2KHSO_5{\cdot}KHSO_4{\cdot}K_2SO_4$, Aldrich) was added to the mixture until completely dissolved. Then, a fixed amount of catalysts (Ru/AC or Ru/ZSM5) was added into the reactor to start the oxidation of phenol. The reaction was run for 2 h and at the fixed time interval, 0.5 mL of a sample was withdrawn from the solution and filtered using HPLC standard filter

of 0.45 μm and mixed with 0.5 mL methanol as a quenching reagent to stop the reaction. Phenol was then analysed on a HPLC with a UV detector at wavelength of 270 nm. The column is C18 with mobile phase of 80% acetonitrile and 20% ultrapure water. For some selected samples, total organic carbon (TOC) was determined by a Shimadzu TOX-5000 CE analyser where 0.5 mL sample was withdrawn, quenched with 3M sodium nitrite solution, and diluted to 20 mL by ultrapure water and examined within 1 h.

In recycling of catalysts for multiple round tests, the spent catalyst was recovered after each run from the reaction mixture by filtration and washed thoroughly with distilled water and dried at 70 ^{o}C for reuse.

3. 3 Result and discussion

3.3.1 Characterisation of ruthenium impregnated activated carbon and ZSM5 catalysts

XRD patterns of RuO_2/AC and RuO_2/ZSM5 are presented in Fig. 3.1. It can be seen, ruthenium species were found in the form of RuO_2 on RuO_2/ZSM5 at 2θ of 28, 35, 40 and 54.3^0. On the other hand, ruthenium oxide was found at 2θ of 28^0 and Ru at 38.4, 42.2, 44 and 69.4^0 on RuO_2/AC. The differences in ruthenium species on the two catalysts were due to the different calcination processes. For RuO_2/ZSM5, the calcination was done in air, whereas the calcination of RuO_2/AC was carried out in nitrogen gas. Ru ions would be reduced by carbon in an inert gas to form Ru metal [27].

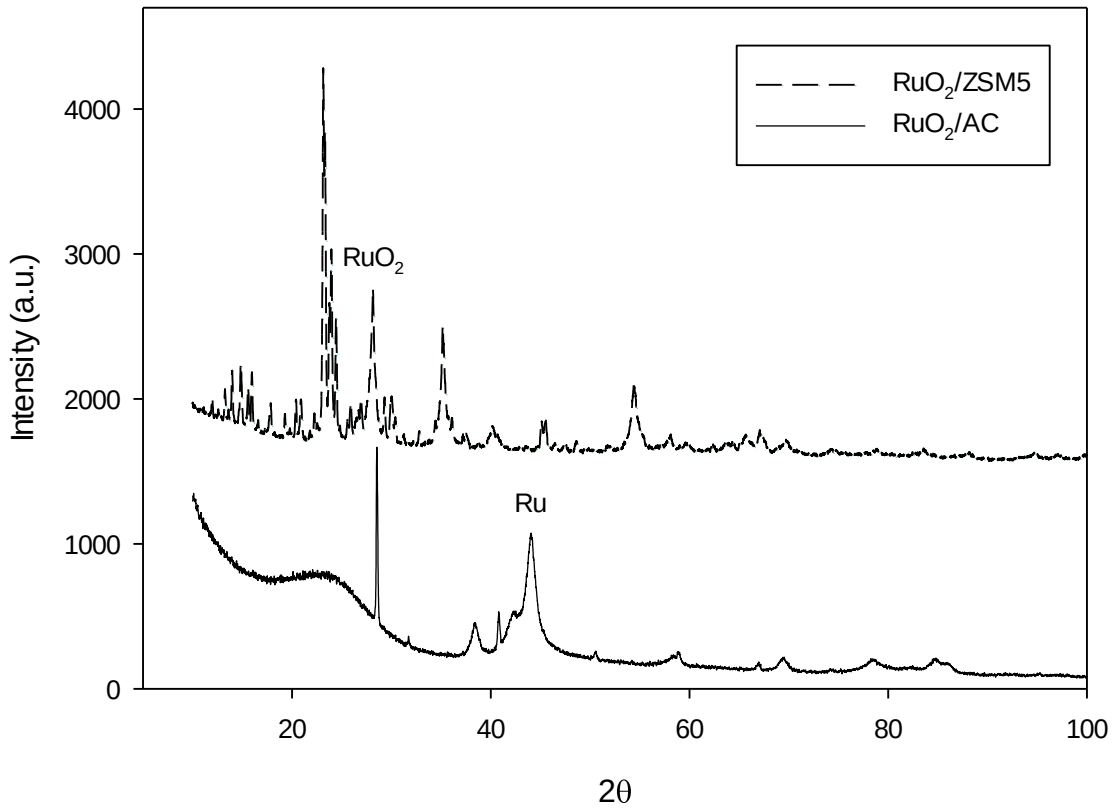

Figure 3.1 XRD spectra of RuO_2/ZSM5 and RuO_2/AC

The texture and morphology of RuO_2/AC and RuO_2/ZSM5 are shown in Fig.3.2. Fig. 3.2A and B show SEM images of RuO_2/AC analysed by a secondary electron detector (SE) and backscattered detector (BSE), respectively. It can be seen that the milled sample has different particle shape and size in a range of 5-60 μm. At the same area, the catalyst sample was also analysed using the BSE analysis and the presence of ruthenium specks is seen at the brighter area in the catalyst particles. It implies that ruthenium is well coated in the activated carbon samples. Further, in the SEM images, no small individual bright particles around the AC particles were observed suggesting that the assimilated ruthenium in the AC is not in the form of isolated RuO_2. This is also confirmed by XRD examination

that RuO_2 is the major species in the RuO_2/AC catalyst sample. Fig. 3.2C and D present SEM photos of RuO_2/ZSM5 with SE and BSE measurements, respectively. As seen, RuO_2/ZSM5 presents in smaller particle size. BSE showed brighter area than the image in SE, suggesting a good dispersion of Ru on ZSM5.

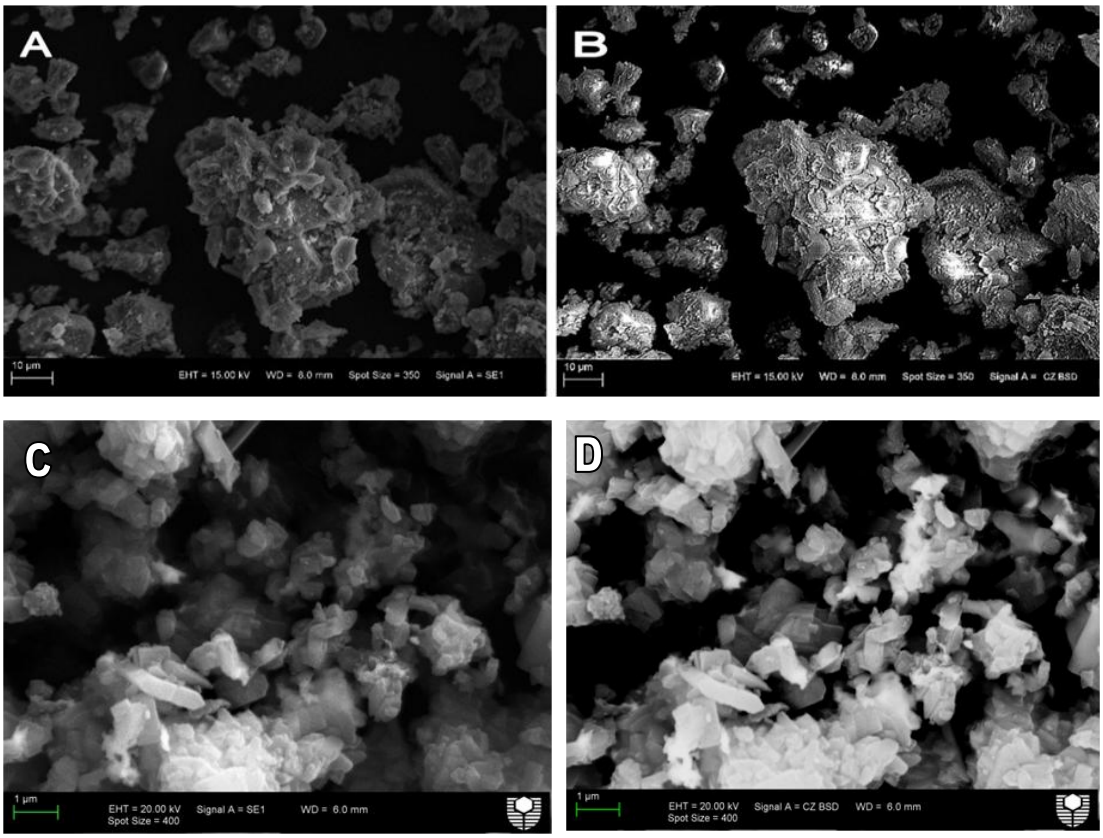

Figure 3.2 SEM images of RuO_2/AC and RuO_2/ZSM5, (A) SE Detector, Ru/AC, (B) BSE Detector, RuO_2/AC (C) SE Detector, RuO_2/ZSM5, and (D) BSE Detector, RuO_2/ZSM5.

Fig.3.3 displays EDS spectra of RuO_2/AC and RuO_2/ZSM5. C, Ru, O and K were found on RuO_2/AC. The presence of K may be due to the chemical activation process of carbon support using KOH. However, K does not affect catalyst activities in reducing phenol. For RuO_2/ZSM5, Si, Al, Ru, and

O are the major elements. Thus the EDS spectra suggest the presence of Ru on both catalysts, confirming XRD and SEM results.

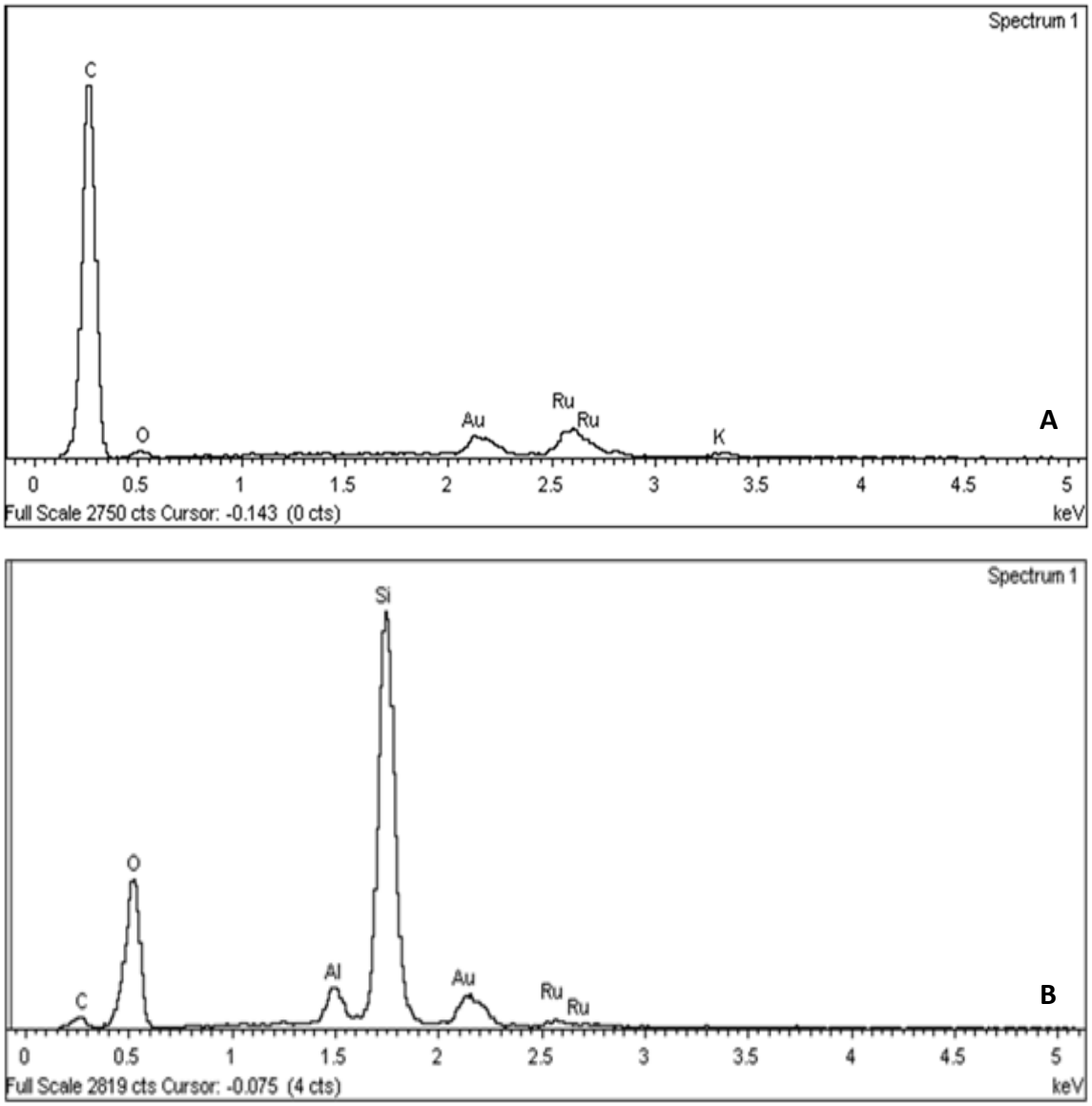

Figure 3.3 EDS spectra of Ru/AC and Ru/ZSM5. (A) Ru/AC , (B) Ru/ZSM5

The catalyst samples were also characterised by N_2 adsorption to identify pore size distribution and specific surface area (S_{BET}). Fig. 3.4 shows N_2 adsorption/desorption isotherms and pore size distributions of RuO_2/AC and RuO_2/ZSM5. As seen in Table 3.1, RuO_2/AC has a higher surface area (1178 m^2/g) than RuO_2/ZSM5 (386 m^2/g). RuO_2/AC also has a higher pore

volume (0.108 cm^3/g) than RuO_2/ZSM5 (0.085 cm^3/g). However, both RuO_2/AC and RuO_2/ZSM5 have a similar pore radius of 15.6 Å and 15.7 Å, less than 20 Å, which means they are microporous materials. The pore size distribution of RuO_2/AC presented two peaks, centred at 1.5 and 3.9 nm, respectively. RuO_2/ZSM-5, however, showed a different profile with three peaks, which are centred at 1.5, 2.9 and 6.3 nm, respectively.

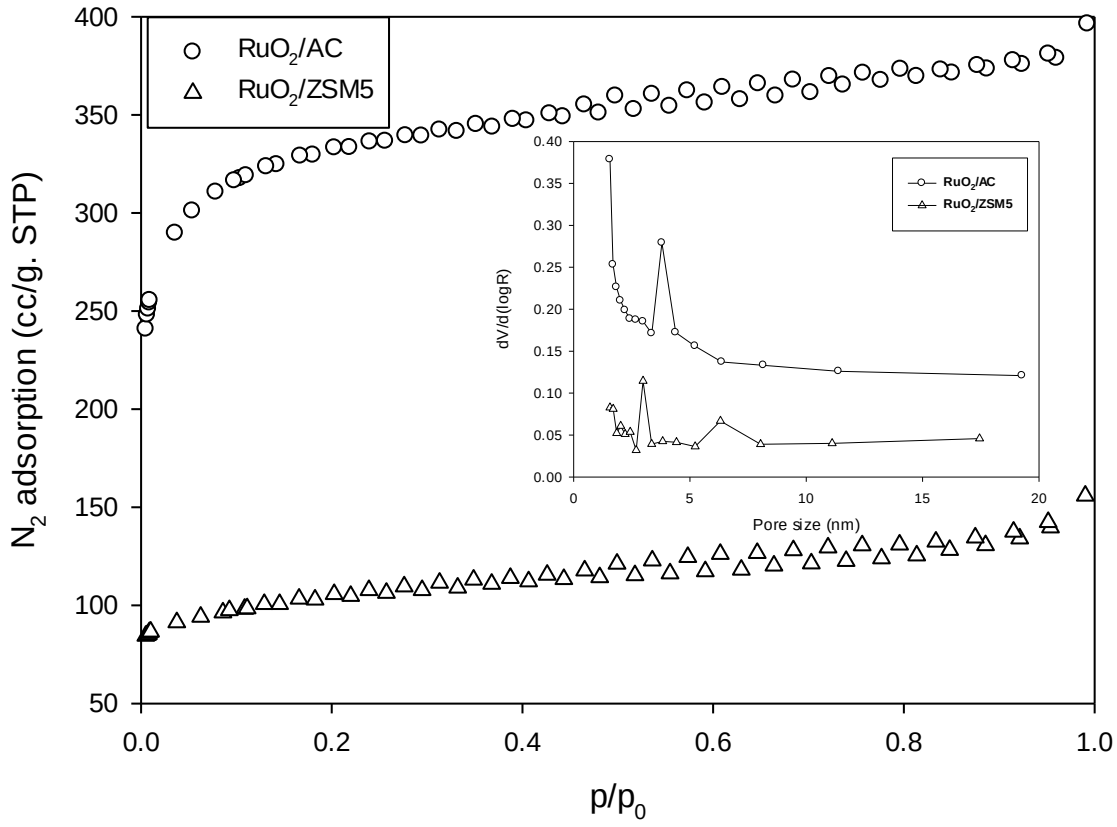

Figure 3.4 N_2 adsorption isotherm and pore size distribution of RuO_2/AC and RuO_2/ZSM5.

Table 3.1. Surface area, pore volume and pore radius of Ru O_2/AC and Ru O_2/ZSM5.

Catalyst	Surface Area (S_{BET}, m^2/g)	Pore Volume (cm^3/g)	Average Pore Radius (Å)
RuO_2/AC	1178	0.108	15.6
RuO_2/ZSM5	386	0.085	15.7

3.3.2 Preliminary study of phenol oxidation

Preliminary tests including adsorption and phenol degradation in aqueous solution on RuO_2/AC and RuO_2/ZSM5 are presented in Fig. 3.5. Generally, all the samples, AC, ZSM5, RuO_2/AC and RuO_2/ZSM5, can adsorb phenol compound despite of at low efficiency. Among them, AC has the highest efficiency in phenol adsorption with 34% removal in 2 h prior to reaching equilibrium. Lower adsorption efficiency of 10% in 2 h can be seen on ZSM5. AC has much higher surface area and pore volume than ZSM5, resulting in higher phenol adsorption. However, phenol adsorption on AC and ZSM5 was decreased when the materials were loaded by ruthenium. The phenol removal efficiencies on RuO_2/AC and RuO_2/ZSM5 were reduced to 27% and 6% in 2 h, respectively. The decrease in removal efficiency of both catalysts is caused by the decrease of surface area and pore volume when ruthenium was loaded covering the support surfaces.

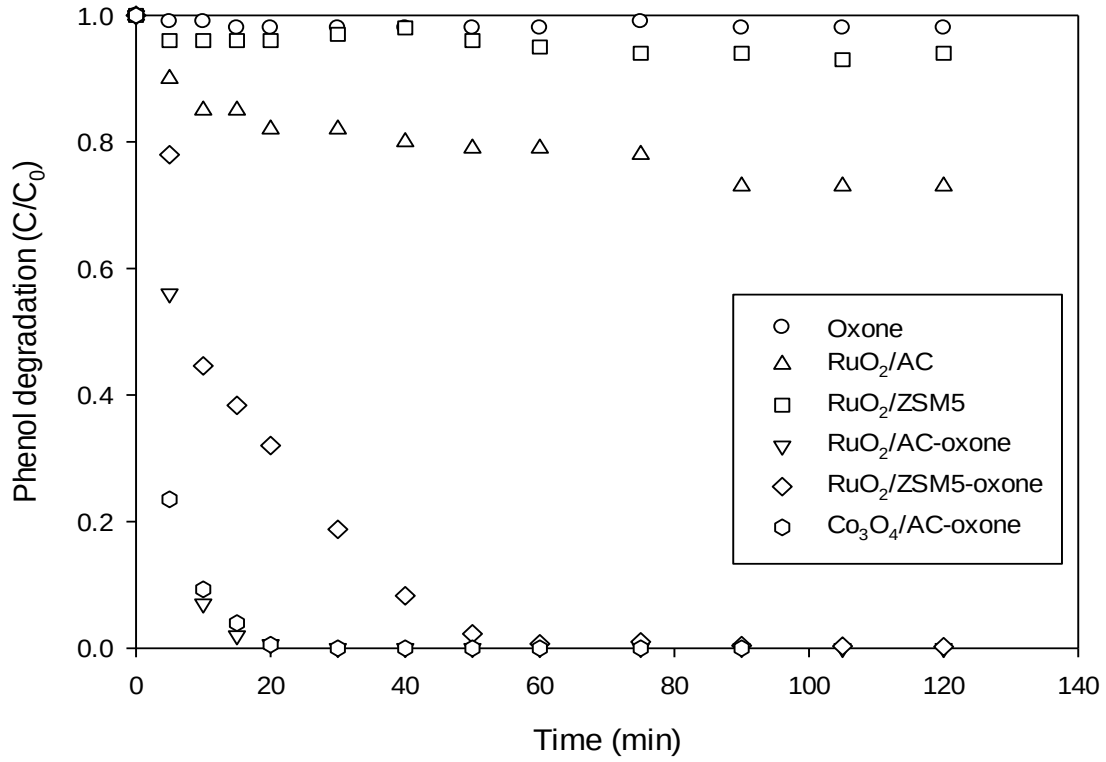

Figure 3.5 Phenol reduction with time in adsorption and catalytic oxidation. Reaction conditions: 0.2 g catalyst loading, 1 g Oxone® in 500 mL phenol solution of 50 ppm, 25 ^{0}C and stirring speed of 400 rpm.

In oxidation tests, addition of PMS without a catalyst did not induce phenol oxidation reaction. Phenol removal would occur when catalysts (RuO_2/AC and RuO_2/ZSM5) and oxidant (PMS) simultaneously were presented in the solution. In comparison of RuO_2/AC-Oxone® and RuO_2/ZSM5-Oxone® systems for phenol oxidation, RuO_2/AC-Oxone® exhibited much better performance producing complete removal of phenol in 20 min while Ru/ZSM5-Oxone® could completely remove phenol in 50 min. For a comparison, Co_3O_4/AC was also prepared and tested. It can be seen that Co_3O_4/AC catalyst exhibited faster initial rate in

phenol degradation, however, the efficiency was the same as RuO_2/AC. The complete removal of phenol could be reached in 20 min. Both catalysts have similar synthesis condition and the active metals of Ru and Co were 5wt% loaded on to AC support.

TOC removal in RuO_2/AC-Oxone® and RuO_2/ZSM5-Oxone® systems was also examined and the results showed that about 70% and 60% of TOC reductions were obtained for RuO_2/AC-Oxone® and RuO_2/ZSM5-Oxone®, respectively, within 1 h.

Anipsitakis and Dionysion [28] investigated several transition metals for activation of H_2O_2 and Oxone® and found that Co(II) and Ru(III) are the best metal catalysts for the activation of peroxymonosulphate. The reaction of Ru(III) with PMS can proceed as below.

$$Ru(III) + HSO_5^- \rightarrow Ru(IV) + SO_4^{-\bullet} + OH^- \quad 3.3$$

According to XRD examination, the major species of ruthenium in RuO_2/AC are Ru and RuO_2. Meanwhile, the ruthenium species in ZSM5 is mainly RuO_2. Thus, it is believed that they are the active sites for activation of peroxymonosulphate (PMS) to produce sulphate radicals in phenol oxidation system. The heterogeneous activation process is proposed as below.

$$S\text{-}Ru(IV) + HSO_5^- \rightarrow S\text{-}Ru(III) + SO_5^{-\bullet} + H^+ \quad \text{(S: solid surface)} \quad 3.4$$

$$S\text{-}Ru(III) + HSO_5^- \rightarrow S\text{-}Ru(IV) + SO_4^{-\bullet} + OH^- \quad 3.5$$

$$C_6H_5OH + SO_4^{-\bullet} \rightarrow \text{several steps} \rightarrow CO_2 + H_2O \quad 3.6$$

RuO_2/AC exhibited higher activity than RuO_2/ZSM5, which can be attributed to several factors. Fig. 3.5 shows that RuO_2/AC presented much high adsorption of phenol than RuO_2/ZSM5. This will promote surface reaction of phenol with sulphate radicals. Our previous investigation showed that AC could induce activation of PMS to produce $SO_5^{-\bullet}$ [11],

which can result in more reduction of phenol. In addition, the multi-valent Ru species (Ru and RuO_2) on AC could induce fast transformation of Ru and promote redox reactions of Ru (Ru-RuO_2) with PMS for formation of sulphate radicals.

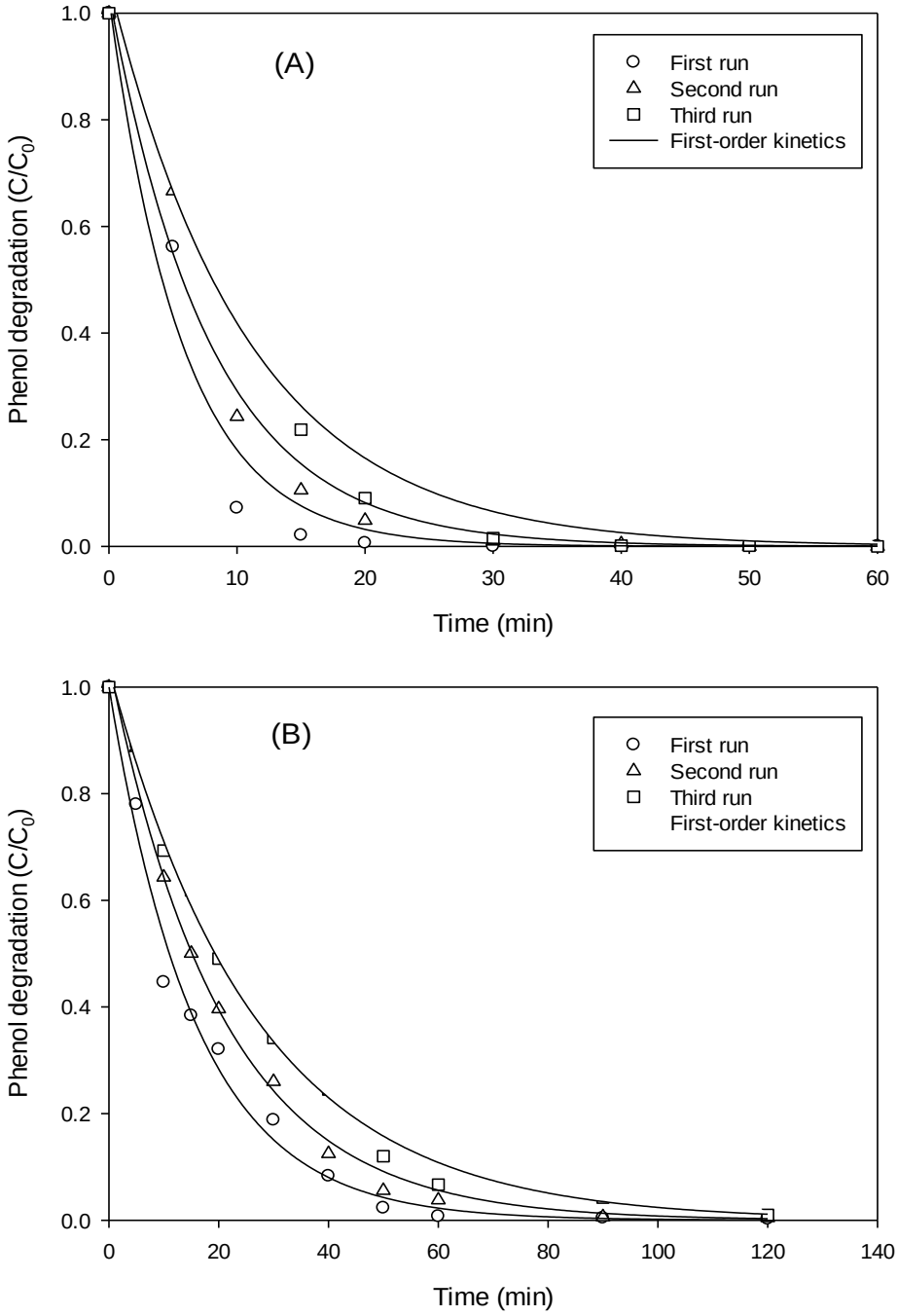

Figure 3.6 Phenol removal in multiple use of (A) RuO_2/AC and (B) RuO_2/ZSM5at 50 ppm, at 1 g Oxone®, 0.2 g catalyst, 25^{0}C.

Both RuO_2/AC and RuO_2/ZSM5 catalysts were also tested after their regeneration by water washing for multiple uses. It can be seen in Fig. 3.6 that, both catalysts showed somewhat deactivation in the second and third runs. However, the deactivation was not so significant. Complete removal of phenol could still be achieved within 1 h for RuO_2/AC and 2 h for RuO_2/ZSM5, respectively. The deactivation occurs presumably due to adsorption of intermediates and a small portion of loose ruthenium leaching from the supports of AC and ZSM5. Our previous investigations also showed that Co_3O_4/AC and Co_3O_4/ZSM5 presented strong stability in activation of PMS for phenol degradation, which is attributed to strong chemical binding of metal with the supports [5, 10].

Table 3.2 Kinetic constants of phenol degradation at different runs.

Catalyst	**Test**	**K (min^{-1})**	**R**
RuO_2/AC	1st run	0.174	0.983
	2nd run	0.130	0.990
	3rd run	0.0928	0.987
RuO_2/ZSM5	1st run	0.0631	0.994
	2nd run	0.0487	0.993
	3rd run	0.0376	0.997

For the reaction kinetics, a general equation of the pseudo first order kinetics was used, as shown in the following equation.

$$C = Co.e^{-k.t} \quad 3.7$$

Where K is the first order rate constant of phenol removal, C is the concentration of phenol at various time (t), C_o is the initial concentration of phenol.

Fig.3.6 also shows the first order kinetics fitting to experimental data and the kinetic constants are presented in Table 3.2. As seen, the experimental data were well fitted by the first-order kinetics with regression coefficients higher than 0.980. The rate constants *(K)* for RuO_2/AC are higher than those of RuO_2/ZSM5, which means RuO_2/AC is able to degrade phenol more rapidly. Several heterogeneous Co catalysts have been tested in PMS activation for phenol degradation. It was found that phenol degradation on Co/SiO_2 [15] and Co/ZSM5 [10] presented zero order kinetics while Co/AC showed the first order kinetics [11].

3.3.3 Effects of reaction parameters on phenol removal

The first parameter measured in this study was phenol concentration which was maintained between 25 - 100 ppm. Fig. 3.7A shows variation of phenol concentration with time at different initial concentrations. Removal efficiency of phenol decreased with increasing phenol concentration. For RuO_2/AC, 100% removal of phenol could be achieved within 20 min at low phenol concentrations (25 - 50 ppm). However, phenol removal was reduced at about 83% in 2 h for 100 ppm phenol. A similar trend can also be seen in Fig. 3.7B using RuO_2/ZSM5. At phenol concentration of 25 -50 ppm, complete removal occurred within 60 min, but for phenol concentration of 100 ppm, removal efficiency was only 52% within 2 h.

In phenol degradation, production of sulphate radicals is the key reaction, which depends on Ru catalysts and PMS (Eqs.4-5). Under the same loading of catalyst and PMS, high phenol concentration would take more time to be degraded, resulting in lower removal efficiency of phenol.

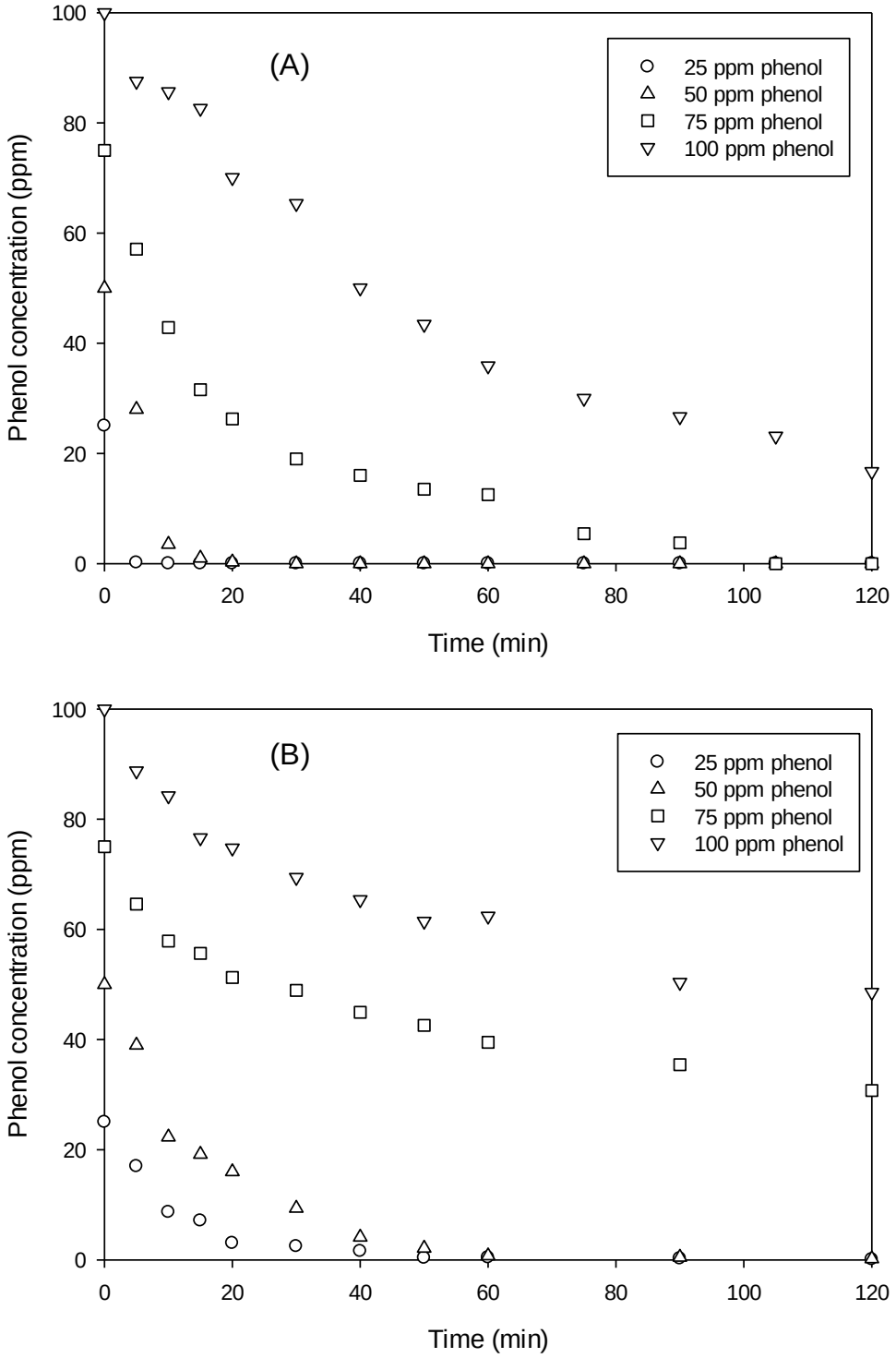

Figure 3.7 Effect of phenol concentration on phenol removal. (A) RuO_2/AC and (B) RuO_2/ZSM5. Reaction conditions: 1 g Oxone®, 0.2 g catalyst, 25 ^{0}C.

Fig. 3.8 shows the effect of catalyst loading on phenol degradation. High catalyst loading in solution would result in higher phenol reduction. This phenomenon is reasonable, because increasing the amount of catalyst will increase the adsorption and also the available catalyst sites to activate PMS. Therefore, the addition of catalysts will increase reaction rate significantly. For RuO_2/AC at 0.1 – 0.4 g/L, complete removal could be achieved within 60 min. For RuO_2/ZSM5, phenol removal was much lower at 0.2 – 0. 3 g/L, but it increased significantly at 0.4 -0.6 g/L. At the loading of 0.4 -0.6 g/L RuO_2/ZSM5 in solution, phenol removal was similar and complete removal could happen in 60 min suggesting an optimal loading of RuO_2/ZSM5 to be 0.4 g/L.

Further, Fig. 3.9 shows that increased concentration of PMS in a solution will accelerate phenol removal significantly on RuO_2/AC and RuO_2/ZSM5. For example, at 0.5 g Oxone®, complete removal of phenol could be achieved in about 90 min. However, an increase in phenol degradation would be very fast when 1 g Oxone® was used where the complete removal occurred within 20 min, an increase of phenol removal rate as high as 4 times. A similar change was seen in Fig. 3.9B for RuO_2/ZSM5. Complete removal was not obtained within 2 h at 0.25 and 0.5 g Oxone® in solution. In contrast, at 1 g Oxone® in solution, complete removal of phenol could occur in about 60 min. The increase of reaction rate at the increased Oxone® concentration is attributed to higher production rate of sulphate radicals for reducing phenol concentration.

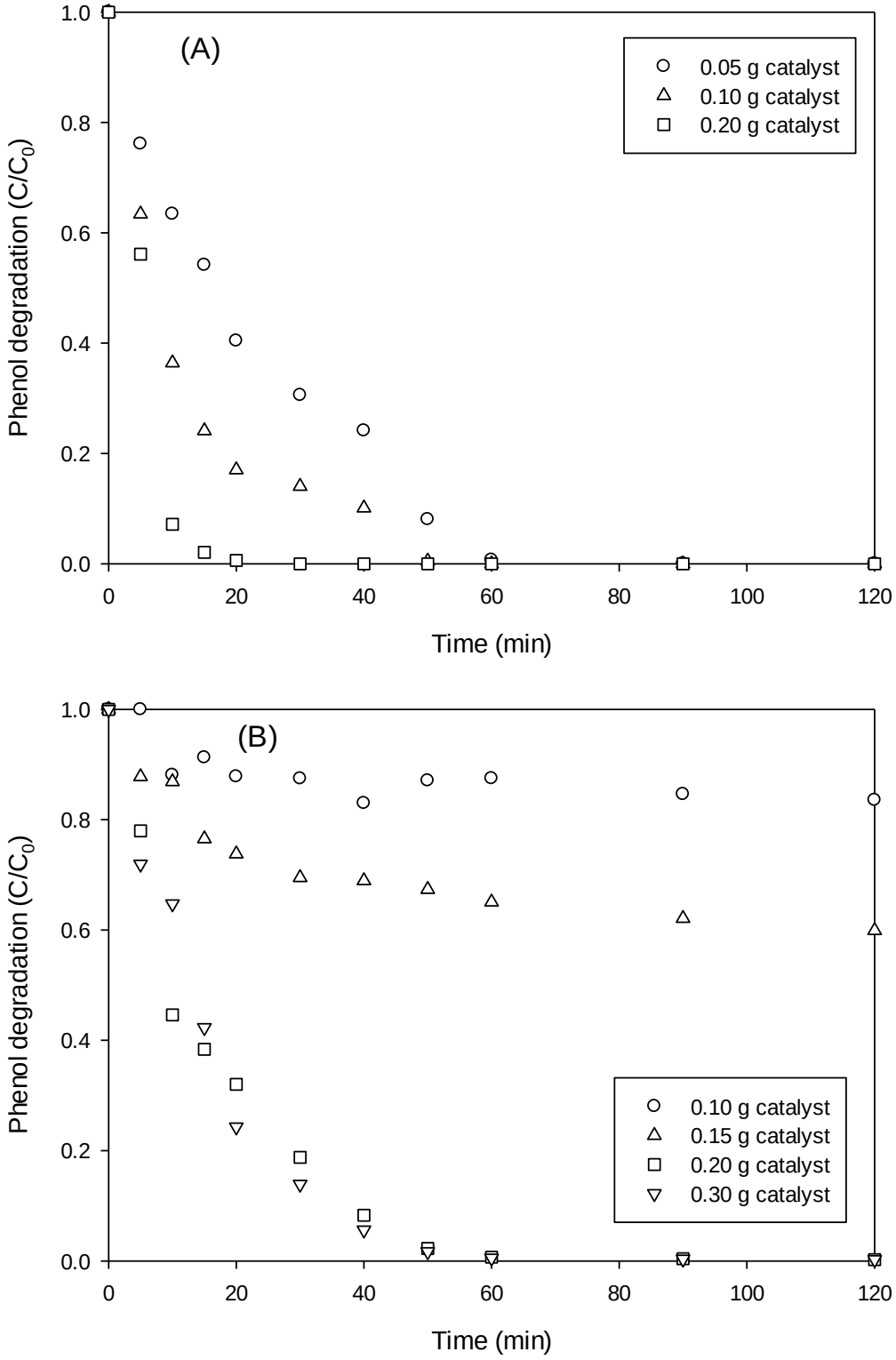

Figure 3.8 Effect of catalyst loading on phenol removal, (A) RuO_2/AC and (B) RuO_2/ZSM5. Reaction conditions: 50 ppm, 1 g Oxone®, 25^0C.

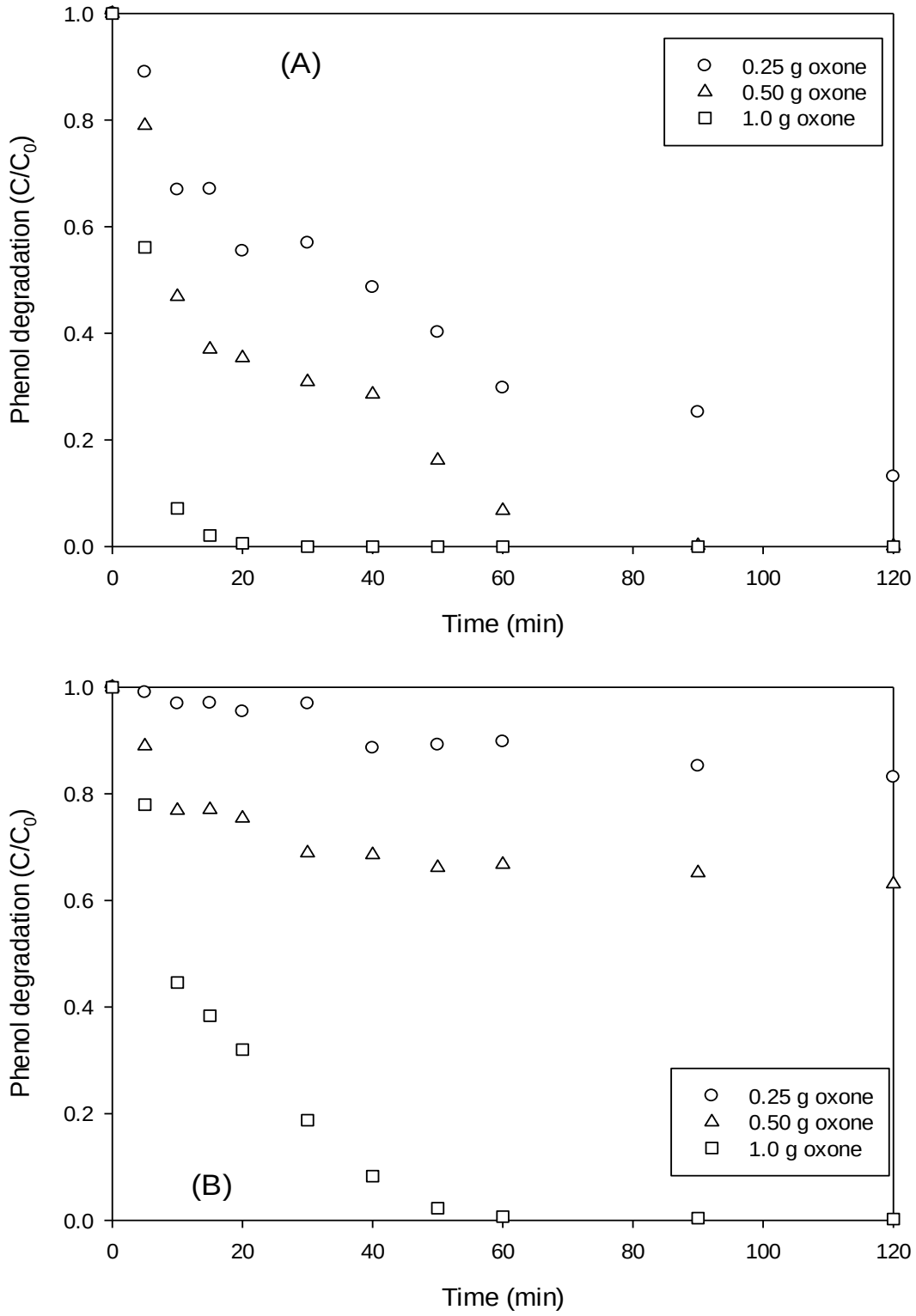

Figure 3.9 Effect of Oxone® concentration on phenol removal, (A) RuO_2/AC and (B) RuO_2/ZSM5. Reaction conditions: 50 ppm, 0.2 g catalyst, 25 ^{0}C.

Effect of reaction temperature on phenol degradation is shown in Fig. 3.10. As can be seen, temperature showed quite significant impact on phenol oxidation process using either RuO_2/AC or RuO_2/ZSM5. An increase in temperature of 10 ^oC would enhance the reaction rate and phenol degradation efficiency by about two times. For example, a complete removal of phenol with Ru/AC-Oxone® at temperature of 25 ^oC was achieved in about 20 min. When the temperature was raised to 35 ^oC, complete removal of phenol would be achieved in about 10 min. Similarly, at temperatures of 45 ^oC, complete removal could be achieved in about 5 min. A same trend also occurred on Ru/ZSM5 as shown in Fig. 3.10B. At 45 ^oC, phenol degradation would reach 100% at 30 min.

Table 3.3 Activation energies of heterogeneous Co catalysts with PMS for phenol degradation.

Catalyst	Activation energy (kJ/mol)	Reference
Co/SiO2	61.7- 75.5	[15]
Co/SBA-15	67.4	[29]
Co/ZSM5	69.7	[10]
Co/AC	59.7	[11]
Co/CX	48.3- 62.9	[30]
RuO_2/AC	61.4	This work
RuO_2/ZSM5	42.2	This work

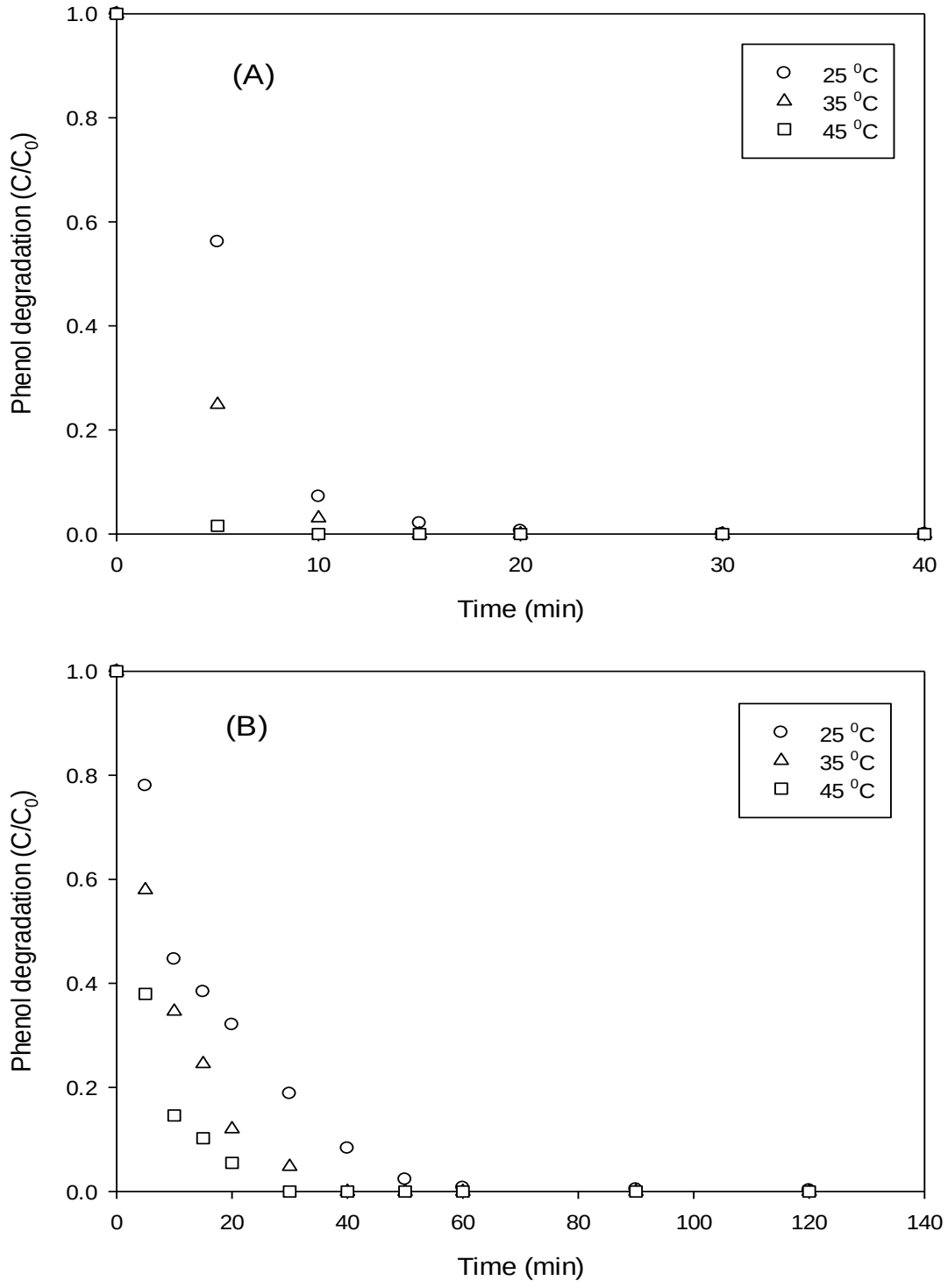

Figure 3.10 Effect of temperature on phenol removal, (A) RuO_2/AC and (B) RuO_2/ZSM5. Reaction conditions: 50 ppm, 1 g Oxone®, 0.2 g catalyst.

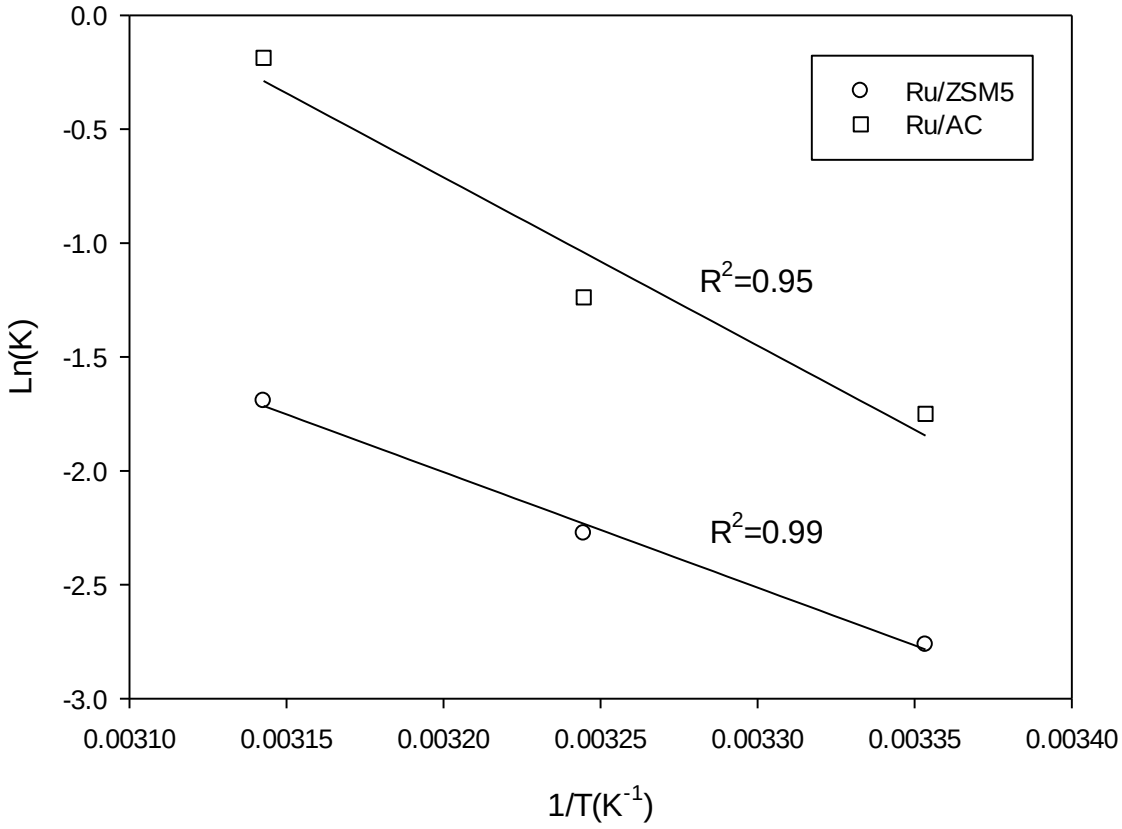

Figure 3.11 Arrhenius plots of phenol degradation on RuO_2/AC and RuO_2/ZSM5.

Fig. 3.11 displays the Arrhenius plots of rate constants with temperature for RuO_2/AC and RuO_2/ZSM5. As shown, the plots presented a good linear correlation and the activation energies for RuO_2/AC and RuO_2/ZSM5 were derived as 61.4 and 42.2 kJ/mol, respectively. Previously, we have investigated several heterogeneous Co catalysts, Co/AC, Co/CX(carbon-xerogel), Co-exchanged ZSM5 (Co-ZSM5), and Co/SiO_2 in phenol degradation by Oxone®. Table 3.3 lists the activation energies of those catalysts. It is shown that Ru/AC has the similar activation energy as Co/AC while Ru/ZSM5 presents lower activation energy than that of Co-ZSM5.

3.4 Conclusions

Activated Carbon (AC) and ZSM5 supported Ruthenium (Ru) catalysts have been successfully synthesised using impregnation method followed by calcination at temperature of 550 ^{0}C. Pore size distribution and specific surface area (S_{BET}) have been identified that RuO_2/AC has a higher surface area (1178 m^2/g) than RuO_2/ZSM5 (386 m^2/g). Further, RuO_2/AC also has a higher pore volume (0.108 cm^3/g) than RuO_2/ZSM5 (0.085 cm^3/g). However, both RuO_2/AC and RuO_2/ZSM5 have a similar pore radius of 15.6 Å and 15.7 Å. RuO_2/AC and RuO_2/ZSM5 are effective catalysts for activation of PMS for the production of sulphate radicals for phenol degradation. RuO_2/AC has better performance of removing phenols than RuO_2/ZSM5. Phenol removal on RuO_2/AC is a combination of oxidation and adsorption. Both catalysts also showed good performance in the second and third runs after regeneration for multiple uses. The concentration of phenol, catalyst loading, concentration of Oxone®, and temperature are important parameters that affect the reaction rate in removing phenol. Kinetic studies showed that phenol oxidation on the catalysts, RuO_2/AC or RuO_2/ZSM5, follows the first order reaction with activation energies of 61.4 and 42.2 kJ/mol, respectively.

References

1. A. Fortuny, J. Font, A. Fabregat, Wet air oxidation of phenol using active carbon as catalyst, Applied Catalysis B-Environmental, 19 (1998) 165-173.

2. S. Chiron, A. Fernandez-Alba, A. Rodriguez, E. Garcia-Calvo, Pesticide chemical oxidation: state-of-the-art, Water Res., 34 (2000) 366-377.

3. A. Camporro, M.J. Camporro, J. Coca, H. Sastre, Regeneration of an activated carbon bed exhausted by industrial phenolic waste-water, J. Hazard. Mater., 37 (1994) 207-214.

4. S. Wang, A comparative study of Fenton and Fenton-like reaction kinetics in decolourisation of wastewater, Dyes and Pigments, 76 (2008) 714-720.

5. P.R. Shukla, S. Wang, H. Sun, H.M. Ang, M. Tade, Activated carbon supported cobalt catalysts for advanced oxidation of organic contaminants in aqueous solution, Applied Catalysis B-Environmental, 100 (2010) 529-534.

6. K.H. Chan, W. Chu, Degradation of atrazine by cobalt-mediated activation of peroxymonosulfate: Different cobalt counteranions in homogenous process and cobalt oxide catalysts in photolytic heterogeneous process, Water Research, 43 (2009) 2513-2521.

7. G.P. Anipsitakis, D.D. Dionysiou, Degradation of organic contaminants in water with sulfate radicals generated by the conjunction of peroxymonosulfate with cobalt, Environmental Science & Technology, 37 (2003) 4790-4797.

8. G.P. Anipsitakis, D.D. Dionysiou, Transition metal/UV-based advanced oxidation technologies for water decontamination, Applied Catalysis B-Environmental, 54 (2004) 155-163.

9. G.P. Anipsitakis, E. Stathatos, D.D. Dionysiou, Heterogeneous activation of oxone using Co_3O_4, Journal of Physical Chemistry B, 109 (2005) 13052-13055.

10. P. Shukla, S. Wang, K. Singh, H.M. Ang, M.O. Tade, Cobalt exchanged zeolites for heterogeneous catalytic oxidation of phenol in the presence of peroxymonosulphate, Applied Catalysis B-Environmental, 99 (2010) 163-169.

11. P.R. Shukla, S.B. Wang, H.Q. Sun, H.M. Ang, M. Tade, Activated carbon supported cobalt catalysts for advanced oxidation of organic contaminants in aqueous solution, Applied Catalysis B-Environmental, 100 (2010) 529-534.

12. X.Y. Chen, J.W. Chen, X.L. Qiao, D.G. Wang, X.Y. Cai, Performance of nano-Co_3O_4/peroxymonosulfate system: Kinetics and mechanism study using Acid Orange 7 as a model compound, Applied Catalysis B-Environmental, 80 (2008) 116-121.

13. Q.J. Yang, H. Choi, Y.J. Chen, D.D. Dionysiou, Heterogeneous activation of peroxymonosulfate by supported cobalt catalysts for the degradation of 2,4-dichlorophenol in water: The effect of support, cobalt precursor, and UV radiation, Applied Catalysis B-Environmental, 77 (2008) 300-307.

14. W. Zhang, H.L. Tay, S.S. Lim, Y.S. Wang, Z.Y. Zhong, R. Xu, Supported cobalt oxide on MgO: Highly efficient catalysts for degradation of organic dyes in dilute solutions, Applied Catalysis B-Environmental, 95 (2010) 93-99.

15. P. Shukla, H.Q. Sun, S.B. Wang, H.M. Ang, M.O. Tade, Nanosized Co_3O_4/SiO_2 for heterogeneous oxidation of phenolic contaminants in waste water, Separation and Purification Technology, 77 (2011) 230-236.

16. L. Hu, X. Yang, S. Dang, An easily recyclable Co/SBA-15 catalyst: Heterogeneous activation of peroxymonosulfate for the degradation of phenol in water, Applied Catalysis B-Environmental, 102 (2011) 19-26.

17. Q. Yang, H. Choi, S.R. Al-Abed, D.D. Dionysiou, Iron-cobalt mixed oxide nanocatalysts: Heterogeneous peroxymonosulfate activation, cobalt leaching, and ferromagnetic properties for environmental applications, Applied Catalysis B-Environmental, 88 (2009) 462-469.

18. K. Pirkanniemi, M. Sillanpaa, Heterogeneous water phase catalysis as an environmental application: a review, Chemosphere, 48 (2002) 1047-1060.

19. L. Oliviero, J. Barbier-Jr, D. Duprez, A. Guerrero-Ruiz, B. Bachiller-Baeza, I. Rodriguez-Ramos, Catalytic wet air oxidation of phenol and acrylic acid over Ru/C and Ru-CeO_2/C catalysts, Applied Catalysis B-Environmental, 25 (2000) 267-275.

20. A. Cybulski, J. Trawczynski, Catalytic wet air oxidation of phenol over platinum and ruthenium catalysts, Applied Catalysis B-Environmental, 47 (2004) 1-13.

21. Z. Kowalczyk, S. Jodzis, J. Sentek, Studies on kinetics of ammonia synthesis over ruthenium catalyst supported on active carbon, Applied Catalysis a-General, 138 (1996) 83-91.

22. P. Gallezot, S. Chaumet, A. Perrard, P. Isnard, Catalytic wet air oxidation of acetic acid on carbon-supported ruthenium catalysts, Journal of Catalysis, 168 (1997) 104-109.

23. M. Carrier, M. Besson, C. Guillard, E. Gonze, Removal of herbicide diuron and thermal degradation products under catalytic wet air oxidation conditions, Applied Catalysis B-Environmental, 91 (2009) 275-283.

24. D.P. Minh, P. Gallezot, M. Besson, Degradation of olive oil mill effluents by catalytic wet air oxidation - 1. Reactivity of p-coumaric acid over Pt and Ru supported catalysts, Applied Catalysis B-Environmental, 63 (2006) 68-75.

25. W.-M. Liu, Y.-Q. Hu, S.-T. Tu, Active carbon-ceramic sphere as support of ruthenium catalysts for catalytic wet air oxidation (CWAO) of resin effluent, J. Hazard. Mater., 179 (2010) 545-551.

26. K.H. Kim, S.K. Ihm, Heterogeneous catalytic wet air oxidation of refractory organic pollutants in industrial wastewaters: A review, J. Hazard. Mater., 186 (2011) 16-34.

27. S. Wang, G.Q. Lu, Effects of acidic treatments on the pore and surface properties of Ni catalyst supported on activated carbon, Carbon, 36 (1998) 283-292.

28. G.P. Anipsitakis, D.D. Dionysiou, Radical generation by the interaction of transition metals with common oxidants, Environmental Science & Technology, 38 (2004) 3705-3712.

29. P. Shukla, H. Sun, S. Wang, H.M. Ang, M.O. Tadé, Co-SBA-15 for heterogeneous oxidation of phenol with sulfate radical for wastewater treatment, Catalysis Today, 175 (2011) 380-385.

30. H. Sun, H. Tian, Y. Hardjono, C.E. Buckley, S. Wang, Preparation of cobalt/carbon-xerogel for heterogeneous oxidation of phenol, Catalysis Today, 186 (2011) 63-68.

Chapter-4

Coal Fly Ash Supported Co_3O_4 catalysts for phenol degradation using peroxymonosulfate

Abstract

Several fly ash (FA) samples derived from Australian (FA-WA) and Brazilian coals (FA-JL and FA-CH) were used as supports to prepare Co oxide (Co)-based catalysts. These Co/FA catalysts were tested in peroxymonosulfate activation for sulphate radical generation and phenol degradation in aqueous solution. The physicochemical properties of FA supports and Co/FA catalysts were characterised by N_2 adsorption, X-ray diffraction (XRD), scanning electron microscopy coupling with energy dispersive spectroscopy (SEM-EDS), elemental mapping, and UV-vis diffuse reflectance spectroscopy. It was found that FA supports did not show adsorption of phenol and could not activate peroxymonosulfate for sulphate radical generation. However, fly ash supported Co oxide catalysts (Co/FA) presented higher activities in activation of peroxymonosulfate for phenol degradation than bulk Co oxide and their activities varied depending on the properties of fly ash supports. Co/FA-JL showed the highest activity while Co/FA-WA showed the lowest activity. Activation energies of phenol degradation on three Co/FA catalysts were obtained to be 47.0, 56.5, 56.0 kJ/mol for Co/FA-WA, Co/FA-JL and Co/FA-CH, respectively.

4.1 Introduction

Currently, large amounts of solid wastes are produced from various industries. Fly ash coming from coal, oil and biomass combustion is one of the major solid wastes and the current practice is disposal in landfills or dumping at sea. In the past years, fly ash has been explored for several applications in adsorption [1-3], material synthesis such as zeolites [4-6], geopolymers [7-9], ceramics [10, 11], and catalysis as supports [12-14].

Wastewater contains many different pollutants, such as dusts, metal ions, and organic compounds. Removal of organic pollutants is an important process in water and wastewater treatments. The processes for organic removal include adsorption, flocculation, membrane separation and oxidation. In the last decades, advanced oxidation processes (AOPs) have emerged as effective techniques to degrade organic compounds for wastewater treatment. Currently, most of AOPs are based on the generation of very reactive species, such as hydroxyl radicals (OH•) that can oxidise a broad range of pollutants quickly and non selectively [15-17]. Apart from OH•, sulphate radicals have been attracting high interest and proposed as an alternative due to their higher oxidation potential [18].

Sulfate radicals can be generated from two oxidants, persulfate and peroxymonosulfate (PMS). For the activation of persulfate and peroxymonosulfate, metal ions are generally used, as shown in the following equations [19, 20].

$$M^{n+} + HSO_5^- \rightarrow M^{(n+1)+} + SO_4^{\bullet-} + OH^- \quad 4.1$$

$$M^{n+} + S_2O_8^{2-} \rightarrow M^{(n+1)+} + SO_4^{\bullet-} + SO_4^{2-} \quad 4.2$$

For peroxymonosulfate activation to produce sulfate radicals, it has been found that homogeneous Co^{2+} is the best metal ion. However, Co^{2+} could

cause environmental problems if presence in water. Heterogeneous activation of peroxymonosulfate would provide a good solution. In the past years, several supported Co systems have been investigated and show high activity [21-28].

Resource recovery is one of the effective strategies in waste management. Using solid wastes for other applications provides a route for solid waste recycle and reduction in waste disposal to landfills, bringing in environmental benefits and economic profits. In this chapter, we report an investigation of preparation of Co oxide catalysts on different sourced fly ash (FA) samples. We will study the effects of fly ash structure and property on the Co/FA catalysts in activation of peroxymonosulfate for sulfate radical production in phenol degradation.

4.2 Experimental section

4.2.1 Materials and catalyst preparation

Fly ash samples were obtained from a coal-fired power station in Western Australia (WA) and two coal-fired power stations, Charqueadas Power Plant (CH) and Jorge Lacerda Power Plant (JL), Brazil. These fly ash samples were labelled as FA-WA, FA-CH, and FA-JL, respectively. Phenol, cobalt nitrate ($Co(NO_3)_2 \bullet 6H_2O$), and oxone ($2KHSO_5 \cdot KHSO_4 \cdot K_2SO_4$) were obtained from Sigma-Aldrich. A stock solution of phenol at 1000 ppm was prepared using deionised water.

Cobalt oxide (Co_3O_4) was obtained by thermally decomposition of $Co(NO_3)_2$ at 500 ^oC for 2 h. For synthesis of Co loaded catalysts, an impregnation method was used. Typically, 1.23 g of $Co(NO_3)_2 \bullet 6H_2O$ were dissolved in 100 mL of ultrapure water. The amount of 1.23 g of $Co(NO_3)_2 \bullet 6H_2O$ is based on molecular calculation to achieve Co/FA catalyst ratio with Co loading of 5wt%. Then 5 g of FAs were added

followed by stirring continuously at 80 °C until total evaporation of H_2O occurred. Furthermore, the sample was dried at 120 °C overnight and calcined at 500 °C for 4 h in air. Then the catalyst was stored in a desiccator until use. In the Co/FA samples, Co loading was kept at 5 wt%.

4.2.2 Characterisation

The crystalline structure of FA and Co/FA powders was characterised by an X-ray diffractometer (XRD, Bruker D8 Advance) equipped with Cu Kα radiation, at accelerating voltage and current of 40 kV and 40 mA, respectively. The surface area was measured by N_2 adsorption/desorption analyser (Quantachrome Nova – 1200). Prior to adsorption, samples were degassed under high vacuum at 150 °C for 12 h. The BET surface areas were obtained by applying the BET equation to the nitrogen adsorption data. For measurements of sample pH, fly ash samples (0.1 g) were placed in 10 mL of deionised water and the mixture was stirred for 24 h in a shaker at 120 rpm. After filtration, the pH of the solutions was measured with a pH meter (MSTecnopon - Mod MPA 210). In cation exchange capacity (CEC) measurements, the samples were saturated with sodium acetate solution (1 M), washed with distilled water (1 L) and then mixed with ammonium acetate solution (1 M). The sodium ion concentration of the resulting solution was determined by optical emission spectrometry with inductively coupled plasma – ICP-OES (Spedtroflame - M120).

The UV-visible diffuse reflectance spectra (DRS) were recorded on a V-570 UV-visible spectrometer (Jasco, Japan) equipped with an integrating sphere, in which $BaSO_4$ was used as a reference material. Scanning electron microscopy (SEM), performed on a Neon 40EsB FIBSEM (Zeiss, Germany), was used to evaluate the morphology, size and textural information of the samples. The integrated energy dispersive spectroscopy

(EDS) and elemental mapping (cobalt) were applied to analyse the dispersion of cobalt in the Co/FA samples.

4.2.3 Catalytic evaluation

Phenol degradation tests were carried out at 25-45 °C in 1 L glass vessel with 500 mL of phenol solution at varying concentrations (ppm) with a constant stirring of 400 rpm. Firstly, 0.20 g catalyst was added into the phenol solution for a while, then oxone was added into the solution at 2 g/L, otherwise indicated. At certain time, water sample (1 mL) was withdrawn into a HPLC vial, 0.5 mL of pure methanol was injected into the vial to quench the reaction. The concentration of phenol was analysed using a Varian HPLC with a UV detector set at λ = 270 nm. A C–18 column was used to separate the organics while the mobile phase with a flowrate of 1.5 mL/min was made of 30% CH_3CN and 70% water. For selected samples, total organic carbon (TOC) was obtained using a Shimadzu TOC-5000 CE analyser.

4.3 Results and discussion

4.3.1 Characterisation of FA supports and Co/FA catalysts

The chemical compositions of three fly ash samples (by weight%) are given in Table 4.1. Fly ash is mainly composed of metal oxides derived from inorganic compounds in coals. Major constituents for all fly ash samples are: SiO_2, Al_2O_3, and Fe_2O_3. The contents of SiO_2 and Al_2O_3 are above 70% for all samples. SiO_2/Al_2O_3 for the three samples is in the order of FA-WA>FA-CH>FA-JL. Higher SiO_2/Al_2O_3 could result in lower pH of solids due to acidity of SiO_2. A comparison of three fly ashes shows that FA-CH has the highest SiO_2 and Al_2O_3 contents but the lowest content of Fe_2O_3. FA-JL has the medium contents of Al_2O_3 and Fe_2O_3, but it has the highest

contents of K_2O, CaO, and MgO. FA-WA has the highest content of Fe_2O_3 but low contents of K_2O, CaO, and MgO.

Table 4.1 Chemical composition (wt%) of fly ash samples obtained from Australian and Brazilian thermal power plants

Components	FA-WA	FA-JL	FA-CH
SiO_2	55.0	50.3	57.5
Al_2O_3	29.3	29.8	32.6
Fe_2O_3	8.8	6.70	3.60
K_2O	0.4	5.30	2.00
CaO	1.6	2.70	1.40
TiO_2	-	2.20	1.60
SO_3	0.1	1.40	0.40
MgO	1.0	1.10	0.70
Na_2O	0.3	-	-
SiO_2/Al_2O_3	1.88	1.69	1.76

The physicochemical properties of three fly ashes are presented in Table 4.2. FA-JL and FA-CH show much high pH, larger than 7, while FA-WA shows lower pH, less than 4. This suggests that FA-JL and FA-CH demonstrate strong basic surface and FA-WA presents acidic surface. This is attributed to the different chemical compositions of the FA samples. Table 4.1 indicates that FA-JL and FA-CH have higher contents of Al_2O_3, K_2O, CaO and MgO, which are basic oxides, making them strong basicity. FA-JL has the highest contents of K_2O, CaO and MgO and thus presenting the highest pH. For LOI (Loss of Ignition) and surface area, FA-JL and FA-WA have higher values than FA-CH. In general, LOI is the indicator of unburned carbon content. Unburned carbons are porous materials formed during high-temperature processing, which will make FA having high surface area. For the three FA samples, CEC is much similar.

Table 4.2 Characteristics of coal fly ashes from Brazil and Australia

Sample	pH	Loss on ignition(LOI) (%)	S_{BET} (m^2/g)	CEC (meq/g)
FA-JL	8.0	15.1	9.6	0.026
FA-CH	7.8	2.60	3.3	0.026
FA-WA	3.7	5.2	15.6	0.029

Fig. 4.1 shows XRD patterns of FA samples and their supported Co catalysts. Three fly ashes show very similar patterns and the crystalline phases were identified mainly as mullite, quartz and minors as hematite and magnetite, which are confirmed from their chemical compositions (Table 4.1). For Co/FA catalysts, Co_3O_4 peaks were identified on all samples, which is due to the decomposition of $Co(NO_3)_2$. It has been reported that $Co(NO_3)_2$ decomposition will produce CoO, Co_2O_3 and Co_3O_4 and that the final product is Co_3O_4. XRD results thus showed that only Co_3O_4 was presented on Co/FA catalysts.

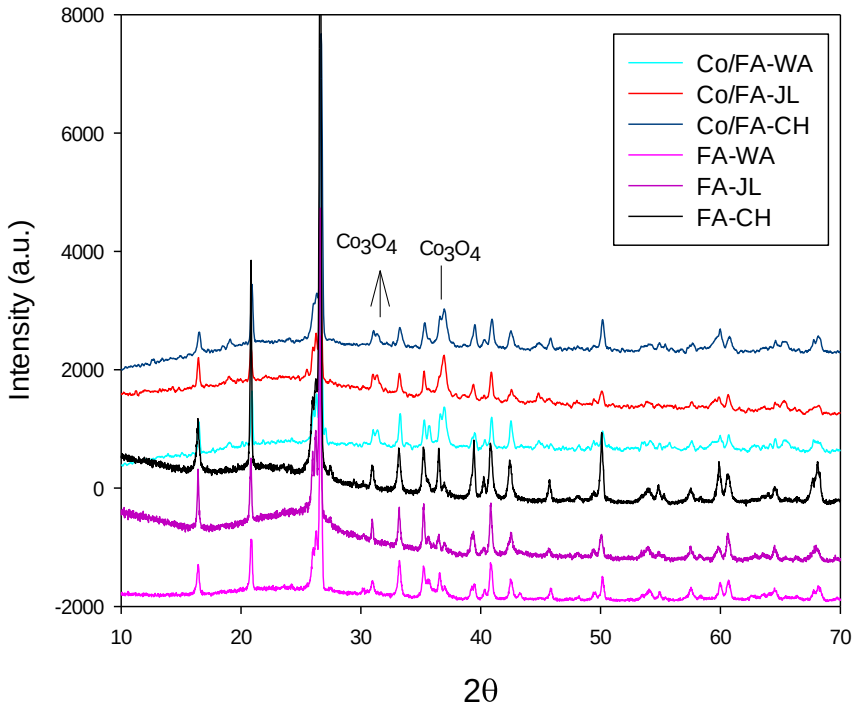

Figure 4.1 XRD patterns of fly ash and their supported Co catalysts.

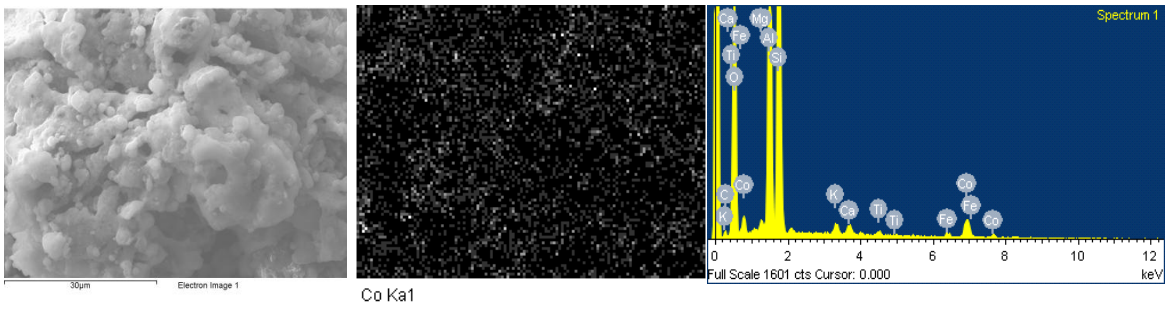

Co/FA-CH

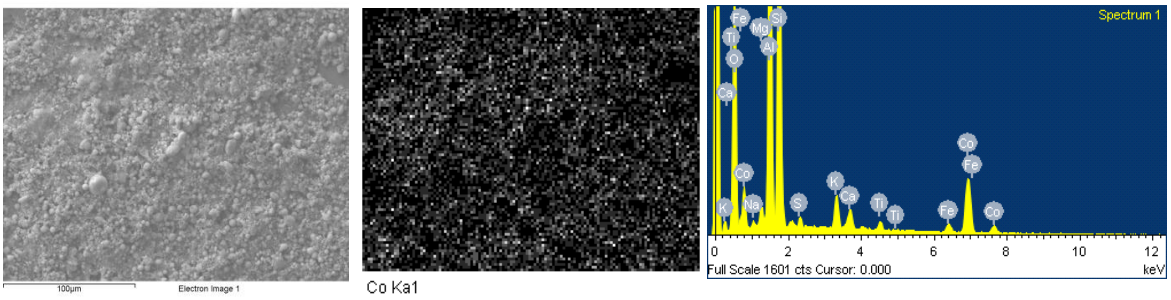

Co/FA-JL

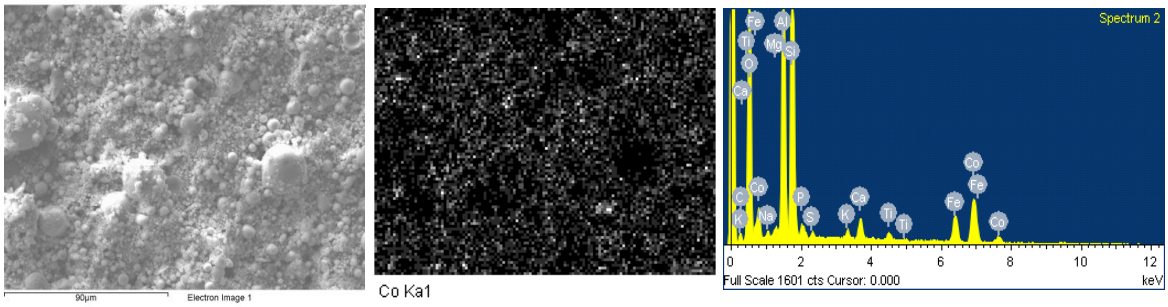

Co/FA-WA

Figure 4.2 SEM micrographs, EDS and Co elemental mapping of Co/FA catalysts.

Fig. 4.2 shows SEM micrographs, EDS spectra and Co elemental mapping of three Co/FA catalysts. As shown, most particles of Co/FA-JL and Co/FA-WA catalysts presented as spherical particles while the particles of Co/FA-CH presented as irregular shape. EDS spectra of three catalysts showed the presence of C, O, Si, Al, Fe, Na, K, Ti, Mg, Ca, S, and Co on catalysts. Co loadings on three catalysts were derived as 5.4, 3.5 and 11.9 wt% on

Co/FA-WA, Co/FA-CH and Co/FA-JL, respectively. Elemental mapping also showed the distribution of Co on the catalysts. Co on Co/FA-JL was much homogeneously distributed on the surface. Co on Co/FA-CH also showed well dispersion but the intensity seemed lower than that on Co/FA-JL. However, Co on Co/FA-WA seemed to have some large black spots, which suggested that Co was not well distributed compared with other two catalysts.

Fig. 4.3 shows UV-vis diffuse reflectance spectra of three Co/FA catalysts. One can see that Co/FA-JL and Co/FA-CH showed much similar profiles and Co/FA-WA presented differently. For Co/FA-WA, two strong and broad bands centred at 400 and 700 nm were observed, which indicate the formation of Co_3O_4. The first band at ca. 400 nm can be assigned to the ligand-metal charge transfer (i.e., $O^2 \rightarrow Co^{2+}$), while the band at about 700 nm is corresponding to the $O^{2-} \rightarrow Co^{3+}$ charge transfer [29, 30]. However, for Co/FA-JL and Co/FA-CH, the first broad band is centred at 460 nm, which suggests the presence of Co^{2+} in tetrahedral coordination.

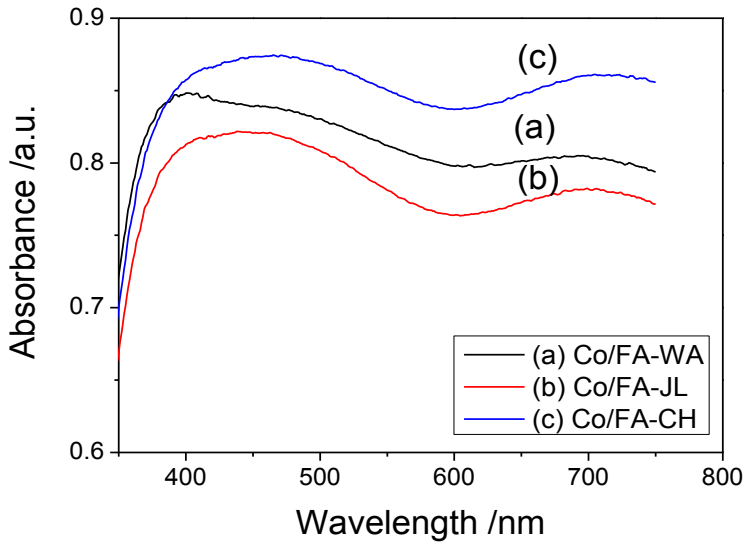

Figure 4.3 UV-vis diffuse reflectance spectra of Co/FA catalysts.

4.3.2 Catalytic activity

Fig. 4.4 shows variation of phenol concentration with time for different solid systems in adsorption and catalytic oxidation. FA did not show strong phenol adsorption with about 5% reduction in phenol concentration at 90 min. For FA/oxone systems, phenol concentration showed a slightly higher reduction than that of adsorption with 10% phenol removal, suggesting that FA could slightly but not effectively activate oxone for sulfate radical production and phenol decomposition.

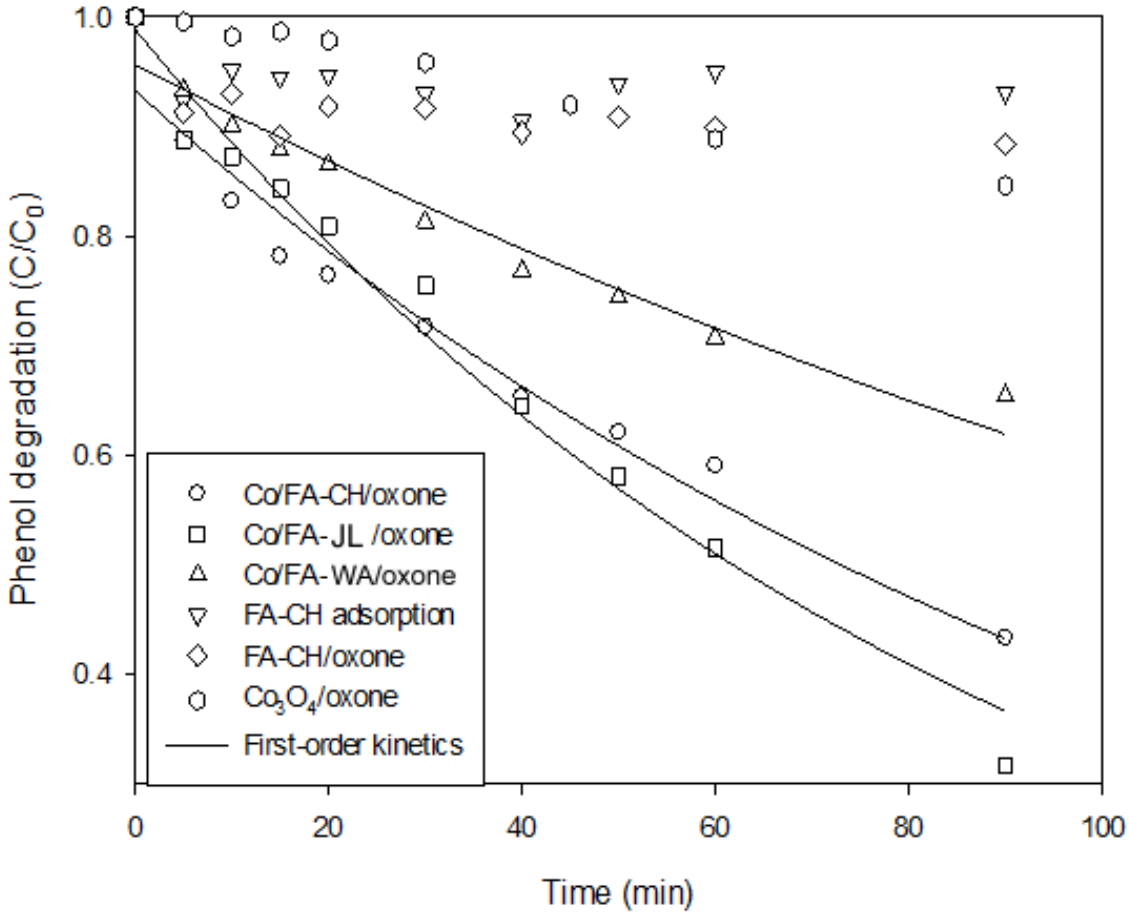

Figure 4.4 A comparison of phenol degradation on Co/FA catalysts. Reaction conditions: [Phenol] =30 ppm, catalyst= 0.4 g/L, oxone= 2 g/L, T= 25 °C.

The activation may be due to the presence of Fe oxides in FA samples. Previous investigations have shown that Fe^{2+} could also activate PMS for sulfate radical generation, but the activity is quite low [19]. Co_3O_4/oxone showed gradual phenol degradation, but phenol removal efficiency was close to that of FA/oxone. Different from FA and Co_3O_4 samples, three FA supported Co catalysts showed much strong phenol degradation, suggesting that dispersive Co oxides are active for reaction with oxone for sulfate radical production. For Co/FA-WA, phenol concentration could be reduced by 40% after 90 min. Co/FA-CH showed better phenol reduction and achieved 56% phenol decomposition at 90 min. Co/FA-JL exhibited the best performance in phenol degradation with 70% phenol reduction at 90 min. The activity of the three catalysts followed an order of Co/FA-JL > Co/FA-CH > Co/FA-WA.

The difference in phenol degradation on three Co/FA catalysts is due to the varying surface properties of the catalysts. XRD and UV-vis diffuse reflectance spectra showed that Co_3O_4 is presented on three Co/FA samples, which will be the active species for activation of PMS. The heterogeneous activation of PMS can be expressed in following equations.

$$\text{S-Co(III)} + HSO_5^- \rightarrow \text{S-Co(II)} + SO_5^{\bullet -} + H^+ \quad \text{S-: support} \qquad 4.3$$

$$\text{S-Co(II)} + HSO_5^- \rightarrow \text{S-Co(III)} + SO_4^{\bullet -} + OH^- \qquad 4.4$$

$$C_6H_5OH + SO_4^{\bullet -} \rightarrow \text{intermediates} \rightarrow CO_2 + H_2O + SO_4^{2-} \qquad 4.5$$

However, bulk Co_3O_4 did not show strong activity in phenol degradation while supported Co_3O_4 produced high phenol removal efficiency, suggesting the important role of Co_3O_4 dispersion. EDS and elemental mapping show dispersion of Co_3O_4 on FA supports is different. EDS and elemental mapping (Fig. 4.2) indicate Co/FA-JL has a higher Co dispersion,

suggesting the more active sites for PMS activation. UV-vis reflectance spectra showed the presence of Co^{2+} in tetrahedral coordination on Co/FA-JL and Co/FA-CH, which can lead to more $SO_4^{\bullet-}$ production (Eq. 4.4). In addition, Table 2 showed that FA-JL and FA-CH have basic surface and FA-WA has strong acid surface. The high surface basicity of FA-JL and FA-CH will promote the reaction with PMS. Zhang et al. [24] investigated cobalt oxide catalysts immobilised on various oxides (MgO, ZnO, Al_2O_3, ZrO_2, P25, SBA-15) for degradation of organic dyes in dilute solutions with PMS and reported that Co/MgO catalysts were the most active. They suggested that the alkaline MgO support helped in (i) dispersing the cobalt oxide nanoparticles well, (ii) minimising the leaching of cobalt ions into the liquid phase, and (iii) facilitating the formation of surface Co–OH complex which is a critical step for PMS activation. Therefore, due to higher dispersion of Co_3O_4, Co^{2+} tetrahedral coordination, and strong basicity of FA-JL, Co/FA-JL exhibited the highest activity in phenol degradation. Liang et al. [31] synthesised Al_2O_3-, SiO_2- and TiO_2-supported Co oxide catalysts and tested them for phenol degradation. They found that Co/Al_2O_3 exhibited higher activity than Co/SiO_2. Table 4.1 shows the lower SiO_2/Al_2O_3 on FA-CH and FA-JL, which could result in higher activity of Co/FA-JL and Co/FA-CH.

Based on phenol degradation curves, a simple model, first order kinetics, was used to fit the data and it produced good results (Table 4.3). The regression coefficients suggest that phenol degradation follows the first-order kinetics. Some supported Co catalysts have been investigated for the activation of PMS in phenol degradation. Kinetic studies indicated that phenol degradation showed first order kinetics on Co/AC [23], similar to Co/FA catalysts in this investigation. The first-order kinetics suggests phenol degradation occurred as surface reaction. HPLC analysis found the

intermediates of hydroquinone and p-benzoquinone. Therefore, phenol degradation could be described in the following scheme (Fig. 4.5).

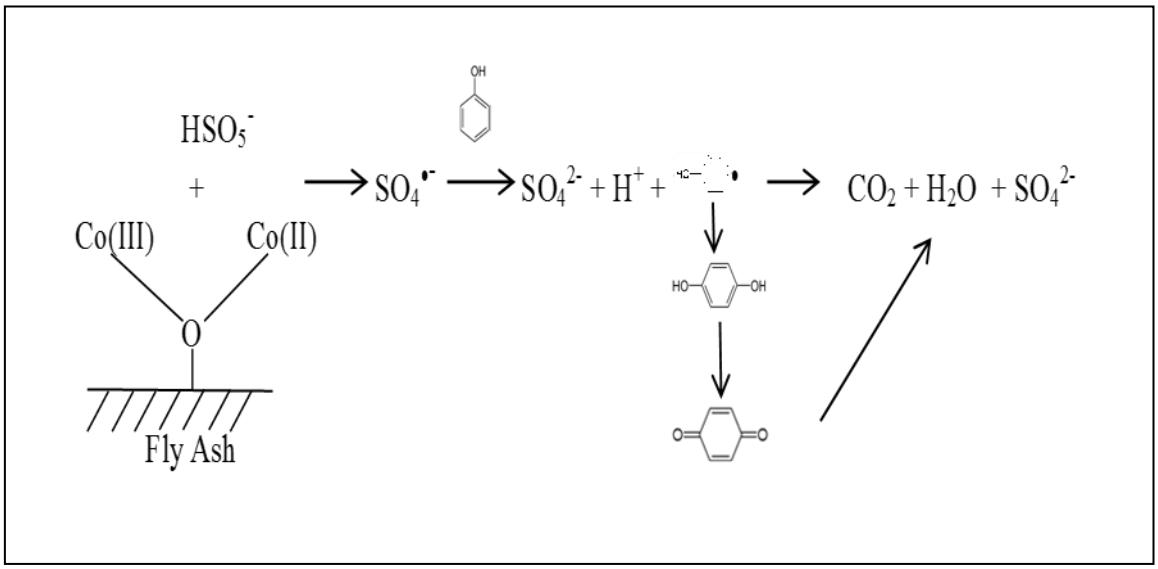

Figure 4.5 Scheme of Co/FA activation of PMS for phenol degradation.

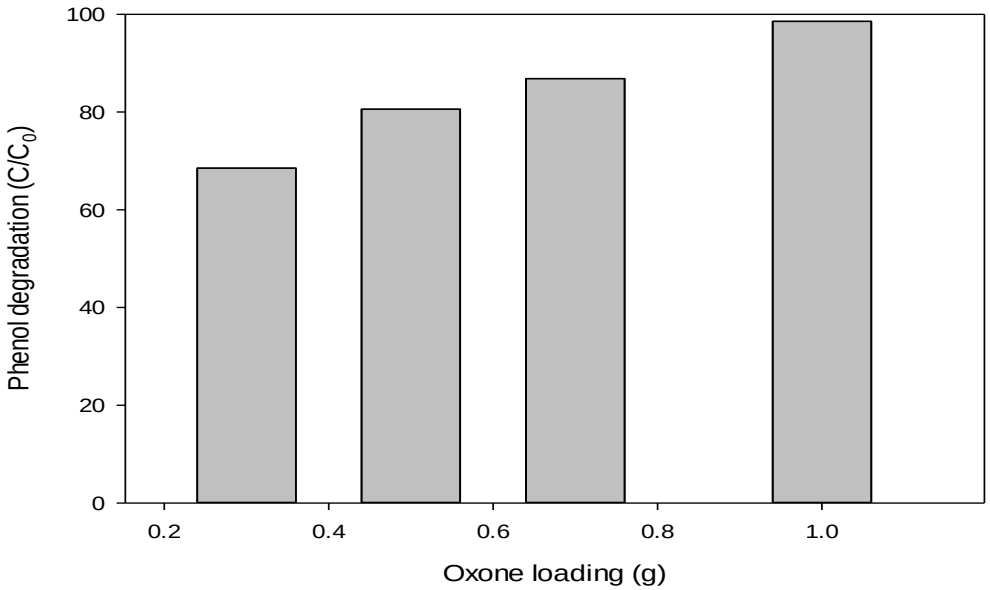

Figure 4.6 Effect of oxone loading on phenol degradation. Reaction conditions: [Phenol] =30 ppm, catalyst= 0.4 g/L, T= 25 °C, reaction time of 90 min.

Table 4.3 Kinetic parameters of first-order model for phenol degradation on Co/FA catalysts

Catalyst	First order kinetics	
	K_1(min^{-1})	R
Co/FA-WA	0.0048±0.0004	0.980
Co/FA-CH	0.0086±0.0006	0.982
Co/FA-JL	0.0111±0.0006	0.990

Fig. 4.6 displays phenol degradation efficiency at 90 min with different oxone loading in solution. Oxone concentration would affect phenol degradation rate and efficiency. Higher oxone loading will increase phenol degradation. At 0.3 g oxone, phenol degradation was about 70% and it could reach 99% at 1 g oxone. Phenol degradation depends on the generation of sulphate radicals. More oxone in solution will produce more sulphate radicals, leading to high phenol reduction.

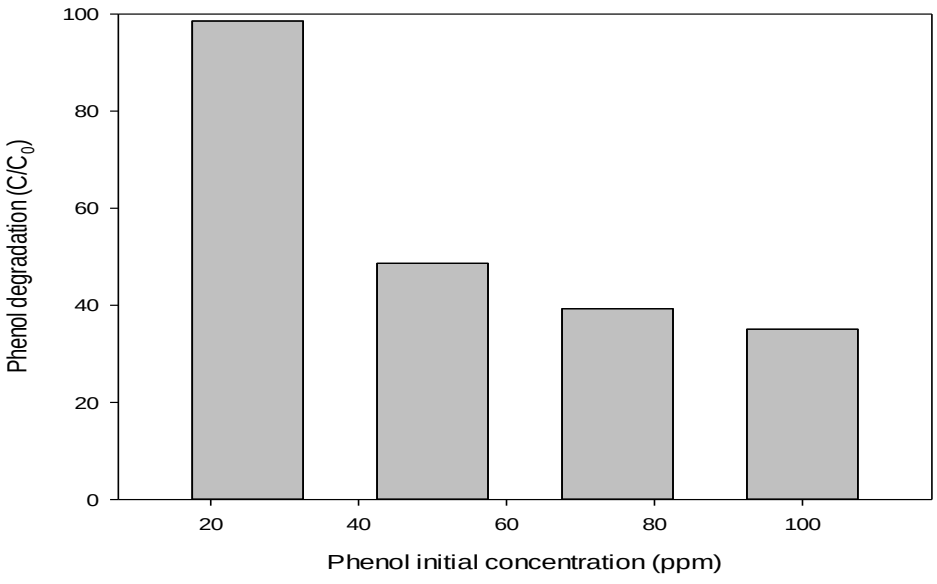

Figure 4.7 Effect of phenol initial concentration on phenol degradation. Reaction conditions: catalyst= 0.4 g/L, oxone= 2 g/L, T= 25 °C, reaction time of 90 min.

Fig. 4.7 illustrates phenol degradation at varying initial phenol concentrations. As can be seen, higher initial phenol concentration will result in low phenol degradation efficiency. At 30 ppm, phenol degradation was 99% but it would reduce to 30% at 100 ppm phenol. As stated before, phenol degradation is dependent on sulphate radicals. At the same concentrations of catalyst and PMS, high amount of phenol in solution will require more time to achieve the same removal rate, thus lowering phenol degradation efficiency.

Fig. 4.8 presents phenol degradation at varying temperatures on three Co/FA catalysts. In general, higher temperature results in high phenol degradation for the three catalysts. At 45 ºC, phenol degradation could achieve 100% at 90, 40 and 50 min on Co/FA-WA, Co/FA-JL, and Co/FA-CH, respectively. Based on the first order kinetics, the reaction rate constants were obtained for the three catalysts at different temperatures. A relationship between the rate constant and temperature could be described by the Arrhenius plots and activation energies were obtained (Table 4.4). The results indicated that Co/FA-JL, and Co/FA-CH presented similar activation energies but Co/FA-WA showed a lower value.

Table 4.4 Activation energies of phenol degradation on Co/FA catalysts.

Catalysts	Ea (kJ/mol)	R^2
Co/FA-WA	47.0	0.993
Co/FA-CH	56.0	0.999
Co/FA-JL	56.5	0.999

For PMS activation by heterogeneous Co catalysts in phenol degradation, few investigations have reported the kinetics and activation energies. We

have studied several heterogeneous Co catalysts on various supports in activation of PMS for phenol degradation. The activation energies obtained are 67.4 [25], 69.7 [22], 59.7 kJ/mol [23] for Co/SBA-15, Co/ZSM5, and Co/AC, respectively. As seen that Co/FAs presented lower activation energy than activated carbon and oxide supported Co catalysts, suggesting Co/FA systems could be promising catalysts.

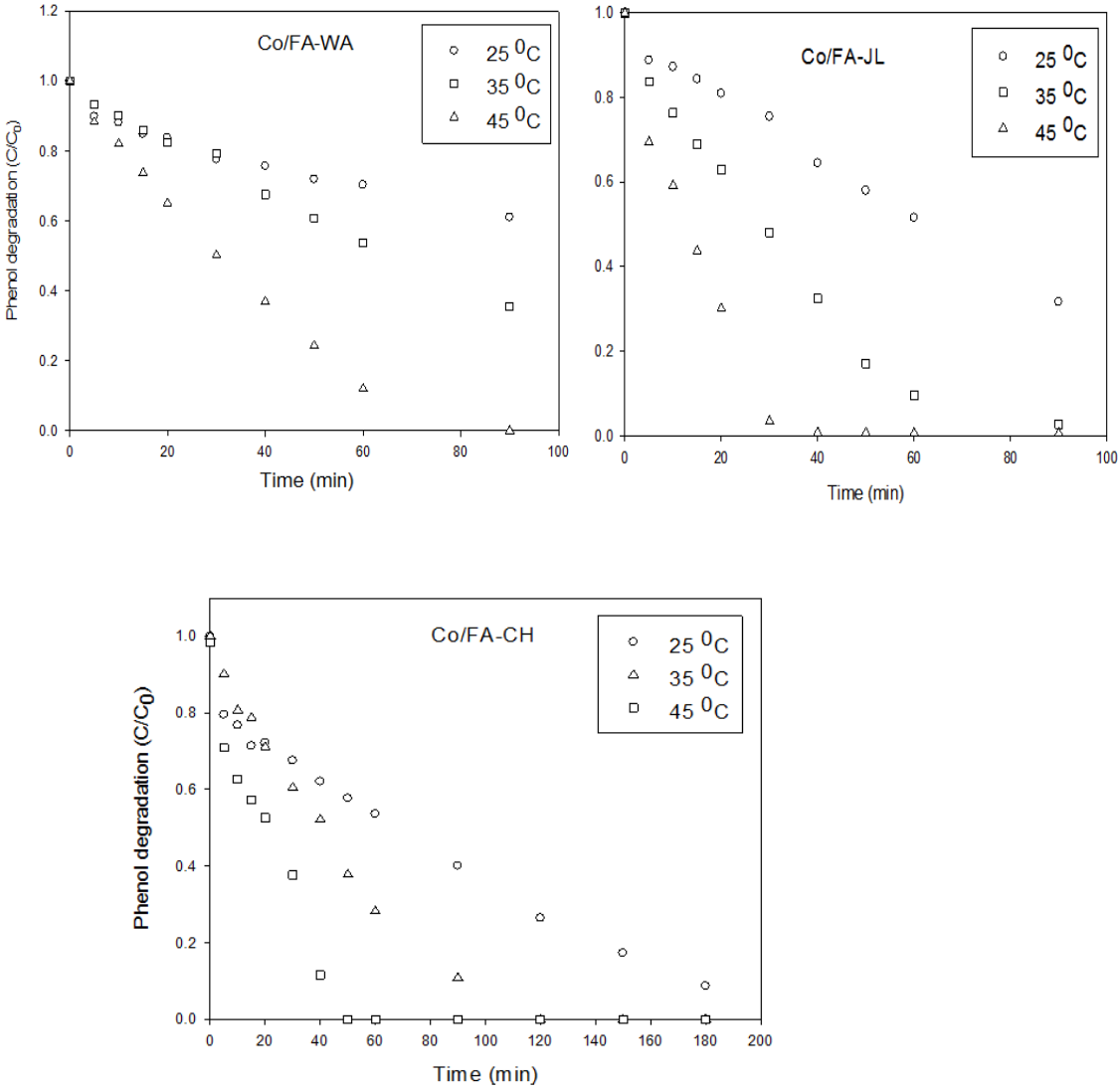

Figure 4.8 Effect of temperature on phenol degradation on Co/FA catalysts. Reaction conditions: [Phenol] =30 ppm, oxone = 2 g/L, catalyst= 0.4 g/L.

4.4 Conclusions

Fly ash based catalysts of FA-WA, FA-JL and FA-CH impregnated active metal Co with active species of Co_3O_4 have been successfully synthesized at calcination temperature of 500 ^{0}C. Based on the characterization, the contents of SiO_2 and Al_2O_3 are above 70% for all type of FA catalysts. These catalysts showed higher activity than supports and bulk Co_3O_4 in activation of PMS for generation of sulphate radicals to oxidatively decompose phenol in aqueous solution. Co dispersion and support basicity strongly influence the activity of Co/FAs. Concentrations of oxone and phenol also influence phenol degradation efficiency. Kinetic studies showed phenol degradation followed a first order kinetics and the activation energies for Co/FA-WA, Co/FA-JL, and Co/FA-CH are 47.0, 56.5, 56.0 kJ/mol, respectively.

4.5 References

1. S. B. Wang, Y. Boyjoo and A. Choueib, *Chemosphere*, 2005, **60**, 1401-1407.

2. S. B. Wang, Y. Boyjoo, A. Choueib and Z. H. Zhu, *Water Research*, 2005, **39**, 129-138.

3. S. Wang and H. Wu, *Journal of Hazardous Materials*, 2006, **136**, 482-501.

4. K. S. Hui and C. Y. H. Chao, *Microporous and Mesoporous Materials*, 2006, **88**, 145-151.

5. H. Tanaka, H. Eguchi, S. Fujimoto and R. Hino, *Fuel*, 2006, **85**, 1329-1334.

6. M. Gross-Lorgouilloux, P. Caullet, M. Soulard, J. Patarin, E. Moleiro and I. Saude, *Microporous and Mesoporous Materials*, 2010, **131**, 407-417.

7. Sindhunata, J. S. J. van Deventer, G. C. Lukey and H. Xu, *Industrial & Engineering Chemistry Research*, 2006, **45**, 3559-3568.

8. J. G. S. van Jaarsveld, J. S. J. van Deventer and G. C. Lukey, *Materials Letters*, 2003, **57**, 1272-1280.

9. S. Wang, L. Li and Z. H. Zhu, *Journal of Hazardous Materials*, 2007, **139**, 254-259.

10. E. Furlani, S. Bruckner, D. Minichelli and S. Maschio, *Ceramics International*, 2008, **34**, 2137-2142.

11. G. Qian, Y. Song, C. Zhang, Y. Xia, H. Zhang and P. Chui, *Waste Management*, 2006, **26**, 1462-1467.

12. S. B. Wang, G. Q. Lu and H. Y. Zhu, *Chemistry Letters*, 1999, 385-386.

13. S. Wang and G. Q. Lu, *Studies in Surface Science and Catalysis*, 2007, **139**, 275-280.

14. S. B. Wang, *Environmental Science & Technology*, 2008, **42**, 7055-7063.

15. J. J. Pignatello, E. Oliveros and A. MacKay, *Critical Reviews in Environmental Science and Technology*, 2006, **36**, 1-84.

16. S. Wang, *Dyes and Pigments*, 2008, **76**, 714-720.

17. M. Pera-Titus, V. Garcia-Molina, M. A. Banos, J. Gimenez and S. Esplugas, *Applied Catalysis B-Environmental*, 2004, **47**, 219-256.

18. G. P. Anipsitakis and D. D. Dionysiou, *Environmental Science & Technology*, 2003, **37**, 4790-4797.

19. G. P. Anipsitakis and D. D. Dionysiou, *Environmental Science & Technology*, 2004, **38**, 3705-3712.

20. G. Zhou, H. Sun, S. Wang, H. Ming Ang and M. O. Tadé, *Separation and Purification Technology*, 2011, **80**, 626-634.

21. Q. J. Yang, H. Choi and D. D. Dionysiou, *Applied Catalysis B-Environmental*, 2007, **74**, 170-178.

22. P. Shukla, S. B. Wang, K. Singh, H. M. Ang and M. O. Tade, *Applied Catalysis B-Environmental*, 2010, **99**, 163-169.

23. P. R. Shukla, S. B. Wang, H. Q. Sun, H. M. Ang and M. Tade, *Applied Catalysis B-Environmental*, 2010, **100**, 529-534.

24. W. Zhang, H. L. Tay, S. S. Lim, Y. S. Wang, Z. Y. Zhong and R. Xu, *Applied Catalysis B-Environmental*, 2010, **95**, 93-99.

25. P. Shukla, H. Sun, S. Wang, H. M. Ang and M. O. Tadé, *Catalysis Today*, 2011, **175**, 380-385.

26. P. Shukla, H. Q. Sun, S. B. Wang, H. M. Ang and M. O. Tade, *Separation and Purification Technology*, 2011, **77**, 230-236.

27. H. Sun, H. Tian, Y. Hardjono, C. E. Buckley and S. Wang, *Catalysis Today*, 2011, 186, 63-68.

28. Q. J. Yang, H. Choi, Y. J. Chen and D. D. Dionysiou, *Applied Catalysis B-Environmental*, 2008, **77**, 300-307.

29. T. A. Zepeda, T. Halachev, B. Pawelec, R. Nava, T. Klimova, G. A. Fuentes and J. L. G. Fierro, *Catalysis Communications*, 2006, **7**, 33-41.

30. R. Xu and H. C. Zeng, *Langmuir*, 2004, **20**, 9780-9790.

31. H. Liang, Y. Y. Ting, H. Sun, H. M. Ang, M. O. Tadé and S. Wang, *Journal of Colloid and Interface Science*, 2012, **372**, 58-62.

Chapter-5

Heterogeneous Catalytic Oxidation of Aqueous Phenol on Red Mud Supported Cobalt Catalysts

Abstract

Red mud (RM), an industrial waste from alumina refinery industry, was used as a support for preparation of Co-oxide-based catalysts (Co/RM). The samples were characterized by N_2 adsorption, X-ray diffraction (XRD), scanning electron microscopy (SEM), energy dispersive X-ray spectroscopy (EDS), and UV-vis diffusive reflectance spectroscopy. The heterogeneous catalytic activity was evaluated in aqueous phenol degradation using peroxymonosulphate (PMS) as an oxidizing agent. It was found that Co_3O_4 was highly dispersed on RM surface and that pre-treatment of red mud (RM-T) would significantly influence catalytic activity. Co/RM-T catalysts exhibited high effectiveness in heterogeneous activation of PMS to produce sulphate radicals for phenol degradation compared with Co/RM-NT. Phenol degradation followed first-order kinetics and activation energies on Co/RM-T and Co/RM-NT are 46.2 and 47.0 kJ/mol, respectively.

5.1 Introduction

Industrial activities produce large amounts of organics-containing wastewater, which is hazardous to the environment and has to be processed before discharge into natural water bodies. There are many types of organics in wastewater; however, one of the most important class of water pollutants is phenol and its derivatives due to their strong toxicity to many living organisms even at low concentrations [1]. These pollutants have been considered on the EPAs priority list since 1976 [2]. Phenol and its derivatives can be found from many industries as by-products such as petroleum refining, petrochemical, pharmaceutical, plastic and pesticide chemical industries [3, 4]. Among the possible technologies for wastewater treatment, advanced oxidation processes (AOPs) using chemicals as oxidants are the most suitable processes to degrade toxic organics in aqueous solution due to low operation cost, no need for special equipment, less energy consumption, and high conversion of the organic pollutants [5-7].

Homogenous catalytic oxidation using Fenton's reagent (H_2O_2 and ferrous ion) has been identified as an effective process to degrade toxic organics in aqueous solutions [8-11]. However, it needs a more process for separation of the catalyst [12]. Moreover, most of the dissolved metal catalysts are harmful to the environment. This disadvantage can be overcome by using heterogeneous catalysts which will be easily recoverable and reusable [13, 14]. Furthermore, heterogeneous catalysis can completely convert organics to CO_2 and H_2O or partially oxidize the organic compounds to less toxic ones [6, 7]. Heterogeneous catalytic oxidation of organic compounds, such as dyes, phenol and its derivatives, have been widely used as a technology for reducing these substances in wastewater from industries [3, 5, 11, 15, 16].

Currently, most AOPs are based on the generation of very reactive species, such as hydroxyl radicals ($OH^{\bullet}$) that oxidise a broad range of pollutants rapidly and non-selectively [11, 17]. Apart from $OH^{\bullet}$, sulphate radicals have also been recently suggested as an alternative due to their higher oxidation potential [18]. For sulphate radical production, the reaction between Co ions and peroxymonosulphate (PMS, HSO_5^-) has been found to be an effective route. The radical generation and organic degradation processes can be described as shown below.

$$Co^{2+} + HSO_5^- \rightarrow Co^{3+} + SO_4^{-\bullet} + OH^- \quad 5.1$$

$$Co^{3+} + HSO_5^- \rightarrow Co^{2+} + SO_5^{-\bullet} + H^+ \quad 5.2$$

$$SO_4^{-\bullet} + H_2O \rightarrow SO_4^{2-} + OH^{\bullet} + H^+ \quad 5.3$$

$$SO_4^{-\bullet} + \text{Organics} \rightarrow \text{several steps} \rightarrow CO_2 + H_2O + SO_4^{2-} \quad 5.4$$

In the past few years, several heterogeneous Co catalysts have been reported for PMS activation. Most of them are supported Co_3O_4 systems using oxides [19-24], carbons [5, 25, 26], and zeolites [27]. Red mud (RM) is a solid by-product from alumina refinery industry. For producing every ton alumina, the Bayer process plant will generate between 1 to 2 tonnes of RM residues [28-30]. Every year, 90 million tonnes of RM are generated globally and 33% of them are created in Australia [30]. RM is mainly composed of fine particles containing alumina, hematite, goethite, boehmite, quartz and gypsum [30, 31]. Furthermore, RM cannot be easily disposed due to its high alkalinity with pH 10-13, this waste residue can cause serious impacts to the environment [31, 32]. Thus, RM needs proper handling to minimize its negative effects on the environment. Nowadays, a great deal of efforts has been done to utilize RM as a coagulant, adsorbent and catalyst for environmentally benign processes [33-38]. Utilization of

industrial solids like RM for other processes can help reduce the solid waste in landfills and produce environmental benefits.

In this chapter, we will report an investigation on the utilization of RM as a catalyst support. Two different cobalt oxide catalysts based on raw RM and water-washed RM were prepared and tested in heterogeneous activation of peroxymonosulphate (PMS) for generating sulphate radicals to degrade phenol in aqueous solution. The influences of catalyst type, oxidant amount, reaction temperature, and phenol concentration were systematically investigated.

5.2 Experimental

5.2.1 RM supports.

A raw RM sample was obtained from an alumina refinery plant in Western Australia, in the form of highly alkaline suspension (pH >12). Prior to use as catalyst supports, two different RM samples were obtained. One RM sample was collected from the suspension by filtration and the solid was dried in an oven at 120 ^{o}C for 24 h. The sample was denoted as RM-NT. The other RM sample was obtained by washing RM-NT several times with ultrapure water to remove alkaline, and drying at 120 ^{o}C for 24 h. This sample was denoted as RM-T.

5.2.2 Synthesis of RM supported cobalt oxide catalysts.

Catalysts, Co/RM-NT and Co/RM-T, at Co 1-5 wt% loading were prepared by a wetness impregnation method. Cobalt nitrate was used as a cobalt precursor due to its better interaction with supports than other Co precursors [19, 39]. Typically, a fixed amount of RM-NT or RM-T was added into a solution of $Co(NO_3)_2 \bullet 6H_2O$ (Sigma-Aldrich) and kept stirring

at 80 ^{o}C until total evaporation of H_2O. After that the solids were dried at 120 ^{o}C overnight and calcined at 500 ^{o}C for 4 h in air. Then the catalysts were stored in a desiccator until use.

5.2.3 Characterization of catalysts.

XRD patterns were obtained on a Bruker D8 (Bruker-AXS, Karlsruhe, Germany) diffractometer using a filtered Cu Kα radiation source, with accelerating voltage 40 kV, current 30 mA and scanned at 2θ from 5 to 70^{o}. N_2 adsorption-desorption was measured on a Gemini 2360 (Micromeritics) to obtain specific surface area using the Brunauer-Emmett-Teller (BET) method. Prior to measurement the samples were degased at 200 ^{o}C for 12 h under vacuum condition. The external morphology and chemical compositions of the samples were observed on a ZEISS NEON 40EsB scanning electron microscope (SEM) equipped with an energy dispersive spectrometer (SEM-EDS). The UV-visible diffuse reflectance spectra (DRS) were recorded on a V-570 UV-visible spectrometer (Jasco, Japan) equipped with an integrating sphere, in which $BaSO_4$ was used as a reference material.

5.2.4 Kinetic study of phenol degradation.

The catalytic oxidation of phenol was carried out in a 500 mL glass beaker containing about 25- 100 ppm of phenolic solutions, which was attached to a stand and dipped in a water bath with a temperature controller. The reaction mixture was stirred constantly at 400 rpm to maintain a homogenous solution. A fixed amount of peroxymonosulphate (PMS from oxone, DuPont's triple salt: $2KHSO_5 \bullet KHSO_4 \bullet K_2SO_4$, Sigma-Aldrich) was added into the solution and allowed to dissolve completely before reaction. Further, a fixed amount of catalysts was added into the reactor to

start the oxidation reaction of phenol. The reaction was carried on for 90 min. At a fixed time interval, 0.5 mL of solution sample was taken from the mixture using a syringe filter of 0.45 μm and then mixed with 0.5 mL methanol to quench the reaction. Concentration of phenol was analyzed using a HPLC with a UV detector at wavelength of 270 nm. The column used was C-18 with mobile phase of 30% acetonitrile and 70% ultrapure water. For selected samples, total organic carbon (TOC) was determined using a Shimadzu TOC-5000 CE analyzer.

5.3 Result and discussion

5.3.1 Characterization of catalysts

The composition of red mud samples has been reported previously [40, 41]. The main components are Fe_2O_3 (60%), Na_2O (16%), Al_2O_3 (15%), SiO_2 (5%), and TiO_2 (5%). XRD patterns of RM, Co/RM-NT and Co/RM-T are shown in Fig. 5.1.

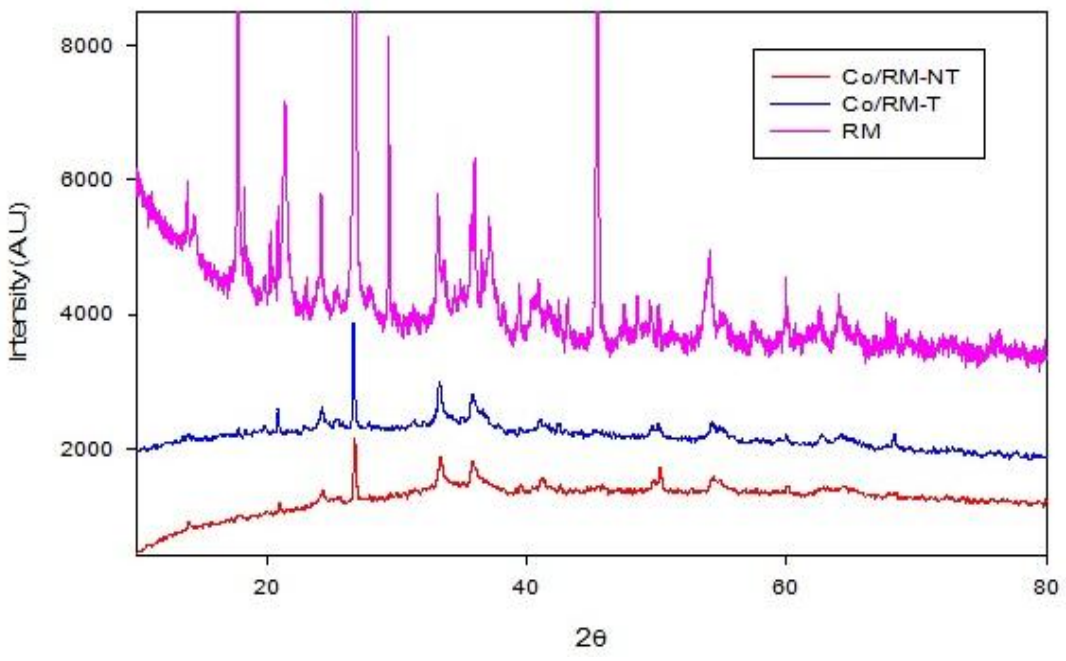

Figure 5.1 XRD patterns of red mud and their supported Co catalysts.

The main phases identified in the RM sample were haematite, goethite, quartz and calcite. Red mud supported Co catalysts have different XRD patterns from the RM support. It can be seen, goethite and calcite were significantly reduced after calcination process, because of decomposition at high temperature, while Co/RM-NT and Co/RM-T showed similar XRD patterns. Cobalt species in crystalline form were not identified on Co/RM-NT and Co/RM-T, possibly due to low Co loading and high dispersion.

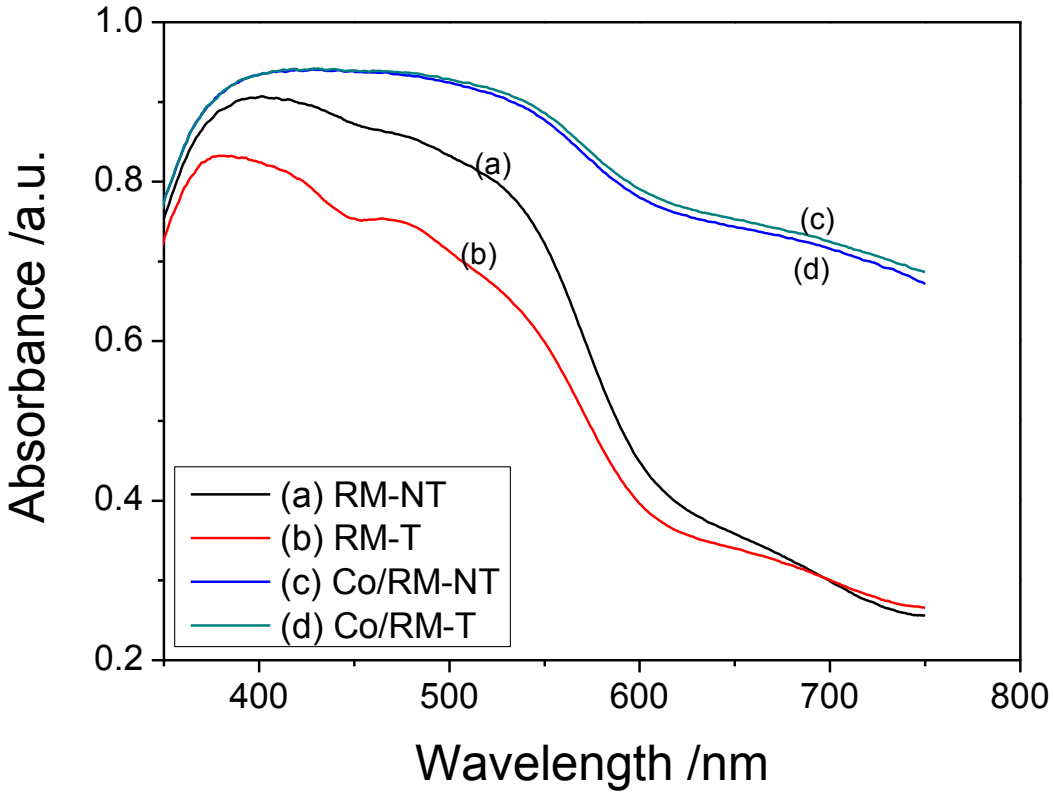

Figure 5.2 UV-vis spectra of RM supports and Co/RM-NT and Co/RM-T.

UV-vis diffuse reflectance spectra of RM and RM support Co catalysts are displayed in Fig. 5.2. RM-NT and RM-T presented a similar pattern,

however, RM-T showed a low intensity. Both Co/RM-NT and Co/RM-T also exhibited similar patterns, but different from the supports. Two strong absorption bands around 400 nm and 700 nm were observed, characteristics of the presence of Co^{2+} and Co^{3+} in catalysts [42-44]. These bands indicate the presence of Co_3O_4 in the catalysts. It is generally believed that calcination of $Co(NO_3)_2$ will result in a final product of Co_3O_4. Although XRD pattern could not display crystallites of cobalt species, UV-vis spectra detected the presence of Co_3O_4 in catalysts.

The BET surface area of RM, Co/RM-T and Co/RM-NT are presented in Table 5.1. The raw RM sample has a surface area of 21 m^2/g. Co impregnation on treated RM has a higher surface area and pore volume compared with the raw material and Co impregnation on untreated RM, which suggests that the washing treatment could improve the porosity of RM by removing some impurities.

Table 5.1. Surface area, pore volume and pore radius of sample

Sample	S_{BET} (m^2/g)	Pore Volume (cc/g)
Co/RM-T	32.0	0.021
Co/RM-NT	22.5	0.011
RM	21.0	-

The morphology and composition of Co/RM-NT and Co/RM-T were observed from SEM images and EDS (Fig. 5.3 and Fig. 5.4, respectively). For SEM analyses, secondary electron (SE) and backscattered (BSE) images were taken to observe the dispersion of Co species on the catalysts. For Co/RM-NT (Fig. 5.3A), it can be seen that the milled sample has different particle size and shape in a range 0.5 – 20 μm. For the same region, the catalyst was also observed using BSE (Fig. 5.3B) and the specks

of cobalt can be seen as the brighter area in the catalyst particles. These indicate that cobalt is well coating on RM supports.

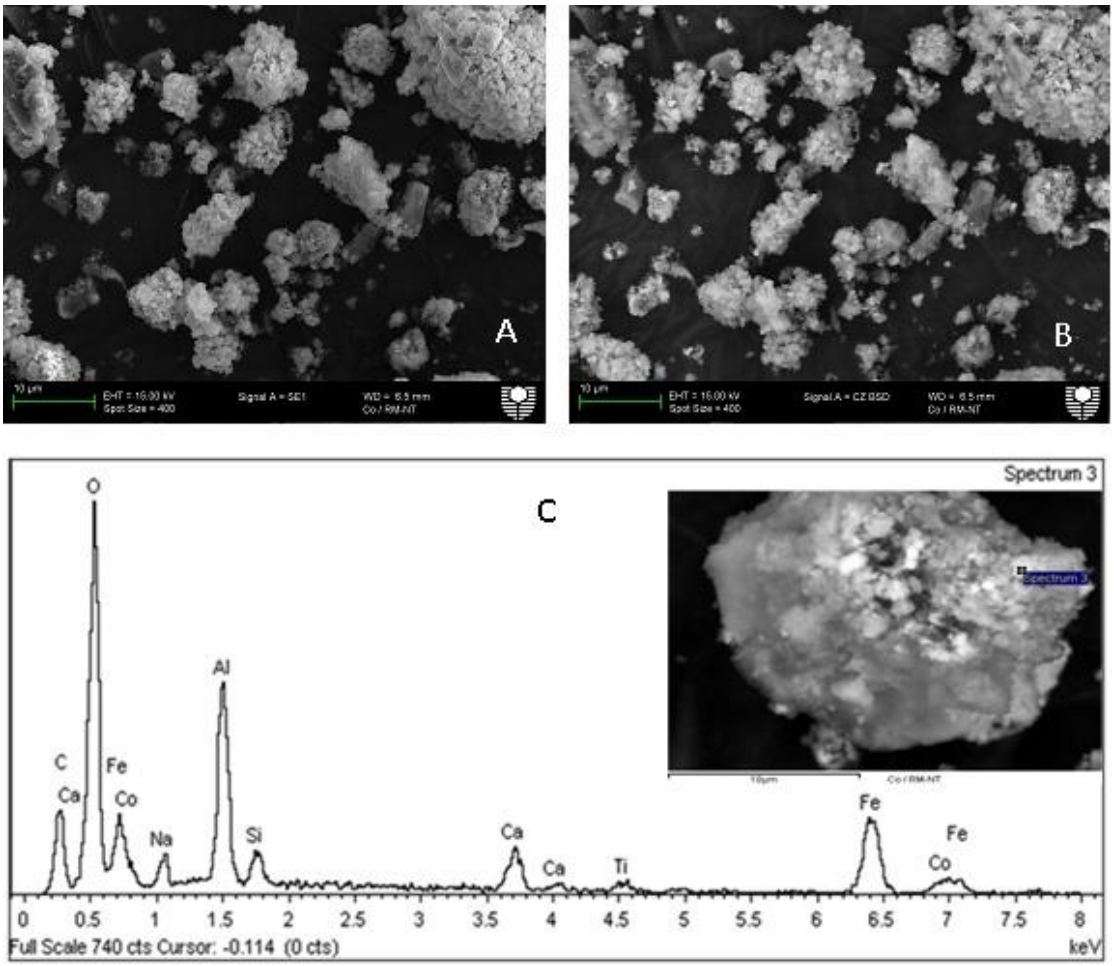

Figure 5.3 SEM images and EDS spectra of Co/RM-NT, (A) SE Detector, (B) BSE Detector, (C) EDS spectra with inset of spectrum image source.

Fig. 5.4A and Fig. 5.4B present SEM images of Co/RM-T with SE and BSE measurements. As seen, Co/RM-T has the similar particle size and shape with Co/RM-NT. BSE also showed bright areas than the image in SE, suggesting a better dispersion of Co on RM-T support. Fig. 5.3C and Fig. 5.4C display EDS spectra of Co/RM-NT and Co/RM-T, respectively.

Elements of C, Ca, Fe, O, Na, Al, Si, Ti, and Co were found on Co/RM-NT. For Co/RM-T, C, Ca, Fe, O, Al, Si, Ti, and Co were also found except Na, probably due to washing process. Thus, EDS results confirm the presence of Co on both catalysts.

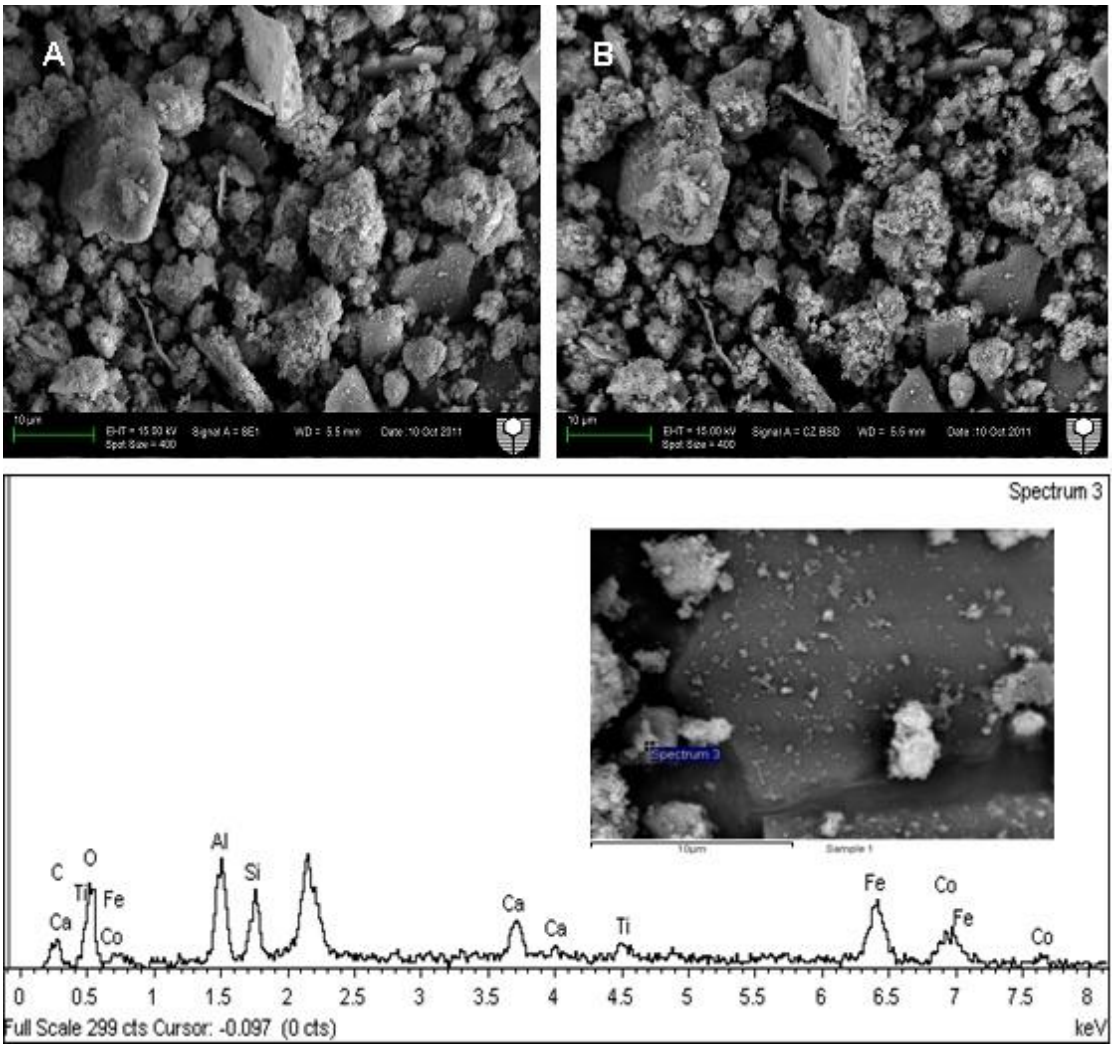

Figure 5.4 SEM images and EDS spectra of Co/RM-T, (A) SE Detector, (B) BSE Detector, (C) EDS spectra with inset of spectrum image source.

5.3.2 Preliminary study of phenol oxidation using catalysts

Fig. 5.5 shows preliminary tests of adsorption and catalytic oxidation of phenol on RM, Co/RM-T and Co/RM-NT in aqueous solution under various experimental conditions. In general, RM-NT, RM-T, Co/RM-NT and Co/RM-T are able to adsorb phenol though at low efficiency. For oxone (PMS) without a solid catalyst, degradation of phenol is less than 3% after 90 min, suggesting that oxone itself could not oxidize phenol.

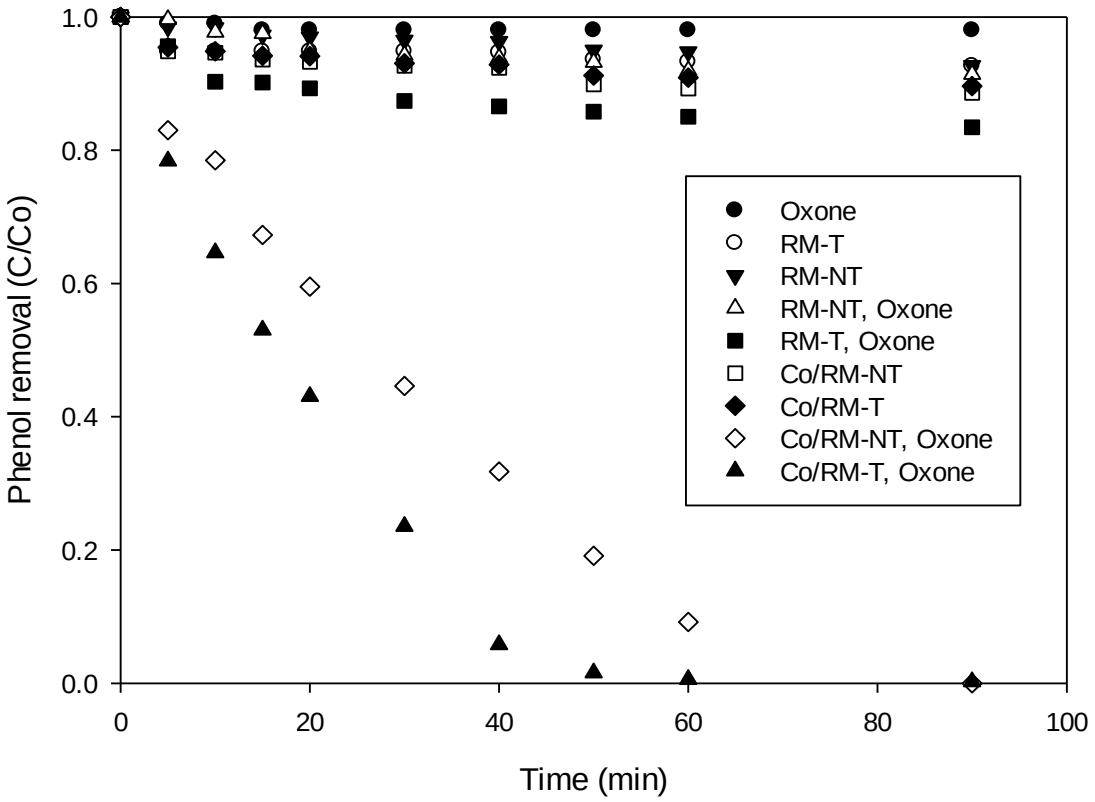

Figure 5.5 Phenol removal with time in adsorption and catalytic oxidation. Reaction conditions: 0.2g catalyst loading, 1 g oxone in 500 mL phenol solution of 25 ppm, 25 ^{o}C.

Furthermore, RM-NT and RM-T particles slightly activated oxone to cause phenol oxidation less than 10% and 17%, respectively. Costa et al. [45] investigated the active sites of red mud for degradation of organic dyes

and reduction of Cr (VI) and the results showed that Fe oxides on RM provides a very important role to generate Fe^{2+} active species, however the Fe^{2+} was less active compared with Co^{2+}. RM supported Co catalysts could produce significant phenol degradation. In Co/RM-T-oxone, phenol could be removed completely from solution in 60 min. Co/RM-NT-oxone, however, could completely remove phenol in 90 min. TOC removal in Co/RM-NT-oxone and Co/RM-T-oxone systems was also measured and results showed that about 64% and 57% of TOC removal were obtained for Co/RM-NT-oxone and Co/RM-T-oxone, respectively, at 60 min.

Generally, catalyst activity strongly depends on support properties. We previously investigated several supported Co catalysts for phenol degradation. Under the similar conditions, Co/RM-T presented better activity than Co/SiO_2 [19], Co/SBA-15 [20], Co/Al_2O_3 [21], Co/TiO_2 [21], Co/ZSM5 [27], Co/FA [24], and the activity is similar to that on Co/AC [5] and Co/CX [25].

Yang et al. [23] studied cobalt species on various supports, TiO_2, SiO_2 and Al_2O_3, for the degradation of 2,4-dichlorophenol in solutions with oxone and reported that only Co_3O_4 crystallites were presented in all supported Co catalysts. Furthermore, the activity of Co_3O_4 on SiO_2 is the highest among other supports due to high surface area. Liang et al. [21] investigated Al_2O_3-, SiO_2- and TiO_2-supported Co oxide catalysts for PMS activation for phenol degradation and they found that Co/TiO_2 exhibited the highest activity due to the high dispersion of Co oxide and high basicity of TiO_2. Zhang et al. [22] investigated MgO-, Al_2O_3-, ZrO_2-, ZnO-, P25- and SBA-15 supported Co catalysts for the degradation of organic dyes in aqueous solution and found that MgO is the best support because it has abundant OH groups of sites which have an important role to promote

high dispersion Co^{2+}. We investigated fly ash (FA)-supported Co catalysts in PMS activation and found that surface properties of the catalysts influence the activity. Higher dispersion of Co_3O_4, Co^{2+} tetrahedral coordination, and strong basicity of Co/FA exhibited the highest activity in phenol degradation [24].

In this investigation, UV-vis diffuse reflectance spectra showed that Co_3O_4 is presented on two Co/RM samples. XRD indicated that Co_3O_4 is highly dispersed on RM supports. SEM images displayed that Co species showed better dispersion on Co/RM-T. BET measurement and adsorption showed that Co/RM-T has a high surface area and adsorption. Therefore, Co/RM-T exhibited higher phenol degradation.

5.3.3 Effects of reaction parameters on phenol degradation

Fig. 5.6 presents phenol degradation efficiency at varying initial concentrations of oxone (0.2-1.0 g). As can be seen, for both Co/RM-NT and Co/RM-T catalysts, the degradation of phenol depended on concentration of oxone. Higher concentration of oxone resulted in more removal efficiency of phenol. For Co/RM-NT, at 0.2 g oxone loading, 80% removal efficiency would be achieved in 90 min, while complete removal would be reached at 0.4 g oxone in 90 min. A similar observation occurred for Co/RM-T catalyst, higher oxone loading would increase removal efficiency of phenol. The complete phenol degradation could be achieved at 0.4 g oxone loading in 60 min. However, at higher oxone loading, no further increase was observed in removal efficiency of phenol. For both Co/RM-NT and Co/RM-T, an optimal oxone loading was achieved at 0.4 g.

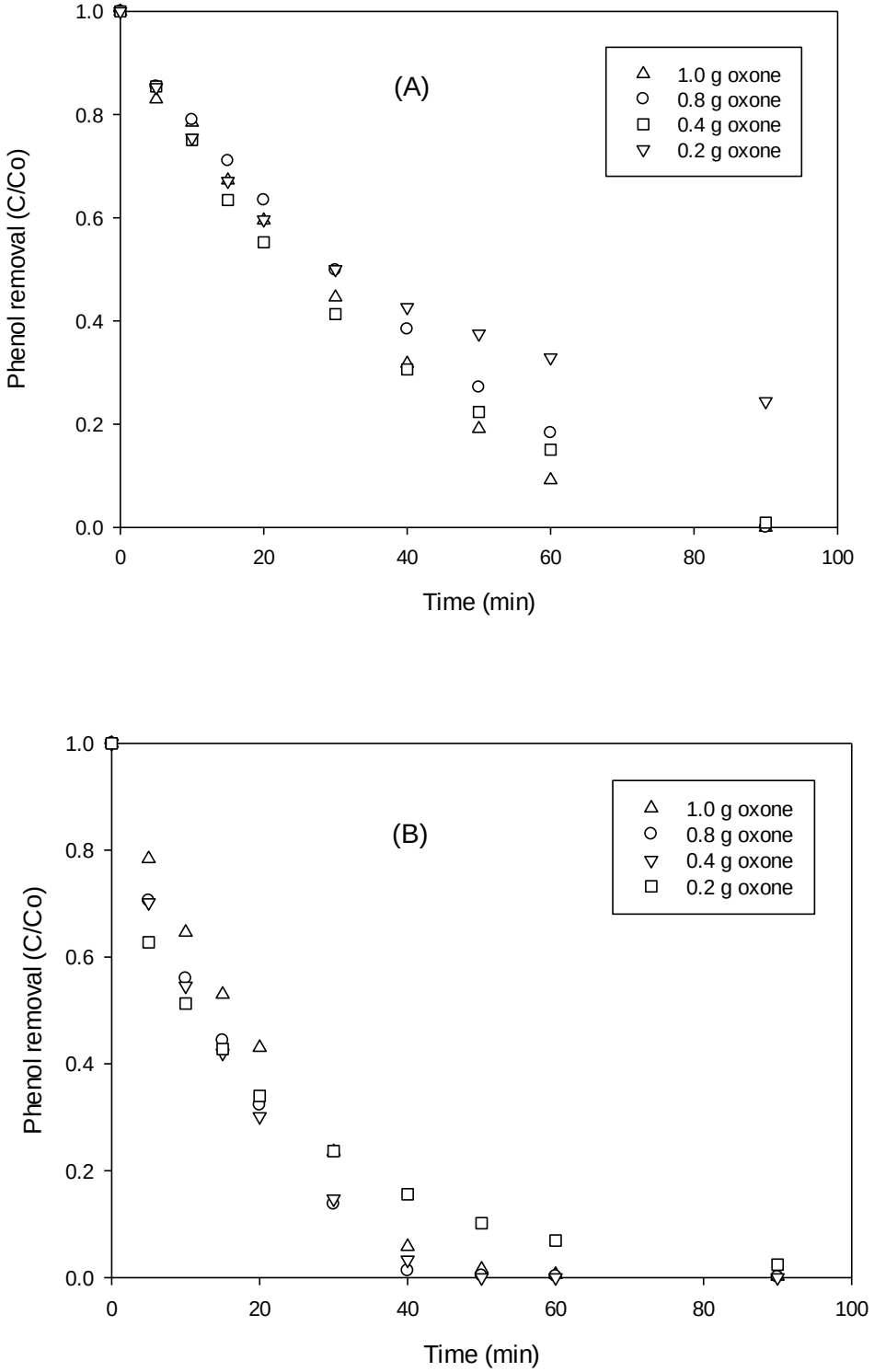

Figure 5.6. Effect of oxone concentration on phenol removal, (A) Co/RM-NT and (B) Co/RM-T. Reaction conditions: 25 ppm, 0.2 g catalyst, 25 ^{0}C.

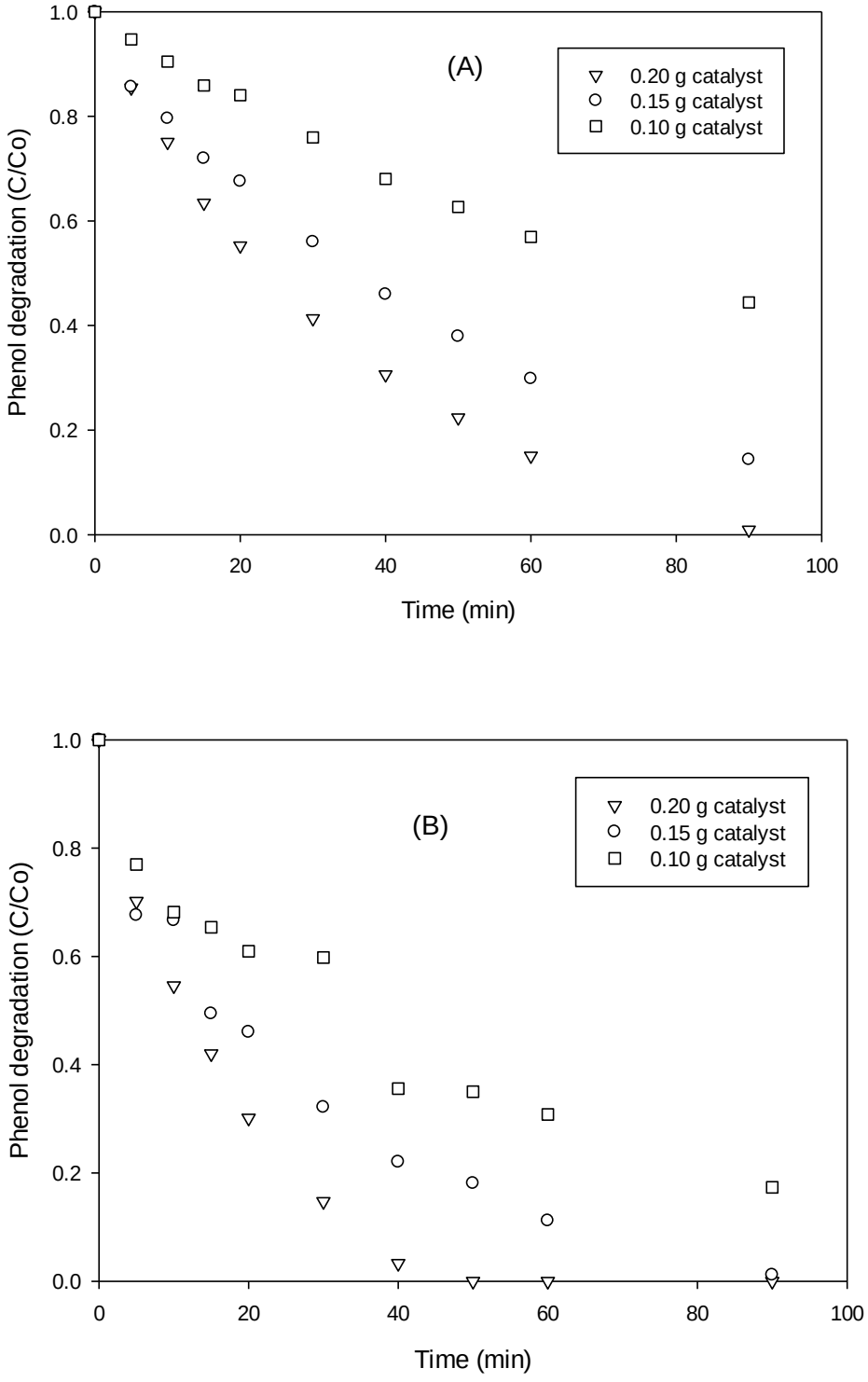

Figure 5.7 Effect of catalyst loading on phenol removal, (A) Co/RM-NT and (B) Co/RM-T. Reaction conditions: 25 ppm, 0.4 g oxone, 25 ^{0}C.

The effect of Co/RM-NT and Co/RM-T loading in solution on phenol degradation is shown in Fig. 5.7. Similar to the effect of oxone loading, an increased amount in both Co/RM-NT and Co/RM-T catalysts in the solutions enhanced the phenol degradation efficiency. At 0.10 g Co/RM-NT (0.2 g/L), phenol removal would be 80% at 90 min, while removal of phenol would reach 100% at 90 min at Co/RM-NT loading of 0.2 g (0.4 g/L). The addition of more catalyst would increase adsorption sites and also provide extra catalyst sites to activate oxone. Therefore, it will result in a significant increase in the rate of reaction. A similar trend occurred on Co/RM-T (Fig. 5.7B), higher catalyst loading could increase degradation efficiency of phenol in solution. At 0.15 g and 0.20 g of Co/RM-T, complete degradation would be achieved in 90 and 50 min, respectively.

It is believed that phenol degradation also depended on initial concentration of phenol in solution. Fig. 5.8 shows phenol degradation at various concentrations between 25 and 100 ppm. At high phenol concentration, removal efficiency tended to decrease. For Co/RM-NT, complete degradation could be reached within 90 min at phenol concentration of 25 ppm, while in the same duration at phenol concentrations of 50, 75 and 100 ppm, degradation efficiency would only be achieved at 80, 50 and 40%, respectively. A similar variation could also be seen in Fig. 5.8B using Co/RM-T. At 25 ppm phenol concentration, 100% degradation efficiency of phenol was achieved within 50 min. At 50 ppm removal of phenol was obtained at about 80% after 90 min. Meanwhile, for phenol concentration of 75 and 100 ppm, removal efficiencies would be reached 60 and 50% within 90 min, respectively.

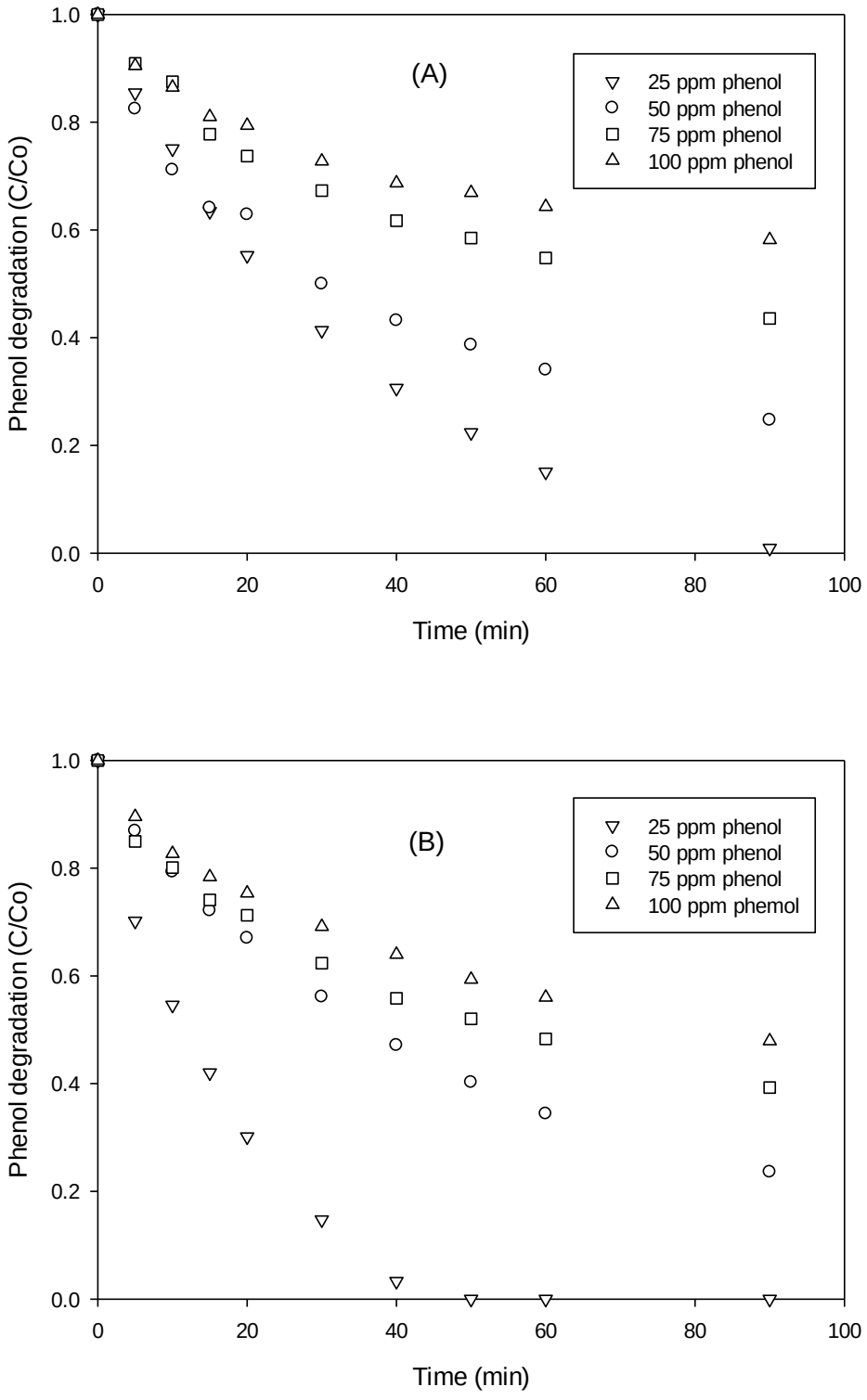

Figure 5.8 Effect of phenol concentration on phenol removal, (A) Co/RM-NT and (B) Co/RM-T. Reaction conditions: 0.4 g oxone, 0.2 g catalyst, 25 ^{0}C.

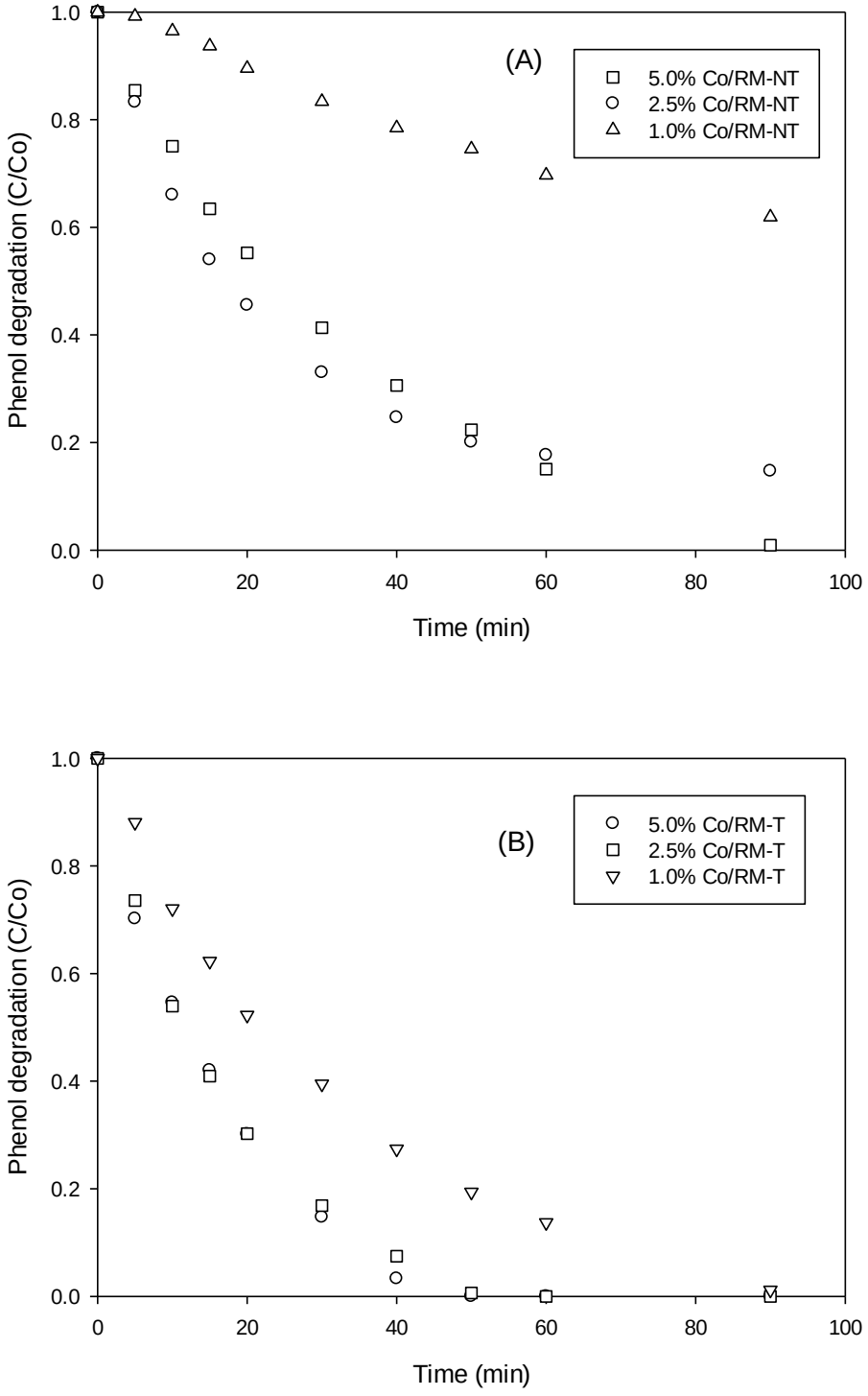

Figure 5.9. Effect of Co loading in Co/RM on phenol removal, (A) Co/RM-NT and (B) Co/RM-T. Reaction conditions: 0.4 g oxone, 0.2 g catalyst, 25 ppm, 25 ^{0}C.

The effect of cobalt loading on RM on phenol degradation was also investigated (Fig. 5.9). As can be seen, cobalt loading on RM showed quite a significant impact on phenol degradation. Higher amount of cobalt loading provides additional sites for generation of active sulphate radicals, thus enhancing the rate of reaction. For Co/RM-NT, the increase in cobalt loading from 1.0 to 2.5 wt% would increase degradation of phenol in more than two times. However, a further increase of Co loading on RM-NT up to 5 wt% would not enhance the rate of reaction. For Co/RM-T, at 1 wt% of cobalt loading, the complete phenol degradation could be achieved within 90 min, while at cobalt loading from 2.5-5 wt%, 100% removal of phenol was achieved within 50 min and no significant improvement in the extent of reaction was observed. The above results suggested the optimal Co loading on RM as 2-5 wt%.

The reaction temperature could play a significant role in phenol removal. Fig. 5.10 shows the reduction of phenol concentration against time at various temperatures of 25 - 45 ^{o}C. The rate of reaction would increase significantly with increased temperature. For Co/RM-NT, complete phenol degradation at temperature of 25 ^{o}C would be achieved in 90 min. Further increase of 10 ^{o}C, 100% degradation efficiency of phenol was achieved within 60 min. At temperature of 45 ^{o}C, phenol removal would reach 100% at 30 min. A same profile was also obtained on Co/RM-T. Complete degradation efficiency of phenol at 25, 35 and 45 ^{o}C would be achieved in 60, 40 and 25 min, respectively.

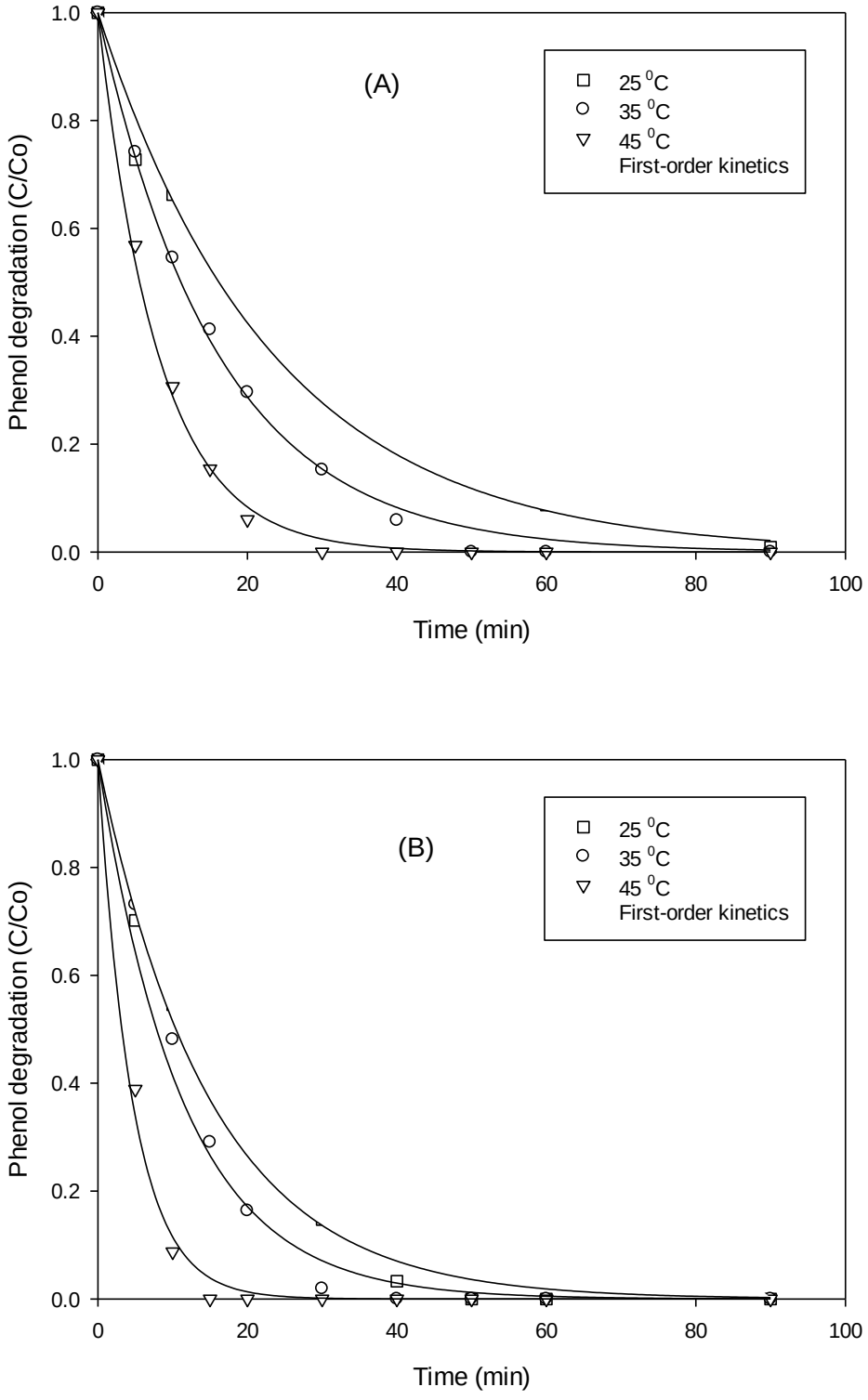

Figure 10. Effect of temperature on phenol removal, (A) Co/RM-NT and (B) Co/RM-T. Reaction conditions: 25 ppm, 0.4 g oxone, 0.2 g catalyst.

In order to estimate the kinetic rates, a general pseudo first order kinetics for phenol degradation was employed, as shown in equation below.

$$\ln\left(\frac{C}{Co}\right) = -k \bullet t \qquad 5.5$$

Where k is the apparent first order rate constant of phenol removal, C is the concentration of phenol at various time (t). C_o is the initial phenol concentration. Data fitting (Fig. 5.10) showed that the phenol degradation could be described by the first order kinetics. Kinetic constants are presented in Table 5.2. As can be seen that kinetic rate of reaction would be increased with increased temperature. The rate constants (k) for Co/RM-T are generally higher than those of Co/RM-NT. Using the first order kinetic rate constants and the Arrhenius equation, the activation energies of Co/RM-NT and Co/RM-T were derived as 47.0 kJ/mol and 46.2 kJ/mol, respectively.

Table 5.2 Kinetic constants of phenol degradation at different temperatures on Co/RM-NT and Co/RM-T catalysts.

Catalyst	Temperature, ^oC	k (min^{-1})	R
Co/RM-NT	25	0.0428	0.968
	35	0.0624	0.990
	45	0.1241	0.989
Co/RM-T	25	0.0664	0.954
	35	0.0882	0.936
	45	0.2163	0.983

5.3.4 Role of Co/Red mud catalyst in phenol degradation

During catalytic oxidation of toxic organics, Co metal oxides on RM provide a significant role to generate Co^{2+} active species which will activate the oxone to produce sulphate radicals. Then, $SO_4^{-\bullet}$ and phenol can react on the catalyst surface to produce simple molecule compounds including CO_2 and H_2O (Eqs.5.1-5.4). Liang et al. [21] investigated TiO_2-, Al_2O_3- and SiO_2-

supported cobalt oxide with oxone for degradation of phenol in dilute solutions. Studies have suggested that production of sulphate radicals is important for phenol degradation due to surface reaction between Co_3O_4 and oxone and that phenol concentration affects its decomposition. Thus, it is believed that heterogeneous surface reactions are major pathways for phenol removal on Co/RM surface as shown in Fig. 5.11. Costa et al. [45] demonstrated the capability of RM and hydrogen peroxide for reduction of Cr(IV). Fe phases will induce reduction of H_2O_2 to produce $OH^{\bullet}$ radicals. The current study using oxone as an oxidant will be in similar consequences.

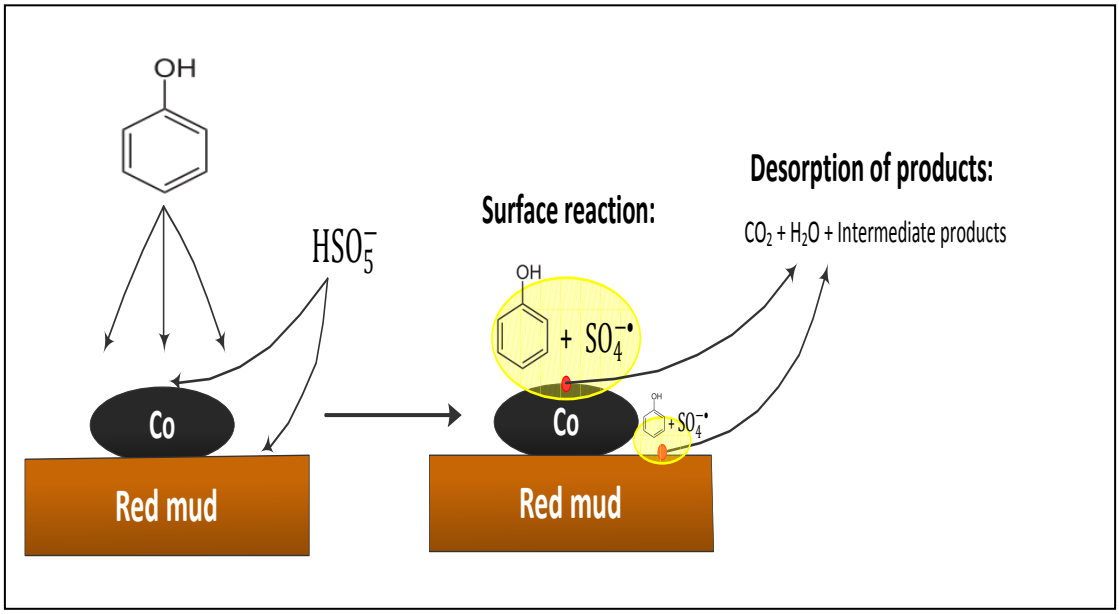

Figure 5.11. Mechanism for degradation of phenol in Co/RM–oxone systems.

5.4 Conclusion

Catalysts of Co/RM-NT and Co/RM-T have been successfully synthesized by dispersed active metal Co of 1-5 wt% by a wetness impregnation method followed by calcination at 500 ^{o}C for 4 h in air on RM supports. The BET surface area of Co/RM-T is 32.0 m^2/g and pore volume is 0.021 cm^3/g while Co/RM-NT has surface area and pore volume of 22.5 m^2/g and 0.011 cm^3/g, respectively. Pretreatment of RM enhanced surface area, resulting in high Co dispersion. Co/RM-NT and Co/RM-T with active metal species of Co_3O_4 are much effective for activation of PMS to produce sulphate radicals for phenol oxidative decomposition. Co/RM-T presented better performance than Co/RM-NT. Several factors influenced the removal efficiency of phenol such as PMS concentration, Co loading in catalyst, phenol concentration, catalyst loading and temperature. Kinetic studies showed that the phenol degradation followed first order reaction and activation energies of Co/RM-NT and Co/RM-T were 47.0 kJ/mol and 46.2 kJ/mol, respectively.

References

1. Dohnal, V.; Fenclova, D., Air-Water Partitioning and Aqueous Solubility of Phenols. *Journal of Chemical & Engineering Data* 1995, 40, (2), 478-483.

2. Keith, L.; Telliard, W., ES&T Special Report: Priority pollutants: I-a perspective view. *Environmental Science & Technology* 1979, 13, (4), 416-423.

3. Fortuny, A.; Bengoa, C.; Font, J.; Fabregat, A., Bimetallic catalysts for continuous catalytic wet air oxidation of phenol. *Journal of Hazardous Materials* 1999, 64, (2), 181-193.

4. Christoskova, S. G.; Stoyanova, M.; Georgieva, M., Low-temperature iron-modified cobalt oxide system: Part 2. Catalytic oxidation of phenol in aqueous phase. *Applied Catalysis A: General* 2001, 208, (1-2), 243-249.

5. Shukla, P. R.; Wang, S.; Sun, H.; Ang, H. M.; Tadé, M., Activated carbon supported cobalt catalysts for advanced oxidation of organic contaminants in aqueous solution. *Applied Catalysis B: Environmental* 2010, 100, (3-4), 529-534.

6. Barrault, J.; Abdellaoui, M.; Bouchoule, C.; Majesté, A.; Tatibouët, J. M.; Louloudi, A.; Papayannakos, N.; Gangas, N. H., Catalytic wet peroxide oxidation over mixed (Al-Fe) pillared clays. *Applied Catalysis B: Environmental* 2000, 27, (4), L225-L230.

7. Huang, C.-P.; Huang, Y.-H., Comparison of catalytic decomposition of hydrogen peroxide and catalytic degradation of phenol by immobilized iron oxides. *Applied Catalysis A: General* 2008, 346, (1-2), 140-148.

8. Garg, A.; Mishra, I. M.; Chand, S., Oxidative Phenol Degradation Using Non-Noble Metal Based Catalysts. *CLEAN – Soil, Air, Water* 2010, 38, (1), 27-34.

9. Zazo, J. A.; Casas, J. A.; Mohedano, A. F.; Gilarranz, M. A.; Rodríguez, J. J., Chemical Pathway and Kinetics of Phenol Oxidation by Fenton's Reagent. *Environmental Science & Technology* 2005, 39, (23), 9295-9302.

10. Imamura, S.; Hirano, A.; Kawabata, N., Wet oxidation of acetic acid catalyzed by Co-Bi complex oxides. *Industrial & Engineering Chemistry Product Research and Development* 1982, 21, (4), 570-575.

11. Wang, S., A Comparative study of Fenton and Fenton-like reaction kinetics in decolourisation of wastewater. *Dyes and Pigments* 2008, 76, (3), 714-720.

12. Gallezot, P.; Chaumet, S.; Perrard, A.; Isnard, P., Catalytic wet air oxidation of acetic acid on carbon-supported ruthenium catalysts. *Journal of Catalysis* 1997, 168, (1), 104-109.

13. Imamura, S.; Doi, A.; Ishida, S., Wet oxidation of ammonia catalyzed by cerium-based composite oxides. *Industrial & Engineering Chemistry Product Research and Development* 1985, 24, (1), 75-80.

14. Esplugas, S.; Giménez, J.; Contreras, S.; Pascual, E.; Rodríguez, M., Comparison of different advanced oxidation processes for phenol degradation. *Water Research* 2002, 36, (4), 1034-1042.

15. Hamoudi, S.; Larachi, F.; Sayari, A., Wet oxidation of phenolic solutions over heterogeneous catalysts: Degradation profile and catalyst behavior. *Journal of Catalysis* 1998, 177, (2), 247-258.

16. Shukla, P. R.; Wang, S.; Ang, H. M.; Tadé, M. O., Photocatalytic oxidation of phenolic compounds using zinc oxide and sulphate radicals under artificial solar light. *Separation and Purification Technology* 2010, 70, (3), 338-344.

17. Pignatello, J. J.; Oliveros, E.; MacKay, A., Advanced Oxidation Processes for Organic Contaminant Destruction Based on the Fenton Reaction and Related Chemistry. *Critical Reviews in Environmental Science and Technology* 2006, 36, (1), 1-84.

18. Anipsitakis, G. P.; Dionysiou, D. D., Degradation of Organic Contaminants in Water with Sulfate Radicals Generated by the Conjunction of Peroxymonosulfate with Cobalt. *Environmental Science & Technology* 2003, 37, (20), 4790-4797.

19. Shukla, P.; Sun, H.; Wang, S.; Ang, H. M.; Tadé, M. O., Nanosized Co_3O_4/SiO_2 for heterogeneous oxidation of phenolic contaminants in waste water. *Separation and Purification Technology* 2011, 77, (2), 230-236.

20. Shukla, P.; Sun, H.; Wang, S.; Ang, H. M.; Tadé, M. O., Co-SBA-15 for heterogeneous oxidation of phenol with sulfate radical for wastewater treatment. *Catalysis Today* 2011, 175, 380–385.

21. Liang, H.; Ting, Y. Y.; Sun, H.; Ang, H. M.; Tadé, M. O.; Wang, S., Solution combustion synthesis of Co oxide-based catalysts for phenol degradation in aqueous solution. *Journal of Colloid and Interface Science* 2012, 372, (1), 58-62.

22. Zhang, W.; Tay, H. L.; Lim, S. S.; Wang, Y.; Zhong, Z.; Xu, R., Supported cobalt oxide on MgO: Highly efficient catalysts for degradation of organic dyes in dilute solutions. *Applied Catalysis B: Environmental* 2010, 95, (1-2), 93-99.

23. Yang, Q.; Choi, H.; Chen, Y.; Dionysiou, D. D., Heterogeneous activation of peroxymonosulfate by supported cobalt catalysts for the degradation of 2,4-dichlorophenol in water: The effect of support, cobalt precursor, and UV radiation. *Applied Catalysis B: Environmental* 2008, 77, (3-4), 300-307.

24. Muhammad, S.; Saputra, E.; Sun, H.; Izidoro, J. d. C.; Fungaro, D. A.; Ang, H. M.; Tade, M. O.; Wang, S., Coal fly ash supported Co_3O_4 catalysts for phenol degradation using peroxymonosulfate. *RSC Advances* 2012, 2, (13), 5645-5650.

25. Sun, H.; Tian, H.; Hardjono, Y.; Buckley, C. E.; Wang, S., Preparation of cobalt/carbon-xerogel for heterogeneous oxidation of phenol. *Catalysis Today* 2012, 186, (1), 63-68.

26. Yao, Y.; Yang, Z.; Zhang, D.; Peng, W.; Sun, H.; Wang, S., Magnetic $CoFe_2O_4$–Graphene Hybrids: Facile Synthesis, Characterization, and Catalytic Properties. *Industrial & Engineering Chemistry Research* 2012, 51, (17), 6044-6051.

27. Shukla, P.; Wang, S.; Singh, K.; Ang, H. M.; Tadé, M. O., Cobalt exchanged zeolites for heterogeneous catalytic oxidation of phenol in the presence of peroxymonosulphate. *Applied Catalysis B: Environmental* 2010, 99, (1–2), 163-169.

28. Mohan, D.; Pittman, J. C. U., Arsenic removal from water/wastewater using adsorbents--A critical review. *Journal of Hazardous Materials* 2007, 142, (1-2), 1-53.

29. Li, L.; Wang, S.; Zhu, Z.; Yao, X.; Yan, Z., Catalytic decomposition of ammonia over fly ash supported Ru catalysts. *Fuel Processing Technology* 2008, 89, (11), 1106-1112.

30. Wang, S.; Ang, H. M.; Tadé, M. O., Novel applications of red mud as coagulant, adsorbent and catalyst for environmentally benign processes. *Chemosphere* 2008, 72, (11), 1621-1635.

31. Liu, Y.; Naidu, R.; Ming, H., Red mud as an amendment for pollutants in solid and liquid phases. *Geoderma* 2011, 163, (1-2), 1-12.

32. Liu, Y.; Lin, C.; Wu, Y., Characterization of red mud derived from a combined Bayer Process and bauxite calcination method. *Journal of Hazardous Materials* 2007, 146, (1-2), 255-261.

33. Li, L.; Wang, S.; Zhu, Z., Geopolymeric adsorbents from fly ash for dye removal from aqueous solution. *Journal of Colloid and Interface Science* 2006, 300, (1), 52-59.

34. Janos, P.; Buchtová, H.; Rýznarová, M., Sorption of dyes from aqueous solutions onto fly ash. *Water Research* 2003, 37, (20), 4938-4944.

35. Mohan, D.; Singh, K. P.; Singh, G.; Kumar, K., Removal of Dyes from Wastewater Using Flyash, a Low-Cost Adsorbent†. *Industrial & Engineering Chemistry Research* 2002, 41, (15), 3688-3695.

36. Zhao, Y.; Wang, J.; Luan, Z.; Peng, X.; Liang, Z.; Shi, L., Removal of phosphate from aqueous solution by red mud using a factorial design. *Journal of Hazardous Materials* 2009, 165, (1-3), 1193-1199.

37. Yue, Q.; Zhao, Y.; Li, Q.; Li, W.; Gao, B.; Han, S.; Qi, Y.; Yu, H., Research on the characteristics of red mud granular adsorbents (RMGA) for phosphate removal. *Journal of Hazardous Materials* 2010, 176, (1-3), 741-748.

38. Ng, P. F.; Li; Wang, S.; Zhu, Z.; Lu, G.; Yan, Z., Catalytic Ammonia Decomposition over Industrial-Waste-Supported Ru Catalysts. *Environmental Science & Technology* 2007, 41, (10), 3758-3762.

39. Schwickardi, M.; Johann, T.; Schmidt, W.; Schüth, F., High-Surface-Area Oxides Obtained by an Activated Carbon Route. *Chemistry of Materials* 2002, 14, (9), 3913-3919.

40. Wang, S.; Boyjoo, Y.; Choueib, A.; Zhu, Z. H., Removal of dyes from aqueous solution using fly ash and red mud. *Water Research* 2005, 39, (1), 129-138.

41. Saputra, E.; Muhammad, S.; Sun, H.; Ang, H. M.; Tadé, M. O.; Wang, S., Red mud and fly ash supported Co catalysts for phenol oxidation. *Catalysis Today* 2012, 190 (1), 68-72.

42. Wei hua Yu, C. Z., Yongxian Fan, Caiying Lou, Dongshen Tong, Mei Fang, Co-supported hexagonal mesoporous silicas for catalytic oxidation of 4-t-butyltoluene. *Indian Journal of Chemistry* 2009, 48A, (July 2009), 946-950.

43. Gu, F.; Li, C.; Hu, Y.; Zhang, L., Synthesis and optical characterization of Co_3O_4 nanocrystals. *Journal of Crystal Growth* 2007, 304, (2), 369-373.

44. Suraja, P. V.; Yaakob, Z.; Binitha, N. N.; Resmi, M. R.; Silija, P. P., Photocatalytic degradation of dye pollutant over Ti and Co doped SBA-15: Comparison of activities under visible light. *Chemical Engineering Journal* 2011, 176-177, (0), 265-271.

45. Costa, R. C. C.; Moura, F. C. C.; Oliveira, P. E. F.; Magalhães, F.; Ardisson, J. D.; Lago, R. M., Controlled reduction of red mud waste to produce active systems for environmental applications: Heterogeneous Fenton reaction and reduction of Cr(VI). *Chemosphere* 2010, 78, (9), 1116-1120.

Chapter-6

Removal of Phenolic Contaminants Using Sulfate Radicals Activated by Natural Zeolite and MCM48 Supported Cobalt Catalysts

Abstract

Two Co oxide catalysts supported on natural zeolites from Indonesia (INZ) and Australia (ANZ) were prepared and used to activate peroxymonosulphate for degradation of aqueous phenol. The two catalysts were characterized by several techniques such as X-ray diffraction (XRD), scanning electron microscopy (SEM), energy dispersive X-ray spectroscopy (EDS), and N_2 adsorption. It was found that Co/INZ and Co/ANZ are effective in activation of peroxymonosulphate to produce sulphate radicals for phenol degradation. Co/INZ and Co/ANZ could reduce phenol up to 100% and 70%, respectively, at the conditions of 25 ppm phenol, 0.2 g catalyst, 1 g oxone, and 25 ºC. Several parameters such as amount of catalyst loading, phenol concentration, oxidant concentration and temperature were found to be the key factors influencing phenol degradation. A pseudo first order would fit to phenol degradation kinetics and the activation energies of Co/INZ and Co/ANZ were obtained as 52.4 and 61.3 kJ/mol, respectively. In addition, Co/MCM48 catalyst was also prepared and tested in phenol degradation. It is found that Co/MCM48 is much better than the other two catalysts in sulfate radical production with activation energy of 80.3 KJ/mol.

Part A : Phenol Removal Using Co/INZ and Co/ANZ

6.1 Introduction

Phenolic compounds are important organic pollutants in wastewater, which can be produced in chemical, petrochemical, and pharmaceutical industries [1-2]. This type of organic contaminants will not be easily removed in primary and secondary treatment processes. Therefore, it is essential to adopt a tertiary treatment such as thermal oxidation, chemical oxidation, wet air oxidation, catalytic oxidation etc, which are generally known as advanced oxidation processes (AOPs) [3-5]. In principle, the AOPs will produce harmless compounds to the environment such as CO_2 and H_2O. Among the AOPs, heterogeneous catalytic oxidation usually has some advantages such as operating at room temperature with normal pressure and low energy. Furthermore, heterogeneous catalysts can be synthesized using cheap materials as supports such as activated carbon, silica, alumina and zeolites [6].

Among the materials, zeolites are important heterogeneous catalysts used in industry. Their key properties are size and shape selectivity, together with the potential for strong acidity. Zeolites also have ion exchangeable sites and highly hydrothermal stability, making them widely used for many applications in separation, ion exchange and adsorption. Natural zeolites are much cheaper than synthetic zeolites due to their wide availability in the world [7]. However, few investigations have been reported in use of natural zeolites for AOPs [8] Currently, most of AOPs are based on the generation of very reactive species, such as hydroxyl radicals (OH•), which will oxidize many pollutants quickly and non selectively [4, 9, 10]. Recently, sulphate radicals have also been proposed as alternative active oxidants due to their higher oxidation potential [11, 12]. For sulphate

radical production, peroxymonosulphate (PMS, HSO_5^-) reaction with Co ions has been found to be an effective route [13-14].

However, the use of cobalt metal ion as a catalyst to activate PMS for generation of sulphate radicals raises an issue of toxicity of the cobalt ions in water, because Co is one of heavy metals which can cause diseases to animals and human beings. Thus, employing Co^{2+}/PMS for oxidation of aqueous pollutants and minimizing the discharge of cobalt in wastewater require development of an efficient heterogeneous catalytic system by incorporating cobalt ions in a substrate. In addition, it is easy to recover the used catalysts after simple separation process. In the past years, several types of heterogeneous cobalt catalyst including cobalt oxides [15, 16], cobalt composite [17] and supported cobalt catalysts have been investigated [18-24].

In this chapter, we investigate cobalt based catalysts supported on Indonesian natural zeolite (INZ) and Australian natural zeolite (ANZ) for heterogeneous generation of sulphate radicals for chemical mineralizing of phenol in the solution. Several key parameters in the kinetic study such as phenol concentration, catalyst loading, oxone concentration and temperature were investigated.

6.2 Materials and Methods

6.2.1 Synthesis of natural zeolite supported cobalt catalysts

Cobalt/Indonesian natural zeolite (Co/INZ) and cobalt/Australian natural zeolite (Co/ANZ) were synthesized using an impregnation method. INZ and ANZ samples were crushed in particle size of 60-100 μm. Cobalt nitrate ($Co(NO_3)_2 \bullet 6H_2O$, Sigma-Aldrich) was dissolved into 200 mL

ultrapure water. Then, INZ or ANZ was added into the solution and kept stirring for 24 h. The solid was dried in an oven at 120 ^{o}C for 6 h. Calcination of the catalysts was conducted in a furnace at 550 ^{o}C for 6 h. For the two catalysts, Co loading was kept at 5 wt%.

6.2.2 Characterization of catalysts

The synthesized catalysts were characterized by XRD, SEM combined with EDS, and N_2 adsorption. Crystalline structure of the materials was analyzed by a X-ray diffractometer (Bruker D8 Advance equipped with a Lynx eye detector, Bruker-AXS, Karlsruhe, Germany) operated at 40 kV and 30 mA. SEM (Philips XL30) with secondary and backscatter electron detectors was used to obtain a visual image of the samples to show the texture and morphology of the catalysts with magnification up to 8000 times. The catalysts were also characterized by EDS (Energy Dispersive X-ray spectroscopy) to identify the structural features and the mineralogy. Furthermore, nitrogen adsorption (Micromeritics Gemini 2360) was used to obtain the BET surface area (S_{BET}). Prior to the analysis, the catalyst samples were degassed under vacuum at 200 ^{o}C for 12 h.

6.2.3 Kinetic study of phenol oxidation

Catalytic oxidation of phenol was conducted in 500 mL phenol solutions with concentrations of 25 - 100 ppm. A reactor attached to a stand was dipped into a water bath with a temperature control. The solution was stirred constantly at 400 rpm to maintain a homogeneous solution. A fixed amount of oxidant of peroxymonosulphate (using oxone, DuPont's triple salt $2KHSO_5 \bullet KHSO_4 \bullet K_2SO_4$, Aldrich) was added to the mixture until completely dissolved. Then, a fixed amount of catalysts (Co/INZ or Co/ANZ) was added into the reactor for running of 3-5 h. At the fixed time

interval, 0.5 mL of solution sample was withdrawn and filtered using a HPLC standard filter of 0.45 μm and mixed with 0.5 mL methanol as a quenching reagent to stop the reaction. Phenol was then analyzed on a HPLC with a UV detector at wavelength of 270 nm. The column is C18 with mobile phase of 70% acetonitrile and 30% ultrapure water.

6.3 Results and Discussion

6.3.1 Characterization of natural zeolite supported cobalt catalysts

XRD patterns of Co/INZ and Co/ANZ are presented in Fig. 6.1. Co_3O_4 peaks were identified on both catalysts, however, the peaks are weaker and broad on Co/INZ. This suggested that dispersion of Co_3O_4 on INZ was higher. N_2 adsorption showed that the BET surface areas of Co/INZ and Co/ANZ are 17.9 and 8.1 m^2/g, respectively. In general, high surface area of a support will result in high dispersion of active metal on the support.

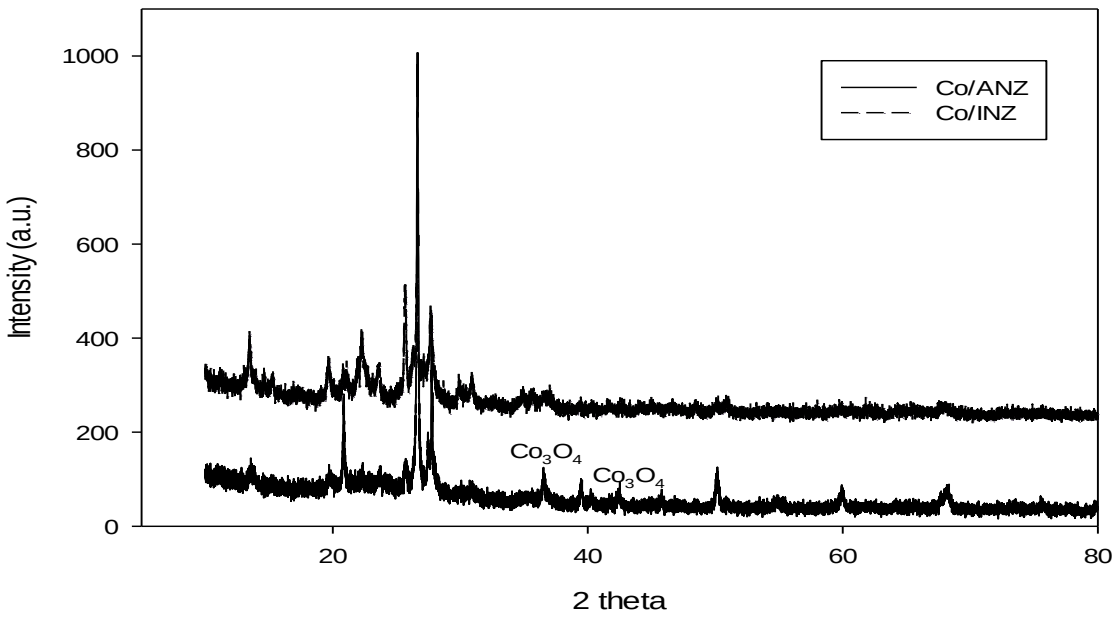

Figure 6.1 XRD patterns of Co/ANZ and Co/INZ.

SEM images and EDS spectra of Co/INZ and Co/ANZ catalysts are shown in Fig. 6.2 and Fig. 6.3. Both secondary electron (SE) and backscattered (BSE) detectors were adopted to observe the dispersion of active cobalt on the catalyst support. From Fig. 6.2A and 6.2B, it can be seen that the BSE detector produces the brighter image than the SE detector at the same observed area. This brighter area refers to the presence of cobalt specks on Co/INZ particles. It also implies that cobalt was well dispersed and coated on the natural zeolite support. The presence of cobalt in the catalyst was also confirmed by EDS spectra (Fig. 6.2C).

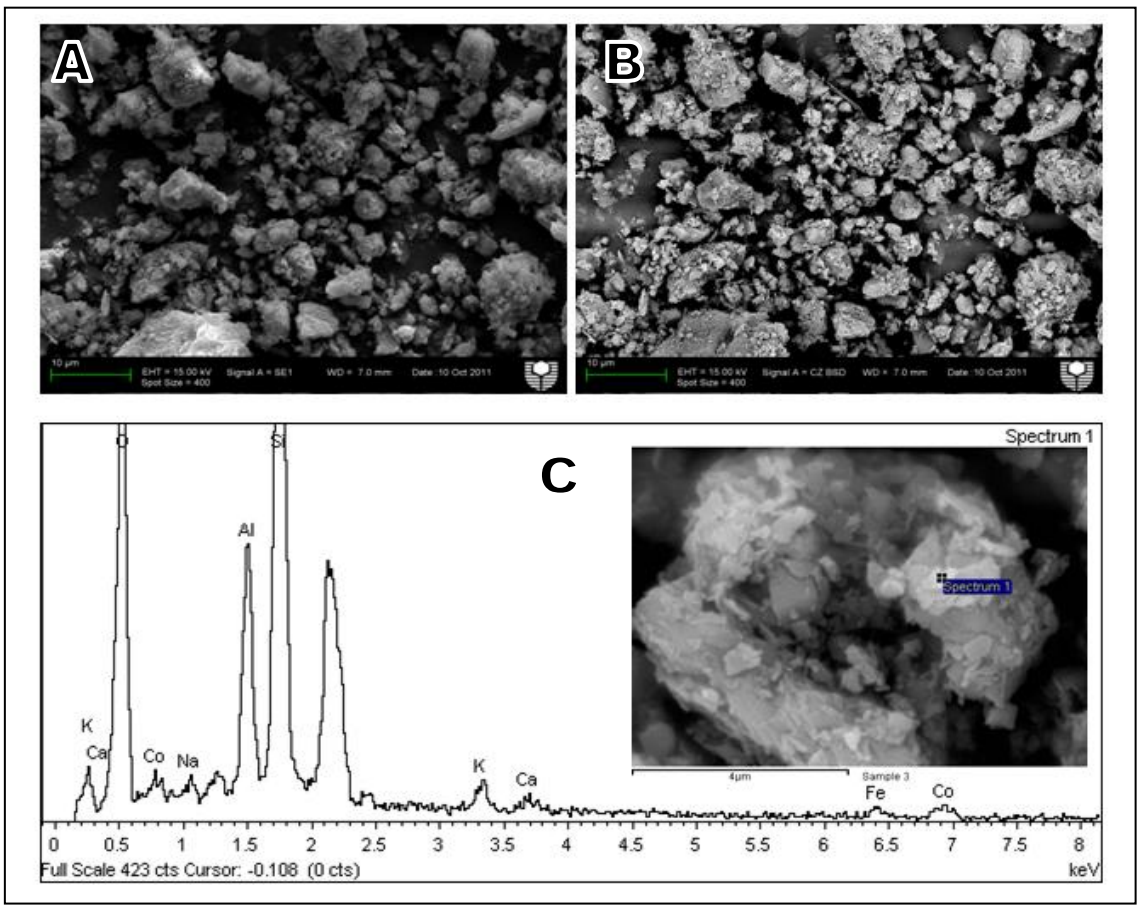

Figure 6.2. SEM images and EDS spectra of Co/INZ, (A) SE Detector, (B) BSE Detector, (C) EDS spectra with inset of spectrum image source

A similar observation was also obtained on Co/ANZ catalyst (Fig. 6.3). However, the particle size of Co/ANZ seems to be larger than Co/INZ. BSE image also shows a good dispersion of cobalt on Co/ANZ surface confirmed by EDS spectra.

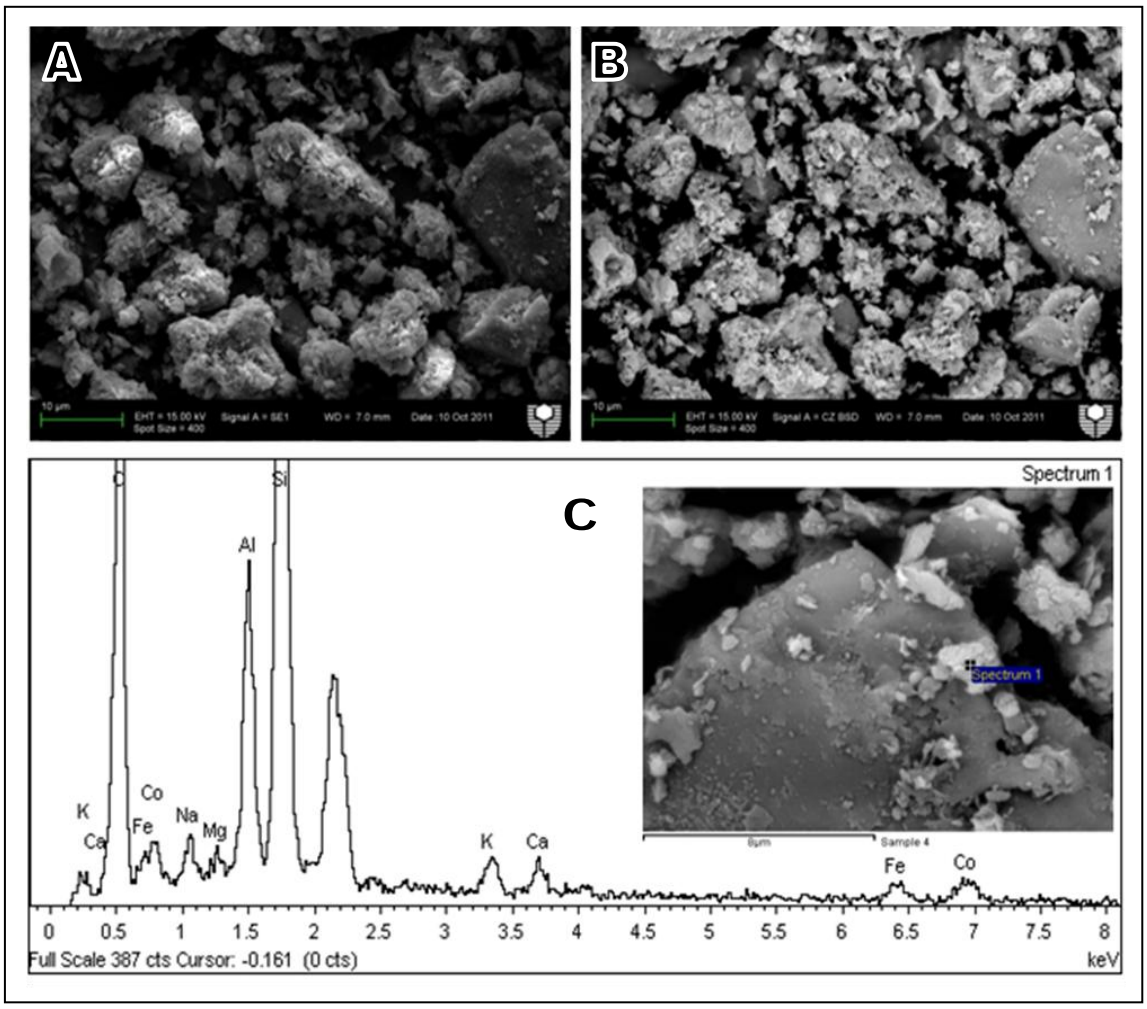

Figure 6.3. SEM images and EDS spectra of Co/ANZ, (A) SE Detector, (B) BSE Detector, (C) EDS spectra with inset of spectrum image source

6.3.2 Phenol oxidation

Adsorption and oxidation of phenol on Co/INZ and Co/ANZ are presented in Fig. 6.4. In the presence of only oxone in phenol solution, no phenol degradation occurred, indicating that oxone itself could not produce sulfate radicals to induce phenol oxidation. Both Co/INZ and Co/ANZ presented low adsorption of phenol at less than 10% in 5 h. However, Co/INZ presented a slight higher phenol adsorption than Co/ANZ, which can be ascribed to higher surface area of Co/INZ.

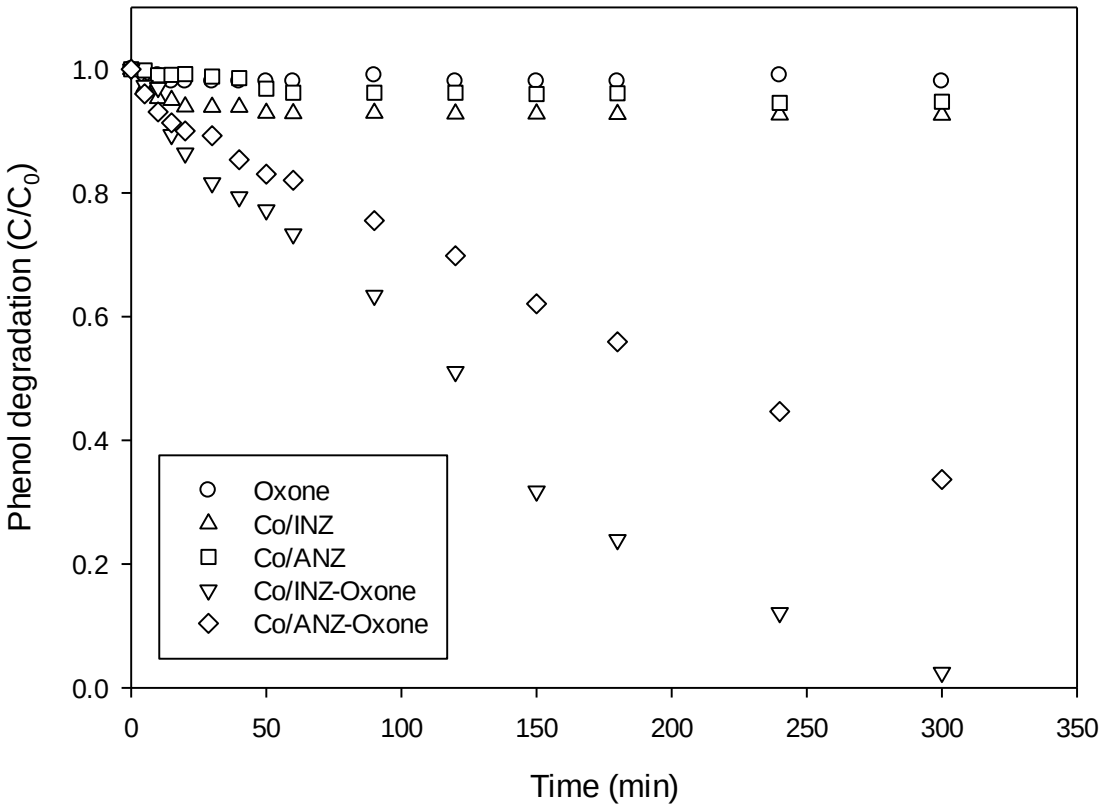

Figure 6.4. Phenol reduction with time in adsorption and catalytic oxidation. Reaction conditions: 0.2g catalyst, 1 g oxone, 25 ppm phenol, 25^{o}C and stirring speed of 400 rpm.

In oxidation tests, Co/INZ with the presence of PMS could degrade phenol up to 100% in 5 h. Meanwhile, Co/ANZ could reach around 70% phenol removal. Significant degradation of phenol in the systems confirms that cobalt in both catalysts could activate PMS to generate sulphate radicals ($SO_4^{-\bullet}$ and $SO_5^{-\bullet}$) for phenol decomposition in solution. XRD analyses showed that Co_3O_4 is major Co species in both catalysts, which will play the role for oxone activation. The reaction mechanism can be listed as below.

$$NZ–Co^{3+} + HSO_5^- \rightarrow NZ–Co^{2+} + SO_5^{-\bullet} + H^+ \quad 6.1$$

$$NZ–Co^{2+} + HSO_5^- \rightarrow NZ–Co^{3+} + SO_4^{-\bullet} + OH^- \quad 6.2$$

Adsorption tests showed that Co/INZ presented a higher phenol adsorption than Co/ANZ. XRD also indicated that Co dispersion on Co/INZ is higher than Co/ANZ. For heterogeneous oxidation, high surface adsorption of phenol and more active Co oxide on surface will promote catalytic activity. Some investigations using different supported Co catalysts have been reported. It was reported that Co/ZSM5 could achieve complete degradation of phenol in 6 h [20] and that Co/SiO_2 could make 100% phenol degradation at 350 min [23]. Therefore, Co/INZ is better than Co/ZSM5 and Co/SiO_2.

Several variables influencing phenol degradations were also investigated. The effect of initial phenol concentration at 25, 50, 75 and 100 mg/L on phenol degradation is shown in Fig. 6.5. Phenol degradation efficiency decreased with increasing phenol concentration. The 100% phenol removal could be achieved at phenol concentration of 25 mg/L in 5 h by using Co/INZ catalyst. While in the same duration at phenol concentrations of 50, 75 and 100 mg/L, removal efficiency obtained are 50, 40 and 30%, respectively. For phenol degradation in Co/INZ-oxone, phenol degradation is dependent on sulphate radicals. Due to the same

concentrations of Co/INZ and PMS, sulfate radical concentration produced in solution will be the same. Thus, high amount of phenol in solution will require more time to achieve the same removal rate, thus lowering phenol degradation efficiency.

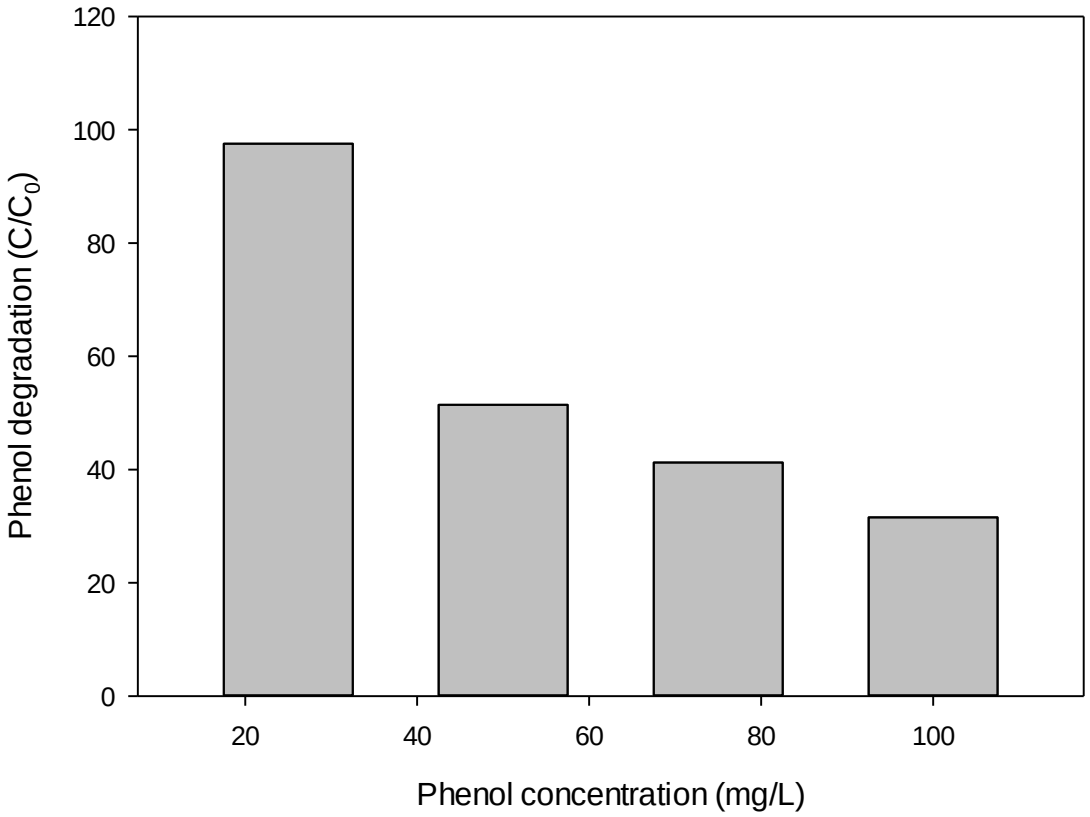

Figure 6.5 Effect of phenol concentration on phenol degradation using Co/INZ catalyst. Reaction conditions: 0.2 g catalyst, 1 g oxone, 25^{o}C and stirring speed of 400 rpm.

Phenol removal efficiency is also affected by catalyst loading in the system as shown in Fig. 6.6. A complete removal of phenol could be reached within 5 h at 0.4 g/L Co/INZ loading. While 70% and 40% removals could be reached at Co/INZ loading of 0.2 and 0.1 g/L, respectively. For phenol

degradation, increased catalyst loading would enhance phenol adsorption and Co oxide to activate PMS, resulting in high phenol degradation.

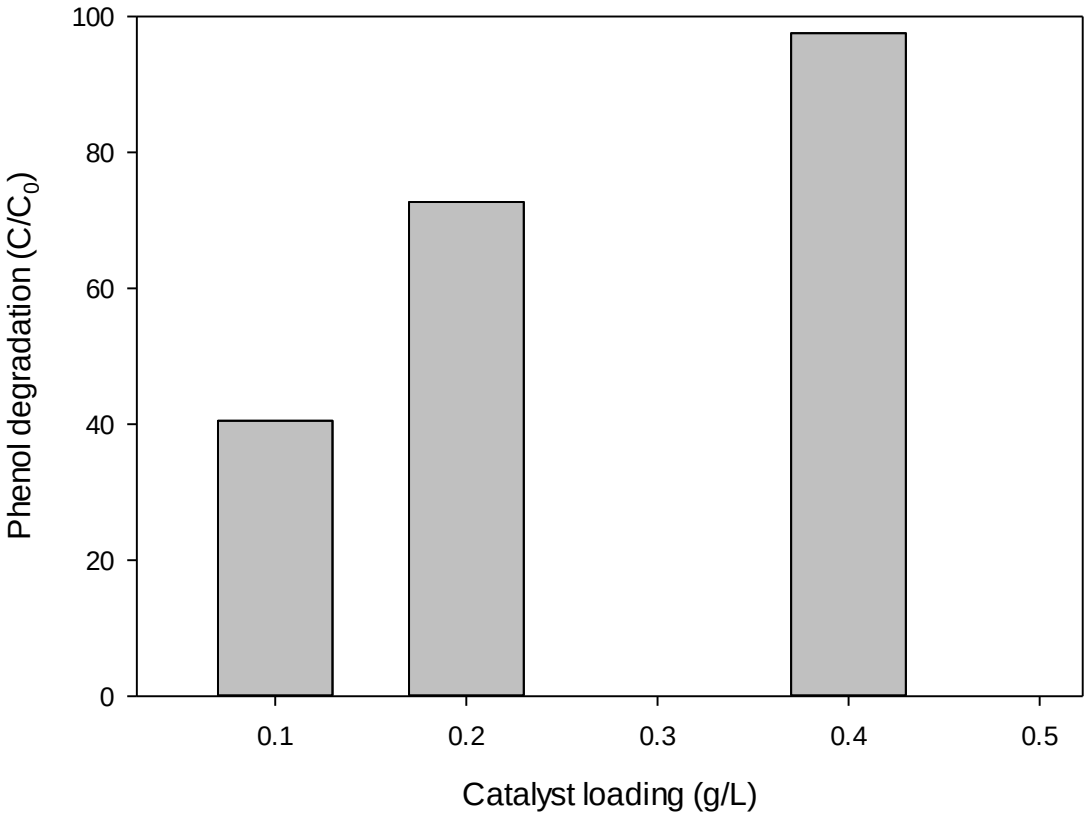

Figure 6.6 Effect of catalyst loading on phenol degradation. Reaction conditions: $[phenol]_0$=25 mg/L, 1 g oxone, 25°C, 300 min.

The effect of oxone concentration on the removal efficiency of phenol is presented in Fig. 6.7. For both catalysts, higher oxone concentration resulted in higher phenol removal. At reaction time of 3 h, the highest removal efficiency of phenol was obtained at 2 g/L oxone and the lowest was at 0.5 g/L oxone on Co/ANZ. However, phenol degradation would reach a similar level after oxone loading higher than 1 g/L on Co/INZ, suggesting the optimal loading at 1 g/L.

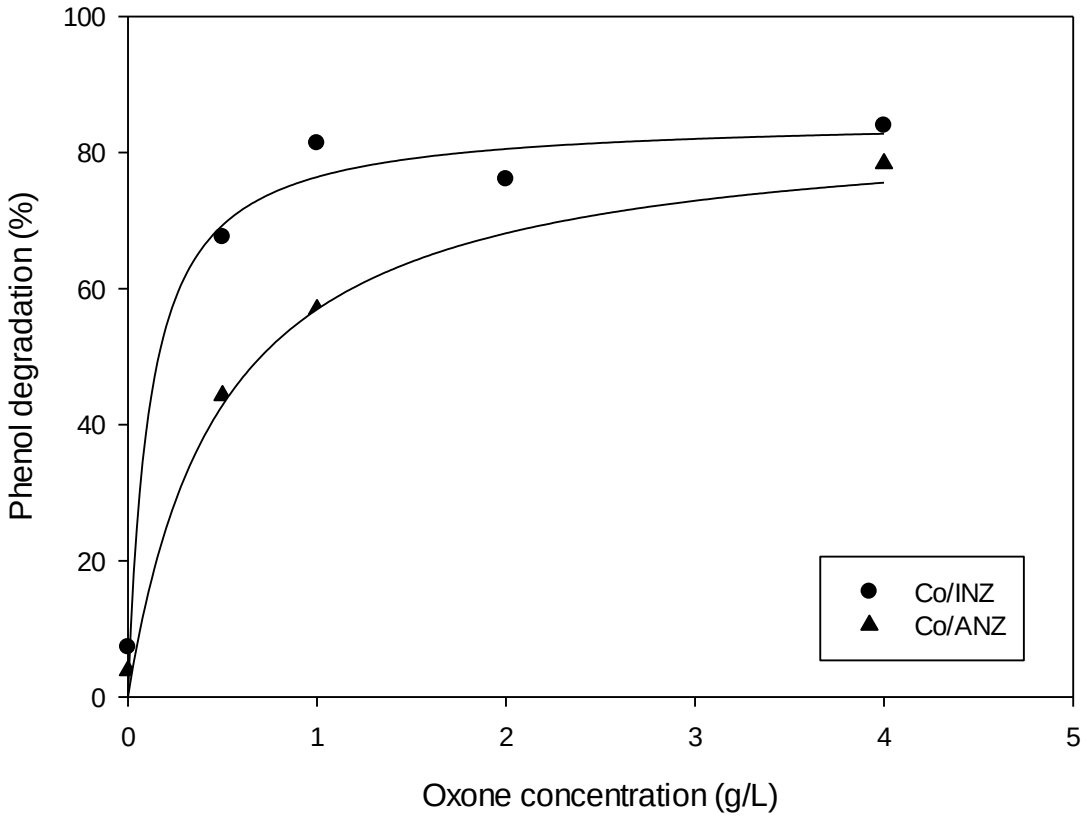

Figure 6.7 Effect of oxone concentration on phenol reduction. Reaction conditions: 0.2 g catalyst, 25 ppm phenol, 25^{o}C and stirring speed of 400 rpm.

In addition, temperature is also a key factor influencing catalyst activity and phenol degradation. Fig.6.8 shows the effect of temperature on phenol degradation. Higher phenol removal was obtained at increased temperature. For instance, at reaction time of 3 h, removal efficiencies of phenol on Co/ANZ at 25, 35, and 45 ^{o}C were 45, 75 and 100%, respectively (Fig. 6.8B). A similar trend is also obtained on Co/INZ catalyst and the removal efficiencies increased from 80% at 25 ^{o}C to 100% at 35 and 45 ^{o}C.

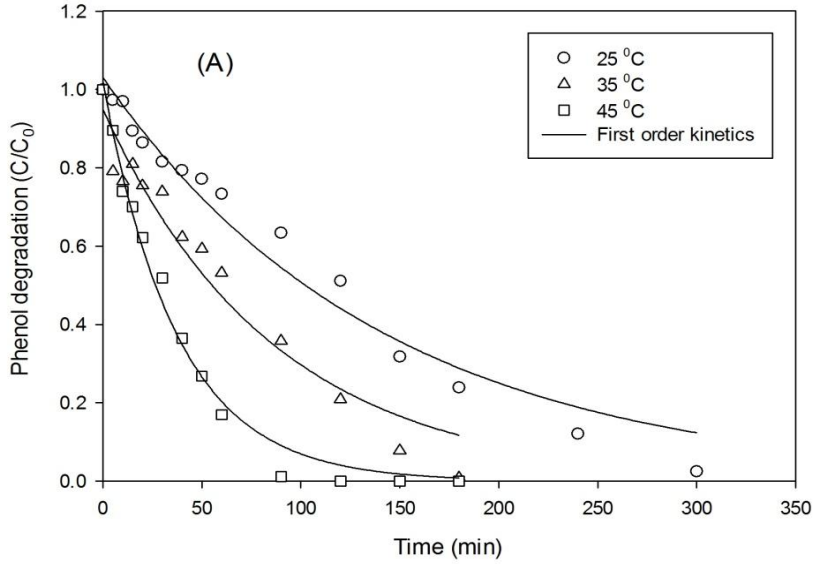

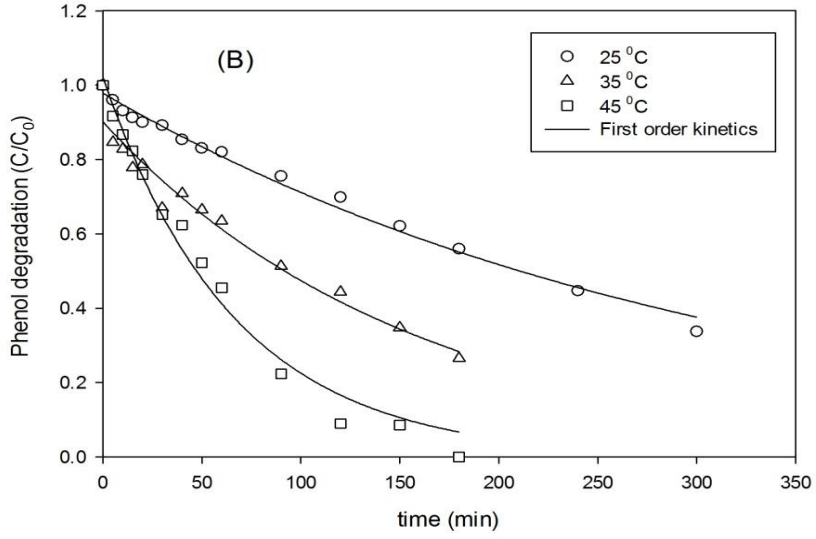

Figure 6.8 Effect of temperature in phenol reduction, (A) Co/INZ catalyst, (B) Co/ANZ catalyst. Reaction conditions : 0.2 g catalyst, 1 g oxone, 25 ppm phenol solution, and stirring speed of 400 rpm.

For variation of phenol degradation with time, a first order model as shown in equation 3.7 can be applied.

Fig. 6.8 also shows the curves of phenol degradation kinetics from the first order model and it is seen that phenol degradation on Co/INZ and Co/ANZ catalysts could be well fitted by the model. Several heterogeneous Co catalysts have been tested in PMS activation for phenol degradation. It was found that phenol degradation on Co/SiO_2 [23] and Co/ZSM5 [20] presented zero order kinetics while Co/AC showed the first order kinetics [21], Chen et al [25] also found the pseudo first-order for decolourisation of acid orange 7 (AO7) in aqueous Co^{2+}/oxone system.

Fig. 6.9 shows the relationship between rate constants *(k)* and temperatures by the Arrhenius correlation. It can be seen that a good relationship for both catalysts was achieved and activation energies for phenol degradation on Co/ANZ and Co/INZ were obtained at 52.4 and 61.3 kJ/mol, respectively.

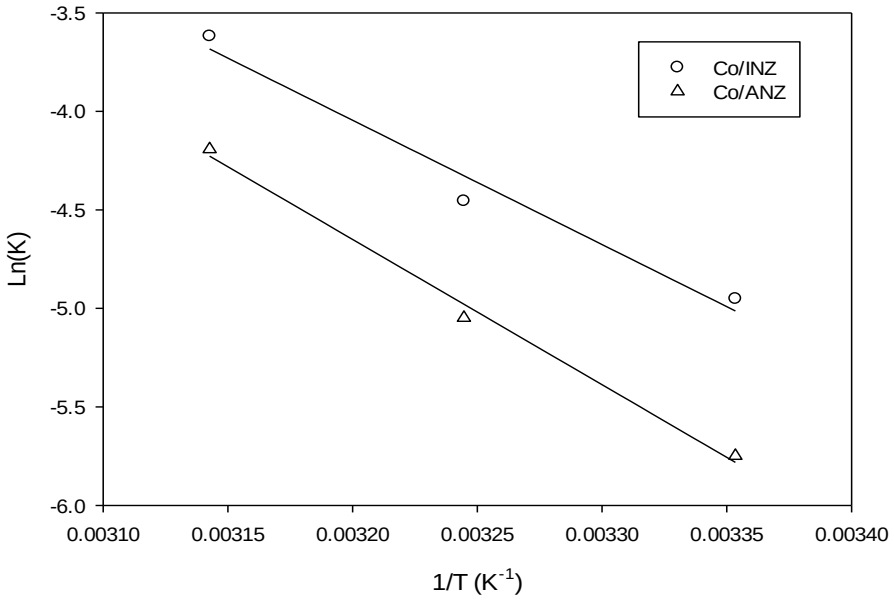

Figure 6.9 Arrhenius plots of phenol degradation on Co/ANZ and Co/INZ.

Part B : Phenol Removal Using Co/MCM48 and Co/INZ

6.4 Introduction

Many chemical industries use phenol as a raw material in their process and discharge the toxic substance in industrial waste streams. Phenol can be in water, wastewater and soil and cause serious problems for human health. Because of its toxic effect even at very low concentration, phenol should be removed completely from the industrial wastes [26]. However, primary and secondary processes in wastewater treatment will not degrade phenol completely into harmless compounds such as H_2O and CO_2. Therefore, tertiary treatment of water becomes important [27].

Further, heterogeneous catalysts can be synthesised using cheap material supports such as activated carbon, zeolite, silica, alumina etc., and can be regenerated for reuse easily [28]. Achieving good coating and dispersion of active metal on a support material with a high surface area is important for obtaining a good catalyst for heterogeneous catalytic oxidation process [29]. It is reported that MCM48 is one of catalyst supports containing high internal surface area and large pore volume [30]. Zeolites including natural zeolite are also important heterogeneous acid catalysts used in industry. They have porous structures revealing regular array of channels and cavities and highly hydrothermal stability, making them promising catalyst supports and adsorbents [31]

The most popular method to degrade organic compounds in wastewater is Fenton reaction which involves of hydrogen peroxide and Fe ion to generate hydroxyl radicals in the solution [32]. Currently, this principle has been developed with many other oxidants such as peroxymonosulphate (PMS) and persulphate which are found more

effective in chemically mineralising various organic pollutants [33-35]. It was reported, in comparison with conventional Fenton reagent, the rate of organic oxidation by sulphate radicals is higher. The sulphate radicals are less dependent on pH in the reaction [13].

Several types of heterogeneous catalyst including Co-oxides [15, 36], Co-composites [37] and Co supported catalysts have been studied [20, 23, 38, 39, 40]. The catalyst supports used are activated carbon (AC), ZSM5, silica, alumina, etc. In this part, we present MCM48 and natural zeolite supported Co catalysts in phenol degradation using peroxymonosulphate.

6.5 Experimental

6.5.1 Synthesis of cobalt based catalysts

Cobalt (Co)/MCM48 and Co/Natural-Zeolite were synthesised using an impregnation method. A fixed amount of cobalt nitrate (Sigma-Aldrich) was added into 200 mL ultrapure water. Next, catalyst supports (MCM48 and Australian Natural Zeolite) were added into the solution and kept stirring for 7 h. After that, the suspension was evaporated in a rotary evaporator at temperature of 50 ^{0}C under vacuum. The solids were dried in an oven at 120 ^{0}C for 6 h and then calcined at 550 ^{0}C for 6 h in a furnace.

6.5.2 Characterisation of catalysts

The synthesised catalysts were characterised by X-ray diffraction (XRD), scanning electron microscopy (SEM) with energy dispersive X-ray spectroscopy (EDS), and N_2 adsorption. The XRD (Siemen, D501 diffractometer) was used to identify the structural features and the mineralogy of the catalysts. The XRD pattern was obtained using filtered Cu Kα radiation with accelerating voltage of 40 kV and current of 30 mA.

The samples were scanned at 2θ from 5-100^{o}. Scanning electron microscopy (SEM, Philips XL30) with secondary and backscatter electron detectors was used to obtain a visual image of the samples to show the texture and morphology of the catalysts with magnification up to 8,000 times. Energy-dispersive X-ray spectroscopy (EDS) was also used to detect Co particles on supported catalysts. The catalysts were analysed by nitrogen adsorption-desorption (Autosorb-1) to identify the BET surface area. Prior to the analysis, the catalyst samples were degassed under vacuum at 200 ^{o}C for 12 h.

6.5.3 Kinetic study of phenol oxidation

Catalytic oxidation of phenol was conducted in 500 mL phenol solutions at concentrations of 25, 50, 75 and 100 ppm. A reactor attached to a stand was dipped into a water bath with a temperature controller. The solution was stirred constantly at 400 rpm to maintain homogeneous solution. A fixed amount of peroxymonosulphate (using Oxone®, DuPont's triple salt $2KHSO_5 \bullet KHSO_4 \bullet K_2SO_4$, Aldrich) was added to the mixture until completely dissolved. Then, a fixed amount of catalysts (Co/MCM48 or Co/ANZ) was added into the reactor to start the oxidation of phenol. The reaction was run for 2-5 h. At some time interval, 0.5 mL of a sample was withdrawn from the solution and filtered using HPLC standard filter of 0.45 μm and mixed with 0.5 mL methanol as a quenching reagent to stop the reaction. Phenol was then analysed on a HPLC with a UV detector at wavelength of 270 nm. The column is C18 with mobile phase of 30% acetonitrile and 70% ultrapure water. For some selected samples, total organic carbon (TOC) was determined by a Shimadzu TOX-5000 CE analyser.

6.6 Result and Discussion

6.6.1 Characterisation of Co/MCM48 and Co/ANZ catalysts

The XRD patterns of Co/MCM48 and Co/ANZ are shown in Fig. 6.10. For Co/MCM48, no Co oxide peaks were observed, probably due to fine particles and high dispersion of active cobalt on the support surface. On the other hand, cobalt oxide species were found at 2θ coordinate of 26.5, 36.8 and 42.4 and 59.5^0 on Co/ANZ.

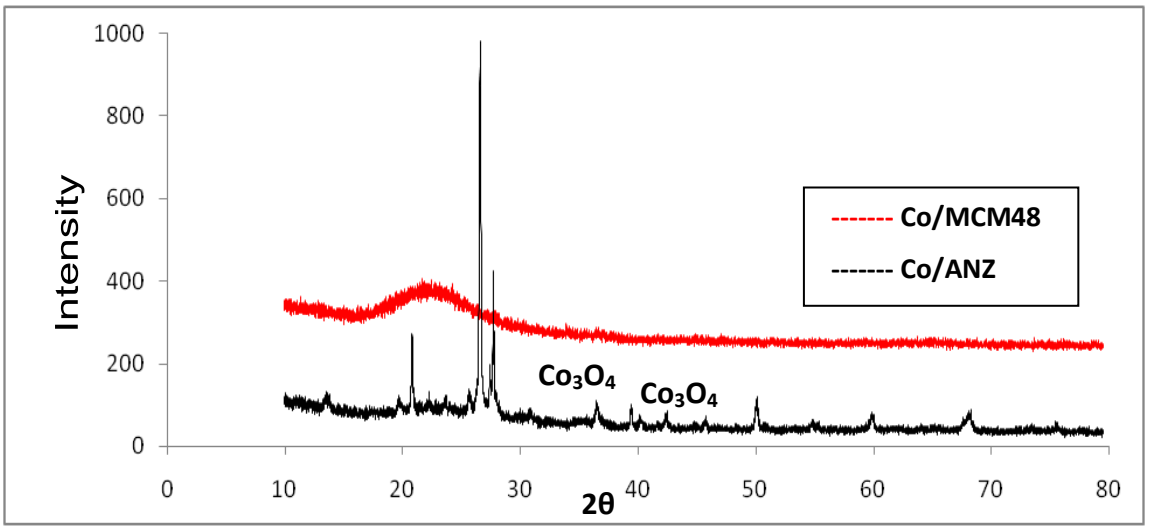

Figure 6.10 XRD spectra of Co/MCM48 and Co/ANZ.

Figure 6.11 and Figure 6.12 show the SEM image with EDS spectra of Co/MCM48 and Co/ANZ catalysts, respectively. It is clear that the morphology of Co/MCM48 is in form of sphere with a particle size below 1 micron. The BSE image (Fig. 6.11B) is brighter than the SE one (Fig 6.11A), which could indicate that cobalt has been well coated on MCM48 support. EDS spectra also show the presence of Co on the surface of MCM48.

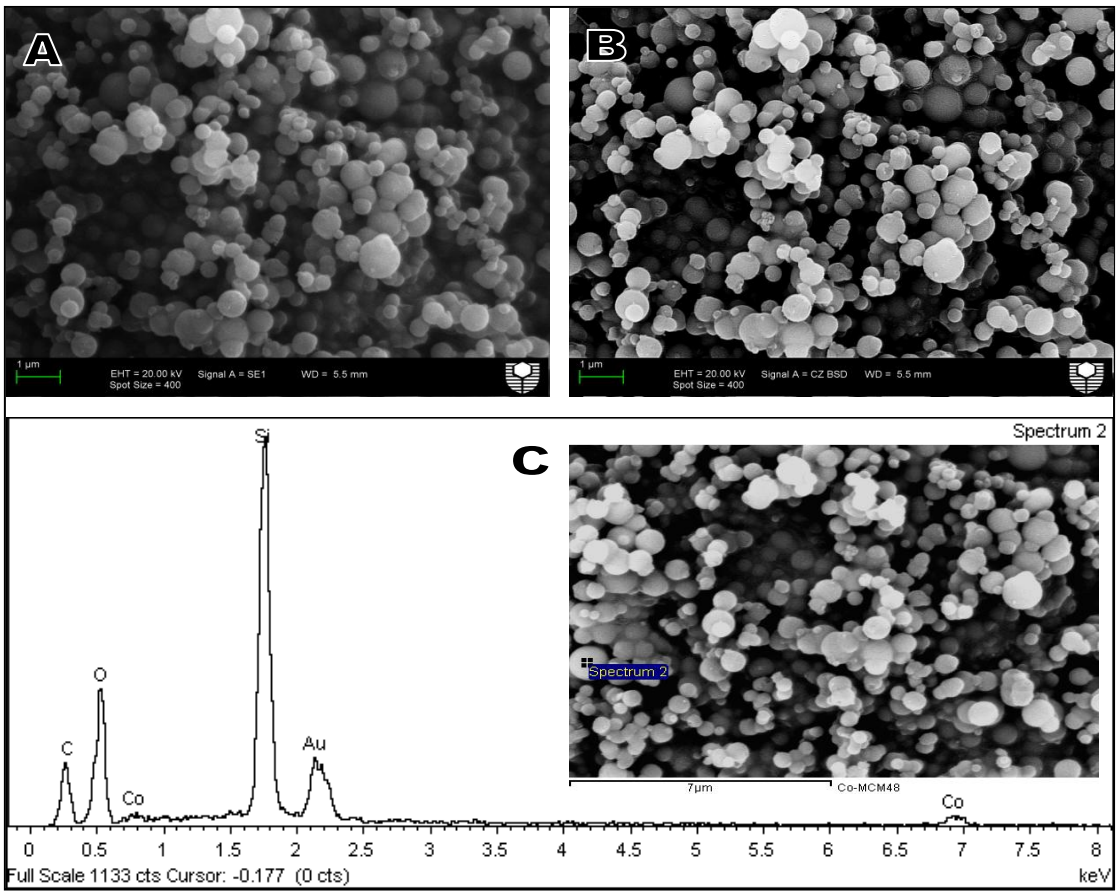

Figure 6.11. SEM images and EDS spectra of Co/MCM48, (A) SE Detector, (B) BSE Detector, (C) EDS Spectra with insert of spectrum image source

Figure 6.12 shows that Co/ANZ presents as larger particles in different sizes. The BSE image (Fig. 6.12B) is much brighter than the SE one (Fig 6.12A), indicating the presence of Co. EDS spectra (Fig. 6.12C) shows the presence of several other metals such as Fe, Ca, K, Si. Al, which come from ANZ. Some of the EDS spectra showed that no cobalt on the surface of the catalyst support. This suggests a low dispersion of Co metal on ANZ surface due to large particle size of ANZ and small surface area.

S_{BET} surface areas of the two catalysts were obtained from N_2 adsorption. Co/MCM48 has a surface area of 797 m^2/g while Co/ANZ only has surface

area of 8 m^2/g. High surface area of a support made a better dispersion of Co on MCM48, which can be confirmed from SEM and EDS results.

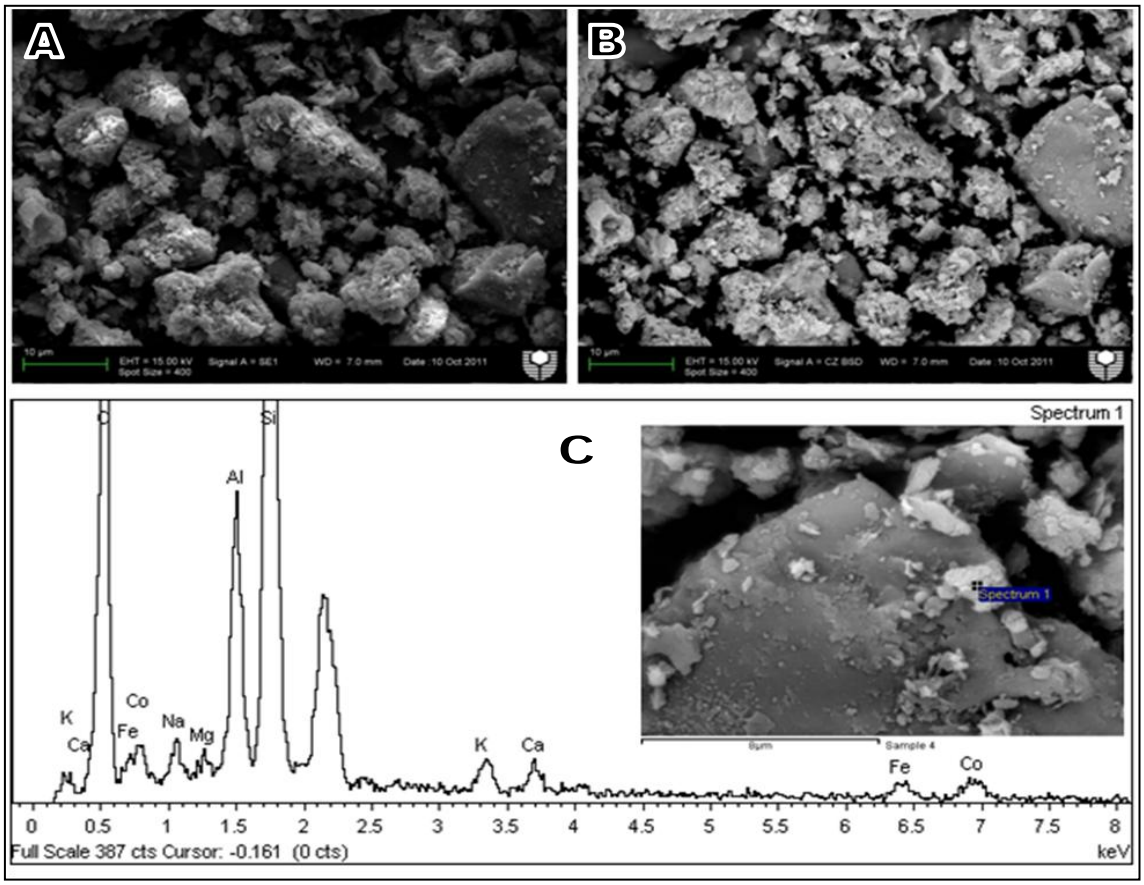

Figure 6.12 SEM Image and EDS Spectra of Co/ANZ, (A) SE Detector, (B) BSE Detector, (C) EDS Spectra with insert of spectrum image source

6.6.2 Preliminary study of phenol oxidation

A series of preliminary tests including adsorption of phenol on Co/MCM48 and Co/ANZ were conducted and the results are shown in Figure 6.13. Phenol did not show degradation with Oxone®, suggesting that Oxone® itself could not be activated at low temperature to produce sulfate radicals.

Co/MCM48 presented phenol adsorption at 19% and Co/ANZ showed phenol removal efficiency of 11% without the presence of Oxone®. But Co/MCM48 and Co/ANZ could activate Oxone® to generate sulphate radical ($SO_4^{-\bullet}$) for the reduction of phenol in solution. Co/MCM48 could reduce 100% phenol to zero within 20 min while Co/ANZ could only reach 17% phenol removal efficiency in the same time. In this experiment, the highest phenol removal by the Co/ANZ is 77% within 5 h. The following reactions show the formation of sulphate radicals.

$$Co^{2+} + HSO_5^- \rightarrow Co^{3+} + SO_4^{\bullet-} + OH^- \quad 6.4$$

$$Co^{3+} + HSO_5^- \rightarrow Co^{2+} + SO_5^{-\bullet} + H^+ \quad 6.5$$

$$SO_4^{\bullet-} + H_2O \rightarrow SO_4^{2-} + OH^\bullet + H^+ \quad 6.6$$

$$SO_4^{-\bullet} + \text{organics} \rightarrow \text{several steps} \rightarrow CO_2 + H_2O + SO_4^{2-} \quad 6.7$$

TOC measurements showed that TOC reductions in Co/MCM48-Oxone® and Co/ANZ-Oxone® were 67% and 23% at 90 min, respectively. The lower reduction in TOC than phenol concentration was due to the generation of intermediates during the reaction.

For phenol degradation, a pseudo first order kinetics was used to describe variation of phenol concentration versus time (Eq. 6.3). It can be seen (Fig. 6.13) that the first order kinetics showed a good fit to the experiment. Several heterogeneous Co catalysts have been tested in PMS activation for phenol degradation. It was found from previous research that phenol degradation on cobalt based catalyst zero order and firs order kinetics [20, 21, 23, 25].

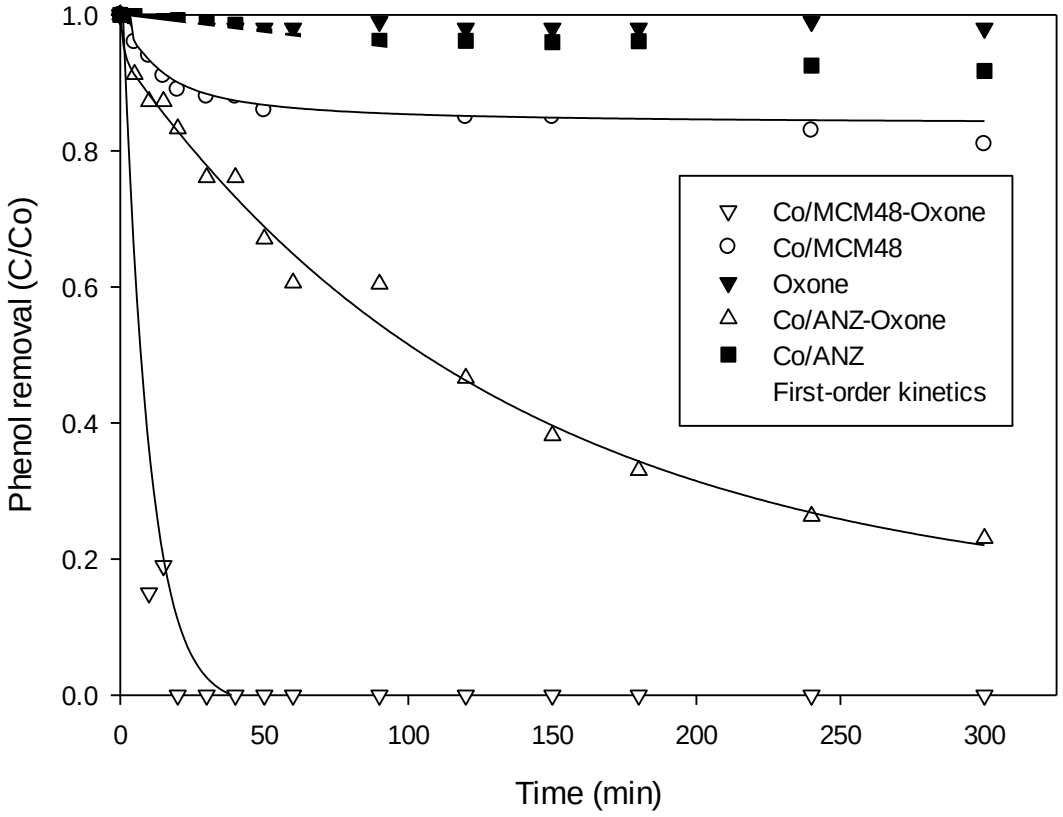

Figure 6.13 Preliminary test of phenol degradation by oxidation and adsorption

6.6.3 Effects of reaction parameters on phenol degradation

The influence of phenol concentration on phenol removal was shown in Figure 6.14. Generally, higher concentration of phenol causes the lower phenol removal efficiency. For instance, at the reaction time of 20 min, phenol conversion for 25, 50, 75 and 100 ppm on Co/MCM48 are 100%, 81%, 39% and 10%, respectively. Complete removal of phenol at 25, 50, and 75 ppm could be achieved at time of 20, 60 and 120 min, respectively, whereas complete removal of 100 ppm phenol could not be achieved within 120 min. A similar tendency also occurs in Co/ANZ-Oxone®

system. After 20 min, phenol removal efficiencies at the concentrations of 25, 50, 75 and 100 ppm are 10%, 6%, 3% and 2%, respectively. Phenol removal using Co/ANZ is relatively slower than Co/MCM48. After 5 h, phenol degradation at phenol concentrations of 25, 50, 75 and 100 ppm are 92%, 73%, 50% and 30% respectively.

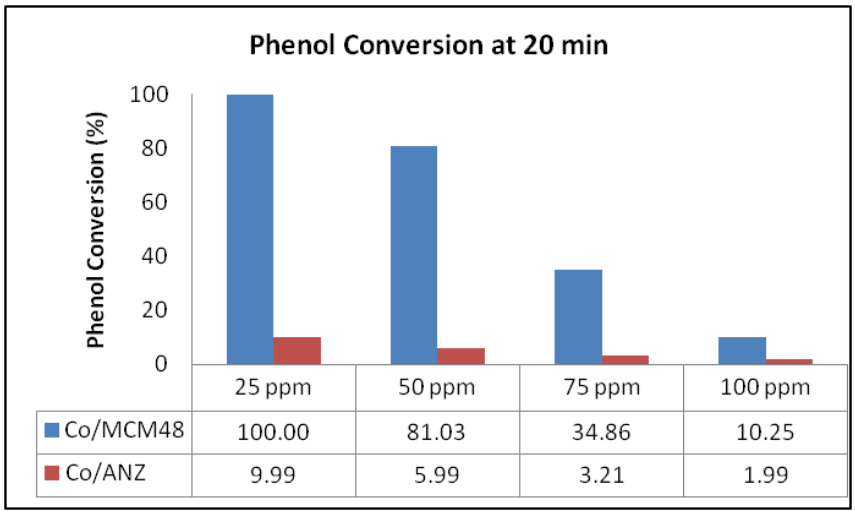

Figure 6. 14 Phenol removal using Co/MCM48 and Co/ANZ at different phenol concentration

Effect of catalyst loading on phenol degradation is shown in Figure 6.15A. It is shown that higher catalyst loading in solution would result in higher phenol reduction. This is reasonable because increased amount of catalyst will increase phenol adsorption and also the available catalyst sites to activate PMS. Therefore, more catalysts will make reaction rate much faster. For Co/MCM48, at loading of 0.05 g, 0.1 g and 0.2 g, phenol removal efficiency at 120 min are 20%, 79% and 100%, respectively. Due to low efficiency in phenol degradation (20% in 2 h) on Co/MCM48 at loading under 0.1 g in solution, an optimal loading at 0.2 g Co/MCM48 in solution (0.4 g/L) was selected.

A similar trend was occurred with Co/ANZ. For instance, at 2 h, Co/ANZ at 0.05 g, 0.1 g and 0.2 g in solution resulted in 14%, 27% and 30% of phenol conversion, respectively. From the experiment data, it can be seen that Co/ANZ showed much slower rate in phenol degradation than Co/MCM48.

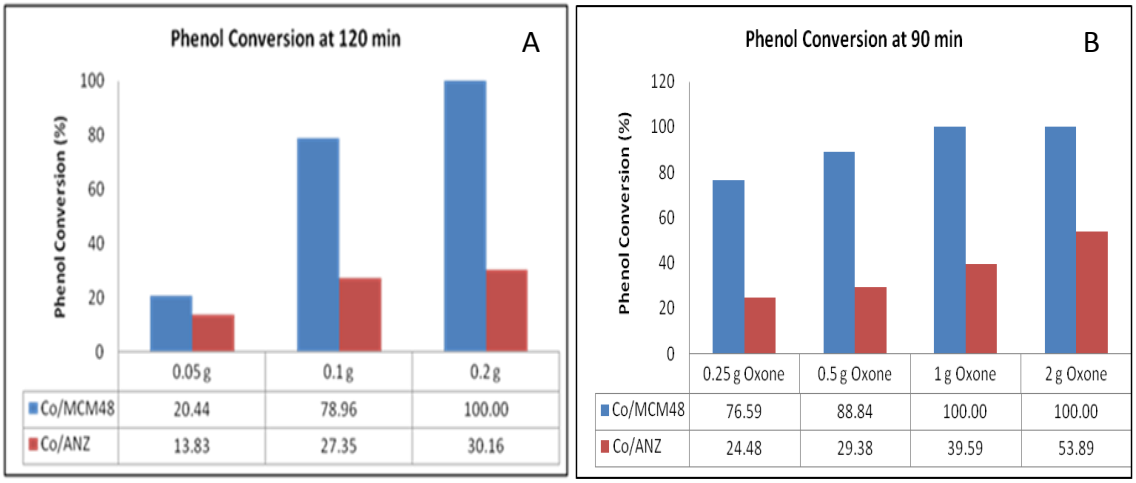

Figure 6.15 Phenol removal using Co/MCM48 and Co/ANZ (A) Different amount of catalyst loading (B) Different Oxone® concentration

As a source of PMS, Oxone® also plays an important role in phenol degradation through the heterogeneous catalytic oxidation process. The effect of Oxone® concentration on phenol removal is presented in Figure 6.15B. Higher Oxone® concentration will cause the phenol removal faster. This is because of high generation of sulfate radicals in solution. For Co/MCM48, 1 g Oxone® in solution is the optimal because phenol conversion reaches 100% at 90 min. For Co/ANZ, phenol degradation increases with increasing concentration of Oxone® showing 24%, 29%, 39% and 54% in 90 min at 0.25, 0.5, 1 and 2 g Oxone®, respectively.

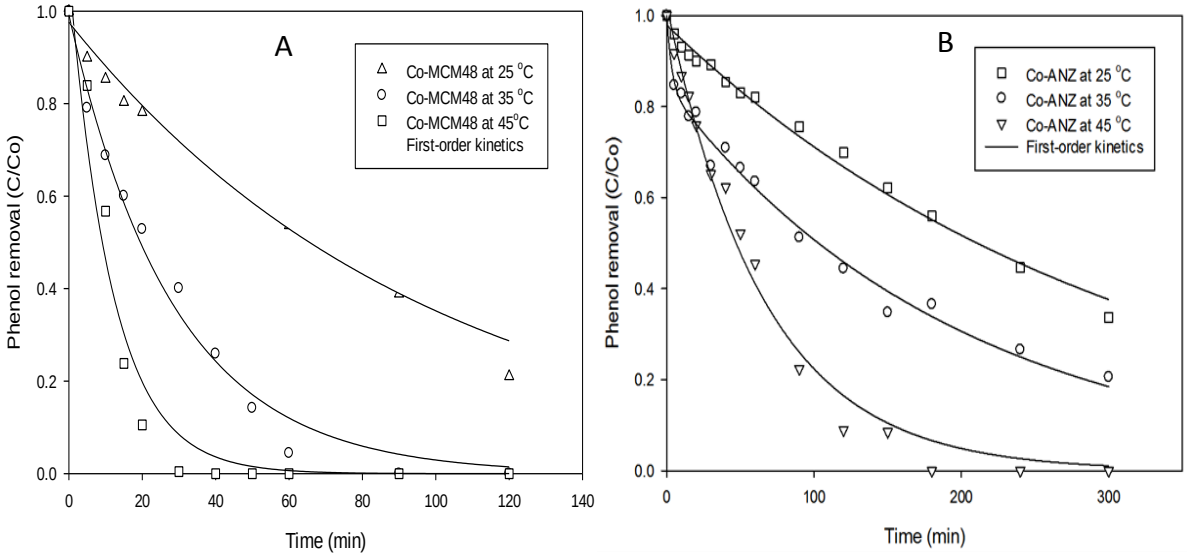

Figure 6.16 Effect of temperature on phenol removal, (A) Co/MCM48 and (B) Co/ANZ

The effect of reaction temperature on phenol degradation is shown in Fig. 6.16. As can be seen, temperature showed quite significant impact on phenol oxidation process using either Co/MCM48 or Co/ANZ. From these experiments, complete removal using Co/MCM48 at 35 and 45°C occurred at 60 and 30 min, respectively. While at 25°C, complete removal could not be reached within 2 h. For Co/ANZ, complete removal of phenol could not be reached within 5 h at temperatures of 25 and 35°C, while complete removal of phenol could be obtained at temperature 45° C in 3 h.

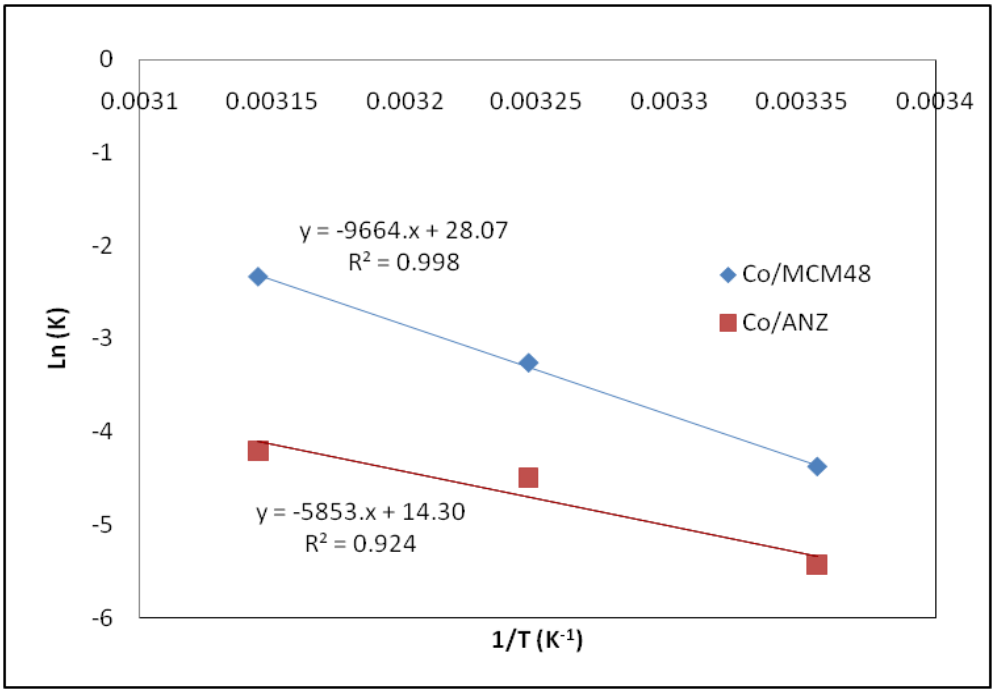

Figure 6.17 Arrhenius plots of phenol degradation on Co/MCM48 and Co/ANZ

Based on the first order kinetic model, the reaction rate constants were obtained for both catalysts at three different temperatures. The Arrhenius plots were presented in Fig. 6.17. It can be seen that a good correlation between rate constant and temperature for both catalysts was achieved and activation energies for phenol degradation on Co/MCM48 and Co/ANZ were derived as 80.3 and 52.4 kJ/mol, respectively. Table 6.1 shows the activation energies of some catalysts for phenol degradation using Oxone®. Compared with other supported Co catalysts, Co/MCM48 has higher activation energy and Co/ANZ shows a medium value of activation energy.

Table 6.1 Activation energies of heterogeneous catalysts with PMS for phenol degradation.

Catalyst	Activation energy (kJ/mol)	Reference
Co/SiO2	61.7- 75.5	[23]
Co/SBA-15	67.4	[22]
Co/ZSM5	69.7	[20]
Co/AC	59.7	[21]
Co/CX	48.3- 62.9	[41]
Ru/AC	61.4	[42]
Ru/ZSM5	42.2	[42]
Co/MCM48	80.3	This work
Co/INZ	61.3	This work
Co/ANZ	52.4	This work

6.7 Conclusions

Synthesis of zeolite and MCM48 based catalysts has been well done by dispersing active metal cobalt on the support material surface through impregnation. Characterization results by XRD and SEM-EDS confirm that the active metal cobalt on the support surface is in form of Co_3O_4. In oxidation tests, Co/MCM48, Co/INZ and Co/ANZ are effective catalysts for generating sulphate radicals in the presence of PMS to degrade phenol. Among these three catalysts, Co/MCM48 has the best activity in removing phenol than Co/INZ and Co/ANZ. Further, phenol removal is a combination of oxidation and adsorption processes. The concentration of phenol, catalyst loading, concentration of oxone, and temperature are key parameters affecting the reaction rate in phenol degradation. Kinetic studies show that phenol oxidation on the Co/MCM48, Co/INZ and Co/ANZ follows the first order reaction with the activation energies of 80.3, 61.3 and 52.4 kJ/mol, respectively.

References

1. Ahmaruzzaman, M. (2008). Adsorption of phenolic compounds on low-cost adsorbents: A review, *Advances in Colloid and Interface Science*, *143*, 48-67.

2. Busca, G., Berardinelli, S., Resini, C., Arrighi, L. (2008). Technologies for the removal of phenol from fluid streams: A short review of recent developments, *J Hazard Mater*, *160*, 265-288.

3. Parmeggiani, C., Cardona, F. (2012). Transition metal based catalysts in the aerobic oxidation of alcohols, *Green Chemistry*, *14*, 547-564.

4. Wang, J.L., Xu, L.J. (2012). Advanced Oxidation Processes for Wastewater Treatment: Formation of Hydroxyl Radical and Application, *Critical Reviews in Environmental Science and Technology*, *42*, 251-325.

5. Shukla, P., Fatimah, I., Wang, S.B., Ang, H.M., Tade, M.O. (2010). Photocatalytic generation of sulphate and hydroxyl radicals using zinc oxide under low-power UV to oxidise phenolic contaminants in wastewater, *Catal Today*, *157*, 410-414.

6. Saputra, E., Muhammad, S., Sun, H., Ang, H.M., Tadé, M.O., Wang, S. (2012). Red mud and fly ash supported Co catalysts for phenol oxidation, *Catal Today*, *DOI: 10.1016/j.cattod.2011.10.025*.

7. Wang, S.B., Peng, Y.L. (2010). Natural zeolites as effective adsorbents in water and wastewater treatment, *Chem Eng J*, *156*, 11-24.

8. Valdes, H., Farfan, V.J., Manoli, J.A., Zaror, C.A. (2009). Catalytic ozone aqueous decomposition promoted by natural zeolite and volcanic sand, *J Hazard Mater*, *165*, 915-922.

9. Dhakshinamoorthy, A., Navalon, S., Alvaro, M., Garcia, H. (2012). Metal Nanoparticles as Heterogeneous Fenton Catalysts, *Chemsuschem*, *5*, 46-64.

10. Wang, S. (2008). A Comparative study of Fenton and Fenton-like reaction kinetics in decolourisation of wastewater, *Dyes Pigments*, *76*, 714-720.

11. Zhou, G.L., Sun, H.Q., Wang, S.B., Ang, H.M., Tade, M.O. (2011). Titanate supported cobalt catalysts for photochemical oxidation of phenol under visible light irradiations, *Sep Purif Technol*, *80*, 626-634.

12. Ling, S.K., Wang, S.B., Peng, Y.L. (2010). Oxidative degradation of dyes in water using Co^{2+}/H_2O_2 and Co^{2+}/peroxymonosulfate, *J Hazard Mater*, *178*, 385-389.

13. Anipsitakis, G.P., Dionysiou, D.D. (2003). Degradation of organic contaminants in water with sulfate radicals generated by the conjunction of peroxymonosulfate with cobalt, *Environ Sci Technol*, *37*, 4790-4797.

14. Anipsitakis, G.P., Dionysiou, D.D. (2004). Radical generation by the interaction of transition metals with common oxidants, *Environ Sci Technol*, *38*, 3705-3712.

15. Anipsitakis, G.P., Stathatos, E., Dionysiou, D.D. (2005). Heterogeneous activation of oxone using Co_3O_4, *J Phys Chem B*, *109*, 13052-13055.

16. Chen, X.Y., Chen, J.W., Qiao, X.L., Wang, D.G., Cai, X.Y. (2008). Performance of nano-Co_3O_4/peroxymonosulfate system: Kinetics and mechanism study using Acid Orange 7 as a model compound, *Appl Catal B-Environ*, *80*, 116-121.

17. Yang, Q., Choi, H., Al-Abed, S.R., Dionysiou, D.D. (2009). Iron-cobalt mixed oxide nanocatalysts: Heterogeneous peroxymonosulfate activation, cobalt leaching, and ferromagnetic properties for environmental applications, *Appl Catal B-Environ*, *88*, 462-469.

18. Yang, Q., Choi, H., Chen, Y., Dionysiou, D.D. (2008). Heterogeneous activation of peroxymonosulfate by supported cobalt catalysts for the degradation of 2,4-dichlorophenol in water: The effect of support, cobalt precursor, and UV radiation, *Appl Catal B-Environ*, *77*, 300-307.

19. Hu, L., Yang, X., Dang, S. (2011). An easily recyclable Co/SBA-15 catalyst: Heterogeneous activation of peroxymonosulfate for the degradation of phenol in water, *Appl Catal B-Environ*, *102*, 19-26.

20. Shukla, P., Wang, S.B., Singh, K., Ang, H.M., Tade, M.O. (2010a). Cobalt exchanged zeolites for heterogeneous catalytic oxidation of phenol in the presence of peroxymonosulphate, *Appl Catal B-Environ*, *99*, 163-169.

21. Shukla, P.R., Wang, S.B., Sun, H.Q., Ang, H.M., Tade, M. (2010b). Activated carbon supported cobalt catalysts for advanced oxidation of organic contaminants in aqueous solution, *Appl Catal B-Environ*, *100*, 529-534.

22. Shukla, P., Sun, H.Q., Wang, S.B., Ang, H.M., Tade, M.O. (2011a). Co-SBA-15 for heterogeneous oxidation of phenol with sulfate radical for wastewater treatment, *Catal Today*, *175*, 380-385.

23. Shukla, P., Sun, H.Q., Wang, S.B., Ang, H.M., Tade, M.O. (2011b). Nanosized Co_3O_4/SiO_2 for heterogeneous oxidation of phenolic contaminants in waste water, *Sep Purif Technol*, *77*, 230-236.

24. Hardjono, Y., Sun, H.Q., Tian, H.Y., Buckley, C.E., Wang, S.B. (2011). Synthesis of Co oxide doped carbon aerogel catalyst and catalytic performance in heterogeneous oxidation of phenol in water, *Chem Eng J*, *174*, 376-382.

25. Chen, X., Qiao, X., Wang, D., Lin, J., Chen, J. (2007). Kinetics of oxidative decolorization and mineralization of Acid Orange 7 by dark and photoassisted Co^{2+}-catalyzed peroxymono sulfate system, *Chemosphere*, *67*, 802-808.

26. Fortuny, A., Font, J., and Fabregat, A. (1998). Wet air oxidation of phenol using active carbon as catalyst, *Appl. Catal. B-Environ*. 19, 165-173.

27. Chiron, S., Fernandez-Alba A., Rodriguez, A. and Garcia-Calvo, E. (2000). Pesticide chemical oxidation: state-of-the-art, *Water Res*., **34**, 366-377.

28. Camporro A., Camporro M.J., Coca J. and Sastre H. (1994). Regeneration of an activated carbon bed exhausted by industrial phenolic wastewater, *Journal of Hazardous Material,* 37, 207-214.

29. Liou, T.H., and Lai B.C. (2012). Utilization of e-waste as a silica source for the synthesis of the catalyst support MCM-48 and highly enhanced photocatalytic activity of supported titania nanoparticles, *Applied Catalysis B: Environmental* 115, 138– 148

30. Kim, T.W., Chung, P.W and Lin V.S.Y. (2010). Facile Synthesis of Monodisperse Spherical MCM-48 Mesoporous Silica Nanoparticles with Controlled Particle Size, *J. Chem. Mater.* 22, 5093–5104

31. Song W., Grassian, V.H., Larsen, S.C. 2005, *High yield method for nanocrystalline zeolite synthesis,* Journal of The Royal Society of Chemistry, Chem. Comm., pp. 2951-2953.

32. Wang, S. (2008). A comparative study of Fenton and Fenton-like reaction kinetics in decolourisation of wastewater, *Dyes Pigments,* 76, 714-720.

33. Chan K.H. and Chu W. (2009). Degradation of atrazine by cobalt-mediated activation of peroxymonosulfate: Different cobalt counteranions in homogenous process and cobalt oxide catalysts in photolytic heterogeneous process, *Water Research,* 43**,** 2513–2521

34. Ling, S.K., Wang, S. and Peng, Y. (2004). Oxidative degradation of dyes in water using Co^{2+}/H_2O_2 and Co^{2+}/peroxymonosulfate, *J. Hazard. Mater.* 178**,** 385–389.

35. Fernandez, J., Maruthamuthu, P., Renken A. and Kiwi, J. (2004). Bleaching and photobleaching of Orange II within seconds by the oxone/Co^{2+} reagent in Fenton-like processes, *Appl. Catal. B: Environ. 49, 207–215.*

36. Chen, X.Y., Chen, J.W., Qiao, X.L., Wang, D.G., and Cai, X.Y. (2008). Performance of nano-Co_3O_4/peroxymonosulfate system: Kinetics and mechanism study using Acid Orange 7 as a model compound, *Applied Catalysis B-Environmental,* 80, 116-121.

37. Yang, Q., Choi, H., Al-Abed, S.R. and Dionysiou, D.D. (2009). Iron-cobalt mixed oxide nanocatalysts: Heterogeneous peroxymonosulfate activation, cobalt leaching, and ferromagnetic properties for environmental applications, *Applied Catalysis B-Environmental* 88, 462-469.

38. Yang, Q.J., Choi, H., Chen, Y.J. and Dionysiou, D.D. (2008). Heterogeneous activation of peroxymonosulfate by supported cobalt catalysts for the degradation of 2,4-dichlorophenol in water: The effect of support, cobalt precursor, and UV radiation, *Applied Catalysis B-Environmental* 77, 300-307.

39. Yang, Q.J., Choi, H. and Dionysiou, D.D. (2007). Nanocrystalline cobalt oxide immobilized on titanium dioxide nanoparticles for the heterogeneous activation of peroxymonosulfate, *Applied Catalysis B-Environmental* 74, 170-178.

40. Zhang, W., Tay, H.L., Lim, S.S., Wang, Y.S., Zhong, Z.Y. and Xu, R. (2010). Supported cobalt oxide on MgO: Highly efficient catalysts for degradation of organic dyes in dilute solutions, *Applied Catalysis B-Environmental,* 95, 93-99.

41. Sun, H., Tian, H., Hardjono, Y., Buckley, C.E. and Wang, S. (2012). Preparation of cobalt/carbon-xerogel for heterogeneous oxidation of phenol, *Catal. Today*, 186, 63-68.

42. Muhammad, S., Shukla, P.R., Tade, M.O. and Wang, S. (2012). Heterogeneous activation of peroxymonosulphate by supported ruthenium catalysts for phenol degradation in water, *Journal of Hazardous Materials,* 215-216, 183-190

Chapter-7

Photocatalytic oxidation in phenol removal using Ru/TiO_2 and Ru/Al_2O_3 catalysts

Abstract

Ru/TiO_2 and Ru/Al_2O_3 catalysts have been synthesized using impregnation method followed by calcination at temperature of 550 ^{0}C. The synthesized catalysts were characterized by XRD, SEM and EDS. Based on characterization results, the active phase of Ru in form of RuO_2 was well dispersed on the support surface. The catalysts were then used in photocatalytic oxidation of phenol in the presence of peroxymonosulphte (PMS) as an oxidant and UV-light from a Mercury lamp which is categorized as UV-C, with wavelength in range of 200-280 nm. Both catalysts are effective for application of photocatalytic oxidation of phenol in the presence of PMS and UV. Further, activation of PMS for the production of sulphate radicals for phenol degradation in this study is generated by the interaction PMS-Catalyst and PMS-UV. The photo catalysts of Ru/TiO_2 and Ru/Al_2O_3 can increase the removal efficiency of 10-15%. The activity in phenol removal of Ru/TiO_2-PMS-UV is slightly higher than Ru/Al_2O_3-PMS-UV. Both catalysts also showed good performance in the second and third runs after regeneration for multiple uses. Kinetic studies showed that phenol oxidation on the catalysts, Ru/TiO_2 and Ru/Al_2O_3 in the presence of PMS and UV follows the first order reaction.

7.1 Introduction

Generally, the removal technique of pollutants from waste water using sunlight such as UV-light is called photolysis. In this process, wastewater solution is irradiated with UV to produce hydroxyl radicals which is playing as an oxidant agent in the degradation of organic waste in the water.

Removal efficiency of these contaminants will be better with the addition of semi-conductors such as TiO_2, ZnO, Al_2O_3 and others. The semiconductor absorbs the UV radiation more efficiently than pollutants to produce active hydroxyl radicals. To date, TiO_2 photocatalyst has been the more widely used than other metal oxides such as ZnO, ZrO_2, SrO_2, CdS etc [1].

TiO_2 has been extensively used due to low cost, low toxicity, chemical and photochemical stability, high photocatalytic activity, and biocompatibility [2-3]. However, some drawbacks of TiO_2 such as the low quantum yield of TiO_2 for practical applications, a high refractive index and limited photoactivity have been reported [4-8]. Further, TiO_2 generally has relatively low surface area which influences the adsorption of organic pollutants on the surface particle and also reduces photocatalytic activity [9].

Some works are developed to overcome the disadvantages of pure TiO_2 such as mixed-phase of TiO_2, which includes anatase–rutile, anatase–brookite, brookite–rutile, and anatase–TiO_2 (B) [10-14]. One of the TiO_2 mixed phase is Degussa P25, which consists of 80% anatase and 20% rutile. This material exhibits higher photocatalytic activity than its pure-phase of TiO_2.

To enhance the photocatalytic activity TiO_2 can be done in some modification such as TiO_2 doping with other metals or noble metals [15-16]. Another is immobilization of TiO_2 over support materials which have high surface areas, such as activated carbon, zeolite, silica, and Al_2O_3 [18-21]. By using this method, the surface area as an important factor influencing adsorption rate and photocatalytic efficiency, will increase significantly. Then the surface area determined pre-adsorbed pollutant molecules on TiO_2 particles facilitates degradation [17]. Some researchers also reported that ZnO which has a band gap of 3.2 eV is an effective catalyst in oxidation of dyes, penolic compound and also on the treatment of groundwater pollutants [22-24]. In another recent study, Al_2O_3 was also found to be a sensitive photocatalyst under UV illumination [9].

A further development is reported that the addition of small amounts of oxidants such as hydrogen peroxide results in the more active hydroxyl radical formation. The combination of oxidants and photocatalyst will have an excellent performance in removal of highly refractory compounds. In addition to hydrogen peroxide and ozone, other oxidants include peroxymonosulfate (PMS). The PMS can generate sulfate radicals by UV or catalyst and has lot of interest due to the high redox potential. Several studies have reported about the use of sulfate radicals in the photocatalytic oxidation of organic contaminants in wastewater in the presence of TiO_2 and UV-light radiation [25-29].

In this chapter, we conducted photocatalytic oxidation of phenol by using photocatalyst of Ru impregnated TiO_2 and Al_2O_3 in the presence of PMS as an oxidant and UV-light.

7.2 Experimental

7.2.1 Experimental setup of photocatalytic oxidation

The photocatalytic experiment is run in a 1 liter double jacket reactor which was placed in UV cupboard with a constant mixing at 400 rpm. The reactor was irradiated with a 500 W (max) of UV-Mercury lamp which is categorized as UV-C, with wave length in range of 200-280 nm from the lamp housing of Oriel 66905 powered by Newport 69911. The radiation temperature was controlled by cooling water which was flowed through an external jacket in the housing lamp. The cooling water was also circulated through the reactor jacket to control reaction temperature. An external tube was dipped in reactor for sample withdrawal at a certain time. The experimental setup sketch can be seen in Fig. 7.1.

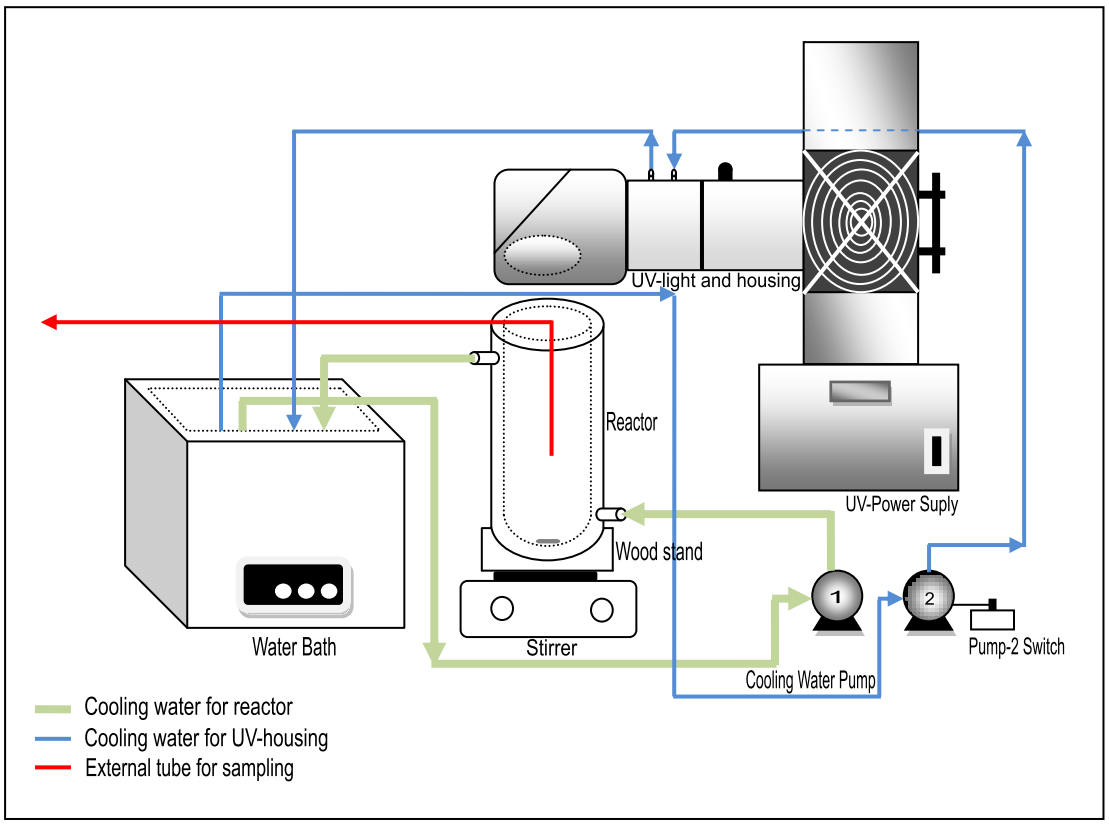

Figure 7.1 Experimental setup of photocatalytic oxidation

7.2.2 Synthesis of ruthenium catalysts on TiO_2 and Al_2O_3 supports

Ru/TiO_2 and $Ru/\alpha\text{-}Al_2O_3$ catalysts were synthesized following a general impregnation method. A fix amount of ruthenium chloride (Sigma-Aldrich) was added into 200 mL ultrapure water until the ruthenium compound was dissolved. Next, TiO_2, (Degussa P25, surface area 55.5 m^2/g, obtained from Degussa, Germany) was added to the solution and kept stirring for 24 h. The amount of Ru were calculated to meet the Ru loading ratio of 5 wt% agains TiO_2. The suspension was then evaporated in a rotary evaporator at temperature of 50 ^{0}C under vacuum. Further, the catalyst was recovered and dried in an oven at 120 ^{o}C for 6 h. Calcination of the catalyst was conducted in a furnace at 550 ^{o}C for 6 h in air. Then the catalyst was stored in a desiccator until use. The same method was also conducted to synthesize $Ru/\alpha\text{-}Al_2O_3$.

7.2.3 Characterisation of catalysts

Both synthesised catalysts of Ru/TiO_2 and $Ru/\alpha Al_2O_3$ were characterised by X-ray diffraction (XRD), scanning electron microscopy (SEM) with energy dispersive X-ray spectroscopy (EDS), and N_2 adsorption. The XRD (Siemen, D501 diffractometer) was used to identify the structural features and the mineralogy of the catalysts. The XRD pattern was obtained using filtered Cu Kα radiation with accelerating voltage of 40 kV and current of 30 mA. The samples were scanned at 2θ from 5-100^o. Further, to obtain a visual image and identify the texture and morphology of the catalysts, SEM (Philips XL30) with secondary and backscatter electron detectors was used. Energy-dispersive X-ray spectroscopy (EDS) was also used to detect Ru particles on TiO_2 and Al_2O_3 supported catalysts.

7.2.4 Kinetic study of phenol photocatlytic oxidation

Phenol (Aldrich) was used to prepare a stock of 5000 ppm. From this stock solution four different concentrations of phenol of 25, 50, 75 and 100 ppm were made and used in catalytic oxidation of phenol. The solution was stirred constantly at 400 rpm to maintain homogeneous solution. Next, a fixed amount of peroxymonosulphate (Oxone®, DuPont's triple salt $2KHSO_5 \cdot KHSO_4 \cdot K_2SO_4$, Aldrich) was added to the mixture until completely dissolved. Then, a fixed amount of catalysts Ru/TiO_2 or $Ru/\alpha\text{-}Al_2O_3$ was added into the reactor. And finally, the power of UV-light which has different power 200, 300 and 500 W was switched on to start the oxidation of phenol. The reaction was run for 1 h and at the fixed time interval, 0.5 mL of a sample was withdrawn from the solution and filtered using HPLC standard filter of 0.45 μm and mixed with 0.5 mL methanol as a quenching reagent to stop the reaction. Phenol was then analysed on a HPLC consisted of isocratic pumps from Varian with a UV-Vis detector at wavelength of 270 nm. The column is C18 with mobile phase of 70% acetonitrile and 30% ultrapure water. Furthermore, the spent catalyst was recovered after each run from the reaction mixture by filtration and washed thoroughly with distilled water and dried at 70 ^{0}C for reuse.

7.3 Results and Discussion

7.3.1 Characterisation of ruthenium impregnated TiO_2 and Al_2O_3

The characterization of synthesized catalysts shows that the active metal of Ruthenium has been well dispersed and coated on the support surface of titanium oxide and alumina. The active phase of ruthenium is in form of RuO_2 at XRD 2θ pattern peaks of 28, 35, 40 and 54.3^0 as can be seen in Fig. 7.2 below.

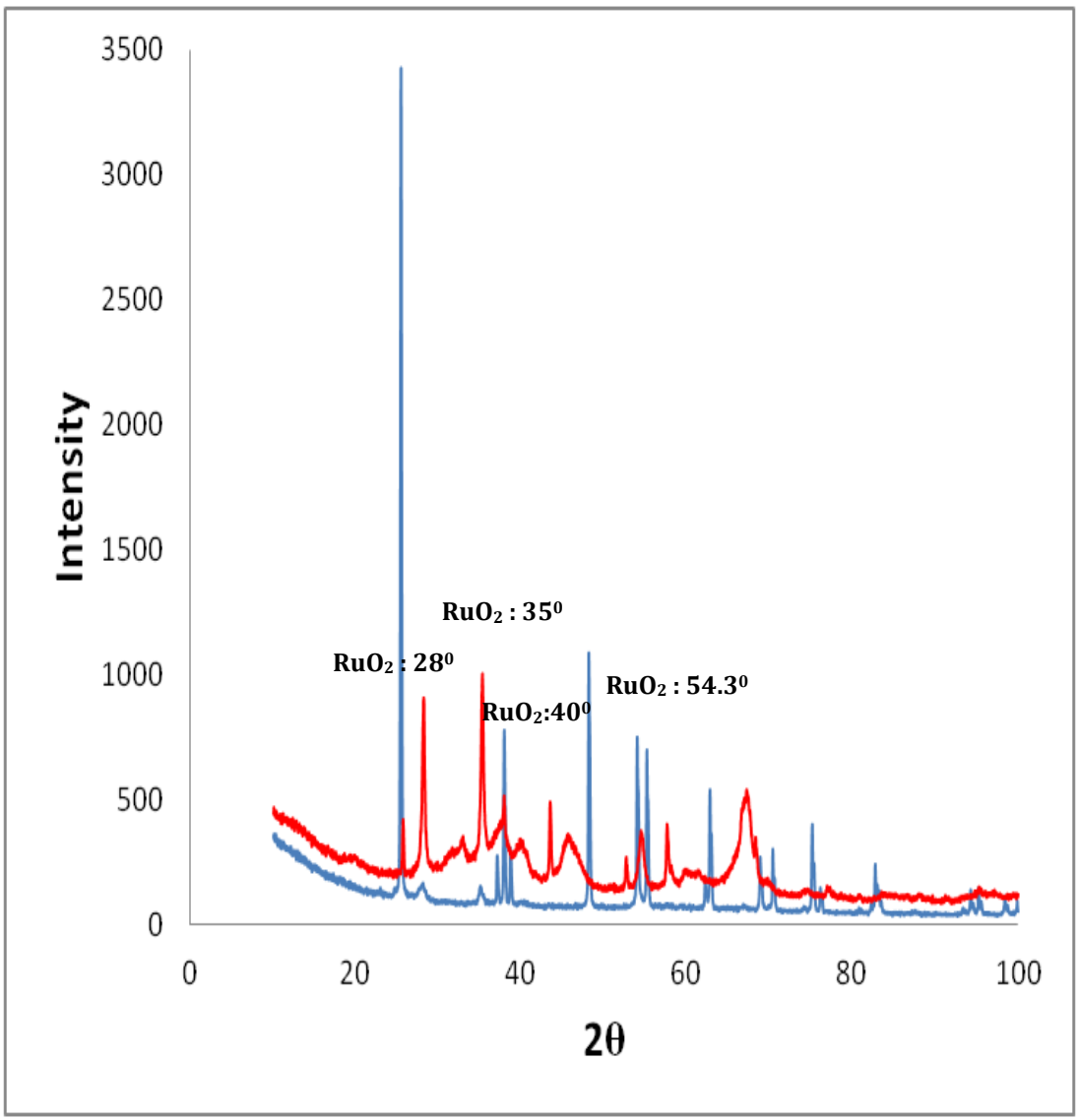

Figure 7.2 XRD pattern of Ru/TiO_2 and Ru/Al_2O_3

The presence and dispersion of active metal ruthenium on the support surface were also confirmed by EDS spectra as can be seen in Fig. 7.3 and Fig. 7.4. Among five spectrum spot selected, all indicate that there are ruthenium on surface of titanium oxide and alumina.

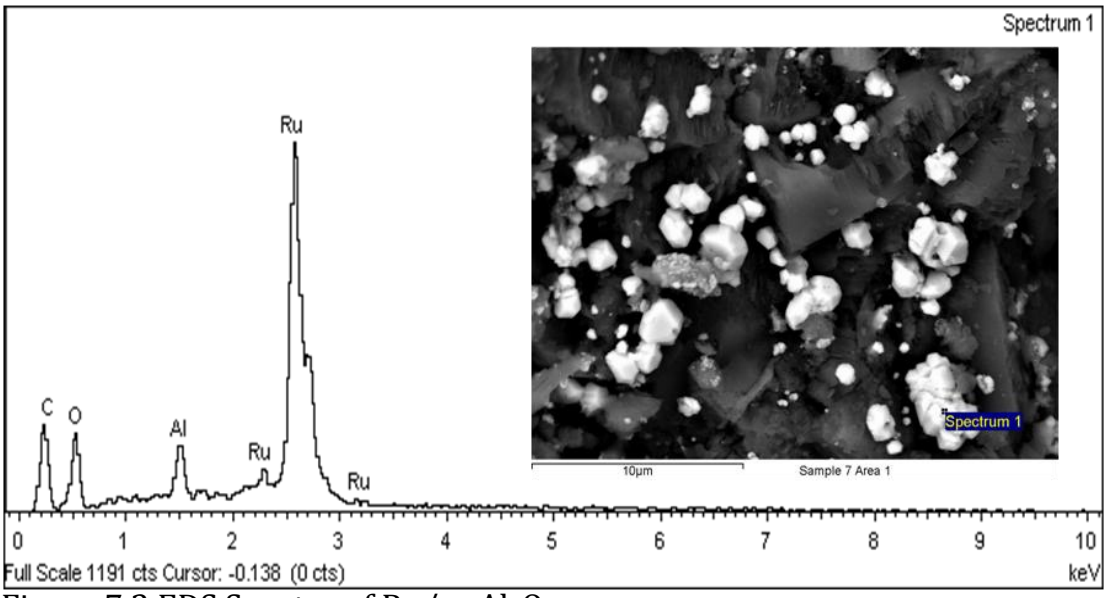

Figure 7.3 EDS Spectra of Ru/ α-Al_2O_3

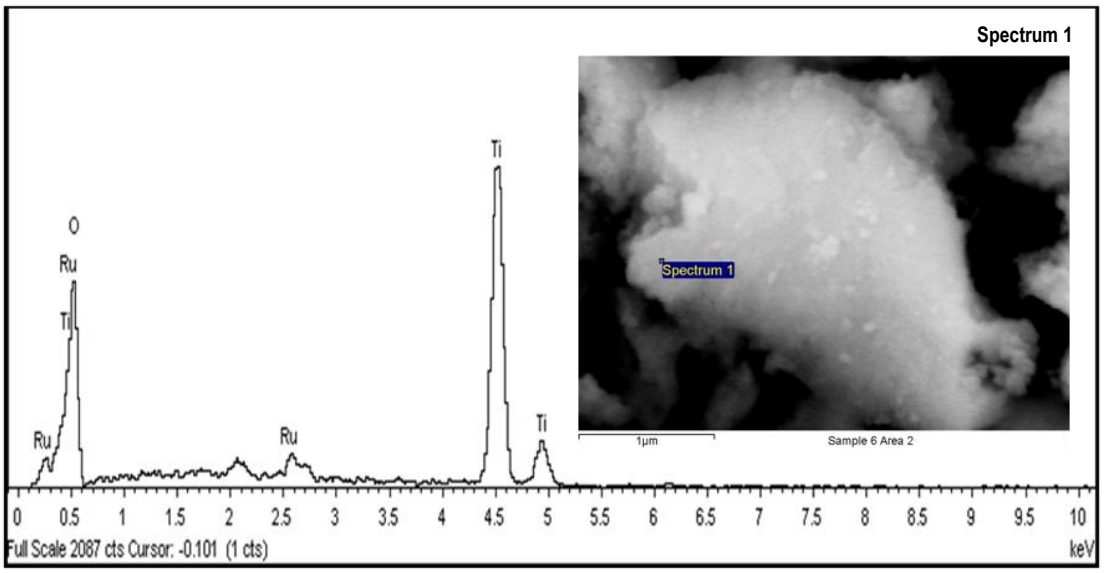

Figure 7.4 EDS Spectra of Ru/ TiO_2

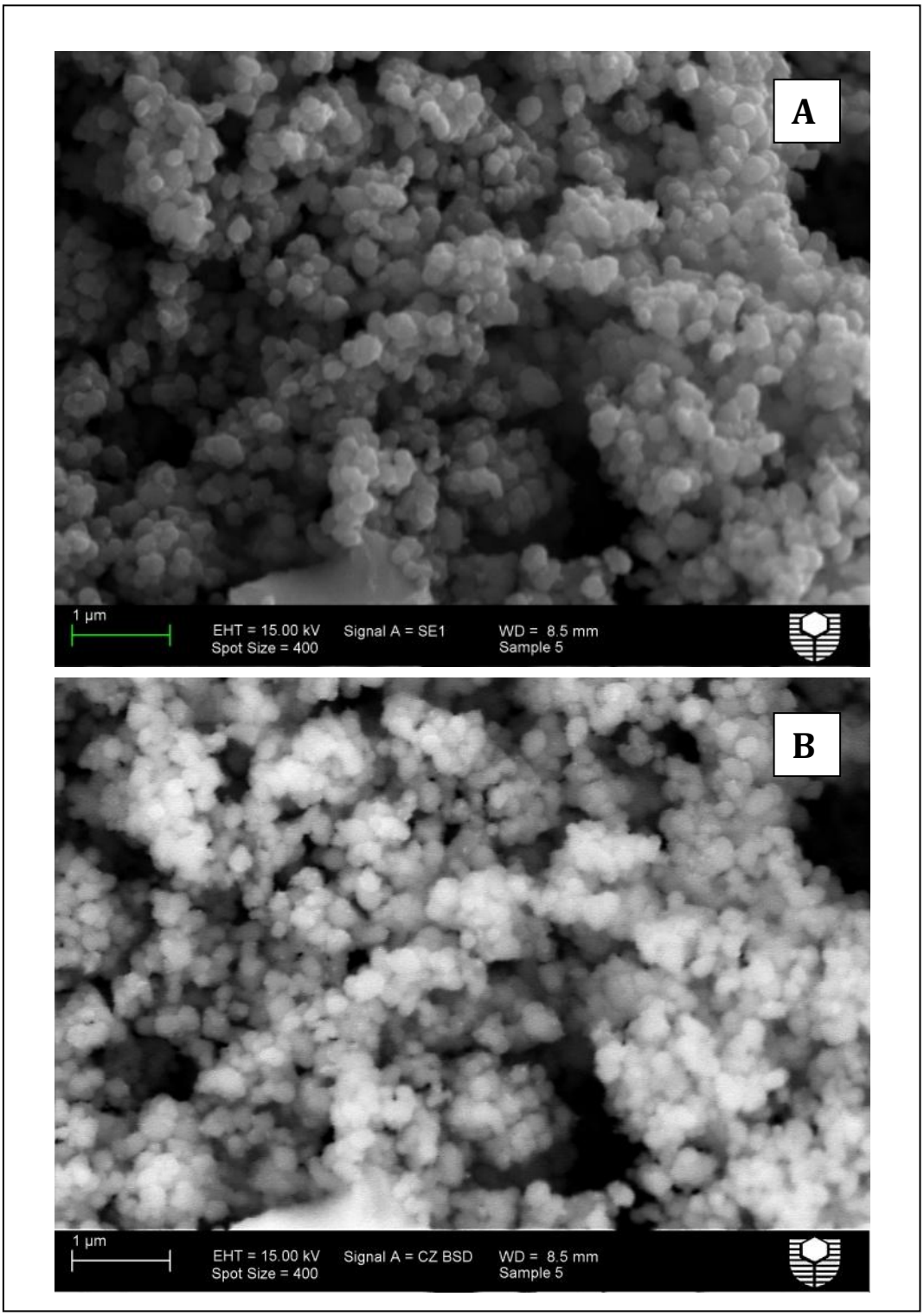

Figure 7.5 SEM Image of Ru/TiO_2, (A) SE detector, (B) BSD detector

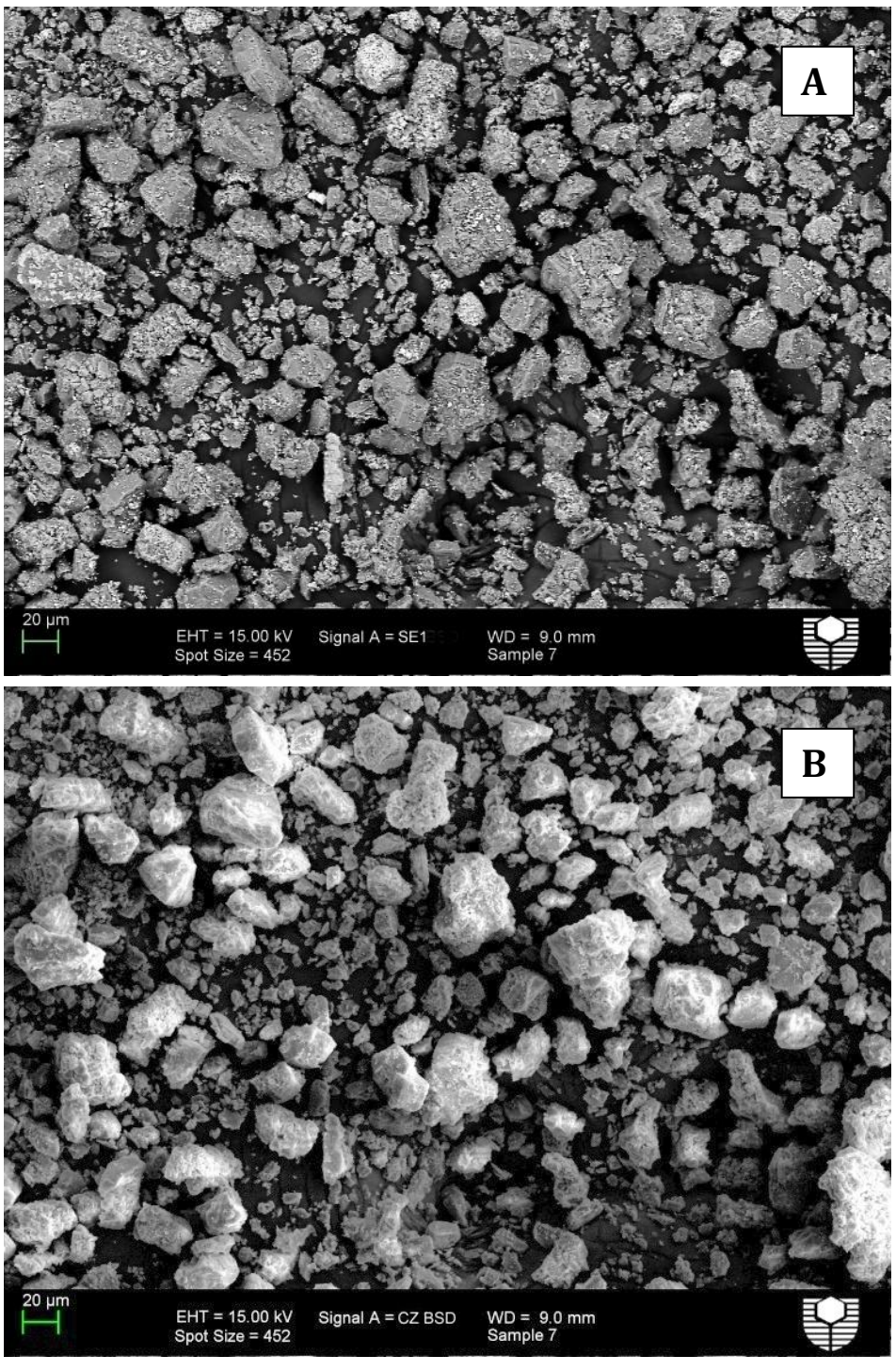

Figure 7.6 SEM Image of Ru/Al_2O_3, (A) SE detector, (B) BSD detector

Further, SEM images as shown at Fig. 7.5 and 7.6 describe the morphology of both catalysts of Ru/TiO_2 (Fig.7.5) and Ru/Al_2O_3 (Fig. 7.6). As seen in the picture, Ru/TiO_2 has much smaller particle size than Ru/Al_2O_3. The presence of ruthenium on the support surface was also analysed by secondary electron detector (SE) and backscattered detector (BSD) of SEM. By using BSD detector at the same area, the presences of ruthenium specks are seen at the brighter area in the catalyst particles. It implies that ruthenium is well coated in the titanium oxide (Fig. 7.5B) and alumina (Fig. 7.6B).

7.3.2 Preliminary study of photocatalytic oxidation of phenol

Preliminary tests of photocatalytic oxidation with various samples are shown in Fig. 7.7. The process was run at reaction conditions of 0.2 g catalyst loading, 1 g of Oxone ® in 500 mL phenol solution of 50 ppm, 25 ^{0}C, stirring speed of 400 rpm and 300 Watt UV-light.

Generally, it is seen that a process involving the catalyst and UV-light give better phenol removal efficiency. As shown in Fig. 7.7, complete removal of phenol by a combination of catalysts Ru/TiO_2, Oxone and UV reaction can be achieved within 60 minutes. In the same time, photocatalitic oxidation using Ru/Al_2O_3, Oxone and UV provides about 90% removal efficiency. Similar trend is also seen using TiO_2/Oxone/UV system. It can be seen that Ru/TiO_2 showed slightly better performance than Ru/Al_2O_3. Another interesting fact is that the phenol removal efficiency can reach 85% by simply using UV and Oxone only. This means that the presence of a catalyst Ru/Al_2O_3 or Ru/TiO_2 in the treatment system only improves phenol removal efficiency in the range of 10-15%. Further, it is also confirmed that UV-light is effective to generate sulfate radical of PMS (Oxone) to degrade phenol as seen in the following Eq. 7.1.

$$HSO_5^- + h\nu \rightarrow SO_4^{-\bullet} + OH^- \quad 7.1$$

$$SO_4^{\bullet-} + C_6H_5OH \rightarrow C_6H_5OH - SO_4^{\bullet-} \xrightarrow{-SO_4^{2-}} C_6H_5OH^{\bullet+} \quad 7.2$$

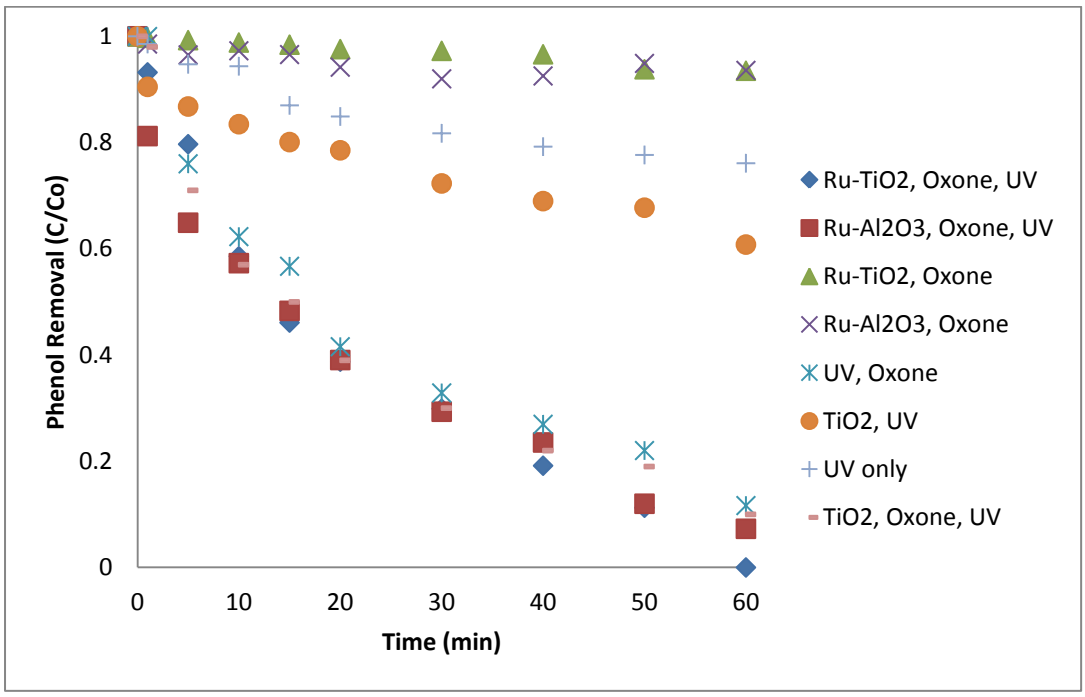

Figure 7.7 Phenol removal in adsorption and photocatalytic oxidation

On the other hand, the presence of photocatalysts of Ru/TiO_2 and Ru/Al_2O_3 gives additional acceleration in sulfate radical production in photocatalytic oxidation system. As can be seen from XRD spectra that the main active phase of the catalyst would be RuO_2 therefore, it is believed that the phenol removal mechanism is as presented below.

$$\text{S-Ru(IV)} + HSO_5^- \rightarrow \text{S-Ru(III)} + SO_5^{-\bullet} + H^+ \quad \text{(S: solid surface)} \quad 7.3$$

$$\text{S-Ru(III)} + HSO_5^- \rightarrow \text{S-Ru(IV)} + SO_4^{-\bullet} + OH^- \quad 7.4$$

$$C_6H_5OH + SO_4^{-\bullet} \rightarrow \text{several steps} \rightarrow CO_2 + H_2O \quad 7.5$$

After their regeneration by water washing, both Ru/TiO_2 and Ru/Al_2O_3 catalysts were also tested for multiple uses (Fig. 7.8). It can be seen that,

both catalysts showed somewhat deactivation in the second and third runs. However, the deactivation was not so significant. The deactivation occurs presumably due to adsorption of intermediates and a small portion of loose ruthenium leaching from the supports of TiO_2 and Al_2O_3.

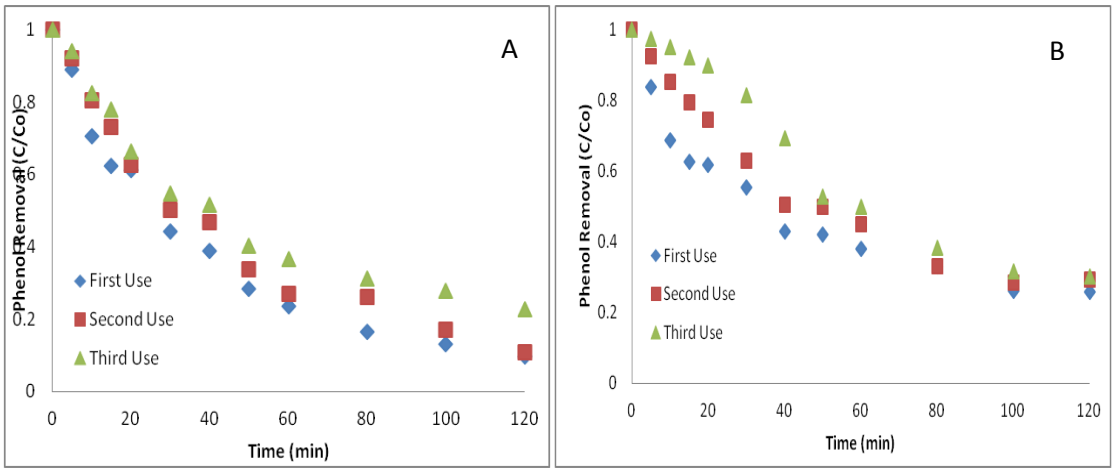

Figure 7.8 Phenol removal in multiple use of photocatalyst (A) Ru/TiO_2 and (B) Ru/Al_2O_3 at 50 ppm, at 1 g Oxone, 0.2 g catalyst, 25^{0}C, 200W UV

7.3.3 Effect of UV-light intensity on phenol removal

It is well know that UV radiation is defined as the electromagnetic radiation with wave length range of 10-400 nm. The UV itself consists of V-UV (vacuum UV, 100-200 nm), UV-C (200-280 nm), UV-B (280-320 nm) and UV-A (320-400 nm) as described in Fig. 7.9 [30]. This research used three different UV-light intensities of 200W, 300W and 500W. Among them the 300W power of UV has the optimum result in phenol removal. The UV-light source is Mercury Lamp which irradiaties the UV-C light with wavelength in range of 200-280. This kind of UV is the UV spectral range of interest for the UV photolysis application [30].

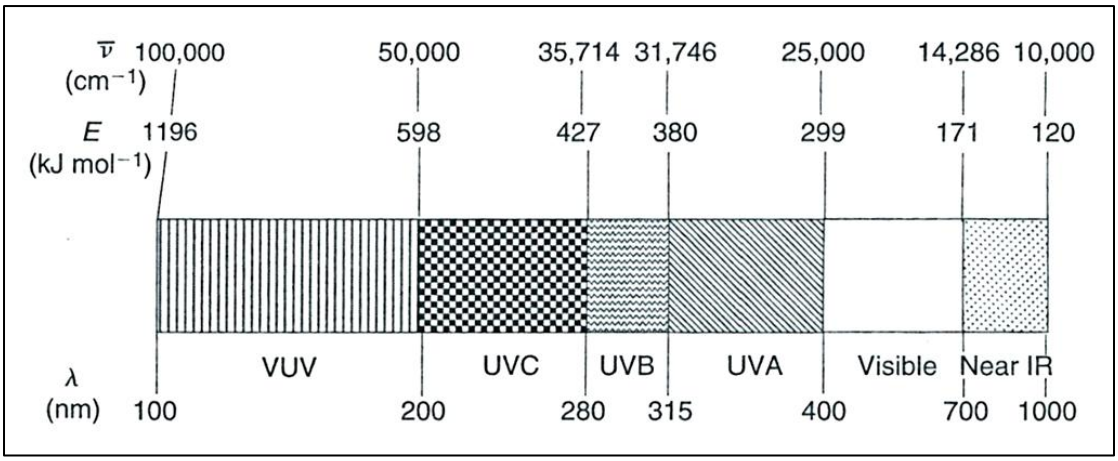

Figure 7.9 Spectrum of the electromagnetic radiation

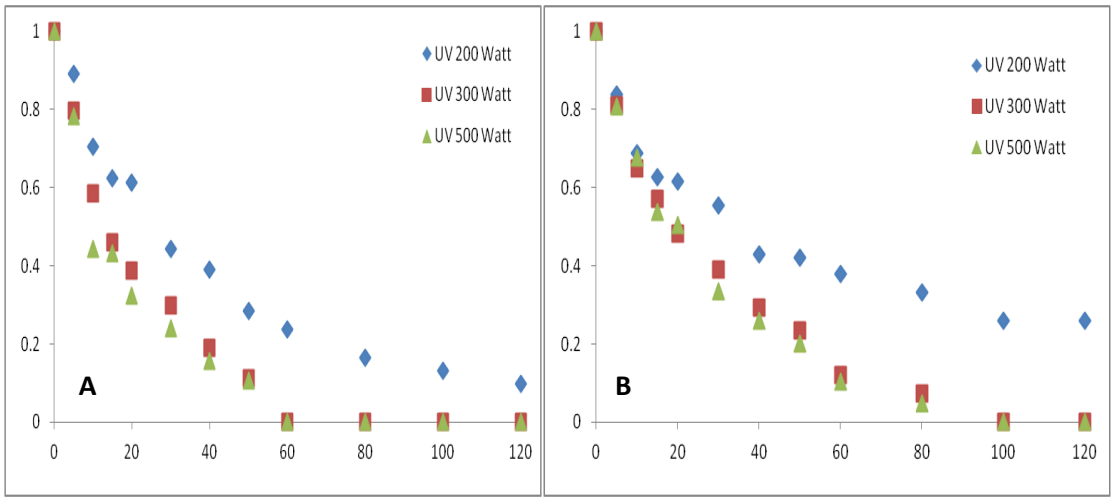

Figure 7.10 Photocatalytic oxidation of phenol at different UV-light intensity, (A). Ru/TiO_2 catalyst and (B). Ru-Al_2O_3 catalyst.

Further, the effect of UV-light intensity on phenol removal is presented in Fig. 7.10. As can be seen, at 60 minutes, complete removal of phenol can be reached using UV power of 300W and 500W while about 75% of phenol removal by 200W. Similar result is presented in Fig. 7.10B using Ru/Al_2O_3, complete removal of phenol is reached within 100 minutes at 300W and 500W of UV power while at 200W, 60% of removal efficiency is obtained.

7.3.4 Effects of reaction parameters on phenol removal

The first parameter is the effect of catalyst loading on phenol degradation. According to Fig. 7.11, the greater of the amount of catalyst used, the higher of phenol reduction efficiency is. This phenomenon is reasonable, because increasing the amount of catalyst will increase the adsorption and also the availability of catalyst sites to activate oxone. The same trend also occurred with Ru/Al_2O_3 in Fig. 7.11B. For instance, at reaction time of 60 minutes, removal efficiency of 80%, 70% and 40% can be obtained by catalyst loading of 0.2g, 0.1g and 0.05g respectively. However, at 120 minutes, the removal efficiency seems not too different. It is probably due to low amount of remaining phenol in the treatment system.

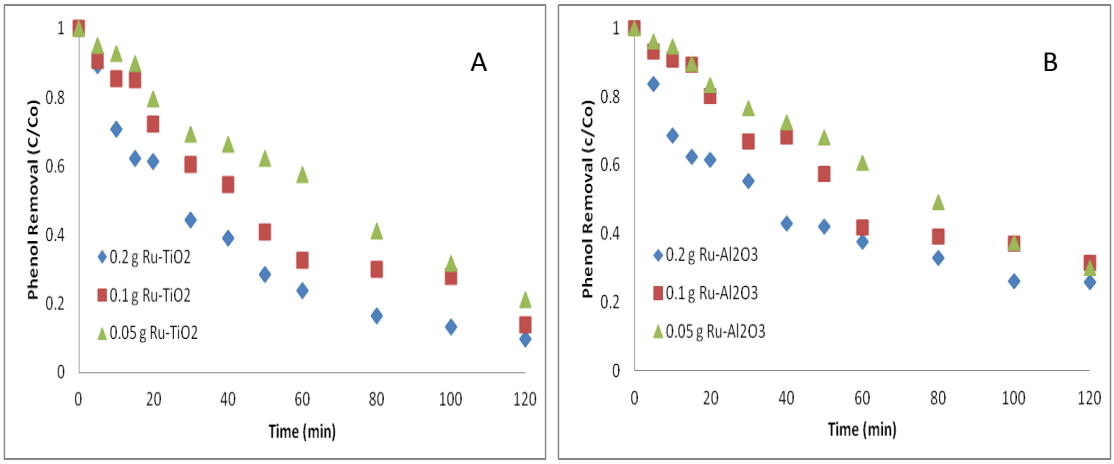

Figure 7.11 Phenol removal in different catalyst loading (A) Ru/TiO_2 and (B) Ru/Al_2O_3 at 50 ppm, at 1 g Oxone, 25^0C, 200W UV

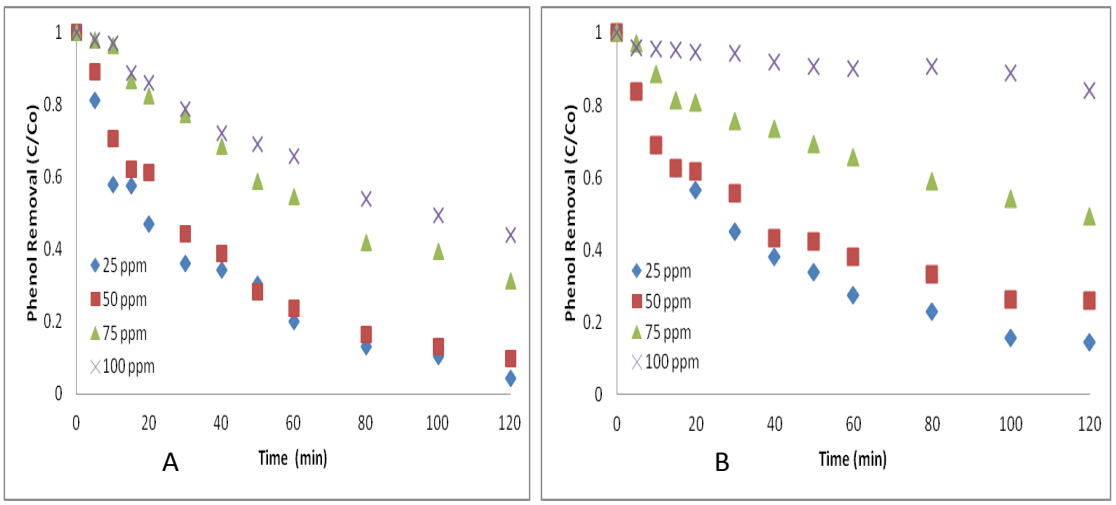

Figure 7.12 Phenol removal in different concentrations of phenol (A) Ru/TiO_2 and (B) Ru/Al_2O_3 at 0.2g catalyst, 1 g Oxone, 25^{0}C, 200W UV

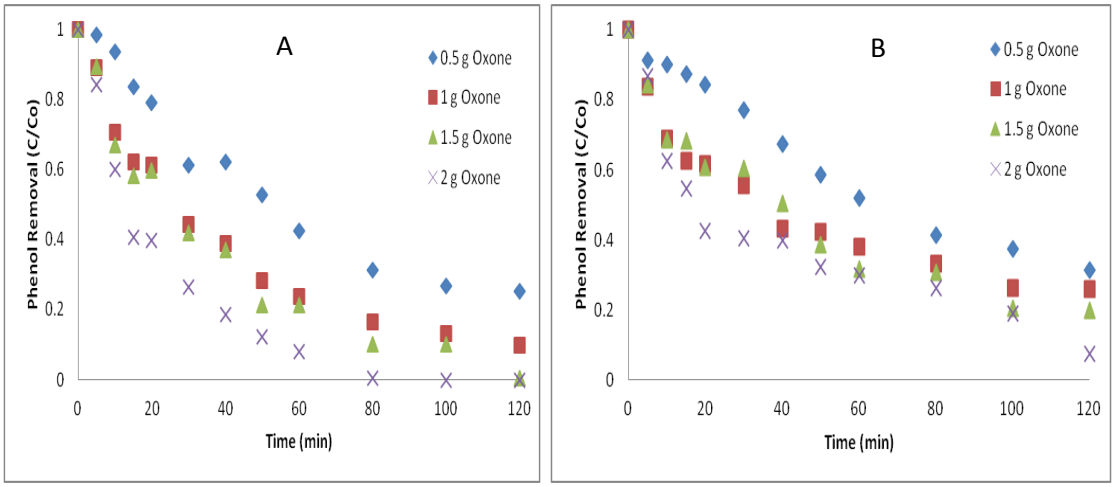

Figure 7.13 Phenol removal in different Oxone concentration (A) Ru/TiO_2 and (B) Ru/Al_2O_3 at 0.2g catalyst, 1 g Oxone, 25^{0}C, 200W UV

The second parameter measured in this study was phenol concentration in a range of 25 - 100 ppm, as shown in Fig. 7.12. Generally, removal efficiency of phenol decreases with increasing phenol concentration. For instance at 120 minutes phenol removal efficiency on Ru/TiO_2 at

concentrations of 25 ppm, 50 ppm, 75 ppm and 100 ppm are 95.67%, 90.16%, 68.72% and 55.88% respectively. Similar trend is also found in Ru/Al_2O_3.

The third parameter investigated is oxone concentration. Figure 7.13A (Ru/TiO_2) shows that increased concentration of oxone in a solution will accelerate phenol removal. By using 2g oxone, complete removal can be achieved in about 80 minutes. Similar trend is also observed in Fig. 7.13B using Ru/Al_2O_3 even with removal efficiency slightly lower than Ru/TiO_2. The increase of reaction rate at the increased oxone concentration is caused by higher production of sulphate radical for reducing phenol.

7.3.5 Phenol photocatalytic oxidation kinetics

Phenol degradation in photocatalytic without an oxidant is occurred with heterogeneous reaction in the catalyst surface. Basically, phenol is directly oxidized on the active holes on catalyst surface. So intermediate compound is formed and continued with the formation of end products. However, by adding an oxidant such as PMS, the main process will be the formation of sulfate radical which is generated by interaction between PMS and the catalyst (Ru/TiO_2 or Ru/Al_2O_3) or caused by interaction between PMS and UV-light. The phenol molecule reduction is fit with the first order kinetics. A general equation of the pseudo first order kinetics can be used, as shown in the following equation.

$$\frac{dC}{dt} = -(k.C) \qquad 7.6$$

Where k is the first order rate constant of phenol removal, C is the concentration of phenol at various time, Co is the initial concentration of

phenol. By integrating the equation above, the profile decrease in phenol concentration can be further elaborated in the following equation.

$$C = Co.e^{-k.t} \qquad 7.7$$

The Eq. 7.7 become

$$\ln (C/C_0) = -k.t \qquad 7.8$$

The rate constant can be determined by plotting of $\ln(C/C_0)$ with time, as presented in Fig. 7.14.

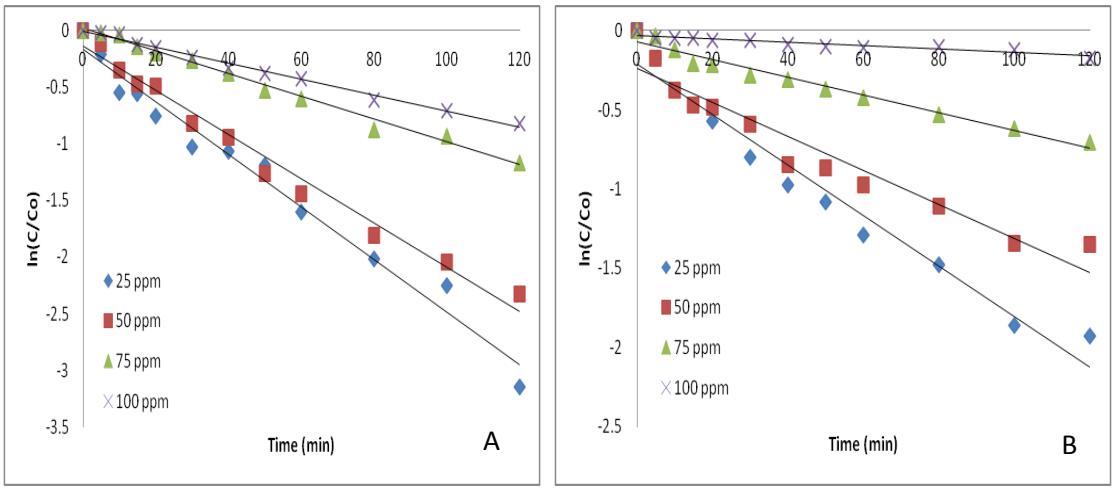

Figure 7.14 Pseudo first order kinetics (A). Ru/TiO_2 and (B). Ru/Al_2O_3

From data fitting, it is obtained that this reaction can be represented by the pseudo first order kinetics. This can be validated from the values of R^2, which are above 0.9 as shown in Table 7.1. The calculated rate constants are also presented in Table 7.1. The rate constant *(k)* shows that in general the value of *k* for Ru/TiO_2 is higher than Ru/Al_2O_3, which means the Ru/TiO_2 is able to degrade phenol more rapidly than Ru/Al_2O_3.

Table 7.1 The rate constants at various concentrations of phenol

Catalyst	Phenol Concentration							
	25 ppm		50 ppm		75 ppm		100 ppm	
	k	R^2	*k*	R^2	*k*	R^2	*k*	R^2
Ru/TiO_2	0.0232	0.9767	0.0195	0.9809	0.01	0.9903	0.0071	0.9908
Ru/Al_2O_3	0.016	0.9666	0.0108	0.9255	0.0056	0.9675	0.0011	0.9863

7.4 Conclusion

Two photocatalysts of Ru/TiO_2 and Ru/Al_2O_3 have been successfully synthesized using an impregnation method. Both catalysts are effective for application of photocatalytic oxidation of phenol in the presence of PMS and UV-light. In this study, phenol can be removed within 1 hour from the solution. Activation of PMS for the production of sulphate radicals for phenol degradation is generated by the interaction PMS-Catalyst and PMS-UV. The photocatalysts of Ru/TiO_2 and Ru/Al_2O_3 can increase the phenol removal efficiency by 10-15%. The activity in phenol removal of Ru/TiO_2-PMS-UV is slightly higher than Ru/Al_2O_3-PMS-UV. Both catalysts also showed good performance in the second and third runs after regeneration for multiple uses. The concentration of phenol, catalyst loading and concentration of Oxone® are important parameters that affect the reaction rate in removing phenol. Kinetic studies showed that phenol oxidation on the catalysts, Ru/TiO_2 and Ru/Al_2O_3 in the presence of PMS and UV light follows the first order reaction.

References

1. N. Serpone, P. Maruthamuthu, P. Pichat, E. Pelizzetti, H. Hidaka, *Exploiting the interparticle electron transfer process in the photocatalysed oxidation of phenol, 2-chlorophenol and pentachlorophenol: chemical evidence for electron and hole transfer between coupled semiconductors.* Journal of Photochemistry & Photobiology, A: Chemistry, 1995. 85(3): p. 247-255.

2. F. Spadavecchia, G. Cappelletti, S. Ardizzone, C.L. Bianchi, S. Cappelli, C. Oliva, P. Scardi, M. Leoni, P. Fermo, *Solar photoactivity of nano-N-TiO2 from tertiary amine: role of defects and paramagnetic species*, Appl. Catal. B: Environ. 96 (2010) 314–322.

3. Y.C. Zhang, Z.N. Du, K.W. Li, M. Zhang, D.D. Dionysiou, *High-performancevisible-light-driven SnS2/SnO2 nanocomposite photocatalyst prepared via in situ hydrothermal oxidation of SnS2 nanoparticles*, ACS Appl. Mater. Interfaces 3 (2011) 1528–1537.

4. S. Cong, Y.M. Xu, *Explaining the high photocatalytic activity of a mixed phase TiO2: a combined effect of O2 and crystallinity*, J. Phys. Chem. C 115 (2011) p. 21161–21168.

5. A.D. Paola, E. Garcia-Lopez, G. Marci, L. Palmisano, *A survey of photocatalytic materials for environmental remediation*, J. Hazard. Mater. 211–212 (2012) p. 3–29.

6. R. van Grieken, J. Marugan, C. Sordo, P. Martinez, C. Pablos, *Photocatalytic inactivation of bacteria in water using suspended and immobilized silver-TiO2*, Appl. Catal. B: Environ. 93 (2009) p. 112–118.

7. H. Xu, L.Z. Zhang, *Controllable one-pot synthesis and enhanced photocatalytic activity of mixed-phase TiO2 nanocrystals with tunable brookite/rutile ratios*, J. Phys. Chem. C 113 (2009) p. 1785–1790.

8. R.G. Nair, A.M. Tripathi, S.K. Samdarshi, *Photocatalytic activity of predominantly rutile mixed phase Ag/TiV oxide nanoparticles under visible light irradiation,* Energy 36 (2011) 3342–3347.

9. Fa-tang Li , Ye Zhao, Ying-juan Hao, Xiao-jing Wang, Rui-hong Liu, Di-shun Zhao, Dai-mei Chen, *N-doped P25 TiO_2–amorphous Al_2O_3 composites: One-step solution combustion preparation and enhanced visible-light photocatalytic activity*, Journal of Hazardous Materials, Vol. 239–240 (2012) p. 118–127

10. T. van der Meulen, A. Mattson, L. Oesterlund, *A comparative study of the photocatalytic oxidation of propane on anatase, rutile, and mixed-phase anatase–rutile TiO2 nanoparticles: role of surface intermediates*, J. Catal. 251 (2007) p. 131–144.

11. G.H. Li, S. Ciston, Z.V. Saponjic, L. Chen, N.M. Dimitrijevic, T. Rajh, K.A. Gray, *Synthesizing mixed-phase TiO2 nanocomposites using a hydrothermal method for photo-oxidation and photoreduction applications,* J. Catal. 253 (2008) p. 105–110.

12. R. Scotti, I.R. Bellobono, C. Canevali, C. Cannas, M. Catti, M. D'Arienzo, A. Musinu, S. Polizzi, M. Sommariva, A. Testino, F. Morazzoni, *Sol–gel pure and mixed-phase titanium dioxide for photocatalytic purposes: relations between phase composition, catalytic activity, and charge-trapped sites*, Chem. Mater. 20 (2008) p. 4051–4061.

13. L. Li, C.Y. Liu, *Facile synthesis of anatase–brookite mixed-phase N-doped TiO2 nanoparticles with high visible-light photocatalytic activity*, Eur. J. Inorg. Chem. (2009) p. 3727–3733.

14. Z.F. Zheng, H.W. Liu, J.P. Ye, J.C. Zhao, E.R. Waclawik, H.Y. Zhu, *Structure and contribution to photocatalytic activity of the interfaces in nano fibers with mixed anatase and TiO2(B) phases,* J. Mol. Catal. A: Chem. 316 (2010) p. 75–82.

15. X.B. Chen, S.S. Mao, *Titanium dioxide nanomaterials: synthesis, properties, modifications*, and applications, Chem. Rev. 107 (2007) 2891–2959.

16. A. Zielinska-Jurek, E. Kowalska, J.W. Sobczak, W. Lisowski, B. Ohtani, A. Zaleska, *Preparation and characterization of monometallic (Au) and bimetallic (Ag/Au) modified-titania photocatalysts activated by visible light,* Appl. Catal. B: Environ. 101 (2011) 504–514.

17. X.X. Yu, S.W. Liu, J.G. Yu, Superparamagnetic-Fe2O3@SiO2@TiO2 composite microspheres with superior photocatalytic properties, Appl. Catal. B: Environ. 104 (2011) 12–20.

18. X.J. Wang, Y.F. Liu, Z.H. Hu, Y.J. Chen, W. Liu, G.H. Zhao, Degradation of methyl orange by composite photocatalysts nano-TiO2 immobilized on activated carbons of different porosities, J. Hazard. Mater. 169 (2009) 1061–1067.

19. R.J. Tayade, R.G. Kulkarni, R.V. Jasra, Enhanced photocatalytic activity of TiO2-coated NaY and HY zeolites for the degradation of methylene blue in water, Ind. Eng. Chem. Res. 46 (2007) 369–376.

20. P. Pucher, M. Benmami, R. Azouani, G. Krammer, K. Chhor, J.F. Bocquet, A.V. Kanaev, Nano-TiO2 sols immobilized on porous silica as new efficient photocatalyst, Appl. Catal. A: Gen. 332 (2007) 297–303.

21. L.C. Chen, F.R. Tsai, C.M. Huang, Photocatalytic decolorization of methyl orange in aqueous medium of TiO2 and Ag–TiO2 immobilized on _-Al2O3, J. Photochem. Photobiol. A 170 (2005) 7–14

22. J. Villasen8or, P. Reyes, G. Pecchi, J. Chem. T echnol. Biotechnol. 72 (1998) 105-110.

23. A. Akyol, H.C. Yatmaz, M. Bayramoglu, Applied Catalysis B, Environmental. 54 (2004) 19-24.

24. A.A. Khodja, T. Sehili, J.F. Pilichowski, P. Boule, Journal of Photochemistry & Photobiology, A: Chemistry. 141 (2001) 231-239.

25. L.B. Khalil, W.E. Mourad, M.W. Rophael, Applied Catalysis B, Environmental. 17 (1998) 267-273.

26. Q.J. Yang, H. Choi, Y.J. Chen, D.D. Dionysiou, Applied Catalysis B-Environmental. 77 (2008) 300-307.

27. A. Fujishima, T. Kato, E. Maekawa, K. Honda, Bulletin of the Chemical Society of Japan. 54 (1981) 1671-1674.

28. M. Bekbolet, I. Balcioglu, Water Science and Technology. 34 (1996) 73-80.

29. R.W. Matthews, S.R. McEvoy, J. Photochem. Photobiol. A : Chem. 64 (1992) 231-246.

30. Parson, S., Williams M. *Advance Oxidation Processes for Water and Wastewater Treatment*, IWA Publishing, London, 2004, p.9

Chapter-8

Conclusions and Future Work

8.1 Concluding remarks

The main objective of this research mentioned in Chapter 1 of this thesis has been well achieved. Several heterogeneous catalysts based on cheap and easy obtained material supports such as Activated Carbon (AC), Fly Ash (FA, Australian: FA-WA, Brazilian: FA-JL and FA-CH), Red Mud (RM: treatment and non treatment), Natural Zeolite (Indonesian: INZ, Australian: ANZ), ZSM5 and MCM48 have been successfully synthesized using an impregnation method. The active metals of Ruthenium (Ru) and Cobalt (Co) have been well coated and dispersed on to the support material surface by impregnation. Further, the synthesized catalysts of Ru/AC, Ru/ZSM5, Ru/Al_2O_3, Ru/TiO_2, Ru/MCM48, Co/FA, Co/RM, Co/NZ, Co/MCM48 have been tested in heterogeneous catalytic oxidation of phenol for waste water treatment in the presence of Oxone®. Particularly for Ru/Al_2O_3 and Ru/TiO_2 catalysts, they have been tested in photocatalytic oxidation of phenol under UV-light. It is proved that the active metals impregnated on the support materials have been well in generation of sulfate radicals from peroxymonosulphate (PMS) which serves as an oxidant agent to degrade phenol contaminant from aqueous solutions. The catalyst activity in the phenol removal varies with a main order of Co/AC = Ru/AC > Co/MCM48 > Ru/ZSM5 = Co/RM-T > Co/FA-JL. In this relation, AC that has large pore volume and surface area and

MCM48 which has a very small particle size exhibit the best results as a support. In the photocatalytic system, the activation of PMS is occurred by the interaction PMS-Catalyst and PMS-UV. The photocatalysts Ru/TiO_2 and Ru/Al_2O_3 can increase the phenol removal efficiency by 10-15% comparing the combination of PMS/UV. Further, it was observed that catalyst loading, phenol concentration, oxidant concentration and temperature are the major factors influencing oxidation process of phenol. It is also noted that degradation of phenol in heterogeneous catalytic oxidation is a combination of oxidation and adsorption process. However oxidation is much faster than adsorption.

8.1.1 Activated Carbon and ZSM5 Supported Ruthenium Catalysts

1. Activated Carbon (AC) and ZSM5 supported Ruthenium (Ru) catalysts have been successfully synthesized using an impregnation method. According to characterization by XRD, SEM and EDS, the active metal species of Ru and RuO_2 are well coated and dispersed on to the support materials.
2. Nitrogen (N_2) adsorption for pore size distribution and specific surface area (S_{BET}) shows that RuO_2/AC has a higher surface area (1178 m^2/g) than $RuO_2/ZSM5$ (386 m^2/g). Further, RuO_2/AC also has a higher pore volume (0.108 cm^3/g) than $RuO_2/ZSM5$ (0.085 cm^3/g). However, both RuO_2/AC and $RuO_2/ZSM5$ have a similar pore radius of 15.6 Å and 15.7 Å. According to the pore radius, both catalysts are microporous materials.
3. Both RuO_2/AC and $RuO_2/ZSM5$ are highly effective in heterogeneous activation of peroxymonosulphate to produce sulphate radicals to degrade phenol. Complete removal of phenol using RuO_2/AC and $RuO_2/ZSM5$ can be reached in 20 min and 60 min, respectively, at

reaction conditions of 50 ppm phenol, 0.2 g catalyst, 1 g Oxone® in 500 mL solution at 25 ^{0}C.

4. Kinetic studies proved that a pseudo first order kinetics would fit to phenol decomposition and the activation energies for RuO_2/AC and RuO_2/ZSM5 were obtained to be 61.4 and 42.2 kJ/mol, respectively.

8.12 Coal Fly Ash and Red Mud Supported Cobalt Catalysts

1. Three types of Fly Ashes (FA-WA, FA-JL and FA-CH) and two Red Mud samples (RM-NT and RM-T) impregnated active metal Co with active species of Co_3O_4 have been successfully synthesized. Based on the characterization, the contents of SiO_2 and Al_2O_3 are above 70% for all types of FA catalysts.
2. FA and RM supports themselves did not show adsorption of phenol and could not activate peroxymonosulfate for sulphate radical generation. However, FA and RM supported Co oxide catalysts presented higher activities in activation of peroxymonosulfate for phenol degradation than bulk Co oxide and their activities varied depending on the properties of fly ash and red mud supports.
3. Generally, FA based catalysts exhibit lower activity than RM systems. Among FA catalysts, Co/FA-JL showed the highest while Co/FA-WA showed the lowest activity. On the other hand, Co/RM-T can completely remove phenol in 60 minutes which is better than Co/RM-NT. For both catalysts, phenol degradation followed the first order kinetics and the activation energies for Co/RM and Co/FA are 66.3 and 47.0 kJ/mol, respectively.

8.1.3 Natural Zeolite and MCM48 Supported Cobalt Catalysts

1. Preparations of zeolite and MCM48 catalysts have been well done by dispersing active metal cobalt on the support material surface through impregnation. Characterization results by XRD and SEM-EDS confirm that the active metal cobalt on the support surface is in form of Co_3O_4.
2. The three catalysts of Co/MCM48, Co/INZ and Co/ANZ are effective catalysts for generating sulphate radicals in the presence of Peroxymonosulphate (PMS) to degrade phenol. Among these three catalysts, Co/MCM48 has the best activity in removing phenol which completes removal of phenol in 40 minutes than the other two with the activity order of Co/MCM48 > Co/INZ > Co/ANZ.
3. Kinetic studies show that phenol oxidation on the Co/MCM48, Co/INZ and Co/ANZ follows the first order reaction with the activation energies of 80.3, 61.3 and 52.4 kJ/mol, respectively.

8.1.4 Ru/Al_2O_3 and Ru/TiO_2 Catalyst on Photocatalytic Oxidation of Phenol in the present of oxidant and UV-light

1. Photocatalysts of Ru/TiO_2 and Ru/Al_2O_3 have been successfully synthesized using impregnation followed by calcination at temperature of 550 ^{0}C for 6 hours in air. The XRD, SEM and EDS characterizations confirm that the active phase of ruthenium in form of RuO_2 has been well coated and dispersed on the supports. The catalysts are effective to activate PMS and generate sulfate radicals for phenol removal.
2. This research also confirms that UVC from Mercury lamp is very effective to generate sulfate radical from PMS. Therefore, the activation of PMS for the production of sulphate radicals in this study is generated by the interaction PMS with Catalyst and PMS with UV. Further, combination of Ru/TiO_2-Oxidan-UV and Ru/Al_2O_3-Oxidant-UV can

increase the phenol removal efficiency about 10-15% compared with Oxidant-UV system only.

3. The activity in phenol removal of Ru/TiO_2-PMS-UV is slightly higher than Ru/Al_2O_3-PMS-UV. Both catalysts also showed good performance in the second and third runs after regeneration for multiple uses.
4. Kinetic studies showed that phenol oxidation on the catalysts Ru/TiO_2 and Ru/Al_2O_3 in the presence of PMS and UV light follows the first order reaction

8.2 Scope of Future Work

1. This research focused on impregnation of active metals of Ru and Co on the cheap and easily obtained material supports such as AC, FA, RM, NZ etc. The synthesized catalysts presented very good performance in phenol oxidation in the presence of PMS. For the future work, it is recommended to conduct the catalyst test with other oxidants such as peroxide, persulphate, permanganate, ozone etc. Further, the catalyst synthesis on similar supports using the other active metals such as Zn, Mn, Ce etc., is also valuable to be implemented. Further, it was also found that little amount of active metal was leach out into the solution. So that it is recommended to examine further the detail of catalyst leaching.
2. In the examination of some synthesized catalysts by using SEM-EDS, it was observed that the dispersed active metals Ru and Co on the support surface was not spred evenly. EDS spectrum spot showed that there are much surface not coated by the active metal. As a result, the performance of catalysts was not optimal in oxidizing phenolic contaminants. Therefore, for the future work, it is needed to improve impregnation method by enhancing initial concentration of active

metal, refine particle size support, increasing stirring and impregnation time, optimizing of drying rate and calcination temperature.

3. One of the TiO_2 drawbacks in relation with its activity on photocatalytic oxidation is its surface area which is relatively low. On the other hand, surface area is an important factor influencing adsorption rate, and photocatalysis. Therefore, for the future work, it is essential to immobilize TiO_2 and other active metal over support materials which have high surface areas, such as activated carbon, zeolite, silica etc.